INVESTIGATION OF THE CLEAVAGE OF THE ESTER BOND IN PHOSPHATE MONOESTERS: ENZYMATIC AND SOLUTION STUDIES OF PHOSPHORYL TRANSFER REACTIONS AND COMPARISON WITH ANALOGOUS SULFURYL TRANSFER REACTIONS

by

Richard H. Hoff

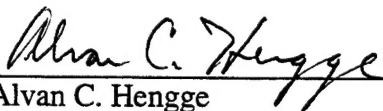A dissertation submitted in partial fulfillment
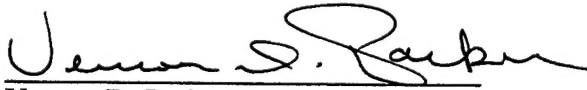of the requirements for the degree

of

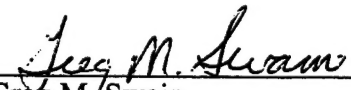DOCTOR OF PHILOSOPHY

in

Chemistry

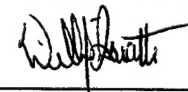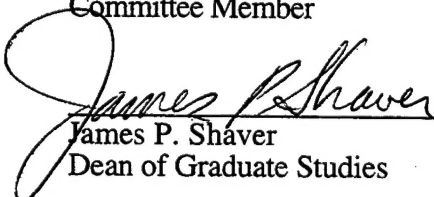Approved:

Alvan C. Hengge Major Professor	Vernon D. Parker Committee Member
Greg M. Swain Committee Member	Robert S. Brown Committee Member
William J. Doucette Committee Member	James P. Shaver Dean of Graduate Studies

UTAH STATE UNIVERSITY
Logan, Utah

1999

ABSTRACT

Investigation of the Cleavage of the Ester Bond in Phosphate Monoesters:

Enzymatic and Solution Studies of Phosphoryl Transfer Reactions

and Comparison with Analogous Sulfuryl Transfer Reactions

by

Richard H. Hoff, Doctor of Philosophy

Utah State University, 1999

Major Professor: Dr. Alvan C. Hengge
Department: Chemistry and Biochemistry

The phosphate ester bond is a ubiquitous species in biochemical systems. Prior studies have elucidated many details of the mechanisms by which this bond is broken. Here this system was further studied through the evaluation of the kinetics of the ester bond cleavage in solution and in enzymatic reactions. The role of solvation was explored by a series of experiments using the extrathermodynamic assumption, which allowed a detailed thermodynamic accounting for the effects of solvent on the reaction. Insights gained into the structure of the transition state through these studies were then applied to the evaluation of several enzymatic systems.

The principal enzyme examined was the protein tyrosine phosphatase from *Yersinia*. Kinetic isotope effects, which provide information on the extent of bond cleavage and charge delocalization in the transition state, were the primary tools of this phase of the study. The mechanism was elucidated through the use of site-directed mutagenesis, which allowed the identification of key roles of particular residues in this enzyme. Further kinetic isotope effect studies were performed with the serine/threonine protein phosphatase-2C, serine/threonine protein phosphatase Lambda, and dual specific

vaccinia-H1-related enzymes for comparison with the *Yersinia* protein tyrosine phosphatase. The chemistry of sulfation has an important role in biochemical systems, but it is not as ubiquitous as that of phosphoryl transfer. The sulfate ester bond has long been held as a close relative of the phosphate ester bond, and it has been proposed that the mechanism of cleavage is similar in spite of a marked difference in activation parameters. In order to broaden the base of knowledge on these related mechanisms, kinetic and kinetic isotope effect studies were conducted with *p*-nitrophenyl sulfate to parallel many of those done with the phosphate. A comparison of the data derived from these studies allowed an explanation to be forwarded for the divergent activation parameters and allowed conclusions to be drawn concerning the mechanism of sulfate ester cleavage.

(262 pages)

DEDICATION

I would like to dedicate this dissertation to the five people who made it possible for me to successfully reach this conclusion to one chapter of my life.

First to my parents, Carolyn and Buddy Hoff, who provided me with the values and experiences that enabled me to seek and know success. They are in my thoughts and prayers always.

Next to my wife, Anne, whose steadfast support and love through the last many years have been the tiebreaker over and over again. I pray that I can make the next twenty years as rewarding for her as she has made the last twenty rewarding for me.

And to my first child, Kimberley, in whom I see every one of Anne's finest qualities reflected. Her quiet strength is a source of wonder and inspiration to me.

Finally to Skyler, the young scientist, who keeps the excitement of discovery fresh and alluring. If I were as smart as he is, I would have finished this a long time ago.

ACKNOWLEDGMENTS

The primary acknowledgment that I need to make for facilitating the accomplishment of this work is to Dr. Alvan C. Hengge. Alvan was quick to grasp the unique needs of a person who is given only a limited amount of time to complete degree requirements. He provided expert assistance and judgment in establishing research goals that were challenging but attainable. His constant attention and unlimited availability to his students laid the groundwork for rapid and intense training, which brought me up to speed in the laboratory. His willingness to use his research resources to get students to conferences provided exposure to world authorities and taught me how to prepare and present my work. I do not think I could have designed a better three-year apprenticeship than I have had in the Hengge lab.

I must also recognize the contributions of my research committee, Dr. Parker, Dr. Brown, Dr. Doucette, and Dr. Swain, to this work. Several members made specific contributions to certain aspects of the work, while all provided useful general guidance throughout the process. Dr. Swain made particular contributions to my efforts to determine pK_as in nonaqueous solution, while Dr. Parker assisted in my investigation of single ion solvation.

A major contribution to this work was made by two collaborators and their students. Dr. Frank Rusnak and his former student, Dr. Pam Mertz, were instrumental in accomplishing all of the work involving the lambda enzyme. Pam produced the enzyme and the mutant that were featured in this work, and she worked through a very difficult kinetic characterization of the enzymes. In addition, she spent two weeks of 16-hour days in Logan performing the bulk of the isotope effects experiments. Dr. Zhong-Yin Zhang and his assistant Dr. Yen-Fang Keng performed a similar service in isolating, purifying, and characterizing the native and mutant Yersinia enzymes.

CONTENTS

LIST OF TABLES

LIST OF FIGURES

.

CHAPTER 1

INTRODUCTION AND LITERATURE REVIEW

Introduction

The Importance of Phosphate Esters. The phosphate ester bond is a critical chemical link in many important biochemical systems in living cells, to the extent that phosphate esters have been said to "dominate the living world."[1] The DNA and RNA that preserve and transcribe all genetic information are phosphate diesters. The key compounds in the maintenance of biochemical energy reservoirs are adenosine triphosphate, creatine phosphate, and phosphoenolpyruvate. As compounds are metabolized and created in countless other biochemical systems, the phosphate or pyrophosphate group is attached, creating phosphate and pyrophosphate esters, all of which have the ester linkage. This phosphate ester linkage is unique in that it can link two other groups and still ionize, which confers on the phosphate ester an ability to resist hydrolysis. The ionization also allows the phosphate ester to be retained within lipid membranes. This combination of stability and retention leads to the ubiquitous role in living systems, and makes the study of phosphate esters an area rich in meaning and interest.

The Nature of Phosphate Esters and the Ester Bond. An understanding of the phosphate ester can begin with the structure and characteristics of phosphoric acid, H_3PO_4. The phosphorus sits at the center of a tetrahedral array of oxygen atoms. Phosphoric acid is a polyprotic acid, which can ionize to give off one proton, or it can subsequently further ionize to yield a second or even a third proton (Figure 1-1). Each ionization has a characteristic solution pH at which the molecule is present as 50% protonated and 50% deprotonated. This pH is called the pK_a for the species. Phosphoric acid has three pK_as, which are 2.1, 7.1, and 12.7.[2] Therefore, at the near-neutral pH that dominates the solution chemistry of biochemical systems, phosphate will be present

almost entirely as the monoanionic and dianionic species. In biochemical systems the form of phosphate shown in Figure 1-1 is referred to as inorganic phosphate, often written as P_i. Most biochemically significant forms of phosphate are not inorganic phosphate, but rather are phosphate esters.

A phosphate becomes an ester simply by replacement of one of the protons with some other chemical entity which provides a bond to the phosphate oxygen, which is represented generally as -R in the structure. Many phosphate esters of biochemical significance are diesters or monoesters. Phosphate triesters have not been found in nature, but were first synthesized in the years prior to World War Two.[3] The triesters were developed into a group of compounds which include highly toxic insecticides and chemical warfare agents. Shown in Figure 1-2 are examples of phosphate monoesters and diesters. Mono-, di-, and triesters have all been the subject of extensive study; this
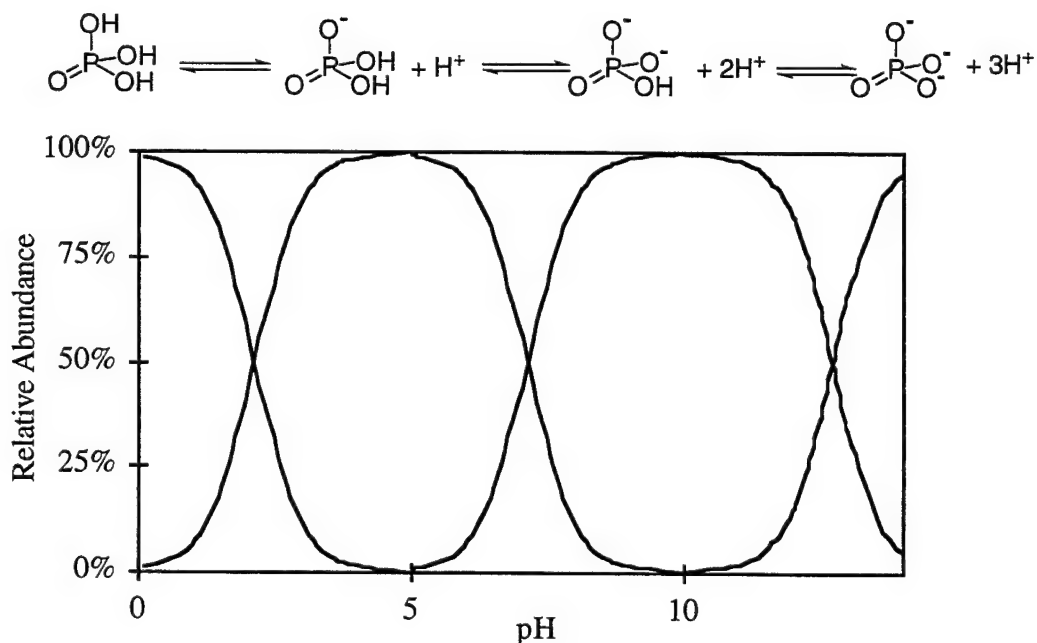
Figure 1-1. The successive deprotonation reactions of phosphoric acid. Under each of the species in the chemical reaction is a curve showing the relative abundance of that species at a given pH. The three points where curves intersect are the pK_as for the deprotonation reactions.

research will focus on the chemistry of monoesters. In a monoester, one of the phosphate oxygens is involved in the link between the phosphorus and the ester group. This oxygen will be referred to as the bridge oxygen in the remainder of this work. The three oxygens that are not involved in the ester bond will be referred to as the nonbridge oxygens.

The chemistry of the phosphate monoester is a substitution reaction. The species which is attached to the phosphate oxygen forms a leaving group, and the phosphorus-oxygen bond becomes labile. Substitution reactions at the tetrahedral phosphate can occur by three limiting mechanisms, as shown in Figure 1-3. The dissociative reaction, designated D_N+A_N in IUPAC nomenclature,[4] is a two-step reaction that proceeds through a free metaphosphate (PO_3^-) intermediate. The associative reaction, designated A_N+D_N, is an addition-elimination pathway in which a stable pentacoordinate intermediate is formed. This pentacoordinate species is called a phosphorane, and it is generally accepted that formation of a phosphorane is accompanied by a shift from tetrahedral to trigonal bypyramidal structure. The concerted mechanism, designated A_ND_N, shows a transition

Generic Phosphate Monoester Glucose-1-phosphate Adenosine Triphosphate
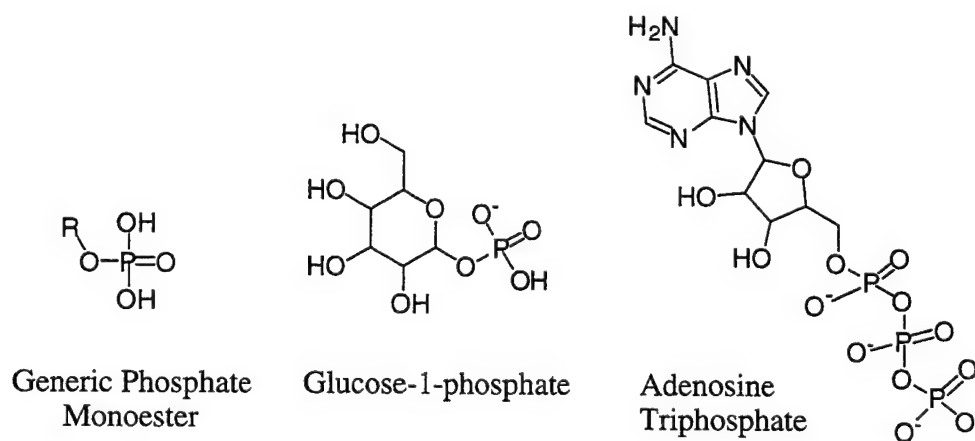
Figure 1-2. Examples of phosphate esters. The generic form is shown in the neutral state, while the glucose-1-phosphate, which is also a monoester, is shown ionized. Adenosine triphosphate has two phosphorus centers which could be viewed as possessing diester character. When there is an ester bond between two phosphate groups, the species is known as an anhydride. Note with adenosine triphosphate that the physiologically stable species carries multiple negative charges.

state where bond cleavage to the leaving group and bond formation by the nucleophile are both occurring. This transition state could have either dissociative or associative character depending on the synchronicity between bond formation and bond cleavage.

The reactions of phosphate monoesters in aqueous solution usually follow the concerted pathway. The mechanism as drawn in Figure 1-3C is pictured to suggest the considerable dissociative character which evidence supports as the mechanism for aqueous reactions. In a dissociative transition state, the sum of the bond orders to nucleophile and leaving group is less than in the ground state. In aqueous solution, the nucleophile is normally water and the reaction is referred to as hydrolysis. In other solvents that can act as nucleophiles, the reaction can be a solvolysis reaction. Alternatively, when a species of greater nucleophilicity than the solvent is introduced as the nucleophile, the reaction is referred to as phosphoryl transfer.
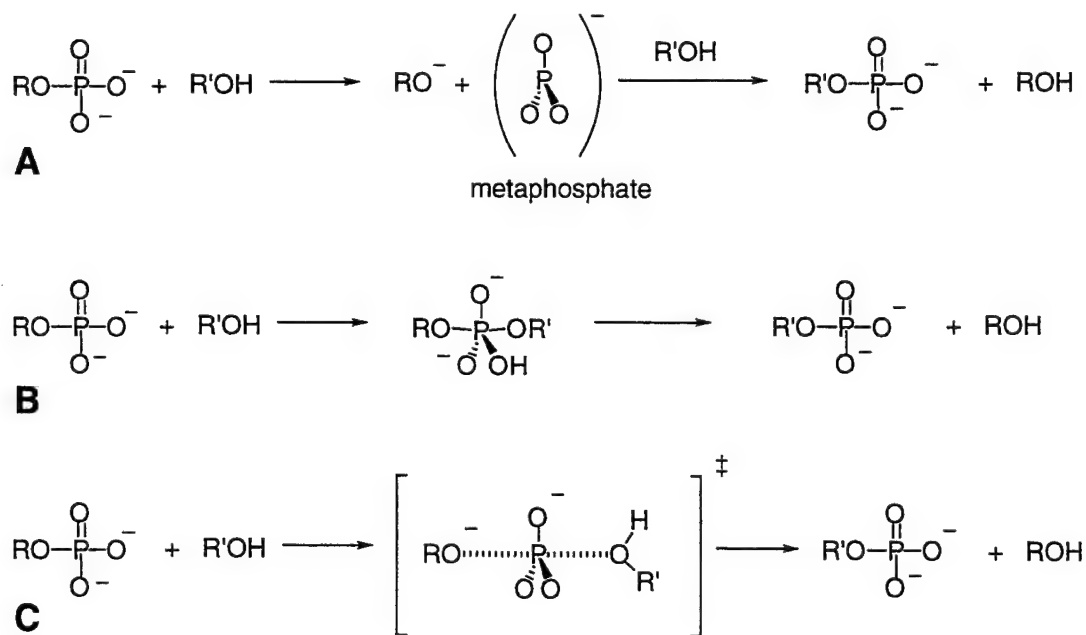
Figure 1-3. The three limiting mechanisms of phosphoryl transfer. **A** is the two-step dissociative mechanism featuring a free metaphosphate intermediate, **B** is the associative mechanism with a phosphorane intermediate, and **C** is the concerted mechanism, shown here with significant dissociative character.

Note that the reactions portrayed in Figure 1-3 all represent the dianion and its mechanistic possibilities. At physiological pH, the monoanion can also be present in significant amounts. Hydrolysis of the monoanion can proceed by two basic mechanisms, as shown in Figure 1-4. In both of these mechanisms the leaving group departs as a neutral species. The key to the difference between these mechanisms is whether the leaving group is protonated in a preequilibrium process, or whether it is protonated as it departs, as part of the formation of the transition state. The first scheme shows the preequilibrium mechanism, which results in an overall stepwise reaction. The second scheme shows the concerted mechanism, with the synchronicity of the proton transfer and the departure of the leaving group remaining undefined, but without the formation of an intermediate. In aqueous solution this proton transfer could be accommodated by a solvent bridge between the donor hydroxyl and the acceptor bridge oxygen.

Literature Review

Uncatalyzed Phosphoryl Transfer in Aqueous Solution. The significance of phosphate monoesters was recognized several years ago; hence the
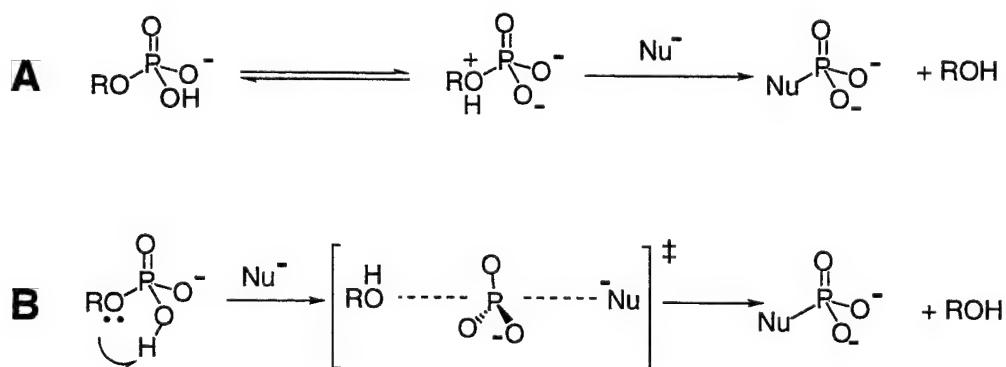
Figure 1-4. The limiting mechanisms for the phosphoryl transfer of the monoester monoanion. **A** shows preequilibrium transfer of the proton from a nonbridge to the bridge oxygen, followed by nucleophilic attack at the phosphorus. **B** is concerted, with undefined synchronicity between proton transfer and nucleophilic attack.

reactions have been fairly well characterized. The study of a class of compounds often begins with simple kinetic experiments in an attempt to relate structure to function. A pH-rate profile of a reaction can give clues as to the impact of protonation on the kinetics of the reaction and allow inferences to be made concerning the mechanism. In such a profile for the reaction of p-nitrophenyl phosphate (pNPP),[5,6] the reaction is seen to have a rate maximum between pH 3 and pH 4 (Figure 1-5). This corresponds to the pH where the monoanion is the predominant species, given pK_1 and pK_2 of 0.3 and 5.0, respectively.[7] The pH rate profile can be mathematically linked to the equilibrium protonation and deprotonation reactions to support the theory that the monoanion is the only reactive species that involves the cleavage of the P-O bond. However, experimental work provides clear evidence of a different mechanism involving the dianion, as will be discussed below. The small upward tail of reactivity that occurs at very high pH is said to
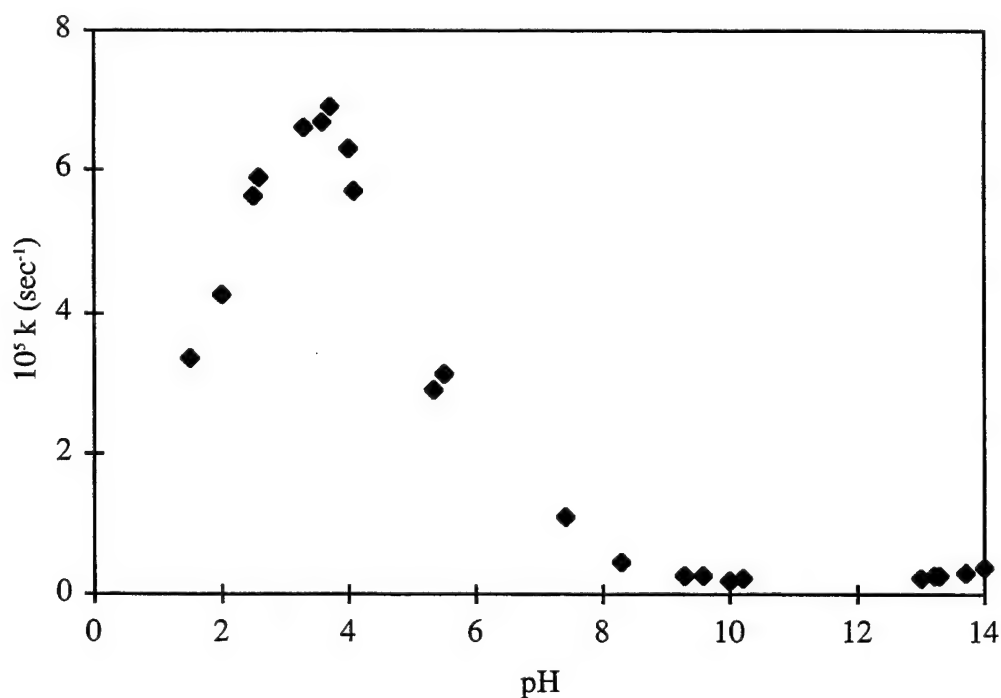
Figure 1-5. The pH/rate profile for the aqueous hydrolysis of p-nitrophenyl phosphate. Data were collected at 73 °C[5] and 39 °C[6] and were corrected for temperature differences and combined to create this plot.

represent the cleavage of the O-C bond between the bridge oxygen and the phenyl ring.[5] Thus the pH rate profile establishes that the reaction of the dianion is much slower than that of the monoanion.

Another means of gathering information concerning the mechanism of a reaction is by varying substituents involved with the reaction and observing the kinetic effects of the structural changes. This method was first developed in classic work by L. P. Hammett[8] and has since been further generalized as the investigation of linear free energy relationships. For phosphate esters, the most obvious application of this work is in an investigation of the relationship between the stability of the leaving group and the rate of the reaction. In the hydrolysis of the monoester dianion, the leaving group departs as a negative ion. Therefore, the leaving group's stability as a negative ion should have an impact on the rate of reaction. The pK_a of the conjugate acid of a negatively charged leaving group provides a measure of the stability of the anion. To quantify the relationship between leaving group and the rate of reaction, the rate constant can be plotted against the pK_a of the leaving group. This plot is called a Brønsted plot and the slope of the line is the β_{LG}, an index of the extent to which leaving group stability affects the reaction. Negative slopes indicate that as the pK_a rises and the leaving group is less stable as an anion, the reaction rate declines. The magnitude of β_{LG} yields a qualitative indication of the extent to which negative charge is developed on the leaving group, and provides insight into the nature of the transition state for the reaction.

A Brønsted study done on phosphate monoesters with aromatic leaving groups found a β_{LG} of -1.23[9] in aqueous solution under conditions where the phosphate was present as a dianion. This is a fairly high value for β_{LG} and indicates that the leaving group has nearly completely broken the bond to the phosphorus in the transition state and is bearing almost a complete negative charge. This could indicate either that a concerted mechanism with a dissociative transition state is active, or that a unimolecular dissociative

mechanism with a late transition state, such as shown in Figure 1-3A, is taking place.

Another means of exploiting the same sort of structure function relationship with this reaction system is to look at the impact of the nature of the nucleophile on the reaction rate. The nucleophilic reactivity of a nucleophile is related to its basicity which can be quantified by the pK_a of its conjugate acid. Therefore a plot of reaction rate versus the pK_a of the nucleophile reveals the extent of the impact of the nature of the nucleophile on the reaction. In a study with *p*-nitrophenolate as the leaving group, and a series of amines as nucleophiles, the β_{NUC} was found to be 0.13.[6] This is a very small value and is evidence that the nature of the nucleophile has little impact on the rate of reaction. The fact that there is some dependence on nucleophilic character does favor the concerted reaction mechanism over the dissociative, where it is difficult to rationalize any involvement by the nucleophile.

By studying the rate of reaction as temperature is varied, and plotting the natural log of the rate constant versus the reciprocal of the temperature, a linear plot is often obtained. This is termed an Arrhenius plot, and the slope of this plot can be used to determine the free energy of activation for a reaction. The Arrhenius plot is the graphic equivalent of the Arrhenius equation (Equation 1).[10]

$$\frac{d(\ln k)}{dT} = \frac{E_a}{RT^2} \tag{1}$$

Once the activation energy is determined, equations 2 through 4 can be used to determine activation parameters $\Delta H^\ddagger$, $\Delta S^\ddagger$, and $\Delta G^\ddagger$.

$$\Delta H^\ddagger = E_a - RT \tag{2}$$

$$\Delta S^\ddagger = \left(\frac{\Delta H^\ddagger - \Delta G^\ddagger}{T} \right) \tag{3}$$

$$\Delta G^{\ddagger} = -RT \ln\left(\frac{kh}{K_B T}\right) \qquad (4)$$

In equation 4, h is the Planck constant, k is the rate constant, and K_B is the Boltzmann constant.

The activation parameters for a reaction provide information on the contributions of enthalpy and entropy to the change from ground state to transition state. Enthalpy is broadly interpreted as indicative of bond breaking or formation, while entropy relates more to the molecularity of the mechanism, or to the effects of solvent reorganization. For the pNPP dianion at pH 10, an evaluation of the activation parameters yielded $\Delta H^{\ddagger} = 30.6$ kcal/mol, $\Delta S^{\ddagger} = +3.5$ eu, and $\Delta G^{\ddagger} = 29.5$ kcal/mol.[6] The large positive enthalpy of activation is consistent with significant bond breaking accompanying the change from ground state to transition state, while the small positive value for the entropy of activation is consistent with a unimolecular process. Both of these values favor the formation of a dissociative transition state, but do not provide conclusive evidence as to whether the mechanism is clearly dissociative or is just a concerted transition state with dissociative character.

The experimental data discussed to this point have formed a convincing case for the position that the hydrolysis of the phosphate monoester dianion proceeds by a dissociative process, but differentiation between a reaction that involves free metaphosphate and one that simply goes through a dissociative concerted transition state is still elusive. When one considers the resemblance of the phosphorus center in the concerted mechanism (Figure 1-3C) and the free metaphosphate intermediate in the dissociative mechanism (Figure 1-3A), the difficulty in differentiating these two is understandable. A possible means of providing a definitive discriminator would be to look at changes in stereochemistry at the phosphorus atom for different phosphoryl transfer reactions. If free metaphosphate was formed, it would be reasonable to expect

that any product would be completely racemic, as the metaphosphate is planar and neither apical approach would be favored. However, racemic product would not be a guarantee of free metaphosphate. An exchange reaction or multiple solvolysis replacements could also result in a racemic product.[11] A chiral product would be an indicator of some degree of associative character, such as that involved in the concerted mechanism.

Two synthetic methodologies were developed for the synthesis of phosphate monoesters made chiral by the use of oxygen isotopes,[12-14] but the results available with these substrates were limited to studies that did not involve phosphoryl transfer to water. For study of transfer to water, the phosphate was made chiral with the addition of two oxygen isotopes and a sulfur atom in the non-bridging positions.[15] The thiophosphoryl transfer to water then yields a racemic thiophosphate product. However, the thiometaphosphate is likely more stable than metaphosphate. When methanolysis of chiral phenyl phosphate substrate was examined, phosphoryl transfer occurred with inversion of configuration,[16] while transfer to *tert*-butanol occurred with racemization.[17] Based on this evidence, it is believed that phosphoryl transfer in water does not involve a free metaphosphate intermediate.

Kinetic Isotope Effects Experiments. Further clarification of the nature of the transition state in this reaction was made through the use of kinetic isotope effects. Kinetic isotope effects are derived from the concept of the zero point energy for bonding between two nuclei. Figure 1-6 shows a Lennard-Jones potential diagram depicting the potential energy curve along an axis between the two nuclei. If one of the nuclei is varied between a heavy isotope and a light isotope of the same element, the nature of the force constant between the two atoms does not change, but the zero point energy does, with the heavier atom residing lower in the potential well.

On this diagram the two isotopes are depicted, with the double-headed arrows representing the energy required to break a chemical bond. Due to the lower position of

the heavier atom on the potential curve, more energy is required to cause dissociation, so it will exhibit a lower kinetic rate at a given temperature. The rationalization of secondary kinetic isotope effects is similar to that explained above, but the effects are expressed as a result of differential effects on changes in bond order or in vibrational degrees of freedom. In situations where bonds are broken or degrees of freedom increase, the lighter isotopes have higher rates and the isotope effect is said to be normal. Since these isotope effects are based on the kinetic effect of isotopic substitution, they are relevant to the transition state of the reaction being investigated. Observation of no isotope effect is indicative of either no participation by the atom in question, or a rate-limiting step that is not chemical.

The notation for kinetic isotope effects is that of Northrop,[18] and consists of a superscript to identify the isotope of concern, the k for kinetic rate constant to indicate that
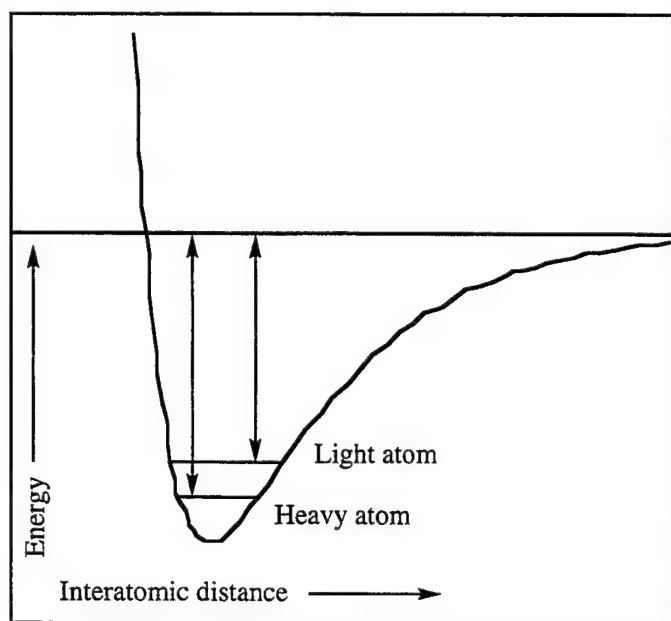
Figure 1-6. Lennard-Jones potential diagram showing the fundamental isotopic energy difference that leads to the observation of kinetic isotope effects. Marked on the potential well are the zero point energies of two isotopes of the same atom. Note the difference in energy required to move these to atoms to infinite separation.[10]

it is a kinetic effect as opposed to an equilibrium effect, and a subscript to indicate more clearly which atom position is of concern. The ^{15}N kinetic isotope effect is written ^{15}k to represent the ratio of rate constants with ^{14}N versus ^{15}N (k_{14N}/k_{15N}). Equilibrium isotope effects can be expressed in a similar manner, using the capital K to represent the effect on an equilibrium constant. The ^{18}O equilibrium isotope effect for the deprotonation of phenol would be written ^{18}K.

Isotope effects for the reaction of the pNPP dianion in aqueous solution were measured at three positions, as shown in Figure 1-7.[19] The ^{15}N kinetic isotope effect measures the extent to which negative charge is delocalized into the p-nitrophenolate leaving group. The nitrogen has an impact on this charge delocalization due to the participation of the quinonoid resonance form, shown in Figure 1-8. A normal isotope effect indicates that negative charge is being delocalized into the phenolate.

The ^{18}O kinetic isotope effects were measured by the remote label method, where

a) The nonbridge phosphoryl oxygen atoms

b) The bridge oxygen atom, the position of bond cleavage

c) The nitrogen atom in the leaving group
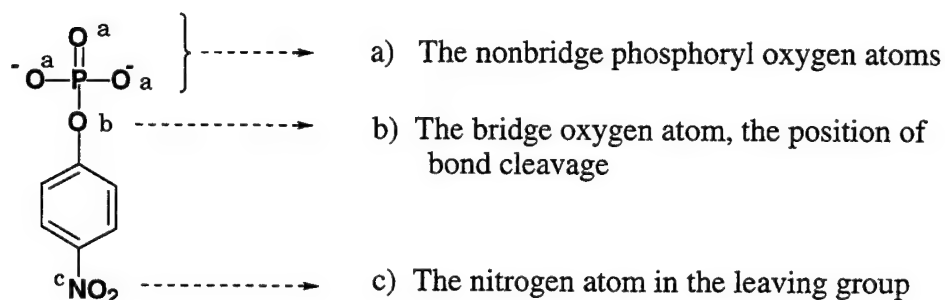
Figure 1-7. Positions of isotopic labeling of p-nitrophenyl phosphate.
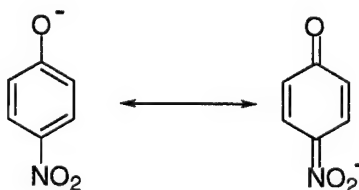
Figure 1-8. Quinonoid form of p-nitrophenolate ion, which contributes to the delocalization of negative charge throughout the ion.

a reporter atom is used to track the effects of a discriminating atom.[20] The substrate was synthesized with the ^{18}O label at the atom of interest and the ^{15}N atom in the nitro group at the remote reporter position. This double-labeled substrate was then mixed with a corresponding ^{14}N/^{16}O compound as shown in Figure 1-9. The kinetic isotope effect of the ^{18}O substitution was measured by tracking the ^{15}N isotope ratios. The observed isotope effect was corrected for the effect of the ^{15}N to give the ^{18}O kinetic isotope effect. The kinetic isotope effect for the bridge ^{18}O ($^{18}k_{bridge}$) provides a measure of the extent to which this bond is broken in the transition state, with a normal isotope effect indicating bond cleavage. The nonbridge ^{18}O isotope effect ($^{18}k_{nonbridge}$) reflects the change in the bond order to the non-bridge oxygens, with a normal isotope effect reflecting a decrease in net bond order.

All isotope effects were measured by the competitive method, which means that a mixture of labeled and unlabeled substrate was subjected to the reaction conditions. The reaction was stopped at partial completion and the nitrophenol product was isolated. The unreacted substrate was then subjected to conditions which converted it completely to nitrophenol, representing the residual substrate, and this was also isolated. By comparing the isotope ratio in the starting material to the ratio in the initial product and to that in the residual substrate, it is possible to make very accurate measurements of the difference in
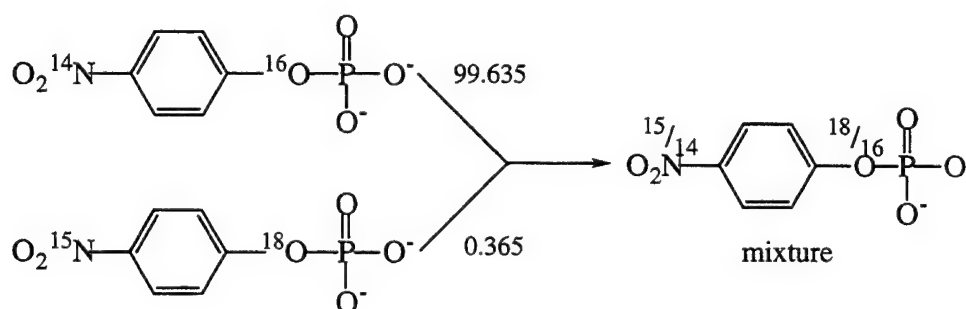
Figure 1-9. The preparation of a double labeled substrate. The ^{15}N/^{18}O double labeled substrate is mixed with the ^{14}N/^{16}O labeled substrate in a ratio such that the level of ^{15}N in the mixture approximates the natural abundance of ^{15}N.

reaction rate of the two isotopic species. From this difference the kinetic isotope effect is calculated, using equations 5 and 6, where R_O is the isotope ratio in starting material, R_P is the ratio in isolated product, R_S is the ratio in residual substrate, and f is the fraction of reaction.

$$\text{isotope effect} = \frac{\log(1-f)}{\log\left[1-f\left(\frac{R_P}{R_O}\right)\right]} \tag{5}$$

$$\text{isotope effect} = \frac{\log(1-f)}{\log\left[(1-f)\left(\frac{R_S}{R_O}\right)\right]} \tag{6}$$

For the pNPP dianion in aqueous solution the kinetic isotope effects, expressed as percents and corrected to 30 °C, are shown in Table 1-1.[19] Kinetic isotope effects with heavy (non-hydrogen) atoms are typically small effects, rarely more than 6%, with theoretical limits of about 7%.[21] These numbers are typically reported either as ratios or as percents. Using the ratio method, a reaction which displayed no impact from isotopic substitution would have an isotope effect of one, an inverse effect would be smaller than one, and a normal effect would be greater than one. The percent method would record 0% for no isotope effect, negative numbers for inverse and positive for normal. As an

Table 1-1. Kinetic Isotope Effects, pNPP Dianion, Aqueous Solution[a]

^{15}k	$^{18}k_{bridge}$	$^{18}k_{nonbridge}$
0.34±.02	2.3±.05	-.07±.05

[a] Data are from Hengge et al.[19] and are expressed as percents.

example, under the ratio method a normal isotope effect might be reported as 1.025, while the same isotope effect as a percent would be 2.5%. For clarity and uniformity, all isotope effects reported in this work will be reported as percents.

The interpretation of these isotope effects begins with the observation that ^{15}k indicates the delocalization of negative charge into the nitrophenol leaving group. This assertion begs the question, "How much charge is on the leaving group?" When considering ^{15}k, the isotope effect on deprotonation of nitrophenol might be expected to represent the upper bound on these isotope effects. For deprotonation, ^{15}K (with the capital letter denoting an equilibrium isotope effect) was measured as 0.23±.01%.[22] With a 0.23% isotope effect for a full negative charge on the phenolate, does the ^{15}k for the dianion, at 0.34%, suggest more than a full charge on the leaving group? The explanation for the experimental result that exceeds the apparent upper bound is that the proximity of the leaving group to the negatively charged metaphosphate-like center causes an induced polarization of the leaving group, forcing more negative charge onto the end farthest away from the phosphorus and enhancing the effect of the ^{15}N isotopic substitution. Another complication in the quantification of the size of the charge is the fact that the O–H bond that is involved in the deprotonation reaction is very different from the P–O bond involved in phosphoryl cleavage due to the differences in electronegativity of phosphorus and hydrogen. This makes the neutral states electronically different and influences the magnitude of the isotope effects involved in going from neutral to charged states. Therefore, the most quantitative evaluation that can be made of the amount of charge on the leaving group is to say that it is virtually a complete negative charge.

The interpretation of the $^{18}k_{bridge}$ result is that the phosphorus-oxygen bond is significantly weakened in the transition state. Again, the goal is to quantify how much the bond is weakened, perhaps to provide a percentage of the bond character that remains. Results from Brønsted plots and other experimental studies suggest that in the dianion,

cleavage of this bond is essentially complete.[23] Thus the isotope effect reported here may represent the upper bound. For comparison, the ^{18}O equilibrium isotope effect on deprotonation is 1.5%. This effect results from the cleavage of a bond to a hydrogen, which should be weaker than the phosphorus-oxygen bond that is broken in the dianion. Therefore, it is reasonable that the dianion $^{18}k_{bridge}$ is slightly higher. The 2.3% obtained with the dianion may be suppressed slightly below a theoretical maximum due to the formation of the same quinonoid form that is responsible for the ^{15}N effects. In this resonance form, the order of the bond to the carbon increases, which compensates for the breaking of the P–O bond. Since this compensating effect is present in all of the isotope effects experiments done with the nitrophenol leaving group, the $^{18}k_{bridge}$ obtained with the dianion is a practical upper limit, and represents nearly complete bond cleavage.

The $^{18}k_{nonbridge}$ result shows an inverse isotope effect; however, when experimental error is taken into account, this isotope effect is essentially zero. In view of the metaphosphate-like phosphorus center in the transition state of the dissociative concerted mechanism, and the classical Lewis diagram visualization of metaphosphate, this isotope effect should be significantly more inverse. Indeed, calculations have shown that the isotope effect should be on the order of -2%.[24] More recent computational work has challenged the classical representation of metaphosphate and suggests that the actual structure is better represented by a hybrid of the resonance structures with a zwitterionic form, with positive charge on the phosphorus, negative charge on the oxygens, and bonds with single-bond character.[25,26] The $^{18}k_{nonbridge}$ results of near zero suggest that this revised representation is more accurate, and that the total bond order to phosphorus may not be conserved in the transition state.[19]

Uncatalyzed Phosphate Monoanion Chemistry. The mechanism for the hydrolysis of the monoanion was examined by many of the same methods that were discussed above for the dianion. In aqueous solution the hydrolysis of the monoanion of

pNPP is 69 times faster than that of the dianion at the same temperature.[9] A Brønsted plot was developed for hydrolysis of phosphoester monoanions and a β_{LG} of -0.27 was calculated.[9] This β_{LG}, which is much smaller than the value for the dianion, applies only to poor leaving groups (phenols with relatively high pK_as). For good leaving groups, with pK_as lower than about 7.4, the dependence on leaving group becomes even smaller. This evidence supports the notion of a concerted proton transfer to the bridge oxygen and bond cleavage, with departure of the leaving group the rate-limiting step. For the poorer leaving groups, the increased dependence of reaction rate on leaving group basicity suggests that the two processes are not synchronous. For the better leaving groups, the rate-limiting step shifts to the proton transfer, and dependence on the leaving group vanishes.

Activation parameters were calculated for the monoanion in aqueous solution in a previous study.[6] The entropy of activation shifts from a small positive number (+3.5 eu) with the dianion to a small negative value (-4.5 eu) with the monoanion, consistent with a shift from a mechanism that is a simple mononuclear dissociation to one that requires the intramolecular impetus of proton transfer. Most of the difference in reaction rate is due to a lower value for $\Delta H^{\ddagger}$ in the monoanion, where it is 25.4 kcal/mol compared to 30.6 kcal/mol for the dianion. This decrease in the bond-breaking energy required is consistent with the protonation of the leaving group, which eases its departure, and the decreased β_{LG} found with the monoanion.

Isotope effects confirm the assertions made above concerning the monoanion mechanism. The measurement of the isotope effects, corrected to 30 °C, found the values reported in Table 1-2. The first characteristic of note is ^{15}k has decreased to near zero. This is consistent with the transfer of a proton to the bridge oxygen. The fact that the isotope effect is not zero lends weight to the argument that proton transfer might lag slightly behind the weakening of the bond to the leaving group. The $^{18}k_{bridge}$ value is also

Table 1-2. Kinetic Isotope Effects, pNPP Monoanion, Aqueous Solution[a]

^{15}k	$^{18}k_{bridge}$	$^{18}k_{nonbridge}$
0.05±.02	1.06±.03	2.24±.05

[a]Data are from Hengge et al.[19] and are expressed as percents.

much lower than it was in the dianion. Three factors influence the magnitude of this isotope effect. The transfer of a proton to the leaving group will produce an inverse effect on the observed isotope effect. Based on other evidence that proton transfer is not complete, the inverse effect will be slightly less than the ^{18}K for protonation, which is -1.5%. The inverse effect due to the change in the order of the C–O bond should be virtually nil for the monoanion, based both on protonation of the leaving group and on the extent of delocalization indicated by ^{15}k. If the dianion result is a maximum observable isotope effect and it is multiplied by the equilibrium effect on protonation, the resultant is 0.8%, a reasonable fit for the observed value with the monoanion. Since the monoanion does not involve the inverse mitigating effect of the C–O bond, the 0.8% value is a lower bound. The qualitative result is that this isotope effect indicates that the bond to the leaving group is largely broken in the transition state.

The nonbridge isotope effect, $^{18}k_{nonbridge}$, is large and normal. If there is little change in bond order, as discussed with the dianion, then this isotope effect is primarily the result of the breaking of an O–H bond. For comparison, ^{18}O equilibrium isotope effects for deprotonation of glycerol-3-phosphate and dihydrogen phosphate monoanions are 1.4% and 1.5% at 67 °C and 65 °C, respectively.[27] Normal isotope effects are also observed with phosphorus diesters and triesters in nonenzymatic reactions, and these have been interpreted as indicating more associative transition states.[28] However, in the case of the monoester monoanion, there is no shift toward a more associative transition state; the normal isotope effect is purely the result of proton transfer.

Effects of Solvation on the Phosphoryl Transfer Mechanism. The nature of the mechanism of phosphate ester hydrolysis in aqueous solution is thus well understood. A considerable amount of attention has been devoted to gaining a similar understanding of the catalytic mechanisms, where rate enhancements of 10^6 to 10^{11}-fold are common. Of particular interest is whether the mechanistic pathways and transition states involved in the enzymatic reactions differ from the uncatalyzed reactions in solution. One approach has been to look at the contribution of the microenvironment of the active site as a possible source of catalytic efficiency. This interest stems from the general observation that enzymatic substrates are essentially desolvated as they are incorporated into the active sites of enzymes. This process of desolvation in living systems involves stripping solvating water molecules away from the substrate, and substituting the fixed dipoles and hydrophobic zones of a protein surface. It is possible to view the transfer from aqueous solution to an aprotic solvent, or a solvent capable of only weak hydrogen bonding, as an approximation of this process. There have been many instances noted of drastic rate enhancements for reactions when they are transferred from water to organic solvents.[19,29,30] Thus, the study of solvent effects on the reaction of phosphate monoesters is believed to be one means of examining microenvironmental effects that relate to enzymatic catalysis.

Several effects have been noted to arise in the aqueous reactions of phosphate monoesters from the addition of cosolvents, or from the reaction in anhydrous solvents that can serve as phosphoryl acceptors. Abell and Kirby found that added DMSO or HMPA accelerated the aqueous hydrolysis of pNPP dianion by up to 10^7-fold, by effects that were attributed to decreased hydrogen bonding to the anionic nonbridge oxygens.[30] Knowles et al. noted that the stereochemical outcome of phosphoryl transfer from pNPP to solvent changed from inversion in aqueous solution to racemization in *tert*-butyl alcohol.[17] This is very significant mechanistically, since it implies the presence of a

diffusable metaphosphate intermediate, which would further indicate a change to a two step mechanism. As a side note to the stereochemical results, this group also found significant rate enhancement in the alcohol, when compared to the aqueous rate. In an attempt to identify transition state changes that induced the observed rate enhancements, the isotope effects for the solvolysis of pNPP in *tert*-butyl alcohol were measured.[19] The results were found to be very close to those for the aqueous dianion, shown in Table 1-1. Thus, the transition states for the two reactions were found to be very similar, and little was revealed about the mechanistic reasons for the observed change in rate. More details about the specific causes of these rate enhancements could be elucidated through further solvent effects studies. For example, determination of the activation parameters in nonaqueous solvent would provide an indication as to whether entropic or enthalpic effects were the force behind rate changes. A study of the energy of solvation could identify whether the effects of nonaqueous solvent are attributed to ground state or transition state energy changes. Computational studies have indicated that solvation may be a major factor in the thermodynamics of phosphoryl transfers,[31] but experimental evidence would provide welcome confirmation of this.

Fundamental Studies on Catalytic Mechanisms. As well as indirect investigation of the enzymatic reaction through modeling active site desolvation with non-aqueous solvents, phosphoryl transfer in enzymatic systems has been the subject of much investigation. Over a hundred phosphatase enzymes are currently known and there are likely many more. A recent review includes a classification system based on substrate specificity that places known phosphatases into three groups: nonspecific phosphatases which catalyze a wide variety of substrates, phosphoprotein phosphatases which accept phosphorylated proteins or peptides, and small molecule specific phosphatases which hydrolyze either a specific small molecule or structurally related molecules.[32] The second group includes three subgroups, one responsible for hydrolyzing proteins phosphorylated

on tyrosine (PTPases), one specific for proteins phosphorylated on serine or threonine, and one subgroup that can accept either of the above classes of substrates. The PTPases and dual-specificity phosphatases have a conserved cysteine residue which serves as the nucleophile, while the serine/threonine phosphatases have an active site which centers on two metal ions. There is little conserved structure across the entire phosphatase family, but all of the phosphatases do have some kind of positive charge at the active site. This has led to investigation of the potential roles for positive charge in catalysis.

One obvious suggestion for the role of positive charge is the stabilization of the negative charges on the phosphorus oxyanions. Since the driving force behind the uncatalyzed aqueous hydrolysis of phosphate esters is the donation of negative charge from these oxygens to the leaving group, any stabilization of negative charge by the positive active site could force the mechanism to shift to a different critical path. The hydrolysis of alkyl phosphorus triesters, where negative charge is not donated to the leaving group, has been shown to proceed by an associative mechanism.[28] Therefore, it can be postulated that a similar effect caused by strong interactions of the oxyanions with positive metal ions could cause the enzymatic reaction of monoesters to be associative. A series of experiments with cobalt complexes of pNPP, measuring the extent of interaction by isotope effects and other methods, showed strong interactions between the phosphoryl oxygens and cobalt.[33] However, the isotope effects results were consistent with a concerted reaction mechanism. While there was some associative character, it was much less than that observed with alkyl triesters.[34] These results imply that metal complexation alone in a phosphatase enzyme is not likely to cause a shift to a truly associative mechanism.

If the metal ions do not cause a shift to a more associative transition state, then what can their role be? In a dissociative transition state, the negative charge shifts from the oxyanions on the phosphate to the leaving group, where it may become more

dispersed. To achieve stabilization of the transition state in preference to the ground state, the enzyme would have to destabilize charge on the nonbridge oxygens. This is intuitively counter to the finding that positive charge in the transition state is common to all phosphatases, where the substrate always bears negative charge. Further examination of the role of metal ions included solution studies which compared β_{NUC} in the presence of metals to that in their absence. It was found that the presence of metals often had a catalytic effect on rate, but did so with no detectable increase in β_{NUC}.[35,36] The results suggested to these investigators that the interactions of metal ions with the nonbridge oxygens were actually anticatalytic and that any rate enhancements were due to interaction of the metal ions with the leaving groups. This leaves the scissile ester oxygen of the leaving group as the likely site for interactions that could stabilize the dissociative transition state.

Another means by which the positively charged centers in an active site could catalyze phosphoryl transfer is by complexation with a nucleophile to facilitate its deprotonation and render it more nucleophilic. In a study of the hydrolysis of phosphorylated pyridines by $Mg(OH)^+$, a rate enhancement of 10^4 was attributed to the greater nucleophilicity of the metal bound hydroxide relative to that of water.[37] A further rate enhancement of 10^2 was attributed to the induced intramoleculearity from the interaction of the metal ion with both the hydroxide nucleophile and the nonbridge oxygens in the transition state. Thus there is evidence that the interaction of metal ions with nonbridge oxygens can be anticatalytic in that it stabilizes the ground state, and catalytic in the stabilization of transition state.

Given the discussion above, there are two apparent means by which positive charge centers, such as metal ions or positively charged amino acid side chains, could affect phosphoryl transfer transition states. One is by stabilizing the negative charge on the leaving group, which would be equivalent to lowering its pK_a. The other would be by

lowering the pK_a of the nucleophile. When one considers the β_{LG} and β_{NUC} from Brønsted slopes, it is apparent that any impact the metal ions have on the leaving group stability will have far more effect on reaction rate than would be produced by a similar change in the efficiency of the nucleophile.

It might also be postulated that stabilization afforded to the nonbridge oxygens is more effective in the planar configuration shown in Figure 1-3 for the associative intermediate or the concerted transition state, than it is in the tetrahedral transition state. This would provide for the intuitively pleasing stabilization of the oxyanions by positive charge and provide a rationalization for transition state being stabilized more than ground state. However, it has been shown[33,38] that even in the dissociative transition state the phosphate substrate does not expand significantly as it goes from ground state to transition state. The nucleophile and the leaving group do not need to move during the reaction and it may be that only the phosphorus undergoes significant translation. There may be little or no movement of the nonbridge oxygens. In an enzymatic process, the reaction coordinate is compressed,[39] making any differential stabilization of ground and transition states through the nonbridge oxygens even more unlikely as a source of catalytic advantage. However, little change in bond length is required for a significant change in bond order, and it may be small conformational changes of the enzyme itself during catalysis that provide for differential stabilization of ground state and transition state.

Another role for positive charge in catalysis is in general acid catalysis, which could occur in either a dissociative or associative transition state. This has already been observed in the difference between reaction rates of the dianion and monoanion of phosphate monoesters, where the intramolecular protonation of the leaving group produces a 69-fold increase in reaction rate.[9] In a dissociative transition state, where the leaving group is nearly completely ionized, proton transfer from a residue activated by

interaction with positively charged centers in the active site should be an energetically favored process. Additionally, protonation of the leaving group will reduce its nucleophilicity, thereby preventing any reversal of the reaction and favoring the transfer of the phosphoryl group. Due to the more limited role of the nucleophile, general base catalysis to activate a nucleophile will provide less rate enhancement. If the general base does not activate the nucleophile for attack, the role of a general base might even be limited to deprotonation of the initial zwitterionic product. While not affecting the transition state, this could tip equilibrium in favor of product formation by preventing a back reaction. This role can be mediated by solvent in aqueous solution, but might become a necessary part of the enzymatic process, where the solvent does not play an active part.

Enzyme Specific Background Information.

(a) General. This research focused on the elucidation of the mechanisms of just two of the phosphatase enzymes, though the two selected are representative of larger groups of enzymes. The two enzymes selected are the PTPase from *Yersinia* (YOP51), and the serine/threonine phosphatase from bacteriophage lambda (λPPase). The YOP51 is an important virulent determinant in the bubonic plague, and is believed to function by dephosphorylating host proteins, thereby disabling the immune system.[40] YOP51 is one of the most active phosphatases known with a rate enhancement of greater than 10^{11} (pNPP substrate, wild type enzyme at pH 5.2, versus uncatalyzed reaction in water)[41] and has been well characterized through x-ray crystallography and kinetic studies. In contrast to the *Yersinia* phosphatase, λPPase is not as well characterized, though crystal structures have been published for other members of the serine/threonine family. The λPPase is classified as a serine/threonine phosphatase based on sequence comparison[42] and kinetic and spectroscopic characterizations[43-45] and is known to have a two-metal ion center. Insights gained into the mechanisms by which these two enzymes function are

believed to generalize to others of their families, though sequence homology is fairly low. For comparison, some of the features of these enzymes are compared to the alkaline phosphatase (AP), a ubiquitous and extremely promiscuous nonspecific phosphatase, which has also been heavily studied.

In the discussion of enzymes and the roles of critical residues, there is a system of abbreviations used by biochemists to refer to specific amino acids in the protein. Amino acids have both a common three-letter abbreviation, which is usually fairly easy to interpret, and a single-letter designation, which is not as easy. Residues in a protein are identified by their sequence number, which provides a means of identifying their location in the secondary structure of the protein. Usually, the sequence number is used with the three-letter abbreviation, as in Arg409, which is an arginine located at residue number 409 in *Yersinia* PTPase. When a residue is mutated, it is common to give both the original amino acid and the replacement, along with the residue number, but in this case the one-letter designation is used. An example is R409K, where the R designates the original arginine, and K designates the replacement lysine, at position 409. In this text, single residues will be referred to with the three-letter abbreviation and position number, while mutations will be designated as shown above. The following single letter designations will be seen in the remainder of this document: A-alanine, F-phenylalanine, P-proline, W-tryptophan, D-aspartic acid, E-glutamic acid, N-asparagine, Q-glutamine, H-histidine, K-lysine, and R-arginine.

(b) Protein-Tyrosine Phosphatase from *Yersinia*. *Yersinia* phosphatase was first identified as possessing protein tyrosine activity in 1990, in a study which also verified the cysteine nucleophile at Cys403 through site-directed mutagenesis.[46] Site-directed mutagenesis, where one residue in a protein is selectively replaced with a different amino acid, has become one of the primary tools in identification of the roles of residues in the mechanisms of enzymatic action. In order to ensure that the

mutagenesis does not have an impact on the secondary structure of the protein, mutated enzymes are purified and tested for resemblance to the wild-type enzyme through chromatography, UV/Vis absorption spectra, and substrate binding constant (K_m) assay.[47]   For YOP51, further work on identifying the key residues and their roles began with a pH-rate profile of the wild type enzyme, shown in Figure 1-10.[41] The general shape of this curve is typical for many PTPases and suggests that there is both a general acid and a general base involved in the catalytic pathway. By selecting the seven acidic residues in the catalytic domain and performing conservative mutations that eliminated the acidic character, the researchers here hoped to identify the residues responsible for the catalysis. While some residues were found to have little effect on k_{cat}, two were found which drastically affected the reaction rate. Overlaid on the pH rate profile at Figure 1-10 are the profiles for three mutants:

A. E290Q - mutation of glutamate to glutamine
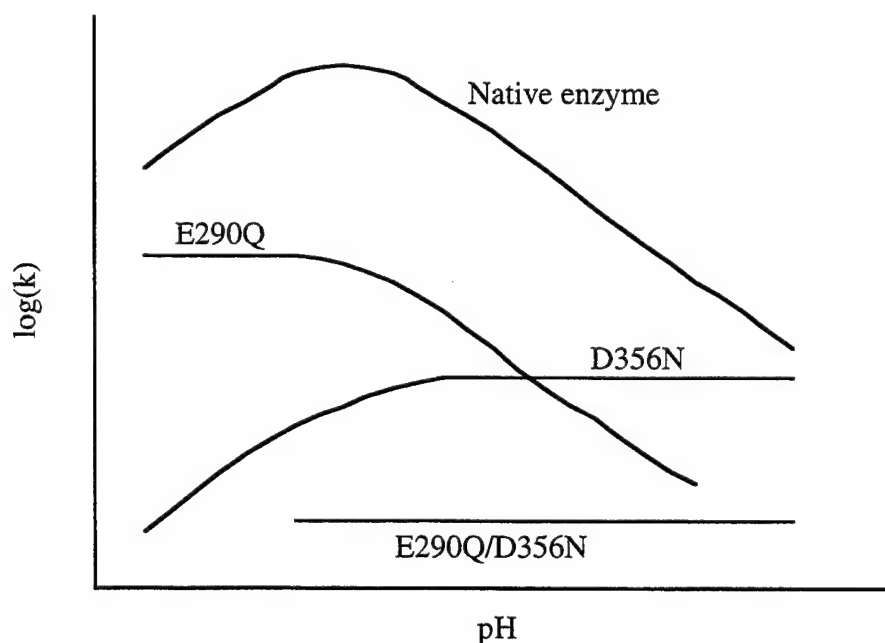
Figure 1-10. Simplification of pH/rate profile for PTPase from *Yersinia* showing native enzyme and mutant activities. Adapted from Zhang et al.[41]

B. D356N - mutation of aspartate to asparagine

C. E290Q/D356N - double mutation including both of the above

Since E290Q eliminates the pH impact on the acidic arm of the wild type profile, the general acid is still competent, but the general base is impaired. Similarly, the D356N mutant eliminates the pH impact on the basic arm of the wild type profile, indicating that the general base still functions. Thus, a general acid role was postulated for the aspartic acid Asp356, and a general base role for glutamic acid Glu290.[41] Additional mutagenesis experiments identified Arg409 as a residue whose absence caused a 10^4 reduction in k_{cat} for the enzyme. Based on inhibition studies and the kinetic results, a role in both substrate binding and transition state stabilization was postulated for this residue.[48] It has also been proposed that the hydroxyl on a conserved serine/threonine residue in PTPases is responsible for hydrogen bonding to the cysteine thiol. This residue (Thr410 in YOP51) could serve to either stabilize the developing negative charge as the enzyme-phosphate intermediate is cleaved, or could merely act to position the complex for nucleophilic attack by water.[49]

Kinetic studies with leaving groups less basic than *p*-nitrophenol found that the basic arm of the pH-rate profile is substrate dependent, with a β_{LG} of 0.16.[50] This suggests that the general acid identified earlier is involved with protonation of the leaving group. Labeling experiments with ^{18}O identified oxygen exchange into organic phosphate in the presence of enzyme, leading to the postulation of a mechanism that proceeds stepwise through reversible substrate binding, phosphorylization of the enzyme, dephosphorylization, and dissociation of inorganic phosphate, as shown in Figure 1-11.

With the elucidation of a crystal structure of the *Yersinia* enzyme, both without a bound ligand and with tungstate, sulfate, or nitrate in the active site, more details of the mechanics of the enzymatic catalysis began to be worked out.[52-54] The nucleophilic cysteine was found to reside at the center of a loop with the potential to bind the

$$E + S \underset{k_{-1}}{\overset{k_1}{\rightleftharpoons}} E \bullet S \underset{k_{-2}}{\overset{k_2}{\rightleftharpoons}} E* \bullet S \overset{k_3}{\longrightarrow} E - P_i \underset{k_{-4}}{\overset{k_4}{\rightleftharpoons}} E + P_i$$

$$ROH$$
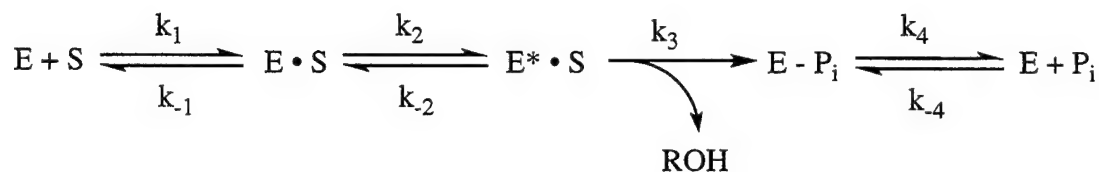
Figure 1-11. Generalized scheme of the catalytic mechanism for YOP51.[51]

phosphate through a network of hydrogen bonds, many of which were with the backbone amide nitrogens. This loop was found to be a general feature among PTPases and was said to constitute a $Cys(X)_5Arg$ active site motif essential for PTPase activity.[48] One very recent study used Poisson-Boltzmann methodology to do a computational analysis of the microdipoles created by the backbone and side chains of this loop, specifically analyzing their impact on the pK_a of the cysteine. The conclusion was that it was the backbone that contributed the stabilization which lowers the pK_a, with only very minor contributions by any side chains.[55]

An unanticipated finding was that the loop containing the putative general acid, Asp356, underwent a conformational change on substrate binding. The movement of the loop (termed the WpD loop for the conserved tryptophan-proline-aspartate sequence) served to trap the oxyanion in the active site and to swing Asp356 closer to the active site by six to eight angstroms.[52] With substrate bound, the orientation of the cysteine nucleophile, the tungsten of the oxyanion, and the oxygen which represents the scissile ester bond of a phosphate monoester were all in-line, consistent with a concerted or with an associative nucleophilic displacement reaction.

The YOP51 enzymatic reaction was examined by isotope effects to provide more information on the nature of the transition state.[51] With p-nitrophenol as the substrate, isotope effects were measured with YOP51 as described above for the solution reactions, and kinetic isotope effects with PTP1, an animal protein tyrosine phosphatase, were measured for comparison. The isotope effects are shown in Table 1-3. These are effects on V/K, and are sensitive up to and including the first irreversible step, the release of

Table 1-3. Kinetic Isotope Effects, YOP51 and PTP1[a]

	^{15}k	$^{18}k_{bridge}$	$^{18}k_{nonbridge}$
YOP51, pH 5.0	-0.01±.03	1.52±.06	-0.02±.13
PTP1, pH 5.5	0.01±.02	1.42±.04	-0.19±.15

[a]Data are from Hengge et al.[51] and are expressed as percents.

p-nitrophenol. Enzymatic isotope effects are also sensitive to commitment factors, and if the commitment factors are too large, isotope effects can be completely suppressed.[51] This is illustrated in Equation 7, which relates the actual ^{18}O isotope effect on a single step in the reaction mechanism (k_3, Figure 1-11) and the commitment factor (c_f, Equation 8) to the observed isotope effect.

$$\text{observed } ^{18}\left(V/K\right) = \frac{\left(^{18}k_3 + c_f\right)}{\left(c_f + 1\right)} \tag{7}$$

$$\text{where } c_f = \left(\frac{k_3}{k_{-2}}\right)\left(\frac{1 + k_2}{k_{-1}}\right) \tag{8}$$

A large commitment factor was apparently the case with alkaline phosphatase, where no isotope effects were observed even at pH well off the optimum.[19] The isotope effects with YOP51 wild-type enzyme show that at the pH optimum there is no negative charge delocalized into the leaving group, leading to the conclusion that the general acid is protonating the leaving group in the transition state. The P–O bond is virtually completely broken, given that the $^{18}k_{bridge}$ value is nearly as large as that for the dissociative transition state for the dianion in water. The $^{18}k_{nonbridge}$ effect is small, leading to the conclusion that the phosphate center interacts with the nonbridge oxygens in a manner that creates a metaphosphate-like transition state. The absence of an inverse isotope effect, which

would result from the transfer of an enzymatic proton to one of the non-bridge oxygens, indicates that there is no proton sharing in the binding interaction and that the binding is purely electrostatic in nature. There is no direct indication of the extent of interaction of the nucleophile in the transition state,[51] but the lack of normal isotope effects in this reaction, and the presence of normal isotope effects in the associative solution reactions of diesters and triesters,[28] provides indirect information.

One other study focused on the dynamics of the WpD loop using time resolved fluorescence anisotropy and steady-state UV resonance raman spectroscopies. These techniques allowed tracking of the rotation of the aromatic side chain of Trp354, which is believed to sit at the hinge end of the WpD loop. The loop was found to alternate between the closed and open forms with a rate constant of almost $3 \times 10^8 \ s^{-1}$.[56] In the presence of ligand, the rate of closure did not change, but the rate of opening dropped, so that the enzyme was present primarily in a closed state with the closed state being stabilized by the ligand. The kinetic effects of the selective mutation of this tryptophan were also examined. A role in oxyanion binding was inferred from the impact of these mutations on K_m, and the suggestion was that this residue interacted with Arg409 to position it for binding. More importantly, the kinetic data made it appear that mutation of this residue disabled the general acid, providing confirmation of its critical contribution to the positioning of the general acid.[47]

In an effort to rationalize the problem of how the positive charges and electrophilic groups in the enzyme can differentially stabilize the transition state over the ground state, some work has been performed to examine the possibility that the hydrogen bonding to the phosphate oxyanions changes along the reaction coordinate. A computational study found that as the phosphate went from the tetrahedral ground state to the trigonal transition state, the equatorial oxygens were spatially expanded, shortening the hydrogen bonds to the phosphate binding loop by 0.05 to 0.1 angstroms.[57] This computational

work was verified by a detailed survey of the differences in X-ray structures of bovine PTPase with vanadate bound versus sulfonate or phosphate. The vanadate has a trigonal bipyramidal structure, resembling the transition state, while sulfonate and phosphate are tetrahedral, resembling ground state substrate. In the survey of experimental data, the hydrogen bond distances were shortened by 0.12 to 0.18 angstroms.[58]

It is the position of this lab that the process of moving a substrate from bulk biologic (aqueous) solution to a catalytic active site involves extensive desolvation. The crystal structures that have been solved with substrate analogs in the active site have all included water molecules modeled in, and these molecules are probably real, given their reproducibility in crystals obtained in different labs and under different conditions. However, the number of water molecules involved in this very limited solvation is quite low. A recent, and very ingenious series of experiments allowed mapping of solvent accessibility of the YOP51 enzyme through a combination of deuterium exchange and mass spectroscopy.[59] It was found that the limited solvent access to the active site became even more limited when a substrate analog was bound. The closing of the WpD loop caused the area around the active site to drastically reduce its solvent accessibility, lending even more weight to the argument that substrate binding is the equivalent of desolvation.

(c) Serine/Threonine Protein Phosphatase Lambda. The PTPase family of enzymes discussed above all form a phosphoryl-cysteine intermediate en route to dephosphorylation of the substrate. Other phosphatases, including the non-specific acid and alkaline phosphatases, also form either phosphoryl-cysteine or phosphoryl-histidine intermediates. However, for the serine/threonine protein phosphatase (Ser/ThrPPase) group, the preponderance of evidence indicates that that no such intermediate is formed and that these enzymes catalyze the direct transfer of the phosphoryl group to water.[60] When considering the comparison of YOP51 and λPPase, the most striking difference in

the two enzymes is the change from a dependence on amino acid side chains for active site positive charge to the presence of two multiply charged metal ions. Based on this tremendous difference, there is widespread interest in investigations of the Ser/ThrPPase group for the purpose of clarifying the roles of the metal ions in catalysis. In the Ser/ThrPPase group are several phosphatases that are essential for a number of signal transduction pathways in eukaryotic cells, such as PP1, PP2A, and calcineurin.[61] These enzymes contain the consensus motif of this family, $DXH(X)_nGDXXD(X)_nGNHD/E$, which has been hypothesized to provide a scaffold for a binuclear metal site.[62,42] In at least one enzyme, calcineurin, this site is known to be a $Fe^{3+} - Zn^{2+}$ center. Although the role of the metal center is not clear, a similar site in the related purple acid phosphatases has been shown to be essential for catalytic activity.[63,64] Crystallographic data have shown that inhibitors and substrate analogs coordinate both metal ions in the PP1 enzyme.[65]

As a class of enzymes, the Ser/ThrPPases are less well understood than the PTPases. The λPPase has proven difficult to characterize, though it has been shown to belong to the Ser/ThrPPase group of enzymes based on substrate specificity and sequence comparison.[42] Electron paramagnetic resonance experiments with λPPase confirmed the accommodation of a binuclear metal center in the enzyme, and site directed mutagenesis of a histidine (His76) which is conserved in other Ser/ThrPPases indicated a perturbation of the ligand environment.[43] Since it was also observed that this mutagenesis did not disturb the assembly of the binuclear metal site, it was inferred that the interaction of the histidine with the metals is not direct, but is more likely through a hydrogen bond to a metal-bound water ligand. Support for this proposition is drawn from crystallographic data for related enzymes, where the histidine is five angstroms from the metal ions.[65-67] The mutagenesis of His76 did result in a reduction in k_{cat} of approximately 10^3 with two different phenyl phosphate substrates, but the K_m was not affected, and a similar result

was seen with calcineurin. The proposed roles for His76 include an active site nucleophile, a participant in the orientation of substrate for nucleophilic attack, assistance in leaving group protonation, or a role in general base catalysis by deprotonation of a metal-coordinated solvent molecule.[43] Mertz et al. use a process of elimination to narrow the possibilities for a role for His76: Based on evidence with related enzymes that the phosphoryl group is transferred directly to solvent the nucleophilic role is rejected, the substrate binding role is rejected based on K_m data, and the leaving group protonation role is eliminated based on the lack of dependence of k_{cat} on leaving group when the histidine is mutated out.[43] This leaves the general base as the most likely hypothesis for His76.

Based on these kinetic and spectroscopic similarities, the active site of λPPase is believed to be very similar to the active site in calcineurin, as shown in Figure 1-12. This figure illustrates a proposed mechanism for transition state stabilization consistent with the evidence discussed above, where the phosphoryl group is coordinated in a bridging position between the two metals and one metal ion participates in the neutralization of the leaving group negative charge.[68,69]

Isotope effects have previously been measured with calcineurin, but not with
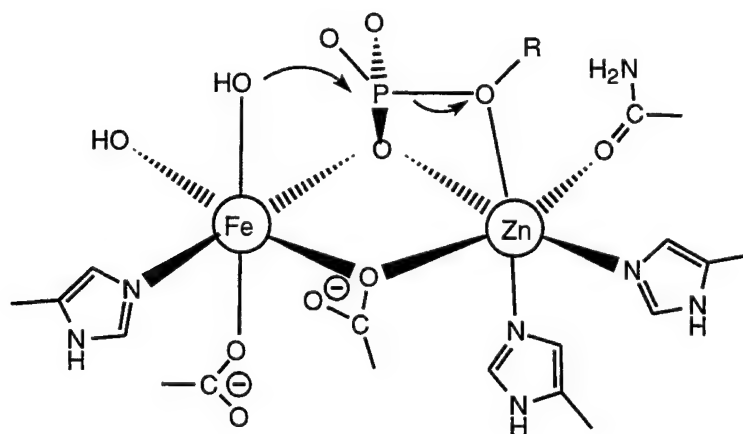
Figure 1-12. A proposed schematic of the active site of the lambda Ser/Thr protein phosphatase. Shown with the phosphoryl group bridging the metals and the zinc ion coordinating to the leaving group.[68,69]

λPPase, allowing some potential inferences to be drawn for the mechanism in λPPase. The isotope effects were measured in the same manner as explained above with YOP51, using the same labeled substrates. The results of these isotope effects experiments are shown in Table 1-4. Interpretation of the isotope effects requires consideration of the generalized scheme of the reaction, shown in Figure 1-13. The isotope effects are sensitive up to the first irreversible step, which here is k_3 (phosphoryl transfer), and the effects observed are the effects on V/K. The absence of a large inverse isotope effect for the nonbridge oxygen atoms is taken as supporting the kinetic evidence that the substrate for the enzymatic reaction is the dianion of pNPP. It is uncertain as to the existence and magnitude of an isotope effect on the binding of pNPP to the metal ions, this could have an impact on the degree to which nonbridge isotope effects were observed. The increase of the $^{18}(V/K)_{bridge}$ as pH changed from 7.0 to 8.5 was interpreted as an observation of the reduction in commitment factor as the pH was moved off of the optimum value, an

Table 1-4. Kinetic Isotope Effects, Calcineurin[a]

	^{15}k	$^{18}k_{bridge}$	$^{18}k_{nonbridge}$
Calcineurin, pH 7	0.06±.05	0.72±.11	
Calcineurin, pH 8.5	0.14±.01	1.15±.12	-0.58±.07

[a]Data are from Hengge and Martin[60] and are expressed as percents.
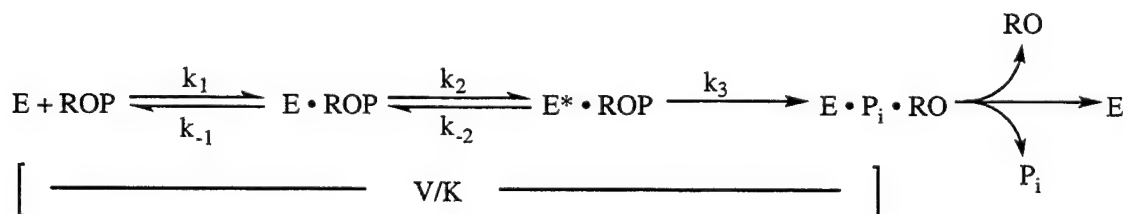
Figure 1-13. Proposed general scheme for Ser/Thr protein phosphatases. The kinetic isotope effect on V/K is sensitive up to the first irreversible step, k_3.[60]

interpretation which is supported by a proportional change in $^{15}(V/K)$. Therefore, this also indicates that chemistry is not completely rate limiting at the pH optimum, and it is possible that the full isotope effects are not expressed even at pH 8.5. The overall picture of the transition state is one where the phosphorus oxygen bond cleavage is advanced, and where proton transfer from enzyme to the leaving group lags behind this bond cleavage. The inverse $^{18}(V/K)_{nonbridge}$ results are related to isotope effects found with metals known to complex strongly to phosphates, hence they indicate coordination between the phosphoryl oxygens and the binuclear metal center. The transition state was not found to have significant associative character.[60]

To what extent are these isotope effects with calcineurin relevant to the interpretation of the λPPase mechanism, and what kind of patterns can be generalized across the entire Ser/ThrPPase group? These questions could be answered by isotope effects studies with λPPase and the His76 mutant.

Sulfuryl Transfer and Its Resemblance to Phosphoryl Transfer. The sections above dealing with enzymatic phosphoryl transfer established the great interest that exists in these systems due to their relevance to many key biochemical pathways. This discussion began with the motivation for choosing phosphates, emphasizing the ability of the phosphate center to form covalent bonds linking two chemical entities while still maintaining ionic charge. Sulfates have also been found in many biochemical systems, with sulfation and desulfation serving as a means to activate and deactivate signal transduction systems. One of the first observations of the importance of sulfuryl transfer in human systems was a classic experiment by Baumann [70] in which he administered phenol to a patient and then showed that it was excreted as phenyl sulfate. Subsequently it has been found that the metabolism of many drugs culminates in the excretion of sulfated forms and this process is the subject of a large body of medical literature.[71] A specific topic of recent interest has been in the regulation of steroid

hormone synthesis through the sulfation induced activation of cholesterol in mitochondria.[72] It has also been noted that in plasma steroids, dehydroepiandrosterone sulfate is second only to cholesterol in abundance and estrone sulfate is the most abundant of the estrogens.[73] Since sulfur lacks the ability to form two covalent bonds and maintain charge, and since sulfate diesters are extremely labile compounds, the biochemically significant species are monoesters. For the purposes of potential biochemical applications, there is value to learning what we can concerning the solution chemistry of sulfate monoesters.

Figure 1-14 shows the sulfate ester linkage and the degrees of protonation available to sulfate monoesters. As in phosphoryl transfer, transfer of the sulfuryl (SO_3^-) group to an acceptor group is termed sulfuryl transfer, when the acceptor is water the reaction is hydrolysis. The literature on sulfuryl transfer is rich with proposed mechanistic similarities between sulfuryl and phosphoryl transfer,[74-78] and the case has been made for an evolutionary link between phosphatase and sulfatase enzymes.[79] However, compared to the volume of research on other hydrolytic mechanisms, such as
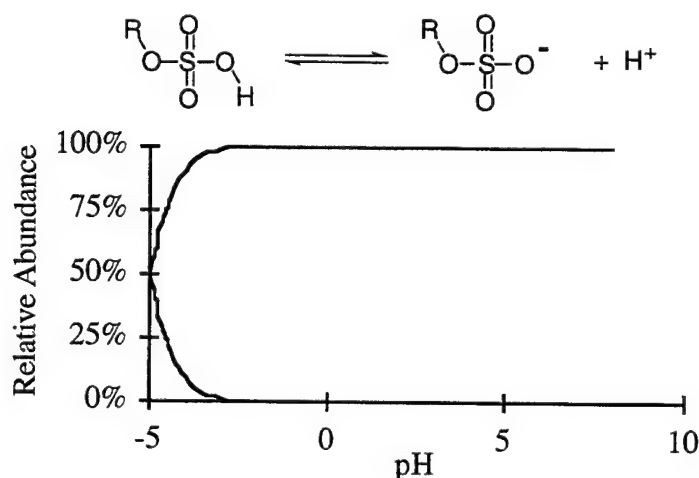
Figure 1-14. Sulfate monoester deprotonation. The generic reaction is shown along with the relationship between the abundance of the species and pH for the pNPS monoester.

phosphate ester hydrolysis, carboxyl ester hydrolysis and amide hydrolysis, comparatively little work has been done on sulfate esters.

Sulfate monoesters can exist in one of two protonation states, namely the anion or the neutral species, as shown in Figure 1-14. At readily attainable pH, the predominant species is the anion, a species which most closely resembles the phosphate dianion, as both lack the intramolecular availability of the proton to facilitate leaving group departure. There is general agreement that the phosphate monoester dianion is hydrolyzed through a dissociative transition state with little nucleophilic involvement.[69] In contrast the uncertainty surrounding the sulfate monoester hydrolysis mechanism is demonstrated by the description of this mechanism in a recent review as "predominantly dissociative in nature with some associative character."[80]

Similarities between sulfate and phosphate monoester hydrolysis have been reported in basic kinetic studies. Sulfate monoester hydrolysis exhibited a pH/rate profile with a plateau at neutral values and acid and base catalyzed rates at pH extremes.[74] Evaluation of linear free energy relationships found that β_{LG} (-1.2) and β_{NUC} (-0.20) were very close to the values for reactions of phosphate monoester dianions.[74,76] The remarkable similarity between the parameters led to the inference that the hydrolysis of the sulfate monoester proceeds through a highly dissociative transition state where the sulfate center resembles sulfur trioxide.[75,81] Such a transition state would resemble that for phosphoryl transfer as shown in Figure 1-3C. However, the validity of interpreting Brønsted parameters in terms of transition state bonding is not universally accepted, and the possibility of a fully dissociative mechanism proceeding by way of a free SO_3 intermediate has been ruled out by stereochemical studies where a sulfate made chiral with oxygen isotopes formed an exclusively inverted product with an alcohol in carbon tetrachloride.[82,83]

The one anomaly in the pattern of similarities between the sulfuryl and phosphoryl

transfer reactions is in the activation parameters for the aqueous reactions. While the pNPP dianion had a $\Delta H^{\ddagger}$ of 30.6 kcal/mol and a $\Delta S^{\ddagger}$ of +3.5 eu at 39 °C,[6] the p-nitrophenyl sulfate (pNPS) monoanion had a $\Delta H^{\ddagger}$ of 24.6 kcal/mol and $\Delta S^{\ddagger}$ of -18.5 eu at 35 °C.[74] The entropies of activation suggest a difference in the molecularity of the two reactions. The small positive number for pNPP hydrolysis is consistent with the proposed dissociative mechanism, while the large negative number for pNPS could be taken as indication that two molecules must interact to form the transition state. Entropies of activation are often on the order of -20 to -30 eu for reactions that have been shown to be bimolecular, allowing the hypothesis to be forwarded that the relatively modest value for pNPS does not require that the reaction is bimolecular.[84] One suggestion is that the increase in activation entropy may be due to increased involvement of solvent in stabilization of the transition state. The issue of solvation in this reaction is one that could provide further information on the extent to which the mechanism resembles phosphoryl transfer. In phosphoryl transfer the rate of reaction of the dianion is about 10,000-fold faster when transferred from water into $tert$-butanol,[19] while for sulfuryl transfer the effects of solvent on rate are mixed.[74,78] Further kinetic studies on the effects of solvent on pNPS solvolysis could allow identification of the source of the difference in activation entropy, relative to phosphoryl transfer. Also with phosphates, the stereochemistry goes from inversion in methanol to racemization in $tert$-butanol inferring the existence of free metaphosphate in the latter case.[14,17] Though one example of a stereochemical experiment with a sulfate monoester in organic solvent was cited above, the possibility of free sulfur trioxide being detected in organic solvent has not been ruled out.

The pH-rate profile for pNPS hydrolysis shows an increase in rate as the proton activity of the solution increases. The pK_a of unsubstituted sulfuric acid is on the order of -3.[2,85] With phosphate, the substitution of the p-nitrophenol group causes a negative shift in pK_a by about two units;[7] assuming a similar effect on the sulfate, the pK_a of

pNPS would be about -5. A plot of percentage of sulfate present in one protonation state versus pH is shown at Figure 1-14. It is obvious that at any pH attainable in aqueous solution it is not possible to have a significant proportion of the sulfate present as the neutral species. Yet the hydrolysis of the protonated sulfate proceeds so much faster than the monoanion that even at pH 0 significant differences are seen in the kinetics of the reaction. A reduced β_{LG} (-0.22)[76] and a solvent deuterium isotope effect of 2.43[78] led to the proposal that the hydrolysis of the neutral species proceeds by a two-step process, as shown in Figure 1-15. Stereochemical studies which could confirm the existence of free SO_3 have not been performed in acid conditions.

Research Questions to Explore

Uncatalyzed Phosphoryl Transfer. Enzymatic catalysis of phosphoryl transfer confers rate enhancements of up to 10^{11} over uncatalyzed reactions. What are the contributing factors to this tremendous acceleration of these reactions? One perspective on the binding of substrate on an enzymatic active site is that the substrate is desolvated as it is bound. By studying the reactions of pNPP in nonaqueous solvent, we hope to shed light on the effect of going from the bulk aqueous state to the active site, which may better resemble organic solvents, or possibly aqueous/organic solvent mixtures. It has been noted that increasing the concentration of nonaqueous solvents accelerates the hydrolysis of some phosphate monoesters.[30] To what extent can the rate of solvolysis of pNPP be accelerated by transfer into a desolvating media? Are there linear free energy relationships
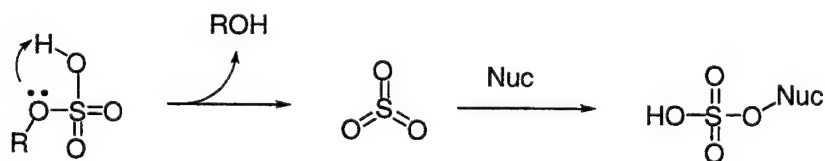
Figure 1-15. Sulfuryl transfer mechanism for neutral sulfate monoester. A two-step mechanism involving a free sulfur trioxide intermediate.

that are expressed in nonaqueous solvent, and if so, what do they indicate about the reaction mechanism? How do the activation parameters in nonaqueous media compare to the aqueous reaction? Rate enhancement infers a reduction in the activation energy for a reaction. In order to reduce activation energy, either the ground state must be destabilized or the transition state must be stabilized, or possibly both could occur. How can the thermodynamics of the transition and ground states be assessed? Is the ground state or transition state perturbed? Is the transition state significantly altered in nonaqueous solvents? What are the implications of this for the enzymatic reaction?

Uncatalyzed Sulfuryl Transfer. It has been postulated that the mechanism of sulfuryl transfer resembles that of phosphoryl transfer, yet there are unexplained differences in the reported kinetic parameters. Linear free energy relationships suggest nearly identical involvement of nucleophile and leaving group for reactions of the phosphate monoester dianion and the sulfate monoester monoanion, yet activation parameters show a large difference in the entropies of activation, and an adequate explanation of this observation has not yet been forthcoming. Since it is believed that insight can be gained from study of the phosphate in nonaqueous solvent, what can be learned from a similar investigation with pNPS? Is the rate enhanced in nonaqueous solvent? By evaluating the activation parameters in nonaqueous solvent, what can be learned about the cause of any change in rate seen? Can a substrate be synthesized with appropriate labels to allow the evaluation of kinetic isotope effects? What is revealed by the isotope effects? Based on kinetic changes under acid conditions, there is believed to be a mechanistic shift, even though the neutral species is present in only a very small minority. Do isotope effects reveal this mechanistic shift? What are the limits of reaction conditions under which isotope effects can be evaluated, and what do kinetic isotope effects at this limit tell us? Given all of the information obtained concerning sulfate monoester hydrolysis, what conclusions can be drawn reference the resemblance between

phosphate monoester hydrolysis and sulfate monoester hydrolysis?

Catalyzed Phosphoryl Transfer.

(a) *Yersinia* **Phosphatase.** The structure of YOP51 PTPase has been solved with and without bound substrate. Key residues have been identified and their roles probed with kinetic studies and spectroscopic techniques leading to some assumptions about the mechanistic details of the phosphoryl transfer process. What additional evidence can the use of isotope effects provide? Is it possible to measure isotope effects with mutated enzymes that have lost a major portion of their catalytic activity and are more susceptible to denaturation than the wild type? What are the limits of the solution conditions under which enzymatic isotope effects can be measured? Are there residues that have catalytic functions that have not yet been identified? Do isotope effects results confirm the suspected roles of the key players? Is the overall picture of the transition state different from the uncatalyzed reaction, and could this difference account for the catalytic rate enhancements observed? If it is not different, what is producing the catalytic effect?

(b) Lambda Ser/Thr PPase. While the three dimensional structure of lambda Ser/Thr PPase has not been solved, the structures of some closely related proteins with significant sequence homology are known. This allows some inferences to be made concerning the structure and function of this binuclear metal center Ser/Thr protein phosphatase. It has been assumed that His76 plays a key role in the catalytic mechanism of this enzyme, but it is not certain what role this is. What can be learned from further kinetic studies of this enzyme and its mutant? There is some uncertainty as to the role of metals in the activity of this enzyme. How is the activity of the enzyme affected by different metals? What are the effects of metals in solution on the isotope effects? Is there a measurable isotope effect on metal binding to the phosphate? Other binuclear metal center enzymes have yielded no information in isotope effects studies due to the rate-limiting nature of a nonchemical step. Can isotope effects even be measured with this

enzyme or is the rate-limiting step a nonchemical step? Are there conditions where chemistry becomes rate-limiting? How do the isotope effects results compare with those for other phosphatase enzymes?

Organization of Remaining Chapters

The research efforts to answer the questions posed above will be presented as a series of papers, presented here as chapters. The first two following chapters (Chapter 2 and Chapter 3) are primarily experimental procedures, outlining some work which was performed and therefore is documented here, but which did not produce significant results. Chapter 4 describes solvent effect studies of phosphoryl transfer and interprets the results in terms of possible applications to enzymatic phosphoryl transfer. Chapters 5 and 6 cover studies of enzymatic phosphoryl transfer dealing with two very different phosphatase enzymes. The objective of these studies was the elucidation of the role of positive charge in the enzyme active site. Chapter 7 presents the results of an investigation of the extent to which phosphoryl transfer resembles sulfuryl transfer, using some of the solvent effect and kinetic isotope techniques used with phosphates to shed light on the sulfuryl transfer mechanism. Following these chapters, some overall conclusions will be drawn as to the extent to which the questions posed here were answered. The conclusion section will also tie together the catalyzed and uncatalyzed pictures of phosphoryl transfer. Additional experimental data and other materials will be included in the Appendices.

References

(1) Westheimer, F. H. *Science* **1987**, *235*, 1173-1178.

(2) Shriver, D. F.; Atkins, P.; Langford, C. H. *Inorganic Chemistry*, 2nd ed.; W.H. Freeman and Company: New York, 1994.

(3) Compton, J. A. F. *Military Chemical and Biological Agents: Chemical and Toxilogical Properties*; Telford Press: Caldwell, NJ, 1987.

(4)   Guthrie, R. D.; Jencks, W. P. *Acc. Chem. Res.* **1989**, *22*, 343-349.

(5)   Barnard, P. W. C.; Bunton, C. A.; Kellerman, D.; Mhala, M. M.; Silver, B.; Vernon, C. A.; Welch, V. A. *J. Chem. Soc. (B)* **1966**, 227-235.

(6)   Kirby, A. J.; Jencks, W. P. *J. Am. Chem. Soc.* **1965**, *87*, 3209-3216.

(7)   Bourne, N.; Williams, A. *J. Org. Chem.* **1984**, *49*, 1200-1204.

(8)   Hammett, L. P. *J. Am. Chem. Soc.* **1937**, *59*, 96-103.

(9)   Kirby, A. J.; Varvoglis, A. G. *J. Am. Chem. Soc.* **1967**, *89*, 415-423.

(10)   Moore, J. W.; Pearson, R. G. *Kinetics and Mechanism*, 3rd ed.; John Wiley & Sons: New York, 1981.

(11)   Herschlag, D.; Jencks, W. P. *J. Am. Chem. Soc.* **1989**, *111*, 7579-7586.

(12)   Cullis, P. M.; Lowe, G. *J. Chem. Soc., Perkin Trans.* **1981**, *1*, 2317-2321.

(13)   Cullis, P. M.; Lowe, G. *J. Chem Soc., Chem. Commun.* **1978**, 512-514.

(14)   Abbott, S. J.; Jones, S. R.; Weinman, S. A.; Bockhoff, F. M.; McLafferty, F. W.; Knowles, J. R. *J. Am. Chem. Soc.* **1979**, *101*, 4323-4332.

(15)   Cullis, P. M.; Iagrossi, A. *J. Am. Chem. Soc.* **1986**, *108*, 7870-7871.

(16)   Buchwald, S. L.; Friedman, J. M.; Knowles, J. R. *J. Am. Chem. Soc.* **1984**, *106*, 4911-4916.

(17)   Friedman, J. M.; Freeman, S.; Knowles, J. R. *J. Am. Chem. Soc.* **1988**, *110*, 1268-1275.

(18)   Northrop, D. B. In *Isotope Effects on Enzyme-Catalyzed Reactions*; Cleland, W. W., O'Leary, M. H. and Northrop, D. B., Eds.; University Park Press: Baltimore, MD, 1977, p 303.

(19)   Hengge, A. C.; Edens, W. A.; Elsing, H. *J. Am. Chem. Soc.* **1994**, *116*, 5045-5049.

(20)   O'Leary, M. H.; Marlier, J. F. *J. Am. Chem. Soc.* **1979**, *101*, 3300-3306.

(21)   Huskey, W. P. In *Enzyme Mechanism from Isotope Effects*; Cook, P. F. Ed.; CRC Press, Inc.: Boston, 1991, p 49.

(22)   Hengge, A. C.; Cleland, W. W. *J. Am. Chem. Soc.* **1990**, *112*, 7421-7422.

(23)   Benkovic, S. J.; Schray, K. J. In *Transition States of Biochemical Processes*; Gandour, R. D. and Schowen, R. L., Eds.; Plenum Press: New York, 1978, Chapter 13.

(24) Weiss, P. M.; Knight, W. B.; Cleland, W. W. *J. Am. Chem. Soc.* **1986**, *108*, 2761-2762.

(25) Horn, H.; Ahlrichs, R. *J. Am. Chem. Soc.* **1990**, *112*, 2121-2124.

(26) Rajca, A.; Rice, J. E.; Streitweiser Jr., A.; Schaefer, H. F. *J. Am. Chem. Soc.* **1987**, *109*, 4189-4192.

(27) Knight, W. B.; Weiss, P. M.; Cleland, W. W. *J. Am. Chem. Soc.* **1986**, *108*, 2759-2761.

(28) Caldwell, S. R.; Raushel, F. M.; Weiss, P. M.; Cleland, W. W. *Biochem.* **1991**, *30*, 7444-7450.

(29) Ramirez, F.; Maracek, J. F. *Pure Appl. Chem.* **1980**, *52*, 1021.

(30) Abell, K. W. Y.; Kirby, A. J. *Tet. Lett.* **1986**, *27*, 1085-1088.

(31) Hayes, D. M.; Kenyon, G. L.; Kollman, P. A. *J. Am. Chem. Soc.* **1978**, *100*, 4331-4340.

(32) Taylor, W. P.; Widlanski, T. S. *Chem. and Biol.* **1995**, *2*, 713-718.

(33) Jones, J. P.; Weiss, P. M.; Cleland, W. W. *Biochem.* **1991**, *30*, 3634-3639.

(34) Rawlings, J.; Hengge, A. C.; Cleland, W. W. *J. Am. Chem. Soc.* **1997**, *119*, 542-549.

(35) Herschlag, D.; Jencks, W. P. *J. Am. Chem. Soc.* **1987**, *109*, 4665-4674.

(36) Admiraal, S. J.; Herschlag, D. *Chem. & Biol.* **1995**, *2*, 729-739.

(37) Herschlag, D.; Jencks, W. P. *Biochem.* **1990**, *29*, 5172-5179.

(38) Cleland, W. W.; Hengge, A. C. *FASEB Journal* **1995**, *9*, 1585-1594.

(39) Kim, E. E.; Wyckoff, H. W. *J. Mol. Biol.* **1991**, *218*, 449-464.

(40) Bliska, J. B.; Guan, K.; Dixon, J. E.; Falkow, S. *Pro. Natl. Acad. Sci. U.S.A.* **1991**, *88*, 1187-1191.

(41) Zhang, Z. Y.; Wang, Y.; Dixon, J. E. *Pro. Natl. Acad. Sci. U.S.A.* **1994**, *91*, 1624-1627.

(42) Lohse, D. L.; Denu, J. M.; Dixon, J. E. *Structure* **1995**, *3*, 987-990.

(43) Mertz, P.; Yu, L.; Sikkink, R.; Rusnak, F. *J. Biol. Chem.* **1997**, *272*, 21296-21302.

(44) Zhuo, S.; Clemens, J. C.; Stone, R. L.; Dixon, J. E. *J. Biol. Chem.* **1994**, *269*, 26234-26238.

(45) Zhuo, S.; Clemens, J. C.; Hakes, D. J.; Barford, D.; Dixon, J. E. *J. Biol. Chem.* **1993**, *268*, 17754-17761.

(46) Guan, K. L.; Dixon, J. E. *Science* **1990**, *249*, 553-556.

(47) Keng, Y. F.; Wu, L.; Zhang, Z. Y. *Eur. J. Biochem.* **1999**, *259*, 809-814.

(48) Zhang, Z. Y.; Wang, Y.; Wu, L.; Fauman, E. B.; Stuckey, J. A.; Schubert, H. L.; Saper, M. A.; Dixon, J. E. *Biochem.* **1994**, *33*, 15266-15270.

(49) Denu, J. M.; Lohse, D. L.; Vijayalakshmi, J.; Saper, M. A.; Dixon, J. E. *Pro. Natl. Acad. Sci. U.S.A.* **1996**, *93*, 2493-2498.

(50) Zhang, Z. Y.; Malachowski, W. P.; Van Etten, R. L.; Dixon, J. E. *J. Biol. Chem.* **1994**, *269*, 8140-8145.

(51) Hengge, A. C.; Sowa, G. A.; Wu, L.; Zhang, Z.-Y. *Biochem.* **1995**, *34*, 13982-13987.

(52) Stuckey, J. A.; Schubert, H. L.; Fauman, E. B.; Zhang, Z.-Y.; Dixon, J. E.; Saper, M. A. *Nature* **1994**, *370*, 571-575.

(53) Fauman, E. B.; Yuvaniyama, C.; Schubert, H. L.; Stuckey, J. A.; Saper, M. A. *J. Biol. Chem.* **1996**, *271*, 18780-18788.

(54) Schubert, H. L.; Fauman, E. B.; Stuckey, J. A.; Dixon, J. E.; Saper, M. A. *Protein Science* **1995**, *4*, 1904-1913.

(55) Peters, G. H.; Frimurer, T. M.; Olsen, O. H. *Biochem.* **1998**, *37*, 5383-5393.

(56) Juszczak, L. J.; Zhang, Z. Y.; Wu, L.; Gottfried, D. S.; Eads, D. D. *Biochem.* **1997**, *36*, 2227-2236.

(57) Alhambra, C.; Wu, L.; Zhang, Z. Y.; Gao, J. *J. Am. Chem. Soc.* **1998**, *120*, 3858-3866.

(58) Zhang, M.; Zhou, M.; Van Etten, R.L.; Stauffacher, C. V. *Biochem.* **1997**, *36*, 15-23.

(59) Wang, F.; Li, W.; Emmett, M. R.; Hendrikson, C. L.; Marshall, A. G.; Zhang, Y. L.; Wu, L.; Zhang, Z. Y. *Biochem.* **1998**, *37*, 15289-15299.

(60) Hengge, A. C.; Martin, B. L. *Biochem.* **1997**, *36*, 10185-10191.

(61) Cohen, P.; Cohen, P. T. W. *J. Biol. Chem.* **1989**, *264*, 21435-21438.

(62) Koonin, E. V. *Protein Science* **1994**, *3*, 356-358.

(63) Vincent, J. B.; Olivier-Lilley, G. L.; Averill, B. A. *Chem. Rev.* **1990**, *90*, 1447-1467.

(64) Kurtz, D. M. *J. Chem. Rev.* **1990**, *90*, 585-606.

(65) Egloff, M. P.; Cohen, P. T.; Reinemer, P.; Barford, D. *J. Mol. Biol.* **1995**, *254*, 942-959.

(66) Klabunde, T.; Strater, N.; Frolich, R.; Witzel, H.; Krebs, B. *J. Mol. Biol.* **1996**, *259*, 737-748.

(67) Kissinger, C. R.; Parge, H. E.; Knighton, D. R.; Lewis, C. T.; Pelletier, L. A.; Tempczyk, A.; Kalish, V. J.; Tucker, K. D.; Showalter, R. E.; Moomaw, E. W.; Gastinel, L. N.; Habuka, N.; Chen, X.; Maldonado, F.; Barker, J. E.; Bacquet, R.; Villafranca, J. E. *Nature* **1995**, *378*, 641-644.

(68) Rusnak, F.; Yu, L.; Mertz, P. *J. Biol. Inorg. Chem.* **1996**, *1*, 388-396.

(69) Hengge, A. C. In *Comprehensive Biological Catalysis*; Sinnott, M., Ed.; Academic Press: San Diego, CA, 1998; Vol. 1, pp 517-542.

(70) Baumann, E. *Ber. Dtsch. Chem. Ges.* **1876**, *9*, 54-58.

(71) Mulder, G. J. *Sulfation of Drugs and Related Compounds*; CRC Press: Boca Raton, FL, 1981.

(72) Lambeth, J. D.; Xu, X. X. *Endocr. Res.* **1989**, *15*, 85-99.

(73) Anderson, C. J.; Lucas, L. J. H.; Widlanski, T. S. *J. Am. Chem. Soc.* **1995**, *117*, 3889-3890.

(74) Benkovic, S. J.; Benkovic, P. A. *J. Am. Chem. Soc.* **1966**, *88*, 5504-5511.

(75) Bourne, N.; Hopkins, A.; Williams, A. *J. Am. Chem. Soc.* **1985**, *107*, 4327-4331.

(76) Fendler, E. J.; Fendler, J. H. *J. Org. Chem.* **1968**, *33*, 3852-3859.

(77) Kaiser, E. T.; Panar, M.; Westheimer, F. H. *J. Am. Chem. Soc.* **1963**, *85*, 602-607.

(78) Kice, J. L.; Anderson, J. M. *J. Am. Chem. Soc.* **1966**, *88*, 5242-5245.

(79) O'Brien, P. J.; Herschlag, D. *J. Am. Chem. Soc.* **1998**, *120*, 12369-12370.

(80) Leyh, T. S. *Crit. Rev. Biochem. Molec. Biol.* **1993**, *28*, 515-542.

(81) D'Rozario, P.; Smyth, R. L.; Williams, A. *J. Am. Chem. Soc.* **1984**, *106*, 5027-5028.

(82) Chai, C. L. L.; Hepburn, T. W.; Lowe, G. *J. Chem. Soc. Chem. Commun.* **1991**, 1403-1405.

(83) Pross, S.; Shaik, S. S. *New J. Chem.* **1971**, *13*, 427.

(84) Benkovic, S. J.; Hevey, R. C. *J. Am. Chem. Soc.* **1970**, *92*, 4971-4977.

(85) Luder, W. F.; Zuffanti, S. *The Electronic Theory of Acids and Bases*; 2nd ed.; Dover Publications: New York, 1961.

CHAPTER 2

A FACILE HIGH-YIELD SYNTHESIS AND PURIFICATION OF TETRABUTYLAMMONIUM TETRABUTYLBORATE[1]

Abstract: Tetrabutylammonium tetrabutylborate is a compound with uses in a wide number of fields of chemistry, but particularly in the area of thermodynamics of solvation. A one-step synthesis of the anion from n-butyllithium and tributylborane, followed by a metathesis reaction with tetrabutylammonium bromide, produces the crude salt in high yield. A purification process involving flash chromatographic techniques and recrystallization produces a product of exceptional purity in 67% yield.

Introduction

When the solvolysis of the dianion of *p*-nitrophenyl phosphate is transferred from water to *tert*-amyl alcohol, tremendous rate enhancements are observed. Evaluation of the kinetic parameters and activation parameters is described in subsequent chapters. The rate enhancement observed is consistent with the observed decrease in the free energy of activation on transfer into *tert*-amyl alcohol. The question that this work seeks to address is the thermodynamic source of the rate enhancement. One way to pursue the answer is by evaluation of the thermodynamics of solvation of the phosphate monoester dianion in both water and in *tert*-amyl alcohol. This will allow a comparison of the ground state energies of the solute in the two solvents.

The free energy of solvation of a solute can be derived from its solubility by use of the relationship between the equilibrium concentration at saturation and the free energy of solvation. The result of this calculation is the overall solvation energy for both the cation and the anion, in the case of ionic solutes. Since the interest here is in the

phosphate dianion, it is desirable to separate the energies of the two ions. This is a common problem in the field of solvation. The development of the extrathermodynamic assumption has led to the establishment of a widely studied field of thermodynamics termed single ion solvation. It is well known that cations and anions are solvated with different efficiencies by a given solvent due to many factors that depend solely on the solvent. The differences in manner of solvation of cation and anion lead to large differences in free energy of solvation. In addition to the solvent dependent effects, with most ionic species the cation and anion themselves are very different in terms of dipoles, charge dispersion, polarizability, and steric bulk. With the extrathermodynamic assumption, these differences are negated by use of cations and anions that include bulky organic groups in their structure, such as n-butyl, isobutyl, or phenyl groups. With these large groups symmetrically arranged around a charged center, a large surface area with very dispersed charge is presented to the solvent. Under these conditions, differential solvation of cation and anion is minimized. The extrathermodynamic assumption states that any energy of solvation for the compound can be equally attributed to cation and anion. This allows the energy of solvation for a single ion to be calculated. When an ion of interest is complexed with one of the partners from an extrathermodynamic pair, its energy of solvation can be determined.

This extrathermodynamic assumption was applied in attempts to determine the energy of solvation of a phosphate monoester dianion, using the subject compound as the starting material. Due to extremely low solubilities, product of high purity was required. Purification steps that had not been previously published with this family of compounds were added to the known but very obscure literature on the synthesis of this compound.

Statement of Problem

The compound tetrabutylammonium tetrabutylborate has a long history of use in

several areas of chemistry,[1] and particularly in studies of the thermodynamics of ion solvation.[2] Until very recently this compound was commercially available, albeit from a single source. Presently there are no commercial sources for tetrabutylammonium tetrabutylborate. Our search of the literature turned up only a single, low-yield (<10%) synthesis for the compound.[3] In addition difficulties in its purification have been reported, and literature melting points for the pure compound range from 109.5 °C[4] to 110.6–112.0 °C.[3]

Summary of Work Performed

We prepared tetrabutylammonium tetrabutylborate in high yield by a modification and simplification of a procedure previously reported for related compounds.[5] Lithium tetrabutylborate, made by reaction of n-butyllithium with tributylborane, was added to a solution of tetrabutylammonium bromide in water. After isolation of the precipitated product, recrystallization using various literature methods afforded material with correct NMR integrations. However, when this material was partitioned between aqueous and organic phases in preparation for thermodynamic studies, the aqueous phase was found to contain small amounts of a contaminating tetrabutylammonium salt, the anion of which gave no proton NMR signal. Repeated aqueous washings and recrystallizations failed to remove the contaminating material. TLC analysis on silica gel plates eluting with acetone/petroleum ether mixtures showed that the relatively nonpolar tetrabutylammonium tetrabutylborate eluted more rapidly than a fainter, contaminating compound which was significantly more polar. Accordingly, flash chromatography was used to afford tetrabutylammonium tetrabutylborate free of the contaminating material, and which had a melting point after recrystallization of 112.5-113 °C. Multigram quantities of pure tetrabutylammonium tetrabutylborate can easily and rapidly be obtained by this method.

Experimental

General Procedures. Reagents were obtained from commercial sources and used as received. Up to the point of combining the two water solutions, preparative steps were performed under a flow of anhydrous nitrogen, but without special equipment to insure inert atmosphere or extraordinary measures to exclude water. NMR analysis was performed with a Bruker ARX400 in d_6-acetone solutions; shifts are reported in parts per million downfield from internal Me_4Si. Melting points were obtained using a Mel-Temp capillary melting point apparatus and are uncorrected. Combustion analysis was performed by Atlantic Microlab, Inc., Norcross, GA, and is reported as percentages.

Synthesis and Purification. Under nitrogen, 0.15 mol of tributylborane (Aldrich, 1.0M diethyl ether solution) was introduced into a large Schlenk flask and 0.15 mol of n-butyllithium (Aldrich, 2.5M solution in hexane, diluted to 1.0 M) was added dropwise over an hour. The solution became warm but no precipitate was formed. When the addition was complete, the solvent was removed under vacuum until the total volume was below 100 mL. This concentrated solution was placed in a -40 °C freezer until a solid formed. Sufficient hexane was added in order to form a slurry and the wet product (lithium tetrabutylborate) was then warmed gently under vacuum as solvent was removed to near dryness. When the product had formed a slurry coating the walls of the flask, after drying for about 2 h, 150 mL of degassed water was added (distilled, deionized water, purged with nitrogen for 30 min). The product dissolved readily in the water, forming a cloudy solution. A separate aqueous solution of tetrabutylammonium bromide (Aldrich) was prepared under normal atmosphere (0.15 mol in 40 mL of water) and this was added all at once to the lithium tetrabutylborate. The addition produced an immediate and plentiful precipitate of the crude final product (tetrabutylammonium tetrabutylborate salt) which was then handled under normal atmosphere. The thick slurry which formed was shaken to ensure complete mixing, and the crude product was washed three times

with 1L of distilled water and dried under vacuum. The yield of crude, dry product was 65.0 g, 89.9%. Yellow color in the dried product indicates inadequate water washing. The dried product was recrystallized from isopropyl ether using the method of Fuchs et al.[3] The product was in the form of small crystalline needles with a melting point of 110.5-111 °C. This product was purified by flash chromatography on silica gel (EM Scientific, 230-400 mesh) eluting with 30% acetone/petroleum ether. Separation of pure product from a tetrabutylammonium salt impurity was observed by TLC and confirmed by NMR analysis of fractions collected from the column. Fractions containing the product were combined for removal of solvent by rotary evaporation. The product was dried under vacuum and recrystallized from isopropyl ether, yielding colorless crystalline needles 0.5-2 cm long. These were dried under vacuum and had a melting point of 112.5-113 °C. Overall yield is 67%. ^{1}H NMR (acetone-d_6) d -0.02 (m, 2H), 0.83 (t, $J=$ 8.8 Hz, 3H), 0.99 (t, $J=$ 8.8 Hz, 3H), 1.17 (m, 4H), 1.44 (m, 2H), 1.84 (m, 2H), 3.46 (m, 2H). An NMR spectrum is at Figure 2-1. Anal. Calcd for $C_{32}H_{72}NB$: C, 79.78; H, 15.06; N, 2.91. Found: C, 79.94; H, 15.11; N, 3.01.
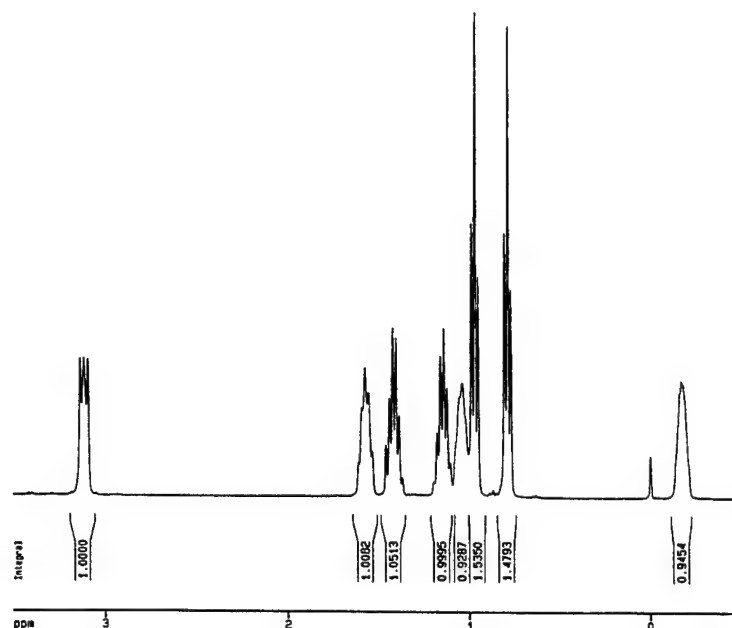
Figure 2-1. An NMR spectrum of tetrabutylammonium tetrabutylborate. Referenced to an internal tetramethylsilane standard at 0 ppm.

References

(1)   For some recent work utilizing the title compound in physical chemistry, analytical chemistry, and electrochemistry, see: (a) Yoshida, K.; Ibuki, K.; Ueno, M. *J. Chem. Soc., Faraday Trans.* **1997,** *93,* 89-92.   (b) Bergmann, K.; Neidhart, B. *J. Anal. Chem.* **1996,** *356,* 57-61. (c) Poole, S. K.; Poole, C. F. *Analyst,* **1995,** *120,* 289-94. (d) Muhuri, P. K.; Hazra, D. K. *J. Chem. Soc., Faraday Trans.,* **1991,** *87,* 3511-13. (e) Dasgupta, D.; Das, S.; Hazra, D. K. *Bull. Chem. Soc. Jpn.,* 1989, *62,* 1246-9.

(2)   For reviews, see: (a) Marcus, Y. *Pure Appl. Chem.* **1983,** *55,* 977-1021. (b) Marcus, Y. *Ion Solvation*; John Wiley and Sons: New York, 1985.

(3)   Fuchs, R.; Bear, J. L.; Rodewald, R. F. *J. Am. Chem. Soc.* **1969,** *91,* 5797-5800.

(4)   Grindley, T.; Lind, J. E. *J. Chem. Phys.* **1972,** *56,* 3602-3604.

(5)   Ford, W. T.; Hauri, R. J.; Hart, D. J. *J. Org. Chem.* **1973,** *38,* 3916-3918.

CHAPTER 3

PARTITIONING OF SOLUTES WITH ION
EXCHANGE MEMBRANES

Abstract: Isotope effects in chemical reactions can be the product of many different processes that take place during a chemical reaction. In order to isolate the isotopic effect on metal-substrate coordination, experiments were designed using ion exchange membrane to allow the partitioning of p-nitrophenyl phosphate anions between two solutions, one of which contained Ca^{2+} ions. The use of isotope labeled phosphates in this partitioning would allow determination of isotope effects on metal coordination. After testing several membrane products provided by commercial sources, we concluded that a membrane with the specific characteristics that we required is not readily available. Ion transport data and performance data for the tested membranes are provided.

Introduction

The primary focus of the research conducted in this lab is the elucidation of the mechanisms of phosphoryl transfer reactions through the use of experimental organic physical chemistry. One of the major techniques used is the study of heavy atom kinetic isotope effects on phosphoryl transfer reactions.

To conduct the kinetic isotope effects studies, substrates for the phosphoryl transfer reactions are synthesized with stable isotopes of nitrogen and oxygen substituted for atoms in critical locations in the compound. Reactions are stopped at partial completion and residual, unreacted substrate and hydrolyzed products are isolated from the reaction mixture. Each of these fractions is analyzed by isotope ratio mass spectrometry, and the extent of disproportionation of isotopes allows calculation of kinetic isotope effects. These are then interpreted in terms of the inferred transition state structure.

A set of kinetic isotope effect data was recently collected for an enzymatic reaction using *p*-nitrophenyl phosphate (pNPP) as the substrate. This particular enzyme requires a divalent metal cation in the active site in order to retain its full catalytic function, and these experiments were performed in the presence of calcium. On consideration of the size of the isotope effects, and interpretation of these in terms of transition state structure, there is some uncertainty whether all of the measured isotope effect can be attributed to the interaction of the substrate with the enzyme. There is potential for significant isotopic effect on the binding of the substrate to the calcium metal alone, and it possible that the measured isotope effects include this binding isotope effect.

The binding of the calcium to the substrate is an effect that is at equilibrium in the reaction mixture, given the conditions used in this lab. Therefore the only way to separate the enzyme kinetic isotope effect from the equilibrium calcium complexation isotope effect is to measure the equilibrium isotope effect on complexation. Direct measurement would require preparing a solution with pNPP and calcium in the solution, instantaneously isolating all pNPP molecules which are complexed with a calcium cation, and measuring the isotopic disproportionation of this population. For obvious reasons, this is not practical.

Another method for direct measurement would be to prepare a solution with a chemically selective boundary in the middle of the container. On one side of the boundary, the solution would initially be rich in calcium cations, and the boundary would not allow any of these cations to pass to the other side. On the other side of the boundary, the solution would initially be rich in pNPP, and the isotopic composition of this solute would be known. The chemically selective boundary would allow the negatively charged aryl phosphate ion to pass freely from one side of the solution to the other. Once the experiment was started, the phosphate would exchange freely across the boundary until an equilibrium was reached between free phosphate on one side and free

and calcium bound phosphate on the other side. If the calcium concentration was maintained high enough to saturate the available phosphate, virtually all phosphate on the calcium side of the boundary would be complexed. If this solution was monitored until it went completely to an equilibrium state, it could be assumed that any isotopic effects on the complexation equilibrium would be expressed. The phosphate on both sides of the boundary could then be isolated and analyzed as described above to quantify this equilibrium isotope effect. This would provide the data necessary to deconvolute the previously measured kinetic isotope effect.

Recent reports on the performance of newly developed membranes and membrane systems used for water purification suggested that it might be possible to achieve the desired partitioning.[1,2] Given the ability of anion exchange membranes to selectively pass anions while restricting the movement of cations, experiments were designed along the lines described above to test the suitability of these membranes for measurements of this sort. Based on a description of the experimental intent in this project, three commercial companies (Ionics, Inc., the Asahi Glass Company of Japan, and Pall Gelman Sciences) provided membranes for the testing described in this report.

Experimental

General. In order to set up multiple experiments simultaneously, an inexpensive, two-chambered vessel with a relatively large porous connection was sought. A Nalgene analytical filter unit, shown in Figure 3-1, was selected that allowed over 150 mL of solution to be used on each side of the partition. These filters are provided as a five-piece unit, consisting of an upper chamber cover, an upper chamber, a cellulose fiber membrane support, a 40-μm pore size membrane (intended for bacterial filtration), and a lower chamber fitted for application of a vacuum device. For the purposes of this work, the membrane was discarded and the cover was sealed to the top with a silicone sealant.
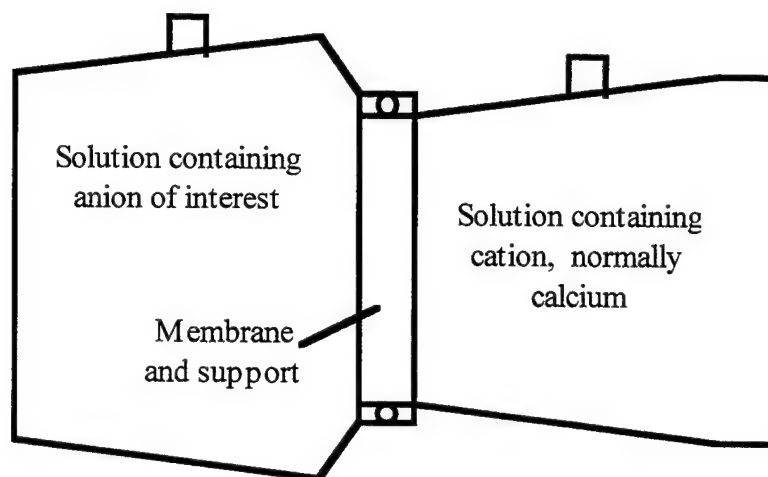
Figure 3-1. Sketch of the membrane testing device.

The top and bottom had an o-ring pressure seal between them that made the junction water tight. The completed assembly was turned on its side to provide two side-by-side volumes, which could be independently filled and sampled, with a support for a 47 mm membrane disc between them. The connecting area, which had a very small opening consistent with the use under vacuum filtration, was drilled to improve hydraulic contact, and holes were drilled in each chamber to allow introduction and sampling of solutions. Due to the slightly different cross sections of the top and bottom chambers, there was a difference in volume of the two solutions used. The anion that was being monitored was always placed in the chamber of higher volume.

Solutions were prepared for testing of solute transport between the two chambers. using distilled, deionized water. When pH control was desired, solutions were buffered to pH 7.0 using 10 mM MOPS (3-(N-morpholino)propanesulfonic acid) buffer. This buffer was selected due to its demonstrated weak interaction with metal cations.[3,4] Overall ionic strength of the solutions on both sides of the membrane was initially equal. Equal liquid levels on both sides of the membrane were maintained to prevent hydraulic head from affecting transport. In order to monitor the calcium ion concentration in solution, a colorimetric titration method was used.[5] An aliquot of the solution was

removed by pipette for the titration and the liquid level was maintained by replacement with stock solution. The pNPP concentration was monitored by placing an aliquot from the chamber into a UV/VIS spectrophotometer cuvet containing TRIS buffer at pH 9.0. Alkaline phosphatase enzyme was added, which cleaved the aryl phosphate quantitatively in about 30 min. The resulting phenol was present as the phenolate ion due to the pH of the solution, and the p-nitrophenolate ion was measured by absorbance at 400 nm.

Prior to initiating the experiments, the membranes were prepared by immersion in a saturated solution of potassium chloride for at least 2 h, followed by washing with distilled, deionized water for at least 30 min. The prepared membranes were then fitted into the opening at the junction of the two chambers. For thicker membranes, no support was used besides the plastic frame integral to the bottom piece. For the thinner membranes, the cellulose fiber support supplied with the filter apparatus was used. The thickness of this support was modified by delaminating it so that the two chambers would seal together well. Once the membrane was in place between the chambers, the solutions were rapidly added evenly to both sides to prevent drying of the membrane and to maintain equivalent hydraulic head. Finally a magnetic stir bar was added to each side and the entire apparatus was placed on a stir plate. Samples were maintained at room temperature.

Membrane Characteristics. The following provides some data concerning the membranes tested. Characterizations provided here are generally those provided by the supplier and were not verified by testing or measurement in this lab.

(a) Supplier: Gelman Sciences[6]

Membrane: SB-6047

Description: Polyether-sulfone copolymer supported quaternary ammonium exchange sites. A strongly basic anion exchange filter with a pore size of 0.45 mm and thickness of 152 mm.

(b) Supplier: Ionics, Incorporated[7]

Membrane: AR103-QDP

Description: A caustic stable membrane with quaternary ammonium exchange sites. Exchange capacity of 2.1 meq/g (gram of dry resin), water content of 35% and a thickness of 600 mm.

Membrane: AR204-SZRA

Description: A general use membrane containing ammonium ions. Exchange capacity of 2.6 meq/g, water content of 46% and a thickness of 600 mm.

Membrane: AR112B-447

Description: A nitrate selective membrane containing ammonium ions. Exchange capacity of 1.9 meq/g, water content of 23% and a thickness of 600 mm.

(c) Supplier: Asahi Glass Company[8]

All of the Asahi Glass membranes were described as dense styrene-divinylbenzene membranes with no pore structure and low hydraulic permeability.

Membrane: AMV

Description: Typical anion exchange membrane with a strongly basic anionic exchange group. Exchange capacity of 2 meq/g, thickness reported as 110-150 mm, measured as 155 mm.

Membrane: ASV

Description: Anion exchange membrane with a strongly basic anionic exchange group, with both membrane surfaces also possessing weakly basic functional groups (tertiary amine). Exchange capacity of 2 meq/g, thickness reported as 110-150 mm, measured as 150 mm.

Membrane: ASO

Description: Anion exchange membrane with a strongly basic anionic exchange group with one membrane surface also possessing weakly basic functional groups. Exchange

capacity of 2 meq/g, thickness measured as 145 mm.

Results and Discussion

Permselectivity Verification. The first experiment was conducted with the Gelman membrane with the intent of verifying its permselectivity for divalent cations. The equilibration apparatus was set up with calcium chloride in one chamber and sodium sulfate in the other, with both solutions at 0.1 M, or an ionic strength of 0.3 M. Any exchange of sulfate ion across the membrane would be apparent by the formation of calcium sulfate precipitate. The exchange of calcium ions across the membrane, which is an undesirable outcome, was monitored by the titration method described above. Calcium transport was observed at rates that were unacceptably high for the proposed partitioning experiments. This experiment was discontinued when precipitate was observed forming on the sodium side of the membrane. The data are shown in Table 3-1. The theoretical equilibrium calcium concentration is calculated as if the calcium present in the reactor was dissolved in the total reactor volume. Thus this number gives a measure of the extent to which calcium transport is not restricted by the membrane.

On dismantling the equilibration apparatus, it was found that much of the surface

Table 3-1. Permselectivity Evaluation with Gelman Membrane

Time (hrs)	$[Ca^{2+}]$ on Ca side (mg/mL)	$[Ca^{2+}]$ on Na side (mg/mL)	% of theoretical $[Ca^{2+}$ equilibrium]
0	4.01	0	0
16	4.01	0.091	6.25
42		0.237	16.3
64	Experiment halted due to formation of precipitate on Na side		

ofthe membrane on the sodium side was fouled with calcium sulfate precipitate. Due to the relatively high sulfate concentration on the sodium side, it can be presumed that as soon as any calcium got through the membrane to the surface on the Na_2SO_4 side, it precipitated. Based on this result, the SB-407 membrane was not investigated further due to its inability to prevent the transport of calcium cations.

The following experiments were performed on the membranes supplied by Ionics, with solutions at lower ionic strength, but using the same set of reagents to test for resistance to calcium ion transport. Results are in Table 3-2. With the concentration of solute on each side of the membrane at 0.05 M, the initial calcium concentration on the calcium side is 2.0 mg/mL, with a potential equilibrium concentration of 0.80 mg/mL throughout the apparatus if calcium is freely transported. The calcium concentration on the calcium side of the membranes was not monitored quantitatively due to the very low level of calcium transport observed.

Based on these data, the AR103 membrane appears to have the best permselectivity for retention of Ca^{2+} ions, with AR204 also showing some resistance to Ca^{2+} transport. AR103 was also the only one of these three membranes to show sulfate precipitation on the calcium side, which demonstrates that it is allowing the transport of

Table 3-2. Perselectivity Evaluation with Ionics Membranes[a]

time (hrs)	AR103-QDP		AR204-SZRA		AR112B-447	
	[Ca^{2+}] on Na side (mg/mL)	[Ca^{2+}] as % of theor.	[Ca^{2+}] on Na side (mg/mL)	[Ca^{2+}] as % of theor.	[Ca^{2+}] on Na side (mg/mL)	[Ca^{2+}] as % of theor.
43	0.004(2)	0.5	0.012(2)	1.5	0.101(5)	12.5
77	0.004(2)	0.5	0.018(2)	2.2	0.095(5)	11.9
101	Stopped due to precipitate formation		0.025(2)	3.2	0.091(5)	11.4

[a]Uncertainty in the last digit is shown in parentheses.

anions across the membrane. Based on these results, and a desire to retest the AR112B-447, all three of these membranes were brought forward to the next round of testing.

Phosphate Transport Evaluation. The next experiment was the final test for the suitability of the membrane for the phosphate-calcium binding measurements. The solutions poised on either side of the membrane were a pNPP/NaCl solution on one side and a $CaCl_2$ solution on the other side. In both solutions used for this experiment, the MOPS buffer was added to maintain the pH at 7.0. This pH ensures that the pNPP was present primarily as the dianion, which is the form of the phosphate monoester that is present in the enzymatic reaction. The pNPP was added as the sodium salt, and began the experiment at a concentration of 1.0 mM. The ionic strength of the solution on the phosphate side of the membrane was made up with NaCl. The calcium side of the membrane was started at 50 mM $CaCl_2$. The ratio of concentration of Ca^{2+} to phosphate was 50:1 based on the results of unpublished spectrophotometric studies done in this lab, which showed that this ratio was sufficient to fully complex the pNPP with calcium.

With this experiment, there were two questions which needed to be answered. First, were the membranes resisting transport of calcium? The data in Table 3-3 show that the AR204-SZRA and AR112B-447 membranes both allowed enough calcium to exchange across the membrane to cause precipitation of calcium pNPP. The AR103-QDP membrane provided sufficient resistance to calcium transport for the purposes of this work. In addition to the prevention of calcium transport, a suitable membrane must also allow the pNPP dianion to freely exchange between the two solutions. The data in Table 3-4, which were only meaningful with the AR103-QDP membrane, demonstrate the capacity of the membrane as an exchange medium for this anion. The pNPP anion was transported across the membrane to some extent, but the transport was not rapid enough to bring the solutions to equilibrium before there began to be significant hydrolysis of the pNPP. This was apparent by the appearance of the yellow-colored *p*-nitrophenolate ion

Table 3-3. Calcium Transport During Phosphate Evaluation Experiment[a]

time (hrs)	AR103-QDP		AR204-SZRA		AR112B-447	
	$[Ca^{2+}]$ on Na side (mg/mL)	$[Ca^{2+}]$ as % of theor.	$[Ca^{2+}]$ on Na side (mg/mL)	$[Ca^{2+}]$ as % of theor.	$[Ca^{2+}]$ on Na side (mg/mL)	$[Ca^{2+}]$ as % of theor.
24	0.001(1)	0.2	0.030(3)	3.8	0.088(5)	10.9
53	0.002(1)	0.5	Stopped due to precipitate formation		Stopped due to precipitate formation	
124	0.009(1)	1.1				
222	0.012(1)	1.5				

[a]Uncertainty in the last digit is shown in parentheses.

Table 3-4. Phosphate Transport Data for Ionics AR103-QDP Membrane[a]

time (hrs)	[Phos] on Phos side (mM)	[Phos] on Ca side (mM)
24	0.94(2)	0.05(2)
53	0.87(2)	0.11(2)
124	0.78(3)	0.18(3)
170	0.79(5)	0.28(5)
222	0.67(5)	0.23(5)

[a]Uncertainty in the last digit is shown in parentheses.

in the solutions. In addition to the appearance of the phenolate ion in solution, the membranes themselves began to become bright yellow in color as they absorbed the phenolate. Due to the inability to reach an equilibrium distribution of phosphate at a rate much faster than the rate of phosphate hydrolysis, these membranes will not be suitable for isotope effects evaluation. The three membranes from Asahi Glass Company were submitted to the same phosphate/calcium transport assessment as the membranes described above. Transport of ions was evaluated at irregular intervals over a period of 12 days. The Asahi Glass membranes were all very resistant to calcium cation transport, with the ASO membrane providing essentially an absolute barrier to movement of the cation. The calcium transport data are shown in Table 3-5.

Phosphate anion transport was limited, with the AMV type membrane demonstrating the highest rate of transport of the anions, as shown in the Table 3-6. This rate of transport of the phosphate anion is not high enough to allow the phosphate-calcium equilibrium exchange equilibrium to be reached before hydrolysis of aryl phosphate becomes problematic.

By the end of the experimental time period, solutions on both sides of the membranes were developing significant yellow color due to the presence of free

Table 3-5. Calcium Transport Data for Asahi Glass Membranes[a]

time (hrs)	ASV		AMV		ASO	
	$[Ca^{2+}]$ on Na side (mg/mL)	$[Ca^{2+}]$ as % of theor.	$[Ca^{2+}]$ on Na side (mg/mL)	$[Ca^{2+}]$ as % of theor.	$[Ca^{2+}]$ on Na side (mg/mL)	$[Ca^{2+}]$ as % of theor.
188	0.006(2)	0.7	0.005(2)	0.6	0 (not detected)	
284	0.005(2)	0.6	0.004(2)	0.5	0 (not detected)	

[a]Uncertainty in the last digit is shown in parentheses.

Table 3-6. Phosphate Transport Data with Asahi Glass Membranes[a]

time (hrs)	ASV		AMV		ASO	
	[Phos] on Phos side (mM)	[Phos] on Ca side (mM)	[Phos] on Phos side (mM)	[Phos] on Ca side (mM)	[Phos] on Phos side (mM)	[Phos] on Ca side (mM)
67	0.94(2)	0.06(2)	0.86(2)	0.14(2)	0.91(2)	0.08(2)
284	0.94(2)	0.06(2)	0.72(2)	0.28(2)	0.87(2)	0.11(2)

[a]Uncertainty in the last digit is shown in parentheses.

p-nitrophenolate ions. The phenolate ion is much smaller than the phosphate ion, and could potentially have a much higher transport rate. Since the assay for phosphate involves enzymatic conversion to free phenolate, there was some concern that the assay might be allowing phenolic transport rates to be included with the phosphate transport rates. Therefore, solutions on both sides of the membranes were analyzed without modification for the presence of free phenolate. Data on phenol transport are shown in Table 3-7.

These data provide support for a couple of possible conclusions. The first is that phenolate anion is transported much more rapidly than the phosphate anion. In all three of these cases, the ratio of phenol concentration on the calcium side of the membrane to phenol concentration on the phosphate side is much higher than the corresponding ratio for the phosphate. This could be interpreted by assuming that as the phenol was formed it was rapidly equilibrated across the membrane. This is further supported by the almost identical phenol concentrations on the two sides of the membranes for all three membranes tested.

A different conclusion that might be drawn is that the membrane is accelerating the rate of hydrolysis of the phosphate, and that this is responsible for the difference in concentration ratios for phenol and phosphate. If the membrane is enhancing hydrolysis of the phosphate as it passes through the membrane pores, then phenol should accumulate

Table 3-7. Phenol Transport with Asahi Glass Membranes[a]

time (hrs)	ASV		AMV		ASO	
	[Phenol] on Phos side (mM)	[Phenol] on Ca side (mM)	[Phenol] on Phos side (mM)	[Phenol] on Ca side (mM)	[Phenol] on Phos side (mM)	[Phenol] on Ca side (mM)
284	0.08(2)	0.04(2)	0.14(2)	0.12(2)	0.08(2)	0.05(2)

[a]Uncertainty in the last digit is shown in parentheses.

faster than the phosphate on the calcium sides of the membranes. Membranes that have higher transport rates for phosphate should also show higher accumulations of phenol, as the AMV does. If the phosphate is actually exchanging from solution to adsorbed membrane phase, and the membrane is enhancing the rate of hydrolysis, then the membrane with the highest transport rate should actually exhibit a higher overall hydrolysis rate than the rate in solution. Again, the AMV membrane demonstrates a higher overall rate of hydrolysis than that observed with the other two membranes.

Summary and Conclusions

None of the membranes tested by this procedure proved to be suitable for the experimental measurement of pNPP dianion transport equilibrium conditions. Given the unsaturated polymer structure of the support medium for the active functional groups on the membranes, it is reasonable to suggest that intermolecular attractive forces between the substituted phenyl rings on the phosphate and the membrane polymer could create conditions not conducive to facile transport of the phosphate dianion through the membranes. In support of this proposition is the observation in this lab of a similar effect with absorption of phenolate ions by cationic exchange resins, such as Dowex. In these resins the functional groups are negatively charged, as is the phenolate ion, and the attractive forces are still strong enough to make use of these resins somewhat problematic.

It is interesting to note that all membranes tested with the *p*-nitrophenyl phosphate

developed intense yellow color over the time course of the experiments. This suggests an affinity of the *p*-nitrophenolate ions for the membrane. The further observation of enhanced rates of hydrolysis of the phenyl phosphate in membranes which exhibited some exchange capacity for the phosphate is also interesting in light of other work being performed in this lab.

The rate of solvolysis of phosphate monoesters is enhanced by up to a factor of 10^7 by the addition of organic solvents to aqueous solutions,[9] and the rates in some pure organic solvents have been shown to be enhanced by up to four orders of magnitude. Based on studies done in this lab, this rate enhancement is believed to be due to the reduced requirement for solvent reorganization to accommodate charge rearrangement in going from ground state to transition state, when this transition is done in the presence of a medium that is less solvating than water. It is proposed that a similar desolvation occurs in the membranes when the phosphate anion is adsorbed into the supporting structure, resulting in a lower entropic cost for achieving the transition state, and an enhanced hydrolysis rate.

Based on the experiments described above, other methods will be pursued to evaluate the equilibrium isotope effects on the binding of metal cations to aryl phosphate dianions.

References

(1)   Strathman, H.; Bauer, B.; Rapp, H. J. *CHEMTECH* **1993**, *23*, 17-24.

(2)   Palaty, Z.; Zakova, A. *J. Membrane Sci.* **1996**, *119*, 183-190.

(3)   Good, N. E.; Winget, G. D.; Winter, W.; Connolly, T. N.; Izawa, S.; Singh, R. M. M. *Biochem.* **1966**, *5*, 467-477.

(4)   Good, N. E.; Izawa, S. *Meth. Enz.* **1972**, *24, Part B*, 53-68.

(5)   Greenberg, A. E.; Trussel, R. R.; Clesceri, L. S., Eds.*Selected Physical and Chemical Standard Methods for Students, Based on Standard Methods for the*

Examination of Water and Wastewater, 16th ed.; American Public Health Association: Washington, DC, 1986.

(6)   Reyes, M. Personal communication.

(7)   Zheng, Y. C. Personal communication.

(8)   Terada, I. Personal communication.

(9)   Abell, K. W. Y.; Kirby, A. J. *Tet. Lett.* **1986**, *27*, 1085-1088.

CHAPTER 4

ENTROPY AND ENTHALPY CONTRIBUTIONS TO SOLVENT EFFECTS ON PHOSPHATE MONOESTER SOLVOLYSIS; THE IMPORTANCE OF ENTROPY EFFECTS IN THE DISSOCIATIVE TRANSITION STATE[1]

Abstract: The solvolysis reactions of a series of aryl phosphates in *tert*-butanol and in *tert*-amyl alcohol have been examined. The dianion of *p*-nitrophenyl phosphate reacts 7500- and 8750-fold faster in these solvents, respectively, than the corresponding aqueous reactions. The monoanion reacts 14- and 16-fold slower, respectively, in *tert*-butanol and in *tert*-amyl alcohol. Analysis of the activation parameters shows that the rate enhancement for the dianion is due solely to entropic factors, while the slower reaction of the monoanion is due to increased enthalpy of activation. The significantly more positive entropy of activation for the solvolysis of *p*-nitrophenyl phosphate dianion in *tert*-butanol supports the original proposal that racemization at phosphorus in this reaction is caused by a switch to a $D_N + A_N$ mechanism, rather than subsequently proposed mechanisms which avoid the formation of metaphosphate. Rate enhancements of similar magnitudes are seen for the dianion reactions of all of the aryl phosphates examined; the plot of the rate constants for solvolysis versus the aqueous pK_a of the leaving phenols has a slope of -1.1, within experimental error of the value for the aqueous reaction. However, in the reactions in *tert*-amyl alcohol, *para*-substituted and *meta*-substituted aryl phosphates fall on separate but parallel lines with *para*-substituted compounds reacting faster than *meta*-substituted reactants with leaving groups of similar pK_a. The pK_a values for a series of *para*-substituted and *meta*-substituted phenols in *tert*-butanol and in *tert*-amyl alcohol

---

were determined and were found to have a linear relationship with the aqueous pK_a values, with no distinction between *para-* and *meta*-substitution. Thus the different Brønsted behavior of *para-* and *meta*-substituted aryl phosphates in these solvents is not due to differential solvent-induced perturbations of the pK_a values of the leaving groups. The mechanistic implications of these results and their relevance to enzymatic phosphoryl transfer are discussed.

Introduction

The chemistry of phosphoryl transfer from phosphate monoesters and diesters is essential and ubiquitous in biological systems. A considerable amount of work over the past decades has been devoted toward gaining an understanding of the mechanisms of these reactions in solution, and toward understanding the mechanisms of enzyme-catalyzed phosphoryl transfer. Of particular interest is whether the mechanistic pathways and the transition states involved in the enzymatic reactions differ from uncatalyzed phosphoryl transfer reactions in solution.

Three distinct reaction mechanisms have been observed for various types of phosphate esters under different conditions, which are illustrated diagrammatically in Figure 4-1.[1,2] Two are two-step mechanisms: A is an S_N1 ($D_N + A_N$ in the IUPAC nomenclature)[3] type of mechanism in which a metaphosphate intermediate is formed in the rate-determining step; this highly reactive species is then attacked by a nucleophile in a subsequent rapid step. Mechanism B is addition-elimination ($A_N + D_N$) and involves nucleophilic attack in the first step to form a pentacoordinate phosphorane intermediate. This intermediate may or may not pseudorotate before expelling a leaving group in a second step. Mechanistic possibility C is a concerted A_ND_N reaction in which the nucleophile enters and the leaving group departs in a single step, with no intermediate.

The primary factor that influences which mechanism is followed is the alkylation state of the phosphate. Monoesters are generally observed to follow, depending on
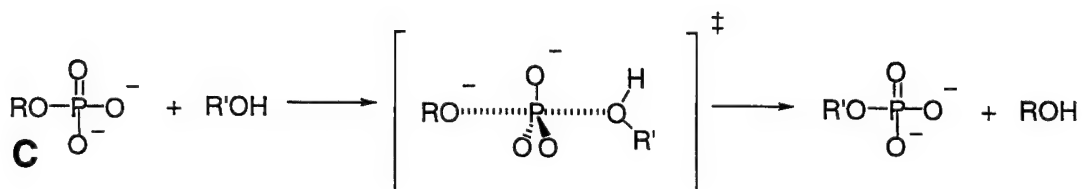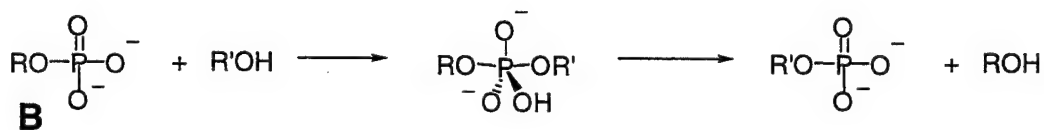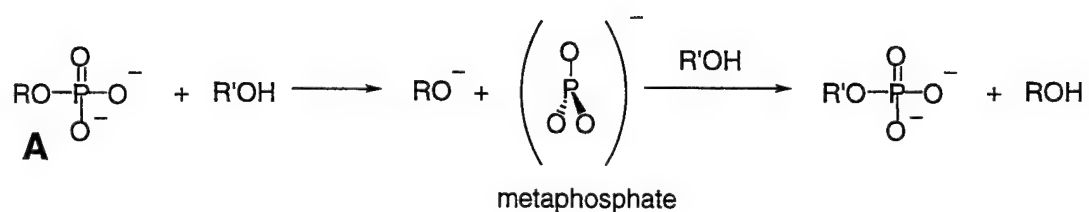
metaphosphate

Figure 4-1. The dissociative (**A**) and the associative (**B**) mechanistic extremes, and the concerted (**C**) pathway for phosphoryl transfer. The concerted pathway is drawn to indicate a dissociative transition state, which is typical for phosphate monoester reactions. At the bottom is the proposed mechanism for the first step in phosphoryl transfers of monoanions; for less basic -OR groups such as phenols the proton transfer to the leaving group may be concerted with P-O bond cleavage.[4]

conditions, either a concerted mechanism with a highly dissociative transition state (in nucleophilic solvents) or, in very non-nucleophilic solvents like *tert*-butanol, a $D_N + A_N$ mechanism with a metaphosphate intermediate. Diesters and triesters follow successively more associative mechanisms, either concerted ones if the leaving group is good (i.e., an aryloxy group) with more nucleophilic participation in the transition state, or fully associative mechanisms via phosphorane intermediates.

Mechanism C for the aqueous hydrolysis of monoester dianions is supported by a very small entropy of activation,[4] a large (-1.2) β_{LG}[5] and a small β_{NUC},[4] and the occurrence of inversion of configuration when the phosphoryl group is made chiral.[6] The reaction of the monoanion is also believed to proceed by a dissociative mechanism, with the proton transferred to the leaving group either in a preequilibrium step as shown in Figure 4-1 or, for less basic –OR groups, simultaneously with P–O bond cleavage.[5] This aqueous reaction also shows a very small entropy of activation[5] and the reaction of pNPP in methanol proceeds with inversion of configuration at phosphorus.[7]

Very large rate accelerations are observed in enzyme-catalyzed reactions of phosphate monoesters. Apart from the direct contribution from catalytic groups, the microenvironment in the active site experienced by the substrate is one possible source of the catalytic efficiency. One technique which has been used to address the effects of microenvironment on phosphoryl transfer reactions is to examine the effect of solvent on the rate and mechanism of the reaction. Several effects have been noted to arise in the aqueous reactions of phosphate monoesters from the addition of organic cosolvents, or from carrying out reactions in anhydrous solutions of alternative phosphoryl acceptors. Abell and Kirby found that added DMSO or HMPA accelerated the aqueous hydrolysis of pNPP dianion by up to 10^6- to 10^7-fold, by effects that were attributed to decreased hydrogen bonding of the solvent to the anionic nonbridge oxygen atoms.[8] Knowles et al. found that the stereochemical outcome of phosphoryl transfer from pNPP, made chiral by

the use of oxygen isotopes, changes from inversion in protic solvents like methanol to racemization in *tert*-butanol.[6] No kinetic studies were reported, but the reported approximate half-life of the reaction in *tert*-butanol was significantly faster than for the aqueous reaction at the same temperature.

In order to better understand the origins of these rate accelerations, we have conducted kinetic and thermodynamic studies of the reactions of a series of aryl phosphate monoesters in anhydrous *tert*-butanol and in *tert*-amyl alcohol, and compared these reactions to the aqueous ones. This report presents the results of those studies.

Experimental

General. Solvents were obtained from commercial sources and all distillations were done under anhydrous nitrogen. *Tert*-butanol was distilled from NaH, *tert*-amyl alcohol (*t*-AOH) was distilled from Mg, pyridine was distilled from CaH_2, and acetone was dried over molecular sieves and distilled. Other solvents were used as received. Tetraphenylarsonium chloride and sodium tetraphenylborate were obtained from commercial sources. Tetraphenylarsonium chloride was recrystallized from acetone, while tetraphenylborate was recrystallized from acetone/toluene.[9]

Synthesis of Aryl Phosphates. Substituted phenyl phosphates were synthesized by the method of Bourne and Williams.[10] The identities of the products were confirmed by both ^1H and ^{31}P NMR analysis. The phosphate monoesters were converted to the free acid forms by cation exchange with Dowex-50X8-100 cation exchange resin in the proton form followed by drying in vacuo. However, with *para*-substituted halogenated phenyl phosphates, cation exchange was accompanied by significant hydrolysis. With these monoesters the bis-cyclohexylammonium salts in water were made 1N in HCl and then extracted three times with diethyl ether. The ether layers were dried over $MgSO_4$, filtered and solvent removed under vacuum. This yielded the pure

acid forms of the phosphate monoesters.

Synthesis and Purification of Tetrabutylammonium and Tetraphenylarsonium Salts.

The synthesis of tetrabutylammonium tetrabutylborate is described elsewhere in detail.[11] The product was confirmed by NMR analysis, elemental analysis, and melting point.

Tetraphenylarsonium tetraphenylborate was synthesized by combining aqueous solutions of tetraphenylarsonium chloride and sodium tetraphenylborate. An aqueous solution was made of each of these compounds, which when combined produced a gel-like suspension of tetraphenylarsonium tetraphenylborate. This product was filtered, dried in vacuo, and recrystallized from nitromethane. ^{1}H NMR analysis confirmed the desired product. Figure 4-2 shows a portion of this NMR spectrum.

Tetraphenylarsonium chloride is noted in the literature for difficulty in obtaining dry material due to the presence of water of hydration.[9] It was necessary to obtain a
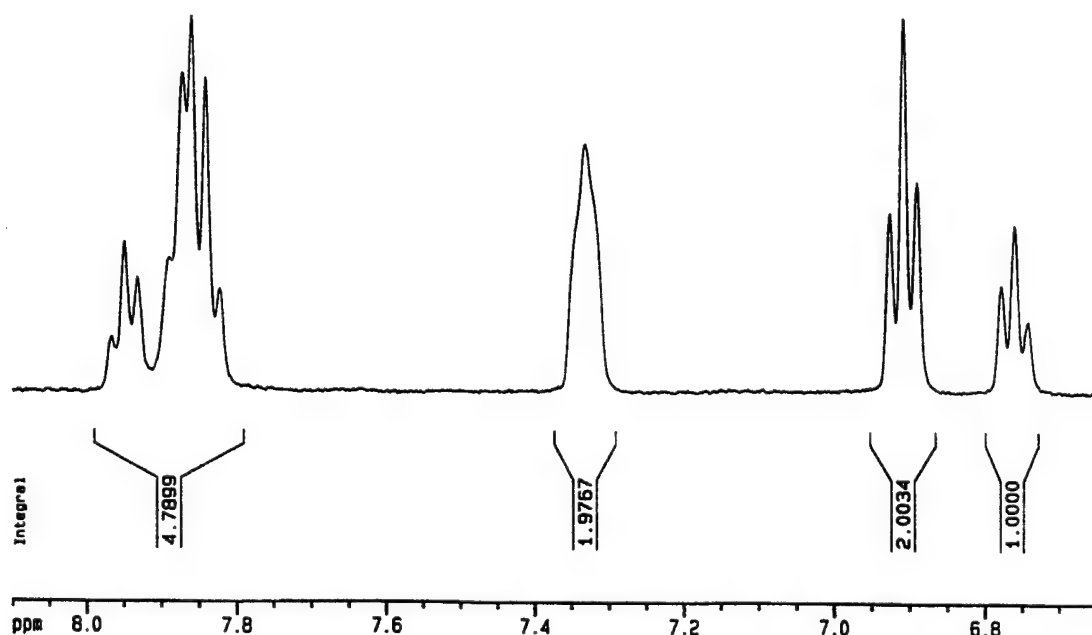
Figure 4-2. 1H NMR of tetraphenylarsonium tetraphenylborate in d_6-acetone. The borate peaks are upfield of the arsonium peaks. δ 6.76 (t, 1H), 6.91 (t, 2H), 7.34 (m, 2H), 7.87 (m, 4H), 7.96 (t, 1H).

water-free tetraphenylarsonium halide for evaluation of its solubility in nonaqueous solvent. Therefore, the anion was exchanged by metathesis in water with sodium iodide, the iodide salt of the tetraphenylarsonium ion being much less soluble in water than the chloride salt, and also much easier to dry. The tetraphenylarsonium iodide was then recrystallized from dry acetone.

Kinetics Methods. The acid form of the substituted phenyl phosphate monoester was dissolved in dried, freshly distilled t-AOH in a dried, screw-top test tube. Typical solution concentrations were 6–20 mM. This solution was brought to the appropriate temperature and a stoichiometric amount of tetrabutylammonium hydroxide (Aldrich 1.0M solution in methanol, stored under nitrogen) was added. To study the dianion reactions, a slight excess of two equivalents of base were added, while to study the monoanion, only one equivalent was added.
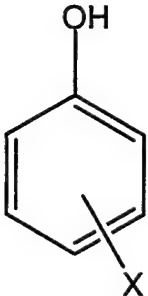
Over time, aliquots were removed and added to measured portions of a solution of 0.1 N NaOH. The reaction rates for phosphate monoesters in basic aqueous solution are many times slower than the rates in t-AOH, so this transfer effectively stopped the reaction. This solution was analyzed spectrophotometrically to determine the concentration of free phenol. The plot of absorbance versus time over the first 1–5% of reaction was analyzed assuming first order kinetics using the initial rates method. To determine initial substrate concentration, an aliquot of the reaction mixture was subjected to complete hydrolysis by alkaline phosphatase in pH 9.0 Tris buffer, 100 mM, containing 1 mM $ZnCl_2$ and $MgCl_2$, and the final absorbance of this solution was determined.

For each different substituted phenol, a spectroscopic study was performed comparing free phenolate to the corresponding phenyl phosphate. For each, a wavelength was selected for kinetic analysis such that no correction for the presence of the aryl phosphate was required. Table 4-1 shows the wavelengths used and an approximate

extinction coefficient for the phenolate ion at that wavelength.

pK$_a$ Determinations. The pK$_a$s in *tert*-butanol and *t*-AOH of the phenols listed in this study were evaluated using the method of Marple and Fritz[12] with an H-cell custom made for this work. A drawing of this cell is shown in Figure 4-3. The description below refers to the procedure using *t*-AOH; the procedure used for *tert*-butanol was identical, with *tert*-butanol replacing *t*-AOH in both reference and titration cells. The reference was an Accumet saturated calomel electrode with a cracked bead junction. This junction extended into a saturated aqueous KCl solution. Above this solution was *t*-AOH, also saturated in KCl, which was in contact with a frit. On the other side of this frit was a solution of *t*-AOH, saturated in tetrabutylammonium bromide. This solution was in contact with a frit which joined the reference assembly to the titration cell. In the titration cell, a glass pH indicating electrode connected to a pH meter was used to monitor pH and electrode potential as titrations were performed at 25°C under nitrogen.

Table 4-1. Wavelengths and Extinction Coefficients for Substituted Phenols Used in This Study

X group	λ_{max}, nm	extinction coefficient ε (M^{-1}cm^{-1})
4-nitro	400	18,320
H	289	4,780
4-cyano	280	29,656
4-amido	295	18,600
3,5-dinitro	408	2,000
3-chloro	242	10,600
3-nitro	404	1,530
4-phenyl	312	13,700

tert-amyl alcohol
saturated in
Bu$_4$NBr

tert-amyl alcohol,
saturated in KCl

Commercial calomel
reference electrode
saturated KCl

Saturated
aqueous KCl

N$_2$ supply

Buret with
(n-Bu)$_4$NOH

Commercial
glass electrode

tert-amyl
alcohol with
phenol
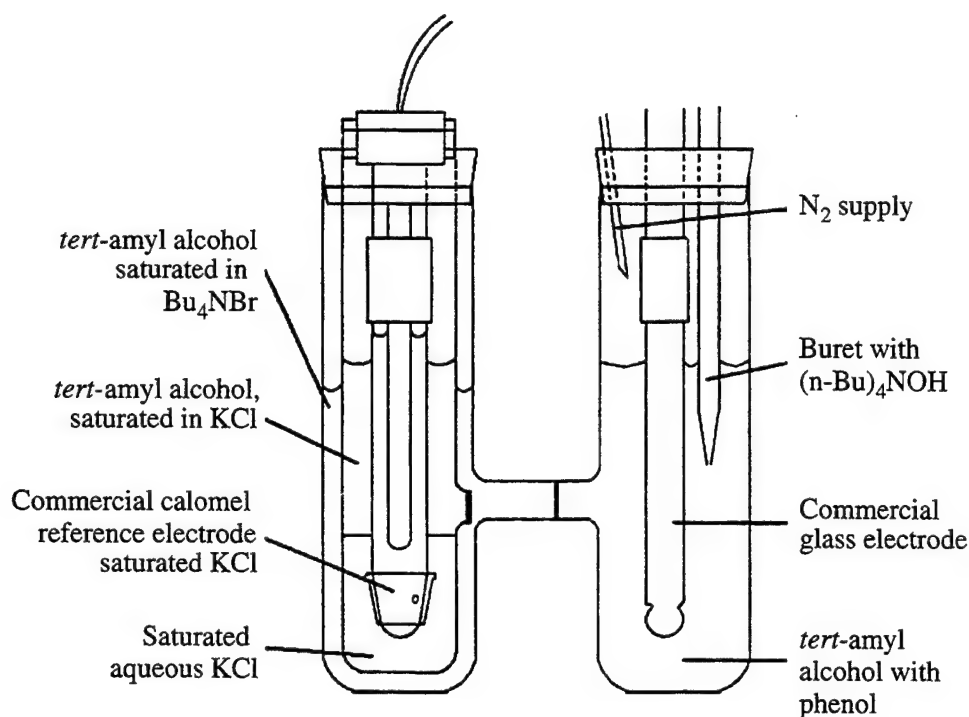
Figure 4-3. H-cell for measurement of pK$_a$ in nonaqueous solvent. Adapted from the design of Marple and Fritz.[12]

Before use of the cell for any data collection, the response of the cell was tested by titration with *p*-toluenesulfonic acid monohydrate. Over a range of five pH units, the response of the cell was found to be 57±1 mV/pH. Phenols were dissolved in *tert*-amyl or *tert*-butyl alcohol, and titrated with tetrabutylammonium hydroxide (Acros Organics, 0.1 N solution in toluene/methanol) that was normalized against a standard HCl solution. The mass of phenol used in each titration experiment was equivalent to about 0.2 mmol, to allow a titration volume of about 2 mL.

Between experiments, the H-cell and reference electrode annular container were cleaned with solvent and distilled water and oven dried. The dried glassware was assembled and filled, beginning with the reference cell solutions. Once solutions were at the proper level, the reference electrode was sealed into this assembly under nitrogen. Dried *t*-AOH was added to the other side of the cell under a blanket of nitrogen, and the glass electrode and titration burette were introduced, with the tip of the titration burette

immersed in the solution. Phenol was added to the cell, with constant stirring, and the cell was allowed to stabilize for at least 10 min. Once the cell voltage was stable, titration was started. Titrations were carried at least to the neutralization point, the data plotted, and the pK_a was calculated by graphic interpolation of the half neutralization point. Experiments in *t*-AOH were performed at least in duplicate. No effort was made to evaluate junction potentials in this cell, as these measurements are intended only for comparison to each other. The stability and reproducibility of the junction potentials was indicated by the reproducibility of the titration results.

One manifestation of the method in this experiment is noted at the beginning of each titration. When the titration is in its early stages, the phenol is predominantly present in the protonated form. Since this is the only electrolyte in the solution where the indicating electrode is located and the titrant is not in significant concentration yet, this solution has almost no charge carriers and the impedance is very high. The very low current flow produces a regular oscillation in the voltage reading of about ± 2 mV, most likely due to the stirring of the solution. As the titration proceeds, phenol dissociates and electrolyte concentration rises, corresponding to the disappearance of this oscillation.

Solubility Experiments. Experiments were performed to evaluate the solubilities of tetrabutylammonium tetrabutylborate, tetraphenylarsonium tetraphenylborate, tetraphenylarsonium iodide, sodium tetraphenylborate, and sodium iodide in *t*-AOH and water. We were unable to reliably quantify the very slight solubilities of the solutes tetrabutylammonium tetrabutylborate and tetraphenylarsonium tetraphenylborate, and others have reported similar problems with direct measurement of these solubilities.[13] For the more soluble salts, a series of tubes was prepared with 5.0 mL of freshly dried *t*-AOH and sufficient mass of dried solute to exceed saturation concentration. Saturation concentrations were estimated based on preliminary experiments of a similar nature. One set of solutions was stirred at the experimental

temperature representing solutions approaching saturation from under-saturation conditions, while another set, representing solutions approaching saturation from super-saturation, was stirred at elevated temperature for a period of time, then allowed to cool to the experimental temperature. Samples were analyzed over time until apparent equilibrium concentrations were reached. Analysis was spectrophotometric (Ph_4AsI at 265 nm, $NaBPh_4$ at 225 nm) for all but NaI, which was quantified by an Ag/Cr colorimetric titration.[14] Some inconsistencies in data were observed, and others have reported the decomposition of the tetraphenyl solutes in alcohols and in water.[9,13,15,16] Due to these problems, the solubility of tetraphenylarsonium tetraphenylborate was not determined directly in either water or t-AOH.

Partitioning Experiments. Phenyl phosphate was prepared in the bis-cyclohexylammonium salt form as described above. Conversion of this compound to the tetrabutylammonium form using cation exchange resin resulted in incomplete exchange. Therefore, the potassium salt was prepared by treating a 10-mM solution of the free acid form with KOH to pH 9, followed by cation exchange using Dowex 50X8-100 resin in the tetrabutylammonium form. A clean solution (8 mM) of the bis-tetrabutylammonium salt of phenyl phosphate was eluted from the column and used without further treatment.

Partitioning experiments were performed with the 8 mM aqueous solution described above at 4 °C in a coldroom. This solution and the alcohol were brought to the experimental temperature, and 5.00 mL of the aqueous solution and 5.00 mL of t-AOH were introduced into screw-top tubes with PTFE lined caps. The tubes were placed on a shaker for a measured period of time. To sample the solutions, tubes were removed from the mixers and centrifuged to speed separation of the layers. All equipment was maintained at the experimental temperature, and all handling of samples was performed in a coldroom. Aliquots were removed by pipette from both the aqueous and organic layers, and introduced into tubes containing premeasured mixtures for spectrophotometric

quantification. These mixtures were prepared such that, after addition of the experimental sample, each tube contained 2.0 mL of 50% ethanol 0.1N in NaOH, 0.5 mL of water, and 0.5 mL of t-AOH. The concentration of phenylphosphate was determined at 267 nm. In addition, samples were scanned for detection of phenolate ion at 289 nm, which would indicate hydrolysis of the phenylphosphate.

Results

Kinetics of Reactions in *tert*-Butanol and *tert*-Amyl Alcohol. Values of the first-order rate constants for the reactions of aryl phosphate dianions and monoanions were determined by spectrophotometrically following the liberation of the free phenols or phenolate anions. The first-order rate constants for the reactions of the monoanion and the dianion of p-nitrophenyl phosphate in both *tert*-butanol and in *tert*-amyl alcohol are shown in Tables 4-2 through 4-5. In these tables the r-squared value is provided as an illustration of the linearity of the initial rates method used. The r-squared value is a statistical measure of the linear correlation of all data points on a line, the closer to 1.00, the better the correlation. The half-lives are provided in appropriate units (either minutes or hours) to give the reader a sense of how the rate constants reported as s^{-1} relate to experimental duration.

The dianion of pNPP was found to undergo phosphoryl transfer to solvent approximately 9000-fold faster in t-AOH than in water, while the monoanion reacted about 16-fold more slowly in t-AOH. Similar results were obtained with *tert*-butanol, where the dianion was about 7500-fold faster and the monoanion 14-fold slower.

The data from these tables gave linear Eyring plots, Figures 4-4 through 4-7, which were used to calculate the enthalpies and entropies of activation, $\Delta H^{\ddagger}$ and $\Delta S^{\ddagger}$. For the purposes of clarity, Eyring plots are shown on the pages with the corresponding tables of data.

Table 4-2. Rate Constants for the Dianion of pNPP in *t*-Amyl Alcohol

T (°C)	k (sec^{-1})	r^2	$t_{1/2}$ (min)
33	5.19×10^{-5}	0.994	223
33	4.74×10^{-5}	1.000	244
33	4.02×10^{-5}	0.999	287
39	1.27×10^{-4}	0.999	91
39	1.52×10^{-4}	0.998	76
39	1.36×10^{-4}	0.999	85
50	9.13×10^{-4}	0.999	13
50	1.06×10^{-3}	0.999	11
50	9.25×10^{-4}	0.999	12
60	3.56×10^{-3}	1.000	3.2
60	2.96×10^{-3}	0.998	3.9
60	3.13×10^{-3}	0.998	3.7

Figure 4-4. Eyring plot for the solvolysis reaction of *p*-nitrophenyl phosphate dianion in *t*-amyl alcohol. Rate constants are in sec^{-1} and temperatures are K. Slope of the plot is $-15,560 \pm 520$, intercept is 35.3 ± 1.6.

Table 4-3. Rate Constants for the Dianion of pNPP in *t*-Butanol

T (°C)	k (sec^{-1})	r^2	$t_{1/2}$ (min)
28	1.56×10^{-5}	0.997	740
28	1.31×10^{-5}	0.996	880
28	1.24×10^{-5}	0.997	930
28	1.38×10^{-5}	0.998	840
35.5	5.83×10^{-5}	0.995	200
35.5	5.99×10^{-5}	0.99	190
35.5	6.83×10^{-5}	0.999	170
35.5	6.72×10^{-5}	1.000	170
35.5	5.10×10^{-5}	0.998	230
43.5	1.83×10^{-4}	0.997	63
43.5	1.84×10^{-4}	0.988	63
43.5	1.84×10^{-4}	0.998	68
53	1.16×10^{-3}	0.995	10
53	1.46×10^{-3}	0.999	7.9
53	1.37×10^{-3}	0.999	8.4
53	1.37×10^{-3}	0.998	8.4
61	2.21×10^{-3}	0.998	5.2
61	2.49×10^{-3}	0.995	4.6
61	2.81×10^{-3}	0.981	4.1
61	2.30×10^{-3}	0.994	5.0

Figure 4-5. Eyring plot for the solvolysis reaction of *p*-nitrophenyl phosphate dianion in *t*-butanol. Rate constants are in sec^{-1} and temperatures are K. Slope of the plot is -15,910 ± 510, intercept is 46.0 ± 1.6.

Table 4-4. Rate Constants for the Monoanion of pNPP in *t*-Butanol

T (°C)	k (sec^{-1})	r^2	t$_{1/2}$ (hr)
43	1.15x10^{-7}	0.950	1670
43	1.49x10^{-7}	0.986	1290
43	1.48x10^{-7}	0.977	1300
56	1.38x10^{-6}	0.999	140
56	1.51x10^{-6}	0.999	128
56	2.05x10^{-6}	0.996	94
65	4.85x10^{-6}	0.986	40
65	4.85x10^{-6}	0.993	40
65	4.54x10^{-6}	0.998	42
76	3.52x10^{-5}	0.995	5.5
76	5.13x10^{-5}	0.995	3.8
76	4.00x10^{-5}	0.998	4.8
76	5.28x10^{-5}	0.985	3.6
76	4.75x10^{-5}	0.997	4.1
76	5.01x10^{-5}	0.997	3.8
76	5.06x10^{-5}	0.996	3.8
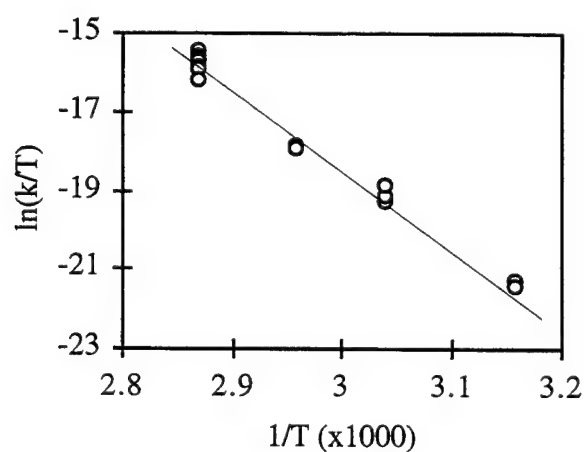
Figure 4-6. Eyring plot for the solvolysis reaction of *p*-nitrophenyl phosphate monoanion in *t*-butanol. Rate constants are in sec^{-1} and temperatures are K. Slope of the plot is -19,680 ± 460, intercept is 40.7 ± 1.3.

Table 4-5. Rate Constants for the Monoanion of pNPP in *t*-Amyl Alcohol

T (°C)	k (sec^{-1})	r^2	t$_{1/2}$ (min)
39	6.58x10^{-8}	0.947	2925
39	7.15x10^{-8}	0.969	2693
39	6.93x10^{-8}	0.983	2777
39	7.02x10^{-8}	0.992	2744
49.5	4,35x10^{-7}	0.988	443
49.5	3.80x10^{-7}	0.990	507
49.5	3.80x10^{-7}	0.996	507
65	3.87x10^{-6}	0.999	50
65	4.43x10^{-6}	0.998	43
65	4.20x10^{-6}	0.998	46
84.5	7.33x10^{-5}	0.998	2.6
84.5	6.65x10^{-5}	1.000	2.9
84.5	6.20x10^{-5}	0.993	3.1
84.5	6.03x10^{-5}	0.997	3.2
84.5	6.85x10^{-5}	0.993	2.8
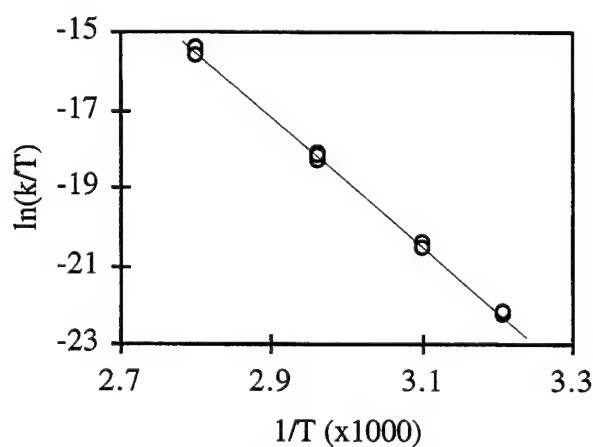
Figure 4-7. Eyring plot for the solvolysis reaction of *p*-nitrophenyl phosphate monoanion in *t*-amyl alcohol. Rate constants are in sec^{-1} and temperatures are K. Slope of the plot is -16,400 ± 120, intercept is 35.3 ± 0.4.

The rate and activation parameter data together with literature values for the aqueous reactions are summarized in Table 4-6 A and B.

The kinetic data for the reactions of the dianions of a series of aryl phosphates in t-AOH are recorded in Table 4-7. These data were used to construct the Brønsted plot in Figure 4-8. The rates for *meta*-substituted and for *para*-substituted compounds fall on separate but parallel lines with slopes of -1.1 ± 0.1.

Phenolic pK$_a$ Values in *tert*-Amyl Alcohol and *tert*-Butanol. The pK$_a$ values for the substituted phenols were measured in anhydrous alcohols as described in the experimental section. The values are tabulated in Table 4-8, and are plotted against their literature aqueous pK$_a$ values in Figure 4-9. The wider range of pK$_a$ values for the phenols in the nonaqueous solvent as compared to the range observed in water is consistent with previous observations.[17]

Solvent Partitioning Studies. Partitioning of the phenyl phosphate dianion between water and t-AOH was studied with the bis-tetrabutylammonium salt of phenyl phosphate. Phenyl phosphate was chosen due to its relatively slow rate of hydrolysis in t-AOH. The experiments were performed at 4 °C in order to further minimize hydrolysis. The free energy of transfer from water to t-AOH is calculated by equation 1 (bis-tbaPP = bis-tetrabutylammonium phenyl phosphate):

$$\Delta G_{tr}(\text{water}/t\text{-AOH})(\text{bis-tbaPP}) = RT\ln(P)[18] \tag{1}$$

where P is the ratio of solubilities in water and t-AOH. The value for P was found to be 9.4 ± 0.1. The free energy of transfer is calculated to be 1.24 ± 0.01 kcal/mol. This represents a destabilization of the ground state of the bis-tetrabutylammonium phenyl phosphate in changing solvent from water to t-AOH.

Single Ion Solvation Studies of the Arylphosphate Dianion. In order to isolate the thermodynamics of the solvation of single ions, extrathermodynamic

Table 4-6. Rates and Activation Parameters for Reactions of p-Nitrophenyl Phosphate

	aqueous	t-butanol	t-amyl alcohol
A. Dianion			
k at 39°C, sec^{-1}	1.6×10^{-8}	1.2×10^{-4}	1.4×10^{-4}
$k_{solv}/k_{aqueous}$	1	7500	8750
$\Delta H^{\ddagger}$, kcal/mol	30.6	31.6 ± 1.0	30.9 ± 0.3
$\Delta S^{\ddagger}$, eu	+3.5	$+24.5 \pm 0.8$	$+23.0 \pm 0.3$
$\Delta G^{\ddagger}$, kcal/mol	29.5	24.0 ± 1	23.7 ± 0.3
source	Kirby and Jencks[4]	this work	this work
B. Monoanion			
k at 39°C, sec^{-1}	1.1×10^{-6}	7.7×10^{-8}	6.8×10^{-8}
$k_{solv}/k_{aqueous}$	1	0.07	0.06
$\Delta H^{\ddagger}$, kcal/mol	25.4	37.1 ± 0.9	32.6 ± 1.0
$\Delta S^{\ddagger}$, eu	-4.5	$+27.7 \pm 0.7$	$+13.4 \pm 0.8$
$\Delta G^{\ddagger}$, kcal/mol	26.8	28.5 ± 0.9	28.4 ± 1.0
source	Kirby and Vargolis[5]	this work	this work

Table 4-7. Rate Constants for Substituted Phenyl Phosphate Dianions in t-Amyl Alcohol

functional group	T (°C)	k (sec^{-1})	r^2	t$_{1/2}$ (hr)
4-cyano	60	1.33×10^{-4}	0.994	1.4
4-cyano	60	1.18×10^{-4}	0.995	1.6
4-cyano	39	3.47×10^{-6}	0.989	56
4-cyano	39	4.13×10^{-6}	0.993	47
4-cyano	39	3.12×10^{-6}	0.996	62
4-cyano	39	3.55×10^{-6}	0.997	54
4-amido	60	2.83×10^{-5}		6.8
4-amido	39	2.98×10^{-6}	0.987	65
4-amido	39	2.53×10^{-6}	0.989	76
4-amido	39	2.25×10^{-6}	0.982	86
4-amido	39	2.70×10^{-6}	0.989	71
3,5-dinitro	39	2.23×10^{-5}	0.993	8.6
3,5-dinitro	39	2.20×10^{-5}	0.998	8.8
3,5-dinitro	39	1.85×10^{-5}	0.987	10
3,5-dinitro	39	1.92×10^{-5}	0.990	10
3-chloro	39	4.73×10^{-8}	0.894	4,070
3-chloro	39	4.33×10^{-8}	0.981	4,440
3-chloro	39	3.35×10^{-8}	0.900	5,750
3-chloro	39	4.88×10^{-8}	0.944	3,940
3-nitro	39	2.78×10^{-7}	0.922	690
3-nitro	39	3.82×10^{-7}	0.859	500
3-nitro	39	4.20×10^{-7}	0.938	460
3-nitro	39	2.65×10^{-7}	0.961	730
4-bromo	39	6.70×10^{-7}	0.994	290
4-bromo	39	8.02×10^{-7}	0.995	240
4-bromo	39	6.88×10^{-7}	0.995	280
4-phenyl	39	8.18×10^{-9}	0.979	23,500
H	39	6.53×10^{-9}	0.993	29,500
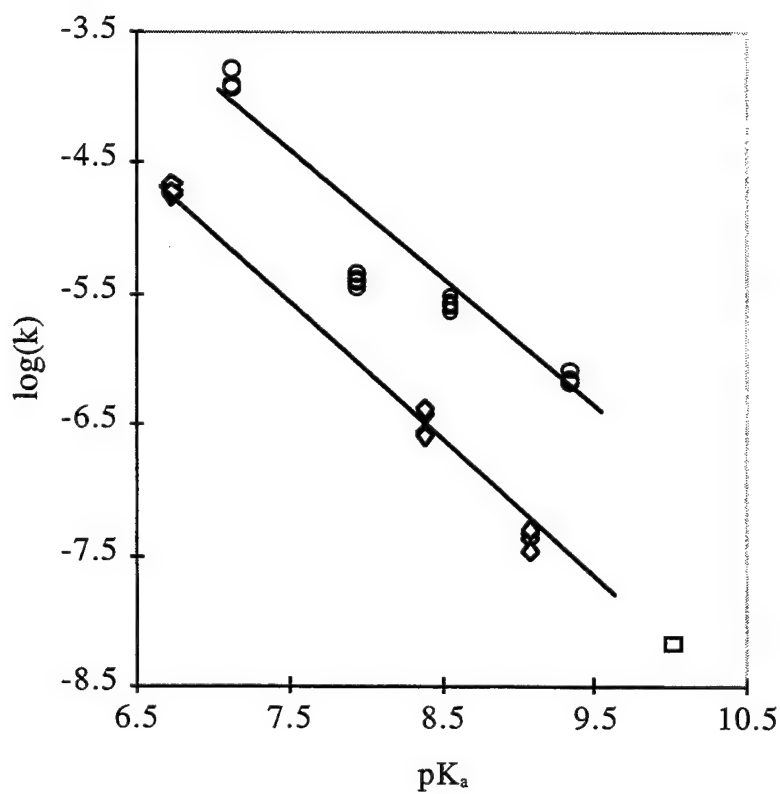
Figure 4-8. Brønsted plot for solvolysis of substituted aryl phosphates in *tert*-amyl alcohol. Circles represent *para*- substituted aryl phosphates, diamonds represent *meta*-substituted aryl phosphates, the square is phenyl phosphate. The slope of the best-fit line for *para*-substituted compounds is -1.14 ± 0.12, and that for *meta*-substituted compounds is -1.11± 0.02.

Table 4-8. pK$_a$ Values for Substituted Phenols in Aqueous Solution in *tert*-Butyl Alcohol and in *tert*-Amyl Alcohol

	pK$_a$		
substituent	aqueous[a]	*tert*-amyl alcohol[b]	*tert*-butyl alcohol[b]
4-nitro	7.14	10.0	10.57(10.48)[19]
4-cyano	7.95	11.83	12.5
4-amido	8.56[20]	13.95	.
4-bromo	9.34	15.00	15.35
4-phenyl	9.51	15.75	
H	10.00	16.20	16.82(16.64)[19]
3,5-dinitro	6.73[21]	9.37	9.98
m-nitro	8.39	12.97	13.84
m-chloro	9.02	14.06	

[a]Aqueous values are from the CRC Handbook of Biochemistry and Molecular Biology, Physical Chemical Data, Part 1 unless otherwise specified. [b]Values in *tert*-butyl and *tert*-amyl alcohol are from this work unless otherwise specified.
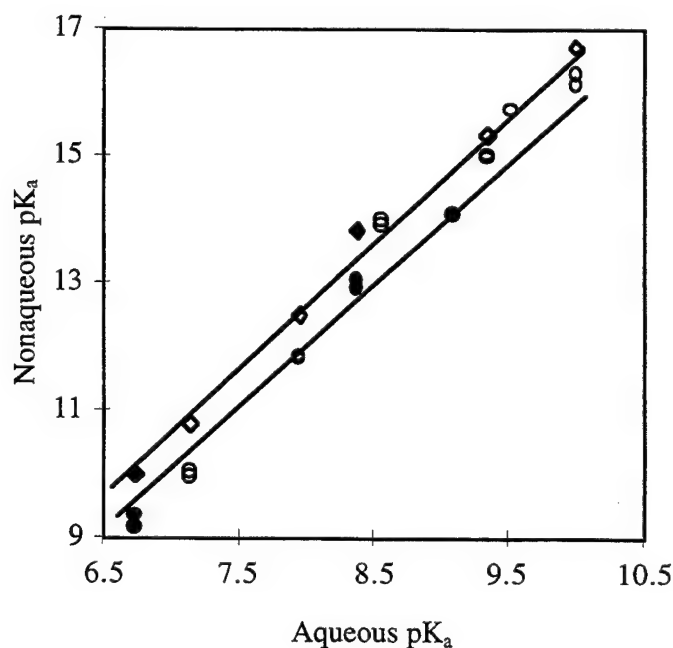
Figure 4-9. Comparison of aqueous and nonaqueous pK$_a$s of the substituted phenols from Table 4-8. Substituted phenolic pK$_a$s in *tert*-butanol are represented by diamonds, and pK$_a$s in *tert*-amyl alcohol are represented by circles. Filled shapes represent *meta*-substituted phenols, open shapes represent *para*-substituted phenols.

assumptions are used. These assumptions are based on the observation that when both the cation and anion of an ion pair are large, structurally similar, and radially symmetric, the charge is essentially shielded from the solvent, and solvent interactions are with a dispersed charge density on the outer surface of the ion. Therefore, solvent interactions with both ions are essentially equal, and any thermodynamic parameters of solvation for the ion pair can be divided equally between the ions. In some applications of the extrathermodynamic assumption investigators have used compounds with somewhat dissimilar structures, for example the use of triisoamylbutylammonium tetraphenylborate.[22] If the extrathermodynamic assumption can be used to equate the thermodynamic contributions of these two ions, then it is reasonable for us to assume that the free energy of transfer from water to t-AOH for the tetraphenylarsonium ion is a good approximation for that of the tetrabutylammonium ion.

The activities of the solutes used in this study were assumed to be close enough to unity to be disregarded, given the dilute concentrations at saturation and the qualitative nature of the conclusions that are drawn. The free energies of solvation can then be approximated from the solubility data using equation 2.

$$\Delta G_s = - RT \ln(K_{sp}) \tag{2}$$

The solubilities of tetrabutylammonium tetrabutylborate and salts of its ions were investigated in an attempt to either directly measure the solubility of tetrabutylammonium tetrabutylborate or to solve for its free energy of solvation through a thermodynamic cycle. These efforts were hindered by the extremely low solubility of tetrabutylammonium tetrabutylborate and the high solubility of some of the salts in t-AOH, which precluded using a thermodynamic cycle to obtain its free energy of solvation indirectly. Due to these difficulties, we decided to use a similar approach with tetraphenylarsonium tetraphenylborate, a more frequently used and widely accepted

subject of studies involving the extrathermodynamic assumption. Since the direct determination of the concentration of Ph_4AsBPh_4 in t-AOH was not reliable, saturation concentrations of Ph_4AsI, $NaBPh_4$, and NaI in t-AOH were measured at 25 °C for use in the thermodynamic cycle shown in Figure 4-10. Solubilities and free energies of solvation in t-AOH are given in Figure 4-10. Applying the extrathermodynamic assumption the free energy of solvation of the Ph_4As^+ ion in t-AOH = 9.4 kcal/mol.

The next step in this process is to compare the $\Delta G_s(t$-AOH) to the ΔG_s(water) to calculate the free energy of transfer of the species from water to t-AOH. The solubility of Ph_4AsBPh_4 in water is very low, and in our hands direct attempts to determine the equilibrium concentration again proved to be unreliable. The high solubilities of NaI and $NaBPh_4$ in water means that activities cannot be assumed to be approximately equal to concentration, and so the thermodynamic cycle approach cannot be used. A literature value for ΔG_s(water) of Ph_4AsBPh_4, which is derived from indirect methods, is 23.5 kcal/mol,[9] which leads to ΔG_s(water)(Ph_4As^+) = 11.8 kcal/mol.

$$Ph_4AsI \quad ---> \quad Ph_4As^+ + I^-$$

$$NaBPh_4 \quad ---> \quad Na^+ + BPh_4^-$$

$$\underline{Na^+ + I^- \quad ---> \quad NaI}$$

$$Ph_4AsBPh_4 \quad --> \quad Ph_4As^+ + BPh_4^-$$
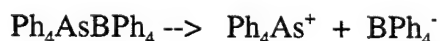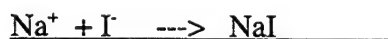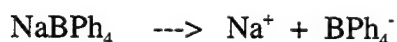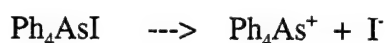
Solute	Solubility (M)	ΔG_s (kcal/mol)
Ph_4AsI	3.31×10^{-5} (1)	12.2
$NaBPh_4$	8.0×10^{-4} (2)	8.4
NaI	2.23×10^{-1} (1)	1.8
Ph_4AsBPh_4		18.8 (calc. from cycle above)

Figure 4-10. The thermodynamic cycle used to determine the free energy of solvation of Ph_4AsBPh_4 in *tert*-amyl alcohol with the concentrations at saturation at 25 °C.

This allows calculation of the free energy of transfer for the Ph_4As^+ ion from water to t-AOH according to equation 3:

$$\Delta G_{tr}(water/t\text{-}AOH)\,(Ph_4As^+) = \Delta G_s(t\text{-}AOH)(Ph_4As^+) - \Delta G_s(water)(Ph_4As^+) \qquad (3)$$

Using our experimental results and the literature value for $\Delta G_s(water)(Ph_4AsBPh_4)$, we obtain a $\Delta G_{tr}(water/t\text{-}AOH)\,(Ph_4As^+)$ of -2.4 kcal/mol. To a first approximation this result is reasonable, given the free energies of transfer from water to various alcohols for the Ph_4As^+ ion as reported by Marcus:[22] -5.8 kcal/mol for methanol, -5.1 kcal/mol for ethanol, and -6.0 kcal/mol for n-propanol; and -3.5 kcal/mol for the BPh_4^- ion in isopropanol.

The experimental cycle to derive the ΔG for transfer of the phenyl phosphate dianion can be completed by measuring the partitioning of bis-tetraphenylarsonium phenyl phosphate between water and in t-AOH. This will allow calculation of the free energy of transfer for the compound, from which the contributions of the tetraphenylarsonium ions can be subtracted. Unfortunately, we were unable to isolate the pure bis-tetraphenylarsonium salt of phenyl phosphate. As an approximation, using the extrathermodynamic assumption that the free energies of solvation for tetraphenylarsonium and for tetrabutylammonium are similar, we can estimate this quantity as follows (PP = phenyl phosphate):

$$\Delta G_{tr}(water/t\text{-}AOH)(PP) = \Delta G_{tr}(water/t\text{-}AOH)((n\text{-}Bu_4N^+)_2\,PP)$$
$$- 2 \times \Delta G_{tr}(water/t\text{-}AOH)(\,Ph_4As^+) \qquad (4)$$

$$\Delta G_{tr}(water/tAOH)(PP) = 1.24\ kcal/mol - 2 \times (-2.4\ kcal/mol) = 6\ kcal/mol \qquad (5)$$

This demonstrates a significant destabilization of the phenyl phosphate dianion in t-AOH relative to water, presumably arising from less efficient solvation by t-AOH.

Discussion

The Impact of Solvation Effects on Catalysis. Phosphate monoesters exhibit bell-shaped pH-rate profiles for hydrolysis with an optimum pH of around 4, and a lower, pH-independent rate at higher pH values, indicating that the monoanionic species is more reactive than the dianion (Figure 1-5). Nevertheless, the less reactive dianion is typically the substrate for phosphatases, and these enzymes exhibit catalytic efficiencies (defined as the ratio of k_{cat} to the uncatalyzed rate constant) of 10^{10} or more. The large rate accelerations provided by phosphatases have led to proposals that, while dissociative transition states occur in uncatalyzed reactions, enzymatic phosphoryl transfer from monoesters may proceed by a more associative mechanism. Since all known phosphatases bear positively charged residues and/or metal ions at their active sites, it is postulated that this charge may function electrostatically in the same way as alkylation does in causing a mechanistic shift, that is, by neutralizing the negative charge on the substrate and enhancing the electrophilicity of the phosphorous atom toward attack. This notion is intuitively attractive since phosphate triesters are considerably more reactive than their monoester counterparts. Another motivating factor has been a perceived difficulty in rationalizing how an enzyme can stabilize a dissociative transition state.[23] Methods by which an enzyme could stabilize a dissociative phosphoryl transfer have been considered.[24]

The descriptive term "dissociative" can be misleading, however; the aqueous hydrolysis reference reaction for phosphatases, while having a dissociative transition state, is nonetheless A_ND_N. Entropy effects are therefore still important, and overcoming entropic barriers is a potential source of catalytic efficiency. Despite this, entropic contributions have been omitted from many discussions of the catalytic efficiencies of phosphatases. A discussion follows of entropic and enthalpic effects in the rate enhancements observed in *tert*-butanol and in *t*-AOH.

The Dianion Reaction. Our work reported in this study was motivated by an interest in analyzing how the microenvironment can affect the kinetics and mechanism of phosphoryl transfer reactions. An essential difference in the phosphoryl transfer from the dianion of pNPP to anhydrous *tert*-butanol, where this acceptor also is the reaction solvent, is the observation of racemization at phosphorus when the reactant pNPP was made chiral by the use of oxygen isotopes.[6] This outcome was interpreted to indicate the formation of a free metaphosphate intermediate. This outcome was in contrast to the observation in more nucleophilic solvents such as methanol, where the product had inverted configuration consistent with nucleophilic participation in the transition state of a concerted mechanism.[7] Because we were interested in performing solvent partitioning studies in order to determine differences in solvation free energies, we also examined reaction in *t*-AOH, which is structurally very similar but is much less miscible with water. Since this alcohol is, if anything, even more hindered as a nucleophile than *tert*-butanol, we assume that the stereochemical course of the phosphoryl transfer reaction in these two alcohols is the same. The very similar kinetics and activation parameters measured for the two reactions support this assumption.

The reduced activation barrier in the tertiary alcohols can occur either by raising the free energy of (destabilizing) the reactant, by lowering the free energy of the transition state, or a combination of both. The portion of the more favorable entropy of activation from reduced solvent reorganization could arise from less effective solvation (increased free energy) of the substrate or from stabilization (reduced free energy) of the transition state, relative to the aqueous reaction. In order to determine the contribution of differences in the free energies of solvation (ΔG_s) of the reactant, we compared the free energies of the tetra-butylammonium salt of pNPP in water and in *t*-AOH. The difference in the solvation free energies in the two solvents, shown as ΔG_{tr} (water/*t*-AOH) in Figure 4-11, represents the free energy of transfer of the substrate from water to the alcohol.

The solvent partitioning experiments thus indicate that the overall reduction in $\Delta G^\ddagger$ of 5.8 kcal/mol in the dianion reaction can be attributed to approximately 1 kcal/mol of ground state destabilization, which presumably reflects less effective solvation of the substrate in t-AOH, with the balance being a transition state effect.

The change to a two-step mechanism in the tertiary alcohols offers one explanation for the faster rate, since the entropy of activation should be more favorable for a reaction involving rate-limiting unimolecular dissociation than for one in which nucleophilic participation by a second molecule occurs. This is revealed in the more favorable $\Delta S^\ddagger$ for the reactions in *tert*-butanol and t-AOH compared to the aqueous reaction. Another possible energetic source for the enhanced rate is the weaker hydrogen-bonding ability of these solvents compared to that of water. The driving force for the dissociative reaction (whether in a fully two-step dissociative mechanism or in a concerted mechanism with a dissociative transition state) can be rationalized as coming from the internal electron donation of the negative charges on the nonbridge oxygen atoms. Indeed, the loss of these charges by alkylation deactivates this pathway and leads to mechanisms with greater
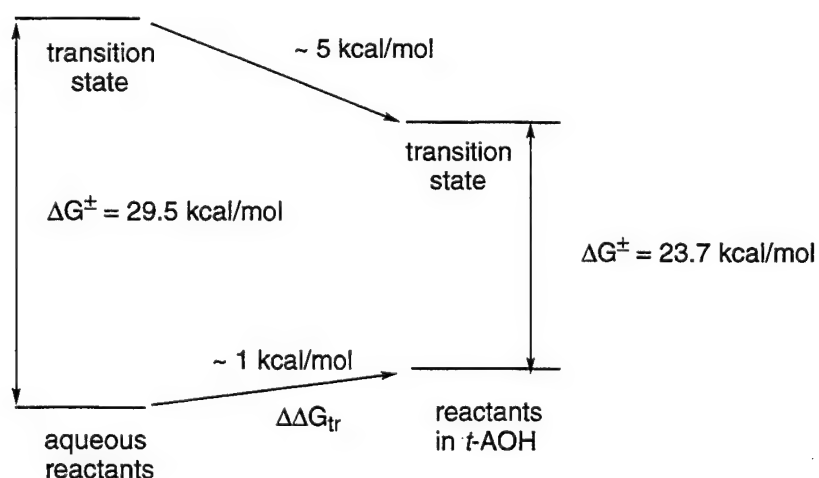
Figure 4-11. Effect of changing solvent on ground state and transition state free energies. Solvent transfer is from water to *tert*-amyl alcohol, with relative free energy based on calculations discussed in the text.

nucleophilic participation. If these charges are less involved in stabilizing interactions such as hydrogen bonds with the solvent, they ought to be more capable of acting as internal nucleophiles in expelling the leaving group. This effect has been postulated to explain the acceleration of the hydrolysis of pNPP dianion in aqueous DMSO or HMPA.[8] In the reactions examined in this study in *tert*-butanol and *t*-AOH, the tetrabutylammonium counterion is also unable to interact effectively with these nonbridge oxygen atoms, due to the steric shielding of the positive charge by the bulky *n*-butyl groups. The single ion ΔG_{tr} of 6 kcal/mol measured for transfer of the phenyl phosphate dianion from water to *t*-AOH confirms that this ion is considerably less solvated in the latter solvent. An increased hydrolysis rate due to the loss of stabilizing hydrogen bonding interactions with the solvent should be analogous to the rate accelerations observed in the alkaline hydrolysis of esters caused by added aprotic cosolvents; the enthalpy of activation for the saponification of ethyl acetate and ethyl benzoate are reduced by 4 and 6 kcal/mol, respectively, in aqueous DMSO versus aqueous ethanol.[25] The increased rates and lower $\Delta H^{\ddagger}$ were attributed to decreased solvation of hydroxide ion. While these are bimolecular reactions and the phosphoryl transfers in the tertiary alcohols are unimolecular, the rate-limiting steps share the features of an anionic species providing the driving force for the reaction, with negative charge becoming more dispersed in the transition state. In the ester saponification reactions a larger destabilization of the reactants relative to the transition state resulted in a significant net reduction in $\Delta H^{\ddagger}$.[25] Thus the expectation is reasonable that rate enhancement caused by desolvation of the dianionic phosphate reactant should show up as a decrease in $\Delta H^{\ddagger}$.

Surprisingly, the activation parameters (Table 4-6A) for the reaction of the dianion of pNPP reveal that the rate enhancements for the reaction in *tert*-butanol and in *t*-AOH are due entirely to a more favorable entropy of activation. The activation enthalpy is unchanged within experimental error from the value in the aqueous reaction. This

indicates that the loss of stabilizing hydrogen bonding interactions with the nonbridge oxygens may not be a major factor in the rate accelerations in these alcohols, and that any such destabilization is evidently felt equally in both the ground state and transition state. A possible alternative explanation for the similar enthalpies of activation is a coincidental compensation for the loss of a stabilizing bonding interaction in the transition state with the nucleophile (present in the aqueous concerted reaction but absent in the stepwise reaction in t-AOH) by a more favorable $\Delta H^{\ddagger}$ for the unimolecular dissociation in t-AOH compared with the same hypothetical process in water. Given a similar degree of bond cleavage to the leaving group in the transition state, the unimolecular dissociation should have a higher $\Delta H^{\ddagger}$ than the concerted reaction since in the latter case the enthalpic cost of bond cleavage is partly offset by formation of the new bond. Though bond formation to the nucleophile in the transition state is small in the aqueous reaction, there should be some enthalpic effect in lowering $\Delta H^{\ddagger}$, which will not be present in the reaction in t-AOH. It is possible that solvation differences lower the enthalpic barrier for unimolecular dissociation in t-AOH by an amount similar to the lost bonding interactions, leaving an unchanged overall $\Delta H^{\ddagger}$. Though perhaps unlikely, this possibility cannot be ruled out.

There are two sources for the more favorable entropy of activation. One is the aforementioned change from a bimolecular concerted reaction in water to a mechanism with rate-limiting unimolecular dissociation. Even though bonding between the phosphorus atom and the nucleophile is thought to be small in the transition state of the aqueous reaction, a solvent molecule must still be recruited to assume an apical position in the trigonal bipyramidal transition state, with an associated loss of entropy. In addition, water is a more highly structured solvent than the tertiary alcohols. Solvent reorganization must occur in the transition state, driven by the change in geometry and in charge distribution. The overall charge of the transition state is the same as that of the ground state; however, since the size of the structure increases and charge is dispersed, a

larger solvation shell is required in the transition state with an accompanying loss in entropy. This solvent effect should be more pronounced in the more highly structured solvent water than in the tertiary alcohols. The latter solvents are not without structure, however, and so the potential entropic acceleration obtainable from eliminating solvent reorganization is probably not fully realized in these solvents.

Although a nucleophilic role is eliminated in the rate-determining step in the reactions in *tert*-butanol and *t*-AOH, isotope effect data[26] indicate that this occurs with no change in the transition state structure of the pNPP reactant. The ^{18}O isotope effects in the non-bridging oxygen atoms and in the bridging oxygen atom and the ^{15}N isotope effects for the reaction of pNPP in *tert*-butanol are very similar to those for the aqueous reaction.[26] That the transition state structure within the reactant is unchanged in the $D_N +$ A_N reaction compared with the $A_N D_N$ one is not surprising in view of the very small degree of bond order to the nucleophile in the transition state of the aqueous reaction. Evidently the loss of this interaction is not accompanied by significant changes in the degree of bond cleavage to the leaving group, or in the transition state structure of the phosphoryl group. Thus the entropic accelerations observed do not result from making the reaction mechanism more dissociative with respect to the degree of transition state bond cleavage to the leaving group, but arise solely from eliminating the need for nucleophilic participation and from possible contributions from solvent reorganization.

A fair question is whether the rate enhancement observed with pNPP also occurs with less activated phosphate esters. The rates were therefore measured for the phosphoryl transfer reaction with a range of substituted phenyl phosphates, and the results were plotted versus the aqueous pK_a values for the leaving groups in Figure 4-8. Although the rates for *meta*- and *para*-substituted aryl phosphates fall on separate but parallel lines, the Brønsted slopes of -1.1 are very similar to the Brønsted slope of -1.2[5]

reported for the aqueous reaction. Thus similar rate enhancements are seen with all of the aryl phosphates tested.

The occurrence of separate lines for *meta-* and *para-*substituted aryl phosphates contrasts with the aqueous reactions where the hydrolysis rates of *meta-* and *para-*substituted phenyl phosphates fall on the same line in the analogous Brønsted plot, both for the reaction of the dianion and for that of the monoanion.[5] We initially hypothesized that the reason might be differential changes in the pK_a values of *meta-*substituted phenols compared to *para-*substituted ones in *t*-AOH. If this were the case, then if the rate constants were plotted against the true pK_a values in the reaction solvent, then the *meta-* and *para-* substituted compounds should fall on the same line as they do in the aqueous reaction.

We measured the pK_a values of the phenols in anhydrous *tert*-butanol and in *t*-AOH using an electrochemical method[19] described in the experimental section. The results are given in Table 4-8. The measured pK_a values in *t*-AOH are higher than those in water and cover a larger span compared to the aqueous values. Both of these effects are expected from the results of previous work on nonaqueous pK_a values of phenols.[17] While there is always some uncertainty in the assignment of absolute pK_a values in nonaqueous solvents, insofar as they can be directly compared with the aqueous values, the method can be counted upon to give precise measurements of the relative nonaqueous pK_a values of the phenols. The pK_a values determined in *t*-AOH are plotted against the aqueous values in Figure 4-9, which reveals a linear correlation between the two values. *Meta-* and *para-*substituted phenols fall on the same correlation line, indicating that there is no anomalous perturbation of pK_a values in the alcohol by *meta-* versus *para-*substituents. Thus the hypothesis that *meta-* versus *para-*substitution causes a differential perturbation in the leaving group pK_a values is incorrect. We are presently uncertain as to the source of the difference in rates between these two classes of compounds in *t*-AOH.

The Monoanion Reaction. The thermodynamic and kinetic data for the monoanion reaction are collected in Table 4-6B. In contrast to the situation in aqueous solution where the monoanions of phosphate monoesters are the more reactive species, in the tertiary alcohols the monoanion reaction is 2000-fold slower than the dianion. The monoanions react more slowly in the alcohols than in aqueous solution, in contrast to the behavior of the dianion. In both alcohols, a more favorable entropy of activation is more than offset by an increased enthalpy of activation.

This increase in $\Delta H^{\ddagger}$ most likely arises from greater difficulty in transferring the proton from a nonbridge oxygen atom of the reactant to the bridging oxygen atom. In the alcohol solvents the pK_a value of the phosphate group will be higher, making proton removal more energetically difficult. In addition, in water this proton transfer could well occur via an intervening water molecule; this would allow a six-membered transition state for the proton transfer process, which is sterically preferable to the four-membered one which would be operative in its absence. The steric bulk of the tertiary alcohols makes them less able to similarly assist in the proton transfer.

Stereochemical studies of the monoanion reaction in *tert*-butanol have not been carried out. Therefore, the more favorable entropies of activation cannot with assurance be ascribed to a change in the molecularity of these reactions, though it is likely. In addition, the reason for the less favorable entropy of activation in the reaction of the monoanion in *t*-AOH compared to *tert*-butanol is uncertain. In both reactions the predominant reason for the slower rates is a higher enthalpic barrier relative to the aqueous reaction.

Significance for Entropic Considerations in Phosphatase Reactions. The results presented here have significance for the enzymatic reactions of phosphatases. Enzymes confer significant entropic advantage relative to uncatalyzed reactions in solution. It has been estimated that 10^8 M is the approximate maximum value for the

advantage of an enzymatic reaction compared with a corresponding bimolecular reaction from entropic advantages, in reactions in which the transition state is relatively tight so that a large loss of entropy is required for its formation.[27] The catalytic benefit of induced intramolecularity in a dissociative phosphoryl transfer reaction has previously been pointed out, and a catalytic enhancement of approximately 10^2-fold was attributed to the positioning of a metal-bound hydroxide ion and phosphoryl group by Mg^{2+} ions in phosphorylated 4-morpholinopyridine/Mg^{2+} complex.[28] In general, however, entropy considerations are often omitted in assessments of the sources for the catalytic efficiencies of phosphatases and in considerations of how these enzymes might catalyze a reaction having a dissociative transition state. This may be because dissociative transition states like those operative in phosphate monoester reactions may seem like unlikely candidates for potential acceleration from entropic effects.

The term "dissociative," while generally an accurate description of the aqueous reaction, may convey the impression that there is no nucleophilic involvement in the transition state. However, the aqueous reference reactions are concerted, with nucleophilic participation in the transition state; even the weak bond formation to the nucleophile in this reaction nonetheless requires its proper positioning in the trigonal bipyramidal transition state. The removal of the associated entropic barrier must be considered as one source of the enzymatic efficiencies of phosphatases. In the ground states of a phosphatase-substrate complex, a nucleophile is already preassociated and the hydration shell has been removed, eliminating the need for solvent reorganization. The rate enhancement observed in these studies of nearly 10^4 is probably a lower limit for the rate enhancement from entropic considerations that are enjoyed by phosphatases. This is not to say that these enzymatic reactions proceed by a metaphosphate intermediate as in the tertiary alcohols. Quite the contrary, with a preassociated nucleophile in place a free metaphosphate intermediate is unlikely. However, the entropic advantage enjoyed in the

enzymatic reaction is the same as that gained from eliminating the need to recruit a disordered solvent molecule to serve the nucleophilic role in the tertiary alcohol reactions. The factor of 10^4 is a significant fraction of the overall catalytic rate enhancement achieved by some phosphatases.

Mechanistic Conclusions. Subsequent to the report of racemization in the reaction of pNPP in *tert*-butanol,[6] alternative explanations have been suggested that avoid the formation of metaphosphate. One is the possibility that a bridge-protonated *tert*-butyl phosphate is initially formed that undergoes reversible and rapid phosphoryl transfer with other solvent molecules before loss of the proton, which is necessary to form a stable product.[29] It has also been postulated that an associative mechanism occurs, forming a pentacoordinate intermediate which may undergo pseudorotations, leading to racemized product.[30] Both of these alternative explanations are unlikely in view of the significantly more positive entropy of activation in the *tert*-butanol reaction. If the first alternative mechanism were operative, since nucleophilic participation is still important in the transition state, no significant change in the entropy of activation should be seen. If the phosphorane mechanism were operative, then the entropy of activation should be large and negative, as it is for reactions of phosphate triesters which have such associative transition states. Typical reactions of this type exhibit entropies of activation of -35 eu,[31] dramatically different from the experimental value reported here. The reported results are in best agreement with the originally reported explanation for racemization, namely, a change to a dissociative S_N1-type of mechanism.

References

(1) Thatcher, G. R. J.; Kluger, R. *Adv. Phys. Org. Chem.* **1989**, *25*, 99-265.

(2) Hengge, A. C. In *Comprehensive Biological Catalysis*; Sinnott, M. Ed.; Academic Press: San Diego,CA, 1998; Vol. 1, pp 517-542.

(3) Guthrie, R. D.; Jencks, W. P. *Acc. Chem. Res.* **1989**, *22*, 343-349.

(4) Kirby, A. J.; Jencks, W. P. *J. Am. Chem. Soc.* **1965**, *87*, 3209-3216.

(5) Kirby, A. J.; Varvoglis, A. G. *J. Am. Chem. Soc.* **1967**, *89*, 415-423.

(6) Friedman, J. M.; Freeman, S.; Knowles, J. R. *J. Am. Chem. Soc.* **1988**, *110*, 1268-1275.

(7) Buchwald, S. L.; Friedman, J. M.; Knowles, J. R. *J. Am. Chem. Soc.* **1984**, *106*, 4911-4916.

(8) Abell, K. W. Y.; Kirby, A. J. *Tet. Lett.* **1986**, *27*, 1085-1088.

(9) Cox, B. G.; Hedwig, G. R.; Parker, A. J.; Watts, D. W. *Aust. J. Chem.* **1974**, *27*, 477-501.

(10) Bourne, N.; Williams, A. *J. Org. Chem.* **1984**, *49*, 1200-1204.

(11) Hoff, R. H.; Hengge, A. C. *J. Org. Chem.* **1998**, *63*, 195.

(12) Marple, L. W.; Fritz, J. S. *Anal. Chem.* **1962**, *34*, 796-800.

(13) Fuchs, R.; Bear, J. L.; Rodewald, R. F. *J. Am. Chem. Soc.* **1969**, *91*, 5797-5800.

(14) Greenberg, A. E.; Trussel, R. R.; Clesceri, L. S., Eds. *Selected Physical and Chemical Standard Methods for Students, Based on Standard Methods for the Examination of Water and Wastewater, 16th Edition*; American Public Health Association: Washington, D. C., 1986.

(15) Alexander, R.; Parker, A. J.; Sharp, J. H.; Waghorne, W. E. *J. Am. Chem. Soc.* **1972**, *94*, 1148-1158.

(16) Popovych, O.; Friedman, R. M. *J. Phys.. Chem.* **1966**, *70*, 1671-1673.

(17) Marple, L.; Fritz, J. S. *Anal. Chem.* **1963**, *35*, 1223-1227.

(18) Leo, A.; Hansch, C.; Elkins, D. *Chem. Rev.* **1971**, *71*, 525.

(19) Fritz, J. S.; Marple, L. W. *Anal. Chem.* **1962**, *34*, 921-924.

(20) Caldwell, S. R.; Newcomb, J. R.; Schlecht, K. A.; Raushel, F. M. *Biochem.* **1991**, *30*, 7438-7443.

(21) Dean, J. A. Ed. *Lange's Handbook of Chemistry*; 13th ed.; McGraw-Hill: New York, 1985, p 842.

(22) Marcus, Y. *Pure Appl. Chem.* **1983**, *55*, 977-1021.

(23) Hasset, A.; Blattler, W.; Knowles, J. R. *Biochem.* **1982**, *21*, 6335-6340.

(24) Admiraal, S. J.; Herschlag, D. *Chem. & Biol.* **1995**, *2*, 729-739.

(25) Haberfield, P.; Friedman, J.; Pinkston, M. F. *J. Am. Chem. Soc.* **1972**, *94*, 71-74.

(26) Hengge, A. C.; Edens, W. A.; Elsing, H. *J. Am. Chem. Soc.* **1994**, *116*, 5045-5049.

(27) Jencks, W. P. *Adv. Enzymol.* **1975**, *43*, 219-410.

(28) Herschlag, D.; Jencks, W. P. *Biochem.* **1990**, *29*, 5172-5179.

(29) Herschlag, D.; Jencks, W. P. *J. Am. Chem. Soc.* **1989**, *111*, 7587-7596.

(30) Florian, J.; Warshel, A. *J. Phys. Chem. B* **1998**, *102*.

(31) Khan, S. A.; Kirby, A. J. *J. Chem. Soc. (B)* **1970**, 1172-1182.

CHAPTER 5

THE EFFECTS ON GENERAL ACID CATALYSIS FROM MUTATIONS OF THE INVARIANT TRYPTOPHAN AND ARGININE RESIDUES IN THE PROTEIN-TYROSINE PHOSPHATASE FROM *YERSINIA*[1]

Abstract: Key roles in the enzymatic mechanism of the protein-tyrosine phosphatase from *Yersinia* have been proposed for the Asp356 (general acid catalysis), Trp354 (hinge pin for a flexible loop that includes the general acid) and Arg409 (substrate binding) residues. The catalytic reactions produced by the native form of the enzyme and the D356N, W354F, W354A, R409A, and R409K single mutants; and the D356N/A-R409A/K double mutants were studied with the substrate *p*-nitrophenyl phosphate using heavy atom kinetic isotope effects and pH dependent kinetic studies. The effects of pH on the kinetic isotope effects with the native enzyme were determined to provide a scale for the magnitude of change in isotope effects as the extent of protonation by the general acid changes. The kinetic isotope effects in the substrate were measured at the nonbridging oxygen atoms [$^{18}(V/K)_{nonbridge}$], at the bridging oxygen atom, the site of bond cleavage [$^{18}(V/K)_{bridge}$], and at the nitrogen atom in the nitrophenol leaving group [$^{15}(V/K)$]. Previous studies have shown that isotope effects clearly reveal the presence or lack of general acid catalysis when Asp356 is altered by mutation. Comparisons of data from the reactions of Trp354 mutants with the native enzyme and general acid mutants reveal that the mutation of Trp354 to phenylalanine causes a partial impairment of the general acid, while mutation to alanine completely disables it. This can be rationalized by examination of the steric implications of these mutations. The mutation of Arg409 to

---

[1]Coauthored by Richard H. Hoff, Alvan C. Hengge, Yen-Fang Keng, and Zhong-Yin Zhang.

alanine and lysine indicated a partial impairment of the general acid. The investigation of the double mutants allowed the isolation of the impact of the arginine residue on the nature of the transition state. Indications from these isotope effects were that the arginine plays an important role in transition state stabilization, but does not alter the distribution of charge. This is in contrast to some proposals concerning the role of positive charge in enzymatic transition states. The combined perspective of kinetic data, substrate binding data, and kinetic isotope effects allows a clarification of the role of Arg409 in positioning substrate and the roles of other enzymatic residues to facilitate catalysis.

Introduction

The catalytic power of many enzymes is intimately connected to their ability to undergo conformational changes, which can allow the repositioning of catalytic groups and the reorienting of the electrostatic environment in the time dimension, or, in other words, at different points along the reaction coordinate. One such family of enzymes is the protein-tyrosine phosphatases, which utilize a general acid to protonate the leaving group in the phosphoryl transfer reaction.[1] The general acid, a conserved aspartate, resides on a flexible loop that is brought into the active site by a conformational change that is induced by substrate binding.[2] It is a simple matter to measure reductions in catalytic efficiency that result from mutations which interfere with conformational changes that are important in catalysis, but it is much more difficult to examine details of how such hindrances in the conformational mobility of an enzyme affect the chemical mechanism or the transition state for catalysis. In this work we have examined in detail changes in the transition state for catalysis that result from mutations to two residues that affect the conformational change that controls general acid catalysis in the *Yersinia* PTPase.

Protein-tyrosine phosphatases (PTPases) have an essential role in signal transduction, and together with protein-tyrosine kinases they control the phosphorylation

level of proteins in the cell. The *Yersinia* PTPase is one member of this enzyme family, which in common with all members of the PTPase family shares the active site signature motif $C(X_5)R(S/T)$.[3] PTPases share a common catalytic mechanism, utilizing a cysteine nucleophile (Cys403 in the *Yersinia* enzyme) in the formation of a thiophosphoryl intermediate which undergoes hydrolysis by water in a second step.[3-5] The invariant arginine residue (Arg409 in *Yersinia* PTPase) functions in substrate binding and in transition state stabilization. The initial phosphoryl transfer step is assisted by general acid catalysis by a conserved aspartate (Asp356 in the *Yersinia* PTPase) that protonates the leaving group.[1] The aspartate resides on a flexible loop that undergoes a major conformational change upon binding of substrate, or small anions such as tungstate.[6] This loop is termed the WpD loop for the conserved Trp-Pro-Asp sequence. The *Yersinia* PTPase has only a single tryptophan residue, which is located at a position that is invariant among all PTPases at one of the hinge positions of the flexible loop. The overall catalytic mechanism including the conformational change involving WpD loop movement is shown in Figure 5-1, and the relative positions of the critical residues are shown in Figure 5-2.

Structural data have shown that Trp354 is located at one of the hinge positions of the WpD loop and has interactions with Arg409 that are important in closure of the loop upon binding of substrate or structurally analogous small anions.[2] Kinetic studies have

$$E + ROPO_3^{2-} \underset{k_{-1}}{\overset{k_1}{\rightleftharpoons}} E \cdot ROPO_3^{2-} \underset{k_{-2}}{\overset{k_2}{\rightleftharpoons}} E^* \cdot ROPO_3^{2-}$$

$$\xrightarrow{k_3} ROH$$

$$E^*-PO_3^{2-} \rightleftharpoons E^* \cdot Pi \rightleftharpoons E + Pi$$
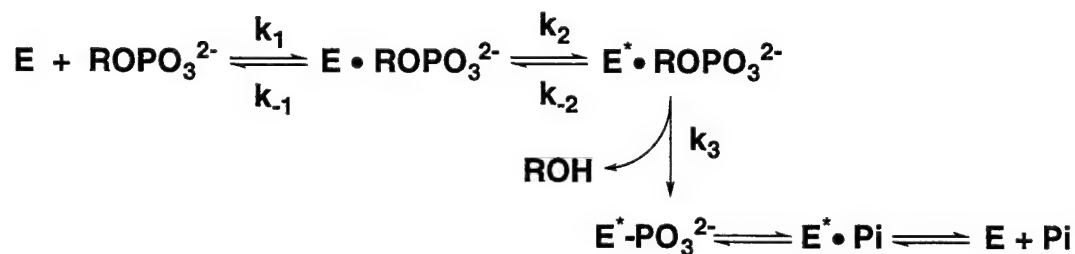
Figure 5-1. Schematic of the overall catalytic mechanism of the YOP51 PTPase phosphoryl transfer reaction.
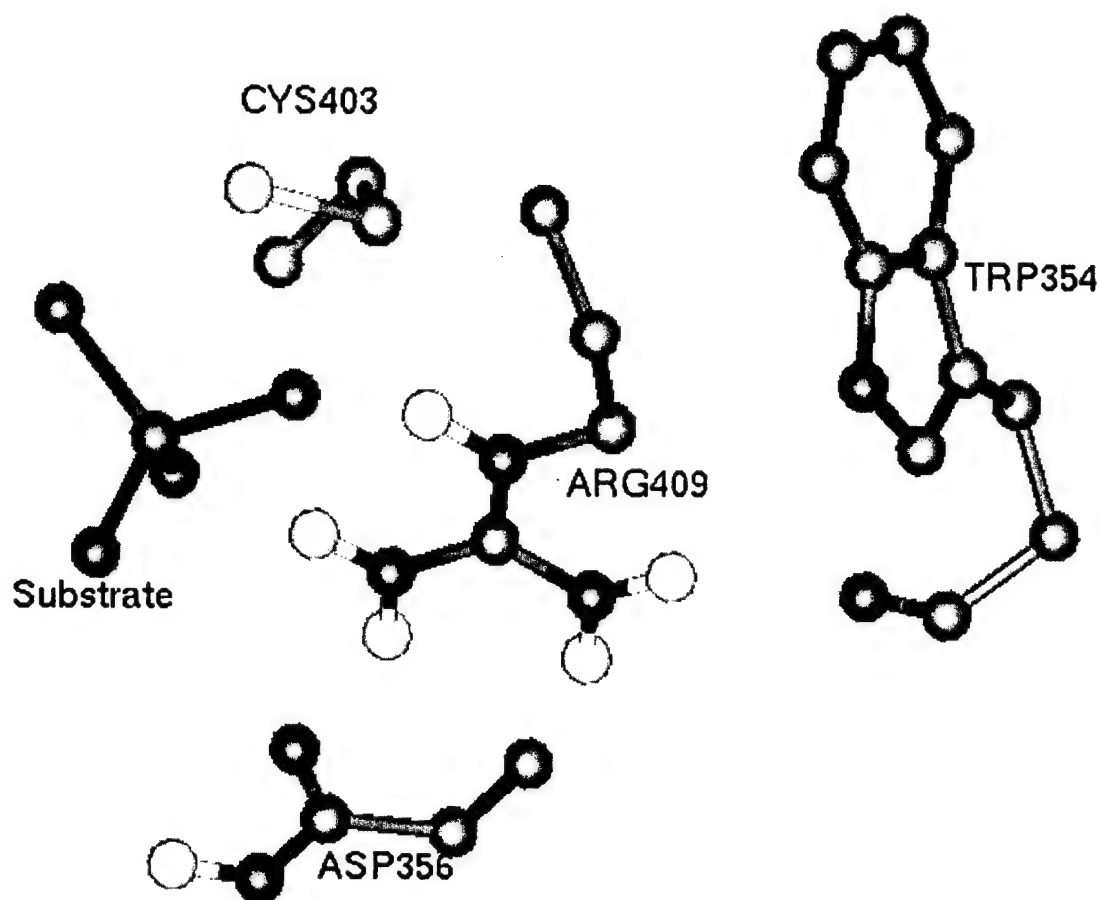
Figure 5-2. Critical residues of *Yersinia* PTPase active site. Relative positions of residues reflect coordinates of crystal structure from Fauman et al.[8] Color codes for all structures shown are: H=white, C=green, N=blue, O=red, S=yellow, and other=magenta.

confirmed that mutation of Trp354 results in impaired catalytic efficiency.[7] The W354F and W354A mutants exhibit k_{cat} values which are decreased 200- and 480-fold, respectively, from the native enzyme using *p*-nitrophenyl phosphate (pNPP) as substrate, while the K_m is relatively unaffected by these mutations. The pH dependency of these mutants suggests that these mutations affect the competence of general acid catalysis, most likely by interfering with movement of the WpD loop on which the general acid resides. Mutation of Arg409 to lysine or to alanine results in decreases in k_{cat} by 17,000- and 14,000-fold, respectively,[9] yet these mutated enzymes still display activity that is

10^4-fold above the uncatalyzed hydrolysis rate. A key role in substrate binding and transition state stabilization has been attributed to this residue. However, the pH dependency of these mutants suggests that these mutations also affect the competence of general acid catalysis.

In this study we report the use of heavy-atom isotope effects to study the mechanistic consequences of mutations to Trp354 and to Arg409. The substrate for the isotope effect measurements was pNPP, which is shown in Figure 1-7 with the positions at which isotope effects have been measured. Prior studies have shown that isotope effects in all three positions are sensitive to the presence or lack of general acid catalysis in the transition state of the reactions of PTPases with this substrate.[10-12] In particular the isotope effects in the leaving group were significantly affected by mutation of the general acid Asp356.

The isotope effects reveal details of how the mutations in the hinge residue Trp354 and the substrate recognition residue Arg409 affect the proper positioning of the general acid, which occurs by movement of the flexible loop. If movement of the loop is impaired, the general acid could be either rendered inoperable, or it may be able to assume a position in which only partial proton transfer is accomplished in the transition state. Comparisons of these isotope effects results with previously reported data from the reaction of the native enzyme and of general acid mutants reveal details of how mutations of the Trp354 and Arg409 residues affect the functionality of the general acid.

Phosphatases utilize differing strategies and functional groups in achieving catalysis, with the only common feature being the presence of positive charge in the active site.[13] The arginine residue in *Yersinia* is of special interest due to its role as the bearer of positive charge in the active site. Evidence from decades of experiments indicates that in solution phosphate monoesters undergo reactions via a loose transition state in which the phosphoryl group resembles metaphosphate.[14,15] In an effort to explain the enormous

rate enhancements observed with enzymatic phosphoryl transfer, there has been speculation that the presence of positive charge changes the transition state to a more associative one. The change from dianionic ground state to metaphosphate in a dissociative process represents a decrease in charge on the phosphoryl group in the transition state.[16] A decrease in negative charge should lead to decreased stabilization afforded by the positive charge in the active site. The positive charge would better stabilize a transition state where negative charge increased, suggesting that the enzymatic pathway may be associative. X-ray structures of a number of phosphoryl transfer enzymes with transition state analogs have been interpreted to favor a transition state that is more associative than the uncatalyzed reaction.[17,18] It has been proposed that the presence of positively charged arginine residues around a transferred phosphoryl group demands an associative transition state for enzymatic phosphoryl transfer.[19]

The evaluation of the isotope effects with the Arg409 mutants will allow an interpretation of the role of the positive charge in the active site. Because this residue plays a role in the positioning of the general acid, the interpretation of isotope effects with Arg409 mutants is somewhat convoluted. By preparing double mutants of the enzyme, it is possible to disable the general acid with one mutation, then examine the effects of Arg409 without the complications of its impact on the general acid. This should allow development of a clearer picture of the specific transition state alterations brought about by the presence of positive charge.

Experimental

Synthesis of Compounds. [^{14}N]-p-nitrophenyl phosphate, [^{15}N, nonbridge-^{18}O$_3$]-p-nitrophenyl phosphate, [^{14}N]-p-nitrophenol, and [^{15}N, ^{18}O]-p-nitrophenol were synthesized as described previously.[20] [^{14}N]-p-nitrophenol, and [^{15}N, ^{18}O]-p-nitrophenol were then mixed to reconstitute the natural abundance of ^{15}N, and then the mixture was

phosphorylated to produce *p*-nitrophenyl phosphate using the same method as referred to above. This mixture was used for determination of $^{18}(V/K)_{bridge}$. The [^{14}N]-*p*-nitrophenyl phosphate and [^{15}N, nonbridge-$^{18}O_3$]-*p*-nitrophenyl phosphate were also mixed to reconstitute the natural abundance of ^{15}N. This mixture was used for determination of $^{18}(V/K)_{nonbridge}$. The isotopic abundance of the mixtures was determined by isotope ratio mass spectrometry.

Isotope Effect Determinations. Isotope effects experiments were run at 100 mM buffer and 1 mM in EDTA. The buffer solutions and corresponding pH ranges were: pH 5-6, acetate; pH 6-7, succinate; pH 7-8, 3,3-dimethyl glutarate; pH 8-9.5, TRIS; and pH 10 and up, CHES (2-(cyclohexylamino)ethanesulfonic acid). Typical isotope effects experiments were performed with a 10 mL reaction volume at a substrate concentration of about 15 mM. Small scale experiments were run to determine the quantity of enzyme required to hydrolyze one third to one half of the substrate in a reasonable amount of time (generally less than twenty four hours) before the activity of the enzyme declined significantly. Reactions were begun with 100 micromoles or more of the substrate and sufficient enzyme used so that background hydrolysis rates were less than 10% of the enzymatic rate. Background rates were determined by parallel solution experiments under the enzymatic experimental conditions, but with no enzyme added.

Isotope effect experiments were run in triplicate and reactions were stopped at extents of reaction ranging from 40% to 60% conversion of substrate. At the time that the reaction was stopped, an aliquot was removed for determination of the precise fraction of reaction. This aliquot was split, with one portion analyzed immediately by placing an aliquot into a measured portion of 0.1 N NaOH and measuring the absorbance at 400 nm. The other portion was placed in TRIS buffer at pH 9.0 with alkaline phosphatase for several hours, followed by a similar measurement of absorbance at 400 nm. The ratio of the absorbances of these two samples gave the extent of reaction.

Reactions were stopped by cooling on ice and titrating to pH 5, followed by extracting three times with an equivalent volume of diethyl ether to quantitatively remove the *p*-nitrophenol which was the product of the enzymatic reaction. The aqueous layer containing the residual substrate was evaporated briefly under vacuum to remove dissolved ether, an equivalent volume of the TRIS pH 9.0 buffer added, and the pH adjusted to 9.0 with NaOH. This sample was treated with alkaline phosphatase to quantitatively hydrolyze all of the remaining substrate. This mixture was then titrated back to pH 5.0 and extracted with ether, the *p*-nitrophenol in this ether fraction representing the residual substrate from the enzymatic reaction. The ether fractions were dried over magnesium sulfate, filtered, and the solvent removed by rotary evaporation. The *p*-nitrophenol was sublimed under vacuum at 90 °C, and 1.0–1.5 mg samples were prepared for isotopic analysis using an ANCA-NT combustion system in tandem with a Europa 20-20 isotope ratio mass spectrometer.

Isotope effects were calculated from the isotopic ratio in the *p*-nitrophenol product at partial reaction (R_p), in the residual substrate (R_S), and in the starting material (R_O). Equation 1 was used to calculate the observed isotope effect from R_p and R_O at fraction of reaction *f*. Equation 2 was used to calculate the observed isotope effect from R_S and R_O.

$$\text{isotope effect} = \frac{\log(1-f)}{\log\left[1 - f\left(\frac{R_P}{R_O}\right)\right]} \tag{1}$$

$$\text{isotope effect} = \frac{\log(1-f)}{\log\left[(1-f)\left(\frac{R_S}{R_O}\right)\right]} \tag{2}$$

Thus each experiment yields two independent determinations of the isotope effect. R_O was determined in two ways. Samples of unreacted substrate were subjected to isotope

ratio mass spectroscopic analysis and, as a control, these results were compared to those from *p*-nitrophenol isolated after complete hydrolysis of substrate using the isolation and purification procedures used in the isotope effect experiments. The agreement of these two numbers demonstrates that, within experimental error, no isotopic fractionation occurs as a result of the procedures used to isolate and purify the *p*-nitrophenol.

The ^{18}O isotope effects were measured by the remote-label method,[21] as previously described for the solution reactions of pNPP.[20] In these experiments the nitrogen atom in the substrate is used as a reporter for isotopic changes at the bridging oxygen atom or the nonbridging oxygen atoms. These experiments yield an observed isotope effect which is the product of the effects due to ^{15}N and to ^{18}O substitutions. The observed isotope effects from these experiments must therefore be corrected for the ^{15}N effect and for incomplete levels of isotopic incorporation in the starting material. The general method for making these corrections is as described by Caldwell et al.[22]

To prepare the substrate for a remote label experiment, a substrate that is depleted in the remote reporter position and natural abundance in all other isotopes is mixed with substrate that is labeled in both the reporter and discriminating atom positions. In order to make accurate corrections, the depleted and the double labeled materials must be characterized to determine the extent of isotopic substitution. For the pNPP substrate used in this work, the following measurements must be made:

z = fraction of ^{15}N in the pure ^{14}N material used to make the double labeled mixture

x = fraction of ^{15}N in the pure double labeled material

y = for $^{18}O_{bridge}$, the fraction of ^{18}O in the double labeled material

for $^{18}O_{nonbridge}$, the fraction of double labeled material that has ^{18}O in all three nonbridge positions

The mixture must then also be characterized to determine the fraction of double

labeled material, defined as b, which should be close to natural abundance for ^{15}N. The measurements made on the isotopic abundance of the mixture components and the mixture itself are then combined to create a correction factor as shown in equation 3.

$$Q = (1-b)\frac{z}{bx} \approx \frac{z}{b} \tag{3}$$

This represents the extent to which light material in the mixture is depleted below natural abundance.

For the ^{18}O isotope effect that we are evaluating, equation 4 is then used to calculate the isotope effect per atom. Inputs to this equation include the observed isotope effect (P), which is a product of the isotope effect of the remote label and the isotope effect of the discriminating atom; the ^{15}N isotope effect (R), derived from natural abundance material; and the number of discriminating atoms (i), which is either one for the bridge ^{18}O or three for the nonbridge.

$$^{18}k(\text{per atom}) - 1 = \frac{\sqrt[i]{\dfrac{P/R}{1 - Q\left(\dfrac{P}{R} - 1\right)}}}{1 - \left(\sqrt[i]{\dfrac{P/R}{1 - Q\left(\dfrac{P}{R} - 1\right)}}\right)\left(\dfrac{1-y}{i}\right)} \tag{4}$$

Equation 4 produces the corrected per atom isotope effect, which is then raised to the power of the number of discriminating atoms to provide the reported isotope effect.

Preparation, Isolation, and Purification of Mutated Enzymes. All work to prepare, purify, and characterize the wild-type and mutant enzymes was done in the laboratory of Dr. Zhong-Yin Zhang. Substitutions at specific residues of the Yersinia

PTPase were made by site-directed mutagenesis according to the procedure of Kunkel.[23] All mutations were verified by DNA sequencing. Wild-type enzyme and all mutants were expressed in *E.coli* and purified to homogeneity as previously described.[24] Chromatographic properties of the mutants showed no significant differences from the native enzyme.

Results

The kinetic isotope effects were measured by the competitive method using an isotope ratio mass spectrometer, which is the most accurate method for determining the small magnitudes of heavy atom isotope effects. Since the competitive method gives isotope effects on V/K,[25] the isotope effects reported are those for the first phosphoryl transfer step, from pNPP to the enzymatic cysteine nucleophile even though hydrolysis of the phosphoenzyme intermediate is the overall rate-limiting step.

Isotope effects for the single mutants were calculated as described in the experimental section and are reported in Table 5-1. A similar list of results for the double mutants is given in Table 5-2. The ^{18}O isotope effects reported in these tables have been corrected for the effect of the remote ^{15}N label and for levels of isotopic incorporation. Multiple determinations were made of each isotope effect and the reported values are the averages of all determinations made under each set of experimental conditions. The isotope effects obtained from the isotopic ratios of product, and those obtained from the isotopic ratios of residual substrate, agreed within experimental error in all cases and were averaged together to give the results shown in the tables.

The substrate for the enzymatic reaction is the dianion of pNPP; the pK_a of this compound has been reported as 4.96 [26] and as 5.05.[27] This means that for the isotope effect reactions conducted at pH 6.0 about 10% of the substrate was present in solution as the monoanion. Fractionation will occur between the monoanion and dianion species at

Table 5-1. Kinetic Isotope Effects for Hydrolysis of pNPP by YOP51 and Mutants[a]

enzyme and pH	$^{15}(V/K)$	$^{18}(V/K)_{bridge}$	$^{18}V/K)_{nonbridge}$
native enzyme, pH 5[b]	-0.01 (3)	1.52 (6)	-0.02 (13)
D356N, pH 6[b]	0.24 (5)	2.75 (16)	0.22 (5)
pH 9	0.26 (2)	3.22 (6)	0.21 (4)
W354A, pH 6	0.21 (2)	3.10 (5)	0.38 (5)
pH 9	0.21 (4)	3.20 (6)	0.36 (5)
W354F, pH 6	0.13 (2)	2.40 (10)	0.15 (8)
pH 9	0.22 (1)	3.20 (10)	0.39 (4)
R409K, pH 6	0.20 (5)	2.73 (3)	0.49 (7)
R409A, pH 6	0.14 (3)	2.00 (5)	0.21 (7)
uncatalyzed aqueous dianion, pH 10[c]	0.34 (2)	2.30 (5)	-0.07 (7)

[a]Matrix includes the pH conditions under which isotope effects were determined. Additional detail is provided in the experimental section. Error in the last digit is in parentheses following each isotope effect. Literature values are provided for comparison. [b]From Hengge et al.[12] [c]From Hengge et al.[20]

Table 5-2. Kinetic Isotope Effects for Hydrolysis of pNPP by YOP51 Double Mutants[a]

enzyme	$^{15}(V/K)$	$^{18}(V/K)_{bridge}$	$^{18}V/K)_{nonbridge}$
R409K/D356N	0.22 (1)	3.17 (2)	0.45 (2)
R409K/D356A	0.23 (1)	3.22 (9)	0.45 (2)
R409A/D356N	0.24 (4)	3.40 (11)	0.27 (5)
R409A/D356A	0.25 (1)	3.10 (11)	0.30 (2)

[a]All experiments were done at pH 6.0. Error in the last digit is in parentheses following each isotope effect.

the nonbridge oxygen position due to the isotope effect for deprotonation of 1.5%.[28] The observed values for ^{18}(V/K)$_{nonbridge}$ in Table 5-1 have been corrected for this isotopic fractionation as previously described.[20] Previously determined[12] isotope effects for the reactions of pNPP with native *Yersinia* PTPase and the D356N mutant are also reported in Table 5-1. Raw data and calculations are in Appendix B, Tables B-1 through B-17.

Discussion

Factors Influencing the Isotope Effects. The overall catalytic mechanism for PTPases is represented in Figure 5-1. Because the competitive method was used to measure the isotope effects in this study, they are effects on V/K and thus are effects on the part of the mechanism up to the first irreversible step, regardless of which step is rate-limiting in the overall enzymatic mechanism. Prior work with the PTPase from *Yersinia* has shown that the chemical step of phosphoryl transfer from pNPP to the enzymatic nucleophile Cys403 is rate-limiting for V/K, both for the native enzyme and for general acid mutants. The kinetic isotope effects with the substrate pNPP are not suppressed by commitment factors, and are the intrinsic ones for the transition state of the phosphoryl transfer step.[12]

Kinetic isotope effects can characterize reactions in detail, in particular yielding information about the structure of the transition state. In phosphoryl transfer reactions, the isotope effects ^{15}(V/K) and ^{18}(V/K)$_{bridge}$ measure charge delocalization in the leaving group and P–O bond cleavage, respectively. The secondary ^{15}(V/K) effect arises from delocalization of charge into the aromatic ring which involves contribution from a quinonoid resonance structure involving the nitro group.[29] The primary isotope effect at the scissile P–O bond, ^{18}(V/K)$_{bridge}$, gives a measure of the degree of cleavage of this bond in the transition state. Phosphate monoesters typically react via transition states characterized by extensive bond cleavage to the leaving group and only a small degree of bond formation to the nucleophile.[14,15] The solution and enzymatic reactions of the

dianion of pNPP exhibit $^{18}O_{bridge}$ isotope effects in the range from 2.02 to 3.0% and ^{15}N isotope effects of 0.28 to 0.39% when the leaving group departs as the negatively charged anion. When the leaving group is protonated in the transition state, as in the reactions of native PTPases, both of these isotope effects are reduced.[10-12,20] Protonation of p-nitrophenol is associated with an inverse ^{18}O isotope effect of -1.5%.[30] A transition state in which P-O bond cleavage and proton transfer are both far advanced would be expected to show an observed $^{18}(V/K)_{bridge}$ isotope effect of about +1.5%. This value is the product of the inverse equilibrium effect for protonation (-1.5%) and the maximum observed $^{18}O_{bridge}$ isotope effect (3.0%), assuming a large degree of P-O bond cleavage. This is very close to the value measured in reactions of pNPP with native YOP (Table 5-1) (1.52 ± 0.06%)[12] as well as with other native PTPases.[10,11] The secondary $^{15}(V/K)$ isotope effect measures charge development in the leaving group. Thus if protonation is synchronous with P-O bond cleavage, the leaving group should remain neutral and this isotope effect should be essentially zero. This is the case in the native YOP reaction ($^{15}(V/K)$ = -0.01 ± 0.03%).

Calculations predict inverse values of $^{18}(V/K)_{nonbridge}$ for dissociative transition states and normal values for tighter transition states where the phosphoryl group resembles a phosphorane.[31] Reported nonbridge ^{18}O isotope effects for reactions of monoester dianions in solution[20] are all small and inverse as predicted. Phosphate diesters and triesters have tighter transition states with considerable nucleophilic participation, and the nonbridge ^{18}O isotope effects for these compounds which have been reported are (with a single exception) normal, in the range of 0.40 to 2.50%.[32,33] The small inverse value for $^{18}(V/K)_{nonbridge}$ measured for the reaction of the native *Yersinia* PTPase with pNPP (Table 5-1) is replaced by a normal value in reactions of general acid mutants (Table 5-1). The same change is seen in the PTP1[12] and Stp1 PTPases,[10] as well as the dual-specificity phosphatase VHR,[11] which all share essentially identical

active sites. This change in the $^{18}(V/K)_{nonbridge}$ isotope effect suggests a transition state with more nucleophilic participation in the general acid mutants. Such a change is consistent with predictions from the Hammond postulate, where deactivation of the leaving group is predicted to result in a later, less dissociative transition state.

Thus, all three isotope effects in the substrate respond to protonation of the leaving group in the PTPase reaction. If movement of the WpD loop is hindered by a mutation in such a way that the extent of proton transfer in the transition state is reduced but not prevented, isotope effects should be observed that are intermediate between those when proton transfer is fully synchronized with P-O bond cleavage (as in the native enzyme) and when the leaving group bears a full charge (as in the general acid mutant).

Isotope effects have been measured for a number of phosphate esters in solution for which kinetic data suggest the range of transition states represented in Figure 1-3.[20,22,29,31-33] The cumulative data indicate that isotope effects can distinguish between the phosphorane-like transition states that exist with associative mechanisms and the metaphosphate-like transition states that characterize the dissociative mechanisms. This should allow detection of an enzyme-induced change in mechanism through the use of isotope effects. Calculations predict inverse nonbridge ^{18}O isotope effects for dissociative transition states and normal values for associative transition states.[31] Experimental results show small inverse $^{18}k_{nonbridge}$ isotope effects (-0.03 to -0.06%) for the pNPP monoester while $^{18}k_{nonbridge}$ for diesters and triesters range from 0.4 to 2.5%. Leaving group isotope effects also mirror what is indicated by linear free energy relationships, with the dissociative monoester reaction displaying ^{15}k effects of from 0.28 to 0.39% and $^{18}k_{bridge}$ of from 2.02 to 3%. The tighter transition states of the diester and triester reactions involve less bond cleavage to the leaving group and typically have ^{15}k effects of from 0.07 to 0.16% and $^{18}k_{bridge}$ in the range 0.39 to 0.60%.

Within this background, the isotope effects for the reactions of the *Yersinia*

PTPase with mutations at Trp354 and Arg409 can be evaluated for the effect of these mutations on the function of the general acid in the transition state of the catalytic reaction. The mutations at Arg409 and the double mutations which eliminate the general acid can further be assessed in terms of the overall associative or dissociative character of the transition state.

Effect of Tryptophan-354 Mutation to Alanine or Phenylalanine.
The isotope effects at pH 6 indicate that function of the general acid is effectively eliminated in the W354A mutant, but is only partially impaired in the W354F mutant. In the case of W354A, the isotope effects in the leaving group, $^{15}(V/K)$ and $^{18}(V/K)_{bridge}$, are very close to their values with the general acid mutant D356N. The same is true for $^{18}(V/K)_{nonbridge}$ where the change from the near zero value for this isotope effect seen in the native enzyme reaction to a small normal isotope effect mirrors the change induced by mutation of the general acid. These data all indicate that protonation of the leaving group is rendered inoperative by the W354A mutation and that the leaving group departs as the anion in the transition state of the catalytic reaction. By contrast for the reaction of W354F each of the isotope effects is intermediate between those for D356N and those for the native enzyme where protonation of the leaving group in the transition state is intact. This indicates that with the W354F mutant, partial proton transfer in the transition state occurs but protonation lags behind P-O bond cleavage, resulting in development of a partial negative charge on the leaving group. When the reactions of both W354A and W354F are examined at pH 9, where the general acid will be almost entirely deprotonated and thus far less effective regardless of its ability to assume proper positioning, the isotope effects for W354A are unchanged while those for W354F increase and are now equal to those for W354A and to those of D356N. This confirms that the general acid, while impaired, is still partially functioning in the W354F mutant at pH 6.

Further evidence of this difference in the extent of acid catalysis operative in these

two mutants is seen in their reported variations of k_{cat} with pH.[7] The W345A mutant shows a pH-rate profile similar in shape to that of D356N,[1] in which the bell-shaped profile of the native enzyme is replaced with a half-bell comprised of an acidic limb and a plateau above pH 5. The W354F exhibits the acidic limb and a maximum at pH 5, and then a small decrease between pH 5 and 6.5 followed by the same plateau value seen with W354A. The reported values for k_{cat} with pNPP at pH 5.5 are 601 s^{-1} for the native enzyme, 2.96 s^{-1} for W354F, and 1.26s^{-1} for W354A.[7]

The differential effects of the two mutations can be rationalized by an examination of the structure of the enzyme. X-ray structures[2,6,8] show that when an oxyanion such as sulfate binds at the active site, the Arg409 residue moves to form bidentate hydrogen bonds with two oxygen atoms of the anion. Structural changes in the active site result in the formation of a new hydrogen bond between Arg409 and the carbonyl oxygen atom of Trp354 (Figure 5-3).

As a result, the indole ring of Trp354 moves into a hydrophobic crevice, making
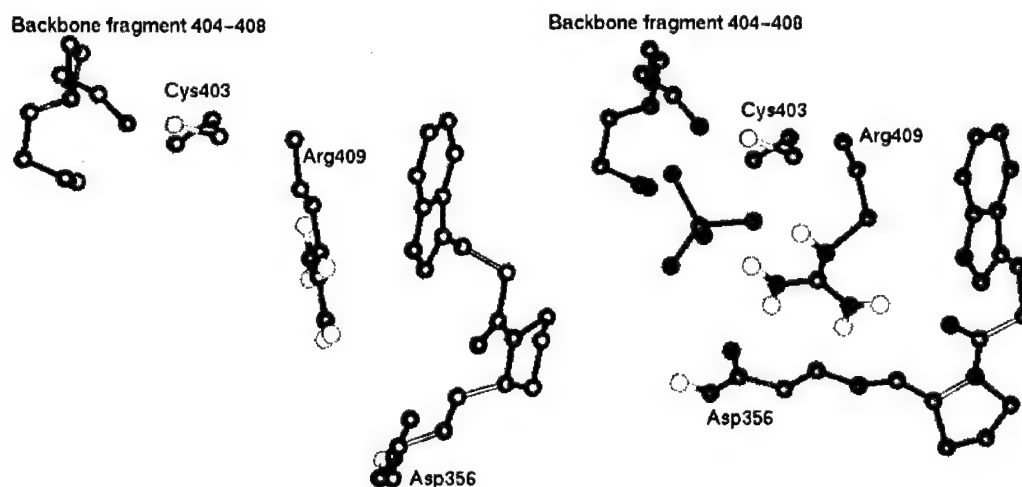
Figure 5-3. *Yersinia* PTPase active site with and without bound ligand. The two versions are from the same perspective. The left sketch has no oxyanion bound while the right sketch has a tetrahedral tungstate bound. In absence of the conformational changes that accompany oxyanion binding, note the orientation of the arginine guanidinium group. The general acid is not in position to protonate the leaving group.[6,8]

van der Waals contacts with the aliphatic portion of Arg409 as shown in Figure 5-4.
These interactions are associated with movement of the WpD loop to attain the closed
position when the oxyanion is bound. The mutation to phenylalanine leaves a more
isosteric side chain in the position occupied by the indole in the native enzyme, which
evidently is sufficient to allow movement of the loop to bring the general acid into
position for partial proton transfer in the transition state. Mutation to alanine completely
removes these van der Waals contacts, and both the pH-rate and isotope effect data
indicate that functioning of the general acid, and by inference movement of the WpD loop,
is inoperative in the W354A mutant. The mutants are shown in Figure 5-5.

Effect of Arginine Mutation to Alanine or Lysine. The R409 residue
not only assists in substrate binding and transition state stabilization, but it also plays a
role in facilitating movement of the WpD loop by way of the conformational changes
described previously. Binding of substrate is also assisted by hydrogen bonds to
backbone amide groups in the active site as shown in Figure 5-6.
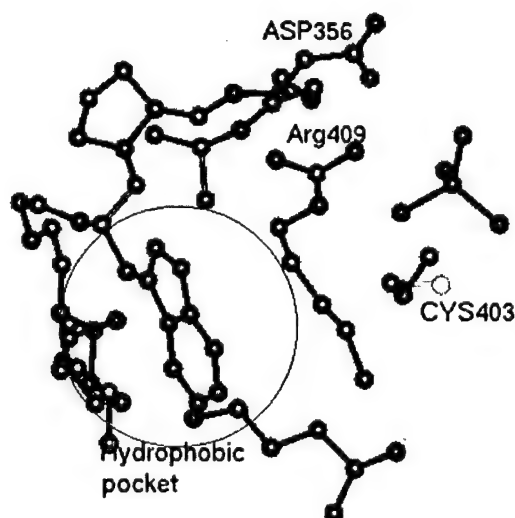
Figure 5-4. Illustration of the hydrophobic pocket occupied by the indole group of
Trp354 when tungstate is bound. The indole group is in black to highlight its position.
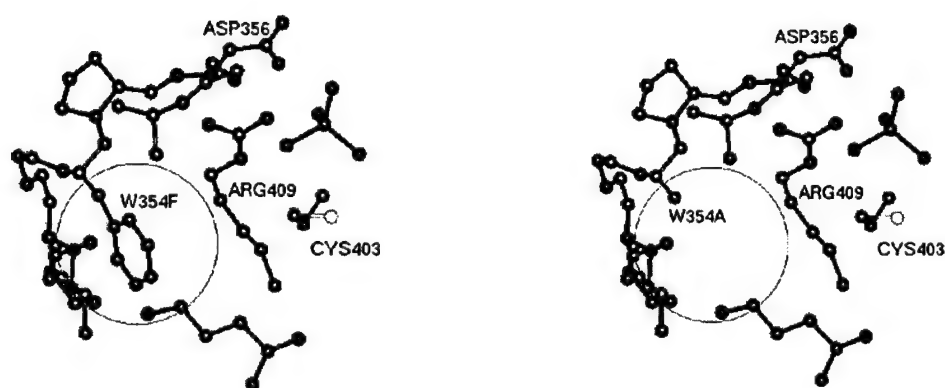
Figure 5-5. Comparison of W354F and W354A mutants. Note the loss of van der Waals contacts with Arg409. Replacement residues are shown in black. Structures were derived by simple graphic replacement, and have not been minimized to reflect secondary structural changes as a result of the replacements.[8]
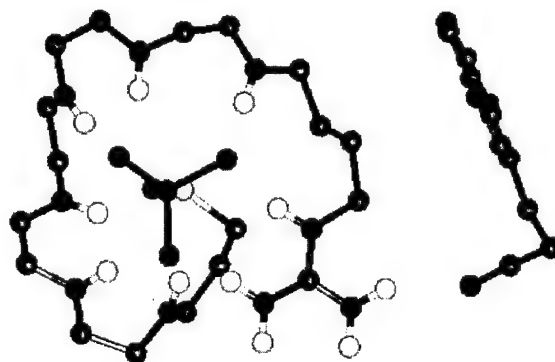
Figure 5-6. Active site of *Yersinia* PTPase with backbone amides between residues 403 and 409 shown. Note the network of potential hydrogen bonds between substrate oxyanions and amide hydrogens. Arg409 contributes to this network, but substrate could bind even in the absence of hydrogen bonds donated by Arg409.[8]

In the R409K mutation the guanidinium group is replaced by an amino group which, while maintaining a positive charge, can donate far fewer hydrogen bonds. In addition the positioning of the cationic group and its hydrogen bonds in the active site are different from their positions in the native enzyme (Figure 5-7). All three isotope effects for the reaction of pNPP with the R409K mutant are close to their values in D356N, indicating that this mutation results in the disabling of general acid catalysis. The leaving group is therefore departing with substantial negative charge. The data for the R409A mutant indicate that partial protonation of the leaving group is occurring in the transition state for catalysis by this mutant. It is interesting, and somewhat counterintuitive, that mutation of arginine to alanine should be less disabling to movement of the WpD loop than mutation of this residue to lysine. This can be explained by considering kinetic data reported earlier for these enzymes.[3]

Table 5-3 compares the k_{cat} and K_m for the mutants and the wild type enzyme. The R409 mutants exhibit k_{cat} values which are some 10^4 less than the native enzyme but are still more than 10^4 faster than the uncatalyzed rate of hydrolysis, indicating that some catalytic power is retained even with the loss of the substrate binding and positioning role
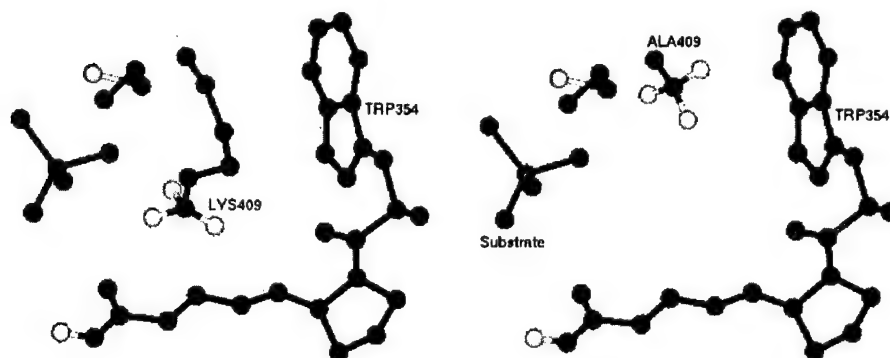
Figure 5-7. Comparison of the R409A and R409K mutants. The R409K mutant retains some apparent potential for binding and positioning other moieties, while the R409A has only backbone amides (not shown here) for this role. Structures shown are simple graphic replacements, and have not been minimized.[8]

Table 5-3. The Kinetic and Binding Effects of the Arginine Mutations[a]

enzyme	$k_{cat}(s^{-1})$	K_m (mM)
wild-type	345	2.6
R409K	0.034	5.0
R409A	0.042	66

[a]All data are from Zhang et al.[3]

of the arginine. Note that the mutation to lysine does little to perturb the binding ability of the enzyme, while the mutation to alanine has a much greater effect. This change in binding is not reflected in the rate of catalysis, where the alanine mutant retains activity essentially equal to the lysine mutant. One possible explanation is that in the lysine mutation the positively charged hydrogen bonding residue is present but the positions of its interactions with the substrate are different than in the native enzyme. Thus the lysine residue could actively participate in the binding of the substrate, but the binding could result in improper positioning for catalysis. The alanine mutation results in a residue in this position which is completely incapable of direct interactions with the phosphoryl group, leaving only the backbone amide hydrogen bonds to position and bind the substrate. Thus the binding affinity is reduced, but the positioning for catalysis is not negatively impacted.

The kinetic data and isotope effect data for the two Arg409 mutants suggest that eliminating the interactions with the arginine residue is less deleterious to the conformational changes accompanying general acid catalysis than substituting a residue which forms hydrogen bonding and electrostatic interactions in a different, improper geometry.

Interpretation of Double Mutant Results. The synthesis of the double mutants involved replacement of the aspartate general acid with either an asparagine or an alanine, neither of which can donate a proton to the leaving group, along with mutation of

Arg409. The elimination of the general acid has the effect of raising the apparent pK_a of the leaving group in the transition state, making it a poorer leaving group. From Hammond considerations, such a change could make the transition state less dissociative, requiring more nucleophilic push than is required in the native enzyme. This effect is seen with the single general acid mutants, where a small normal $^{18}(V/K)_{nonbridge}$ is observed.[12] A similar effect is seen in solution reactions where linear free energy data indicates that increased basicity of the leaving group results in an increase in nucleophilic participation in the transition state.[34] An enforced increase in nucleophilic participation in the transition state should enhance the importance of the cationic arginine residue in catalysis if indeed this residue serves to assist in stabilization of increased negative charge in a more associative transition state. While not testing the effect on the transition state of the native enzymatic reaction, the double mutant experiments constitute a valid test of the proposition that the positive charge of Arg409 alters the nature of the transition state.

Comparison of the double mutant data with isotope effects of the general acid mutants reveals the effect of the Arg409 residue on the transition state. The values for $^{15}(V/K)$ of all the double mutants are within experimental error of those of the general acid mutants, which indicates no change in the amount of negative charge developed on the leaving group in the transition state as a result of mutating Arg409 to lysine or alanine. The $^{18}(V/K)_{bridge}$ isotope effects are slightly higher with the double mutants than with D356N. This change is in the direction expected if the cationic Arg409 favors a more associative transition state which becomes dissociative when Arg409 is mutated; however, the change is very small. Bond cleavage is already large in the general acid mutants, and the additional effect with the added arginine mutation is minimal.

Comparison of the $^{18}(V/K)_{nonbridge}$ isotope effects of the double mutants with the general acid mutant also shows little change. If the Arg409 residue did impart associative character and there was a shift toward more dissociative character in its absence, this

isotope effect should have decreased. The small change observed with these isotope effects was actually an increase. The facts that all isotope changes observed with the double mutants were very small, and that the changes observed were not systematically in the direction that supports an associative mechanism role for the arginine, both suggest that the positive charge of the arginine is not responsible for a change in the mechanism. The role that these data support for the arginine is one of transition state stabilization, not alteration.

These data echo findings from reactions in solution, where the presence of metal ions was shown by linear free energy relationships not to increase the associative character of the transition states of GTP hydrolysis,[35] or of those for reactions of phosphorylated pyridines.[36]

Role of Positive Charge in the Active Site. The perception of the change in negative charge distribution as the phosphate dianion goes from ground state to transition state is that the phosphoryl group loses negative charge and the oxygens become less negative. The problem with this view is that it leaves one unable to rationalize the universal presence of positive charge in the active sites of phosphatase enzymes. Part of the problem with this rationalization can be solved by consideration of recent computational analysis of the electronic structure of metaphosphate. This evidence points to a resonance hybrid, as shown in Figure 5-8, with major contributions from the structures labeled B and C.[37,38]

A   **B**   **C**
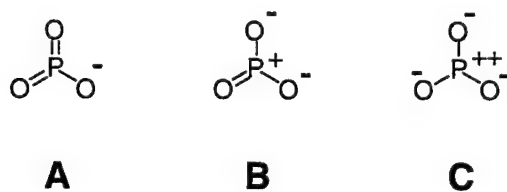
Figure 5-8. The resonance structures which contribute to the actual distribution of charge in metaphosphate.

Given this description, in spite of the reduction in the net negative charge on the phosphoryl group, the charges on the nonbridge oxygens undergo little change as the reactant moves from ground state to transition state. The conformational changes that are undergone by both substrate and enzyme during catalysis provide for stronger interaction between the cationic and hydrogen bonding residues in the transition state than in the ground state. The phosphoryl group also undergoes inversion, which can have the effect of enforcing additional hydrogen bonding interactions as the oxygen-phosphorus bond angle changes.[8,39] Thus the positive charge can be effective in stabilizing the dissociative transition state, and there is no requirement to rely on an associative transition state to justify experimental observations.

Effect of pH on the Isotope Effects of the Native Enzyme Reaction. The isotope effects for the reaction with the native enzyme with pNPP were evaluated at pH values ranging from the pH optimum of 5.5 and higher. In particular we were interested in the isotope effect in the leaving group, which would be expected to increase as the pH was raised to values at which the general acid would be in the incorrect protonation state and unable to transfer a proton to the leaving group. The results, displayed in tabular form in Table 5-4 and plotted versus pH in Figure 5-9, show that indeed the value of $^{15}(V/K)$ did increase as the pH was raised from 5.5 to pH 10.5 but not as rapidly nor to as large a magnitude as might be expected. The values never become as large as that for the D356N mutant (1.0024 at pH 6.0).

One explanation for the slow rise in the magnitude of this isotope effect lies in the relative values for k_{cat} for the native enzyme and for the reaction with the general acid disabled. The D356N mutant has a value for k_{cat} that is 1700-fold smaller than that for the native enzyme. The value for k_{cat} of D356N should be a reasonable estimate for the rate constant for the reaction of the native enzyme form in which the general acid is rendered nonfunctional by deprotonation. The aspartic acid in the active site has been found to

Table 5-4. Variation of Isotope Effects of Native Enzyme with pH

pH	$^{15}(V/K)$	$^{18}(V/K)_{bridge}$	$^{18}(V/K)_{nonbridge}$
5.0	0.9999 (3)	1.0152 (6)	0.9998 (13)
6.0	0.9999 (3)	1.0160 (15)	1.0001 (13)
8.5	1.0008 (3)		
8.75	1.0011 (2)		
9.0	1.0010 (1)	1.0216 (2)	1.0021 (5)
9.5	1.0016 (2)		
10.0	1.0019 (1)		
10.5	1.0019 (2)		
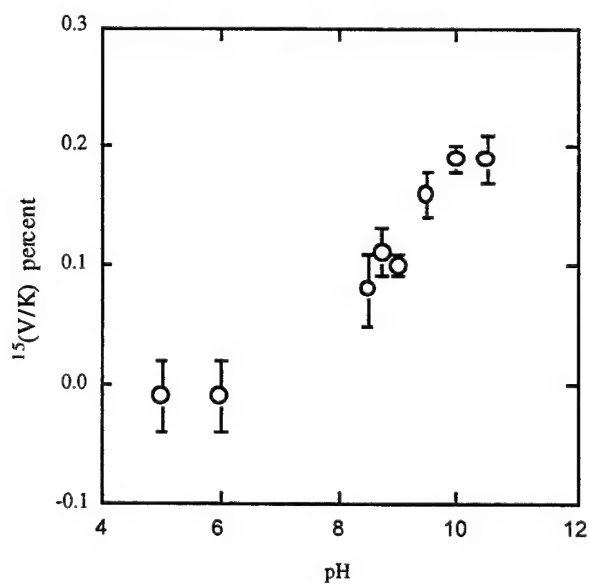
Figure 5-9. Plot of $^{15}(V/K)$ versus pH. Error bars are shown for each data point.

have a pK_a of about 5.2.[7] Thus, at pH 8.5 only about 1/1700 of the enzyme will be in the correct protonation state for general acid catalysis to occur; however, the rate constant for this form of the enzyme will also be 1700 times larger. At pH 8.5 one expects that about half of the turnover will be from the correctly protonated form of the enzyme and the value for $^{15}(V/K)$ should be about midway between that observed when general acid is fully functioning and that when it is deleted by mutation. In fact, at this pH $^{15}(V/K)$ is about one third of the maximum value seen when no general acid catalysis occurs. Given the small magnitudes of this isotope effect this is in reasonable agreement with the prediction.

At still higher pH values it would be expected that this isotope effect should rapidly approach that for D356N, but the $^{15}(V/K)$ isotope effect increases only slowly above this pH and never reaches that seen in the reaction of D356N. We are not certain of the reasons for this behavior. It was noted that at pH values above 9.0 the enzyme was much less stable in solution and precipitation was increasingly evident over time. This indicates that these elevated pH levels result in conformational perturbations to the enzyme, and thus data from reactions above this pH must be interpreted with caution. Due to the large amounts of enzyme needed for the experiments, only the $^{15}(V/K)$ effect was measured across this full pH range; $^{18}(V/K)_{bridge}$ and $^{18}(V/K)_{nonbridge}$ were measured at pH 6.0 and 9.0. The same trend toward the values seen with the D356N mutant was also seen in these two isotope effects. At pH 9.0, $^{18}(V/K)_{bridge}$ is about halfway between that of the native enzyme at the pH-optimum and that of D356N. The value for $^{18}(V/K)_{nonbridge}$ at this pH is identical within experimental error to that of D356N.

The isotope effects for D356N were also measured at pH 9.0. The magnitude of $^{15}(V/K)$ was unchanged from that observed at pH 6.0. The values for $^{18}(V/K)_{bridge}$ and $^{18}(V/K)_{nonbridge}$ are both increased somewhat at pH 9.0. The reason for the small increase in these isotope effects is uncertain.

Conclusions

Mutations to the hinge residue Trp354 affect the functioning of the general acid residue which can be directly measured by isotope effects in the substrate pNPP. Mutation of Trp354 to alanine completely disables general acid catalysis. In the phenylalanine mutant, weak acid catalysis occurs with the proton only approximately half transferred in the transition state and as a result a partial negative charge develops on the leaving group, in contrast to the native enzymatic reaction where protonation is completely synchronous with P–O bond cleavage and the leaving group remains uncharged. The results are indicative of impaired positioning of the flexible loop in both of these mutants, and are consistent with the observation that while W354A has a k_{cat} value that is reduced 480-fold from that of the native enzyme, W354F is slowed only 200-fold. Mutation of the Arg409 residue by either lysine or alanine both result in substantially reduced catalytic turnover. The K_m of the R409K mutant with pNPP is doubled from that of wild type enzyme, while that for R409A is increased more than 30-fold. However, functioning of general acid catalysis is more deleteriously affected in the R409K mutation, where it is completely abolished, while partial proton transfer in the transition state still occurs in the R409A mutant. The reduction in catalytic efficiency in the arginine mutants is due to a combination of loss of transition state stabilization arising from loss of the guanidinium group, and from disruption to the functioning of the general acid catalyst. There was no support found for the proposition that positive charge in the active site forces enzymatic phosphoryl transfer to proceed by a more associative transition state. The role of the invariant arginine residue in Yersinia PTPase was found to be the stabilization of the dissociative transition state.

References

(1)   Zhang, Z. Y.; Wang, Y.; Dixon, J. E. *Pro. Natl. Acad. Sci. U.S.A.* **1994**, *91*, 1624-1627.

(2)   Schubert, H. L.; Fauman, E. B.; Stuckey, J. A.; Dixon, J. E.; Saper, M. A. *Protein Science* **1995**, *4*, 1904-1913.

(3)   Zhang, Z. Y.; Wang, Y.; Wu, L.; Fauman, E. B.; Stuckey, J. A.; Schubert, H. L.; Saper, M. A.; Dixon, J. E. *Biochem.* **1994**, *33*, 15266-15270.

(4)   Cho, H.; Krishnaraj, R.; Bannwarth, W.; Walsh, C. T.; Anderson, K. S. *J. Am. Chem. Soc.* **1992**, *114*, 7296-7298.

(5)   Guan, K. L.; Dixon, J. E. *Science* **1990**, *249*, 553-556.

(6)   Stuckey, J. A.; Schubert, H. L.; Fauman, E. B.; Zhang, Z.-Y.; Dixon, J. E.; Saper, M. A. *Nature* **1994**, *370*, 571-575.

(7)   Keng, Y. F.; Wu, L.; Zhang, Z. Y. *Eur. J. Biochem.* **1999**, *259*, 809-814.

(8)   Fauman, E. B.; Yuvaniyama, C.; Schubert, H. L.; Stuckey, J. A.; Saper, M. A. *J. Biol. Chem.* **1996**, *271*, 18780-18788.

(9)   Zhang, Y. Z. Personal communication.

(10)   Hengge, A. C.; Zhao, Y.; Wu, L.; Zhang, Z.-Y. *Biochem.* **1997**, *36*, 7928-7936.

(11)   Hengge, A. C.; Denu, J. M.; Dixon, J. E. *Biochem.* **1996**, *35*, 7084-7092.

(12)   Hengge, A. C.; Sowa, G. A.; Wu, L.; Zhang, Z.-Y. *Biochem.* **1995**, *34*, 13982-13987.

(13)   Taylor, W. P.; Widlanski, T. S. *Chem. and Biol.* **1995**, *2*, 713-718.

(14)   Thatcher, G. R. J.; Kluger, R. *Adv. Phys. Org. Chem.* **1989**, *25*, 99-265.

(15)   Hengge, A. C. In *Comprehensive Biological Catalysis*; Sinnott, M., Ed.; Academic Press: San Diego, CA, 1998; Vol. 1, pp 517-542.

(16)   Hasset, A.; Blattler, W.; Knowles, J. R. *Biochem.* **1982**, *21*, 6335-6340.

(17)   Matte, A.; Tari, L. W.; Delbaere, L. D. J. *Structure* **1998**, *6*, 413-419.

(18)   Mildvan, A. S. *Proteins* **1997**, *24*, 401-416.

(19)   Schlichting, I.; Reinstein, J. *Biochem.* **1997**, *36*, 9290-9296.

(20)   Hengge, A. C.; Edens, W. A.; Elsing, H. *J. Am. Chem. Soc.* **1994**, *116*, 5045-5049.

(21)   O'Leary, M. H.; Marlier, J. F. *J. Am. Chem. Soc.* **1979**, *101*, 3300-3306.

(22)   Caldwell, S. R.; Raushel, F. M.; Weiss, P. M.; Cleland, W. W. *Biochem.* **1991**, *30*, 7444-7450.

(23) Kunkel, T. A.; Roberts, J. D.; Zakour, R. A. *Meth. Enz.* **1987**, *154*, 367-382.

(24) Zhang, Z. Y.; Clemens, J. C.; Schubert, H. L.; Stuckey, J. A.; Fischer, M. W. F.; Hume, D. M.; Saper, M. A.; Dixon, J. E. *J. Biol. Chem.* **1992**, *267*, 23759-23766.

(25) Northrop, D. B. In *Isotope Effects on Enzyme-Catalyzed Reactions*; Cleland, W. W., O'Leary, M. H., Northrop, D. B., Eds.; University Park Press: Baltimore, MD, 1977, p 303.

(26) Bourne, N.; Williams, A. *J. Org. Chem.* **1984**, *49*, 1200-1204.

(27) Massoud, S. S.; Sigel, H. *Inorg. Chem.* **1988**, *27*, 1447-1453.

(28) Knight, W. B.; Weiss, P. M.; Cleland, W. W. *J. Am. Chem. Soc.* **1986**, *108*, 2759-2761.

(29) Hengge, A. C.; Cleland, W. W. *J. Am. Chem. Soc.* **1990**, *112*, 7421-7422.

(30) Hengge, A. C.; A., H. R. *J. Am. Chem. Soc.* **1994**, *116*, 11256-11263.

(31) Weiss, P. M.; Knight, W. B.; Cleland, W. W. *J. Am. Chem. Soc.* **1986**, *108*, 2761-2762.

(32) Hengge, A. C.; Tobin, A. E.; Cleland, W. W. *J. Am. Chem. Soc.* **1995**, *117*, 5919-5926.

(33) Hengge, A. C.; Cleland, W. W. *J. Am. Chem. Soc.* **1991**, *113*, 5835-5841.

(34) Skoog, M. T.; Jencks, W. P. *J. Am. Chem. Soc.* **1984**, *106*, 7597-7606.

(35) Admiraal, S. J.; Herschlag, D. *Chem. & Biol.* **1995**, *2*, 729-739.

(36) Herschlag, D.; Jencks, W. P. *J. Am. Chem. Soc.* **1987**, *109*, 4665-4674.

(37) Horn, H.; Ahlrichs, R. *J. Am. Chem. Soc.* **1990**, *112*, 2121-2124.

(38) Rajca, A.; Rice, J. E.; Streitweiser Jr., A.; Schaefer, H. F. *J. Am. Chem. Soc.* **1987**, *109*, 4189-4192.

(39) Alhambra, C.; Wu, L.; Zhang, Z. Y.; Gao, J. *J. Am. Chem. Soc.* **1998**, *120*, 3858-3866.

CHAPTER 6

THE TRANSITION STATE OF THE PHOSPHORYL TRANSFER

REACTION CATALYZED BY THE LAMBDA

SERINE/THREONINE PROTEIN

PHOSPHATASE[1]

Abstract: The reactions catalyzed by the Mn^{2+} form of the native bacteriophage λ phosphatase and the H76N mutant were studied with the substrate *p*-nitrophenyl phosphate using kinetic isotope effects and pH-dependent rate studies. The kinetic isotope effects were measured at the nonbridge oxygen atoms [$^{18}(V/K)_{nonbridge}$]; at the bridge oxygen atom, the site of bond cleavage [$^{18}(V/K)_{bridge}$]; and at the nitrogen atom in the leaving group [$^{15}(V/K)$]. The isotope effects at the pH optimum of 7.8 were $1.33\pm0.06\%$ for $^{18}(V/K)_{bridge}$, $0.06\pm0.03\%$ for $^{15}(V/K)$, and $-0.24\pm0.03\%$ for $^{18}(V/K)_{nonbridge}$. These values were constant within experimental error across the pH range from 6.0 to 9.0 and were also unchanged for the slower catalytic reaction resulting when Ca^{2+} was substituted for Mn^{2+}. The results indicate that the chemical step of P–O bond cleavage is rate-limiting, the first metallophosphatase for which this has been shown to be the case. The isotope effects are very similar to those measured for reactions of protein-tyrosine phosphatases, indicating that the two families of enzymes share similar dissociative transition states. The $^{18}(V/K)_{bridge}$ and $^{15}(V/K)$ isotope effects for the H76N mutant were slightly increased in magnitude relative to the native enzyme, but were much smaller than the values expected if the leaving group were departing with a full negative charge. The pH-k_{cat} profile for the native enzyme is bell-shaped with pK_a values of 7.7 ± 0.3 and 8.6 ± 0.4, while K_m values for substrate increased with pH approximately

70-fold across the pH range 5.8 to 9.1. The K_m for the H76N mutant was similar to that observed for native enzyme at high pH and was relatively constant across this pH range. The basic limb of the pH-rate profile is reduced but not abolished in the H76N mutant reaction. The results are discussed in terms of the possible role of His76 and the nature of the transition state for catalysis in the native enzyme and mutant.

Introduction

The regulation of metabolism in organisms from bacteria to higher eukaryotes is accomplished by the reversible phosphorylation of proteins. Protein phosphorylation (by kinases) or dephosphorylation (by phosphatases) occurs primarily on tyrosine, serine, or threonine residues. Interestingly, phosphatase families have evolved which utilize completely different catalytic machinery to accomplish the hydrolysis of phosphate monoester bonds. The protein-tyrosine phosphatases (PTPases) have no metal ions and utilize a conserved arginine for substrate binding and transition state stabilization, a cysteine nucleophile to form a phosphoenzyme intermediate, and general acid catalysis is accomplished by a conserved aspartic acid residue to protonate the leaving group.[1-4] Less is known about the mechanistic details of catalysis by the serine/threonine (Ser/Thr) protein phosphatases, but these phosphatases are distinguished from the protein-tyrosine phosphatases by their use of a binuclear metal center as a key component of catalysis.[5-7] There are four major Ser/Thr phosphatase families distinguished primarily by substrate specificities and susceptibility to specific inhibitors; these are designated types 1, 2A, 2B (also called calcineurin), and 2C. Among the Ser/Thr phosphatase family, crystal structures have been published for the catalytic subunit of rabbit muscle[8] and human[9] PP-1, bovine brain[10] and human[11] calcineurin, and for PP2C[12] as well as for the related enzyme purple acid phosphatase (PAP).[13,14] A variety of experimental evidence indicates that the binuclear metal center in bovine brain calcineurin is a Fe-Zn center. The protein

phosphatase from bacteriophage λ, designated λ protein phosphatase (λPPase), is considered a member of the Ser/Thr protein phosphatase family based on sequence comparisons[6] and on kinetic and spectroscopic characterizations.[15-17]

The x-ray structures of the members of this family indicate that the binuclear metal center has a ligand environment that is very similar to that of purple acid phosphatases. In PAP the stereochemical course of the reaction occurs with inversion of configuration at phosphorus, supporting a mechanism involving direct transfer of the phosphoryl group to water.[18] The nucleophile has been proposed to be an Fe^{3+}-bound hydroxide ion on the basis of rapid kinetic measurements with anions[19] and pH-rate studies.[20] Kinetic studies, solvent isotope effect data, and redox studies with calcineurin are also indicative of a phosphoryl transfer mechanism that most likely proceeds by direct transfer to a metal-bound water molecule.[6,21,22] A schematic of part of the active site of calcineurin was shown in Figure 1-12.

In addition to the ligands of the binuclear metal center, there are several other conserved amino acids within the region of the active site which could participate in catalysis. One of these is a histidine residue which in calcineurin (His151) is within 5 Å of the two metal ions. A histidine residue in this region is conserved in other Ser/Thr phosphatases such as PP1 (His125),[5,6] λPPase (His76), and purple acid phosphatase.[13,14] It has been proposed that this residue could function as a catalytic general acid in the phosphoryl transfer reactions catalyzed by this family of enzymes. Mutation of this residue in λPPase results in substantial kinetic effects[15,17] and spectroscopic differences.[15]

In this study we report the kinetic isotope effects and pH-rate studies on the reaction of p-nitrophenyl phosphate (pNPP) with native λPPase and with the H76N mutant. The substrate is shown in Figure 1-7 with the positions indicated at which isotope effects have been measured. Using this substrate, prior isotope effect studies on

reactions of protein-tyrosine phosphatases have shown that isotope effects reveal the presence or lack of general acid catalysis in the transition state of the catalytic reaction.[23-25] In the PTPase studies each of the isotope effects revealed alterations in the transition state when protonation of the leaving group in the transition state was lost due to mutation of the general acid.

While a number of PTPases have been mechanistically characterized using isotope effects, similar experiments with phosphatases utilizing binuclear metal ion catalysis have been hindered by the fact that the chemical step is less often rate-limiting with pNPP as the substrate. Isotope effects were measured for the reaction of pNPP with calcineurin.[26] Although calcineurin is very similar to λPPase the chemical step of phosphoryl transfer was found to be only partially rate-limiting, thereby leaving the interpretation of the isotope effects in terms of transition state structure somewhat uncertain.[26] Alkaline phosphatase, another phosphatase utilizing binuclear catalysis, showed no kinetic effect with isotopic substitution, consistent with other data indicating that a nonchemical step is completely rate-limiting for k_{cat}/K_M.[27,28]

In the present study we report strong evidence that the chemical step of phosphoryl transfer is fully rate-limiting for k_{cat}/K_M for the reaction of pNPP with λPPase, allowing the full intrinsic isotope effects on the transition state to be observed. In addition the isotope effects for the H76N mutation have been measured, as well as for the native enzyme in which the supplied metal is Ca^{2+} in place of Mn^{2+}, a substitution which results in a reduction in rate of about 17-fold.[16] The results yield information about the transition state of the λPPase reaction, the role of His76, the identity of the substrate as the monoanion or the dianion of pNPP, and the effect of changing the metal ion from Mn^{2+} to Ca^{2+} on the transition state of the reaction. The results also allow an evaluation of the proposal that the normally loose transition state for solution pNPP hydrolysis is altered by coordination of the substrate to the metal ions at the active site and

becomes tighter, with greater bond formation to the nucleophile and less advanced bond cleavage to the leaving group. It has been noted that coordination to divalent metal ions in aqueous solution does not alter the transition state of the hydrolysis reaction.[29] However, the nature of the transition state for enzymatic phosphoryl transfer reactions remains controversial.

Experimental

Synthesis of Compounds. [^{14}N]-p-nitrophenyl phosphate, [^{15}N, nonbridge-^{18}O$_3$]-p-nitrophenyl phosphate, [^{14}N]-p-nitrophenol, and [^{15}N, ^{18}O]-p-nitrophenol were synthesized as previously described.[28] [^{14}N]-p-nitrophenol, and [^{15}N, ^{18}O]-p-nitrophenol were synthesized and then mixed to closely reconstitute the 0.365 % natural abundance of ^{15}N. This mixture was phosphorylated to produce p-nitrophenyl phosphate as the mixture of isotopomers used for determination of the ^{18}(V/K)$_{bridge}$ isotope effect. The [^{14}N]-p-nitrophenyl phosphate and [^{15}N, nonbridge-^{18}O$_3$]-p-nitrophenyl phosphate isotopic isomers were mixed to reconstitute the natural abundance of ^{15}N, and this mixture used for measurement of the ^{18}(V/K)$_{nonbridge}$ isotope effect. Natural abundance pNPP for kinetic experiments was purchased from Sigma.

Kinetic Isotope Effect Determinations. Isotope effects experiments were run at 100 mM buffer and 1 mM dithioreitol (DTT), at 30 °C. DTT is a protective agent for S-H groups, and serves to preserve the function of enzymes that contain cysteine residues by preventing denaturation through cross linking.[30] The buffers used were MES at pH 6.0 and TRIS at pH 7.8 and 9.0. DTT was omitted at pH 9.0. Reactions were begun with 100 micromoles of substrate and sufficient enzyme used so that background hydrolysis rates were less than 10% of the enzymatic rate. Enzymatic experiments were run in parallel with solution experiments to establish background hydrolysis rates under experimental conditions. The extent of reaction was measured by transferring an aliquot

of the reaction mixture into 0.1 N NaOH and measuring the absorbance of product at 400 nm. Isotope effect experiments were run in triplicate and were stopped at extents of substrate turnover ranging from 40% to 60%. Reactions were stopped by removing the samples from the temperature controller and placing them on ice and titrating to pH 5. An aliquot was removed for determination of the precise fraction of reaction. This aliquot was split, with one portion analyzed immediately and one portion placed in TRIS buffer at pH 9.0 with alkaline phosphatase for several hours. After this portion was analyzed, the ratio of the absorbances of these two samples gave the extent of reaction. The remaining reaction solution was extracted three times with an equivalent volume of diethyl ether to quantitatively remove the *p*-nitrophenol, which was the product of the enzymatic reaction. The aqueous layer containing the residual substrate was evaporated briefly under vacuum to remove dissolved ether, an equivalent volume of the TRIS pH 9.0 buffer added, and the pH adjusted to 9.0 with NaOH. This sample was treated with alkaline phosphatase to quantitatively hydrolyze all of the remaining substrate. This mixture was then titrated back to pH 5.0 and extracted with ether, the *p*-nitrophenol in this ether fraction representing the residual substrate from the enzymatic reaction. The ether fractions were dried over magnesium sulfate, filtered, and the solvent removed by rotary evaporation. The *p*-nitrophenol was sublimed under vacuum at 90 °C, and 1.0–1.5-mg samples were prepared for isotopic analysis using an ANCA-NT combustion system in tandem with a Europa 20-20 isotope ratio mass spectrometer.

Methods for calculation of isotope effects were described in the previous chapter. The ^{18}O isotope effects were measured by the remote-label method,[31] as previously described for solution reactions of pNPP.[28] These experiments yield an observed isotope effect, which is the product of the effect due to both the ^{15}N and the ^{18}O substitution. The observed isotope effects from these experiments were corrected for the ^{15}N effect and for incomplete levels of isotopic incorporation in the starting material.[32]

Equilibrium Isotope Effects for Coordination of pNPP to Ca^{2+}. The coordination of pNPP with calcium ion was followed by recording the shift of the UV-VIS spectrum as a function of calcium ion concentration. A 5 mM solution of the disodium salt of pNPP was prepared at pH 7.0 with 100 mM MOPS buffer. Its spectrum was monitored at increasing concentration of $CaCl_2$ at a constant ionic strength of 3.0 M maintained with NaCl.

An estimation of the nonbridge ^{18}O isotope effect for coordination was performed by monitoring the separation in the ^{31}P NMR signals for ^{16}O- and for ^{18}O-labeled pNPP as a function of the concentration of Ca^{2+}. The solution was 5 mM in pNPP, at pH 7.0 (100 mM MOPS buffer). The pNPP consisted of a roughly 1:1 mixture of natural abundance compound and of [nonbridge-$^{18}O_3$]-pNPP. The chemical shifts were followed as calcium ion concentrations were increased from zero to 1000 mM at a constant ionic strength of 3.0 M maintained using NaCl. ^{18}O-substitution causes a small upfield shift in the ^{31}P chemical shift of about 0.02 ppm per ^{18}O. The separation will change as a function of metal ion concentration if there is an isotope effect on the coordination and will reach a maximum at the pK. This technique was introduced by Ellison and Robinson[33] to determine the equilibrium isotope effect for deprotonation of formic acid, and has also been used to measure the isotope effect for deprotonation of phosphate and phosphate esters.[34] A sample spectrum is given in Figure 6-1, showing the upfield shift of the multiply labeled phosphate. The phosphate is primarily $^{18}O_3$ labeled, but there is detectable $^{18}O_2$ labeled compound present. Noticeable in this spectrum and in most of the other spectra recorded is a shoulder on the downfield side of the upfield peak. This most likely represents the $^{18}O_2$ labeled phosphate.

pH-Dependent Kinetic Assays of λ Protein Phosphatase and λ Protein Phosphatase H76N. The preparation, isolation, purification, and characterization of the native and mutant enzyme used in this study were done by
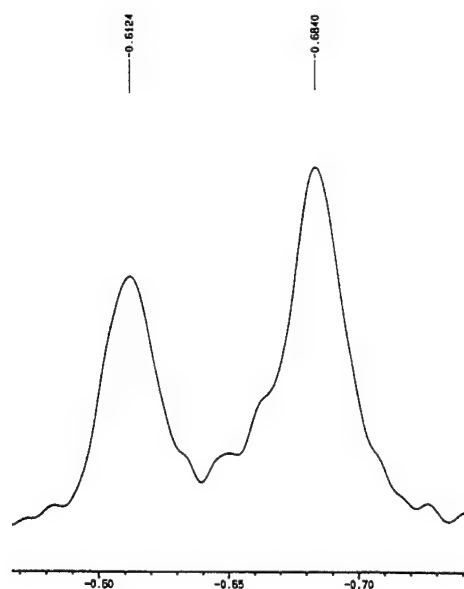
Figure 6-1. Sample of Ca^{2+}-pNPP complexation isotope effect spectra. Peak height shows ratio of unlabeled to labeled phosphate present. The peak on the left is the unlabeled compound, the peak on the right is shifted upfield approximately 0.02 ppm per ^{18}O.

coauthors P. Mertz and F. Rusnak.

The following buffers at 200 mM concentration (2x the final concentration in the assays) were prepared for pH studies: MES for pH 5.8, 6.1, and 6.4; MOPS for pH 6.7, 7.0, and 7.3; Tricine for pH 7.6, 7.9, and 8.2; Bicine for pH 8.5 and 8.8; and CHES for pH 9.1. Stocks of pNPP (0.5 M) were also prepared at each pH by titrating a 1.0 M solution of pNPP with HCl or NaOH to the desired pH followed by dilution with water to the appropriate volume.

Assays contained 100 mM buffer, 1 mM $MnCl_2$, and the appropriate concentration of NaCl to normalize the ionic strength due to varying concentrations of pNPP used in the assays. pNPP was varied in order to determine kinetic parameters at each pH. All reagents except enzyme were incubated for 5 min at 30 °C before initiation of the reaction by addition of enzyme. Reactions were allowed to proceed for 2 min and terminated by addition of 1 mL of 2 M TRIS pH 10, 10 mM EDTA. At this pH, p-nitrophenol is

completely deprotonated. After mixing, the absorbance at 410 nm was read immediately and converted to specific activity using $\varepsilon_{410} = 17,800 \text{ M}^{-1}\text{cm}^{-1}$.

The apparent ionization constants of the enzyme-substrate complex for λPPase were determined by fitting the raw data to the appropriate curve using a nonlinear least squares analysis method.

Separation of pNPP from Contaminant Inorganic Phosphate. A preparation of pNPP containing less contaminating inorganic phosphate (which typically is about 1 mol %) was needed in order to carry out assays with λPPase and λPP(H76N) at high substrate concentrations to avoid product inhibition (K_i orthophosphate = 0.71 mM at pH 7.8).[16] This was completed by ether extractions of pNPP. A solution of pNPP was prepared and acidified with 1 N HCl to a pH of ≈4.5-5 and extracted twice with ether (ratio of ether to aqueous phase ≈ 3:1). The aqueous phase was retained and acidified to pH ~1.0 using 1 N HCl. This was then extracted 5 to 6 times with ether (ratio of ether to aqueous phase ≈ 3:1). Anhydrous $MgSO_4$ was added to the ether phase as a drying agent and removed by filtration. The ether was evaporated to dryness using a rotary evaporator and the yellow oil which remained was dissolved in a few mL of H_2O. The pNPP concentration was determined by dilution of the pNPP stock into 0.5 M MOPS, pH 7.0 using $\varepsilon_{310} = 9500 \text{ cm}^{-1}\cdot\text{M}^{-1}$. The inorganic phosphate concentration of this stock was checked using the Malachite green/ammonium molybdate reagent.[35] Following ether extraction of pNPP, the contamination from inorganic phosphate was 0.14–0.20 mole % compared with ≈1.2 mole % in the commercial sample.

Instrumentation. UV-VIS spectra were recorded on a Cary 1 Bio spectrophotometer equipped with a thermostatted cell holder. ^{31}P NMR data were obtained using a Bruker ARX400 spectrometer operating at 161.976 MHz. The spectra were the sum of 50–2000 (usually <200) scans and were externally referenced to phosphoric acid (0 ppm) in a coaxial tube. The data were resolution enhanced by

gaussian apodization prior to Fourier transformation. Peak width at half height was typically 0.018–0.030 ppm.

Results

Kinetic Isotope Effects. The isotope effects for the enzymatic reactions of λPP with pNPP and their standard errors are given as percents in Table 6-1. The isotope effects obtained from the isotopic ratios of product, and those obtained from the isotopic ratios of residual substrate, agreed within experimental error in all cases and were averaged together to give the results shown in Table 6-1. Six or more determinations of each isotope effect were made. Isotope effects were measured with the wild-type enzyme with Mn^{2+} at the pH optimum of 7.8, at pH 6.0 and 9.0, and separately with Ca^{2+} at pH 7.8. Isotope effects with the H76N mutant were measured at pH 7.8 with Mn^{2+}.

The values for the ^{18}O isotope effects have been corrected for the ^{15}N effects and for levels of isotopic incorporation. Since the enzymatic substrate is likely the dianion of pNPP *(vide infra)* the values for $^{18}(V/K)_{nonbridge}$ in Table 6-1 at pH 6.0 have been corrected for the equilibrium ^{18}O isotope effect of 1.5% on deprotonation,[34] as previously described.[28] The $^{18}(V/K)_{nonbridge}$ values shown are the isotope effects resulting from ^{18}O

Table 6-1. Kinetic Isotope Effects for λPPase Reactions with pNPP[a]

enzyme and conditions	$^{15}(V/K)$	$^{18}(V/K)_{bridge}$	$^{18}(V/K)_{nonbridge}$
native, Mn^{2+}, pH 7.8	0.06 (3)	1.33 (6)	-0.24 (3)
native, Mn^{2+}, pH 6.0	0.06 (2)	1.32 (4)	-0.19 (2)
native, Mn^{2+}, pH 9.0	0.07 (6)	1.43 (5)	-0.08 (1)
native, Ca^{2+}, pH 7.8	0.07 (1)	1.30 (4)	-0.16 (2)
H76N, Mn^{2+}, pH 7.8	0.16 (3)	1.83 (9)	-0.24 (1)

[a]Expressed as percents. Standard errors in the last digit are in parentheses.

in all three nonbridge oxygen atoms. For purposes of comparison the isotope effects for PTPase reactions with the substrate pNPP from previous studies are shown in Table 6-2. Raw data and calculations are in Appendix B, Tables B-18 through B-26.

Ca^{2+} **Titration Isotope Effects.** Data from titration experiments of pNPP with Ca^{2+} are plotted in Figures 6-2 and 6-3, while the same data are displayed in table format at Table 6-3 and 6-4. The UV-VIS experiment following the change in λ_{max} of a 5 mM solution of pNPP as a function of Ca^{2+} concentration indicates complete complexation at about 500 mM metal ion; λ_{max} gradually changed from 311.1 nm in the absence of calcium ion to a plateau value of 309.5 nm at 500 mM Ca^{2+} (Figure 6-2). The ^{31}P NMR data, however, indicate that further complexation occurs at higher calcium ion concentrations and that saturation is approached but is not complete at 1 M Ca^{2+} (Figure 6-3). A likely possibility is that the UV-VIS experiment detects formation of an initial 1:1 complex, while at higher calcium concentrations a 2:1 metal:pNPP complex forms which causes no further change in the UV-VIS spectrum but is detected by changes in the ^{31}P chemical shift. The NMR data indicate that full saturation is approached at approximately

Table 6-2. Kinetic Isotope Effects for PTPase Reactions with pNPP[a]

enzyme and conditions	$^{15}(V/K)$	$^{18}(V/K)_{bridge}$	$^{18}(V/K)_{nonbridge}$
native PTP1, YOP, and VHR (range)	-0.01 to 0.01	1.18 to 1.52	-0.19 to 0.03
native Stp1	0.07	1.60	0.18
general acid (D to N) mutants of PTP1, YOP, VHR and Stp1 (range)	0.19 to 0.34	2.75 to 2.94	0.18 to 0.24

[a] Data from references 23-25 are expressed as percents. Data from the native PTP1, YOP and VHR were very similar and are reported as a range; data from the native Stp1 differ in small but systematic ways from the other three enzymes and are reported separately. Data from the Asp to Asn general acid mutants of all four enzymes were very similar and are reported as a range.
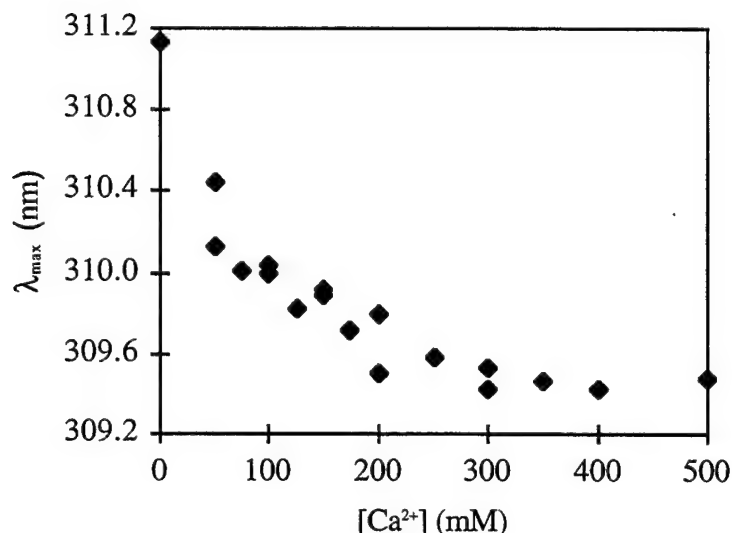
Figure 6-2. The variation of the λ_{max} of a 5 mM solution of pNPP as a function of calcium ion concentration at pH 7.0. Ionic strength maintained at 3.0 M with NaCl.
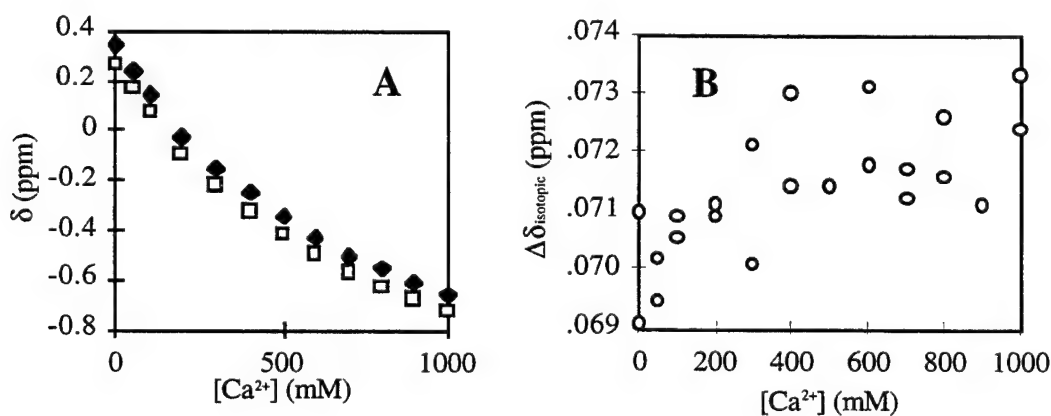
Figure 6-3. Ca^{2+}-pNPP complexation experiment. In A, the ^{31}P chemical shift of a 5 mM solution pNPP is shown as a function of calcium ion concentration. Filled diamonds represent the chemical shift of unlabeled pNPP, open squares represent nonbridge-$^{18}O_3$-labeled pNPP. In B, the difference between the chemical shifts of labeled and unlabeled pNPP is shown as a function of calcium ion concentration. Data from two titrations under identical experimental conditions are shown. For comparison, when the isotope effect for the deprotonation of $^{18}O_3$-labeled phosphate or of $^{18}O_3$-labeled phosphate esters are measured by the same technique, the difference in the isotope-induced chemical shift changes from 0.070 to a maximum of about 0.085 ppm at the pK_a.[36]

Table 6-3. UV-Vis Titration Data[a]

[Ca^{2+}] (mM)	lambda max (nm)	[Ca^{2+}] (mM)	lambda max (nm)	[Ca^{2+}] mM	lambda max (nm)
0	311.13	75	310.01	50	310.13
50	310.45	100	310.04	100	310.04
100	309.99	125	309.82	150	309.92
200	309.5	150	309.89	200	309.5
300	309.53	175	309.72	250	309.58
400	309.43	200	309.79	300	309.43
500	309.48			350	309.46

[a]The λ_{max} of a 5 mM solution of pNPP as a function of calcium ion concentration at pH 7.0, with ionic strength maintained at 3.0 M with NaCl.

Table 6-4. ^{31}P Chemical Shift Data[a]

[Ca^{2+}] (mM)	$\delta_{unlabled}$ (ppm)	δ_{labled} (ppm)	$\Delta\delta_{isotopic}$ (ppm)
0	0.34133	0.27036	0.0710
50	0.24098	0.17081	0.0702
100	0.14255	0.07166	0.0709
200	-0.0248	-0.0959	0.0711
300	-0.1480	-0.2201	0.0721
400	-0.2503	-0.3233	0.0730
600	-0.4260	-0.4991	0.0731
700	-0.5045	-0.5757	0.0712
800	-0.5557	-0.6283	0.0726
900	-0.6051	-0.6762	0.0711
1000	-0.6538	-0.7271	0.0733
0	0.33474	0.26566	0.06908
50	0.23525	0.16580	0.06945
100	0.1779	0.10738	0.07052
200	0.0247	-0.0462	0.0709
300	-0.1170	-0.1871	0.0701
400	-0.2484	-0.3198	0.0714
500	-0.3477	-0.4191	0.0714
600	-0.4968	-0.5685	0.0717
800	-0.5536	-0.6252	0.0716
1000	-0.6497	-0.7221	0.0724

[a]Data are for a mixture of unlabeled and nonbridge $^{18}O_3$-labeled pNPP as a function of Ca^{2+} concentration. Data from two titrations under identical experimental conditions are shown.

twice the Ca^{2+} levels as indicated by the UV-VIS experiment.

Since full complexation could not be achieved, an exact fit of the data to determine the nonbridge ^{18}O isotope effect for formation of this complex could not be done. Therefore, the effect was estimated by comparing the maximum change in the isotopic separation induced by Ca^{2+} complexation with that which has been reported for analogous experiments on the protonation of phosphate esters.[36] The magnitude of the isotope effect will be proportional to the maximum *change* in the separation of the peaks of the isotopic isomers. The deprotonation of phosphate monoesters results in a maximal change of 0.015 ppm and an isotope effect of $1.5 \pm 0.1\%$ at 27 °C[34] (the isotope effect for protonation will be the inverse of this number, -1.5%). Since Ca^{2+} results in a maximal change in this separation of 0.0024 ppm, the isotope effect for complexation by two calcium ions is estimated to be about 16% as large as that for protonation of one of the nonbridge oxygen atoms, or approximately -0.24%. These $^{18}K_{nonbridge}$ values are the isotope effects resulting from ^{18}O in all three nonbridge oxygen atoms.

Enzyme Kinetics Studies. Table 6-5 contains a listing of kinetic data with pH, while plots of log (k_{cat}/K_M) vs. pH for native and H76N λPP, and log k_{cat} vs. pH for native λPP, are presented in Figures 6-4A and 6-4B, respectively. Significant substrate inhibition was observed at pH ≤ 7, requiring increased levels of Mn^{2+} in order to obtain saturating concentrations of substrate. For this reason the reaction was not explored below pH 5.8. A theoretical curve was fit to the data in Figure 6-4B using equation 1, where K_{1app} and K_{2app} are apparent ionization constants of the enzyme-substrate complex.

$$k_{cat} = \frac{k_{cat(max)}}{\left(1 + \frac{[H^+]}{K_{1\,app}} + \frac{K_{2\,app}}{[H^+]}\right)} \qquad (1)$$

The value for k_{cat} (max) was 500 ± 200 sec^{-1}. K_{1app} and K_{2app} yield pK_a values of

Table 6-5. Kinetic Data for λPPase as a Function of pH[a]

pH	k_{cat} (s^{-1})	Km (mM)	MnCl$_2$ (mM)	k_{cat}/K_m (s^{-1}mM^{-1})
		A. Native λPPase pH data		
5.8	30 ± 1	1.0 ± 0.1	15	30
6.1	44 ± 1	1.2 ± 0.1	10	37
6.4	41 ± 2	1.1 ± 0.2	10	37
6.7	102 ± 3	2.8 ± 0.3	10	36
7.0	101 ± 4	2.9 ± 0.5	10	35
7.3	136 ± 4	5.0 ± 0.5	1	27
7.6	180 ± 10	14 ± 4	1	13
7.9	270 ± 40	40 ± 10	1	6.8
8.5	280 ± 20	49 ± 7	1	5.7
8.8	210 ± 20	50 ± 10	1	4.2
9.1	60 ± 20	70 ± 30	1	0.86
		B. H76N λPPase pH data		
5.8	1.6 ± 0.1	22 ± 3	15	0.073
6.4	2.2 ± 0.1	26 ± 4	10	0.085
6.7	3.9 ± 0.2	49 ± 5	10	0.080
7.0	4.1 ± 0.5	40 ± 10	10	0.10
7.6	1.0 ± 0.1	30 ± 10	1	0.033
7.9	1.8 ± 0.2	70 ± 10	1	0.026
8.2	0.93 ± 0.08	35 ± 7	1	0.027
8.5	0.57 ± 0.07	50 ± 10	1	0.011
8.8	0.56 ± 0.04	60 ± 10	1	0.0093

[a]Data in this table generated by coauthors Mertz and Rusnak.
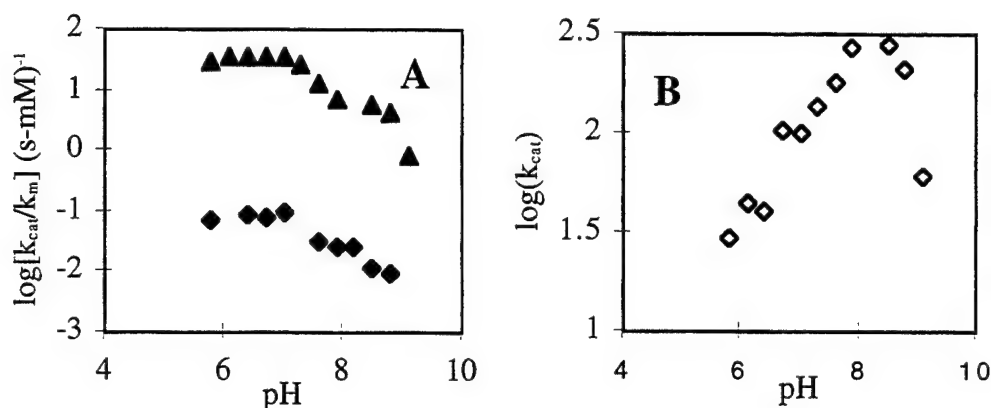
Figure 6-4. Variation of kinetic data with pH for λPPase. A shows the pH- k_{cat}/K_m profile for the hydrolysis of pNPP by wild-type λ protein phosphatase (triangles) and the H76N mutant (diamonds), while B shows the variation in k_{cat} for the native enzyme. B was used for the curve fit described in the text.

7.7 ± 0.3 and 8.6 ± 0.4, respectively. The data in Figure 6-4 and Table 6-5 were generated by Mertz and Rusnak.

Discussion

Factors Influencing the Expression of the Intrinsic Isotope Effects. Experimental data show that the reaction of purple acid phosphatase, which is structurally very similar to the Ser/Thr phosphatases, proceeds with inversion of stereochemistry at phosphorus, consistent with a single-step mechanism.[18] Kinetic and solvent isotope effect data with calcineurin[21,22] also are most consistent with a mechanism involving direct phosphoryl transfer to a metal-bound water molecule without a phosphoenzyme intermediate. This evidence indicates that a model for the catalytic mechanism for the Ser/Thr phosphatases can be represented as shown in Figure 6-5. In this scheme k_2 represents a hypothetical conformational change or other non-chemical step subsequent to substrate binding. There is no direct evidence for such an additional step in the mechanism of λPPase, but it is reasonable to assume for the moment that a conformational change may occur upon substrate binding in order to consider the

possibility that a nonchemical step may be partly or fully rate limiting, thereby affecting the observed enzymatic kinetic isotope effects.

Because the competitive method was used to measure the isotope effects in this study, they are effects on V/K and thus are effects on the part of the mechanism up to the first irreversible step, regardless of which step is rate limiting in the overall enzymatic mechanism. The first irreversible step is likely to be the phosphoryl transfer step from substrate to the metal-bound water, which is shown as k_3 in Figure 6-5. The justifications for representing this step as irreversible are the poor nucleophilicity of p-nitrophenol and the observation that p-nitrophenol is a poor inhibitor of Ser/Thr phosphatases,[21] which suggests that its dissociation from the active site is rapid.

When only one step is isotopically sensitive in an enzymatic reaction, the isotope effect on V/K is described by equation 2.[37]

$$*(V/K) = \frac{\left[*k + c_f + c_r\left(*K_{eq} \right) \right]}{\left(1 + c_f + c_r \right)} \tag{2}$$

In this equation $*(V/K)$ represents either $^{18}(V/K)$ or $^{15}(V/K)$, $*k$ similarly designates the isotope effect on the isotope-sensitive step, $*K_{eq}$ is the equilibrium isotope effect in the forward direction, and the constants c_f and c_r are the forward and reverse commitment factors, respectively.[38] There will be no reverse commitment if the phosphoryl transfer step k_3 is irreversible; data described above indicate that this is the case.[22] Using the mechanism in Figure 6-5, if the chemical step is the only isotope sensitive step, then the isotope effect is given by equation 3.

$$*(V/K) = \frac{\left(*k_3 + c_f \right)}{\left(1 + c_f \right)} \tag{3}$$

$$E + ROP \underset{k_{-1}}{\overset{k_1}{\rightleftharpoons}} E \cdot ROP \underset{k_{-2}}{\overset{k_2}{\rightleftharpoons}} E^* \cdot ROP \overset{k_3}{\longrightarrow} E \cdot P_i \cdot RO$$

with the cycle: $E \cdot P_i \cdot RO \to$ (RO) $\to E \cdot Pi \to$ (Pi) $\to E$; and $E \cdot P_i \cdot RO \to$ (Pi) $\to E \cdot RO \to$ (RO) $\to E$

$$\Big[\xleftarrow{\hspace{3cm}} V/K \xrightarrow{\hspace{3cm}} \Big]$$
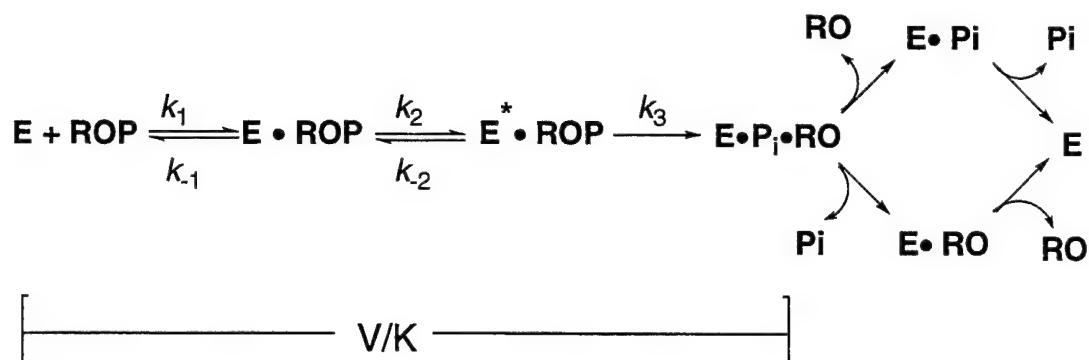
Figure 6-5. Mechanistic scheme for λPPase phosphate ester hydrolysis. Steps sensitive to the measurement of kinetic isotope effects are shown in brackets.

The commitment factor c_f will equal $(k_3/k_{-2})(1 + k_2/k_{-1})$.

To the extent that a nonchemical step such as substrate binding or a subsequent conformational change is rate-limiting, the resulting forward commitment will suppress the magnitude of the isotope effects on the chemical step and can completely abolish them resulting in observed isotope effects of zero percent. Just such a case is observed with alkaline phosphatase, where the absence of kinetic isotope effects[28] as well as other kinetic data[27] indicate that a nonchemical step is completely rate-limiting except for substrates having very poor leaving groups. In the calcineurin reaction, commitments partially suppress the kinetic isotope effects at the pH optimum, although the suppression is reduced and the isotope effects on the chemical step are fully or nearly fully expressed if the reaction is studied at higher pH.[26]

The ratio k_2/k_{-1} is a measure of the fate of the initial enzyme-substrate complex. If the substrate is tightly bound, this ratio will be large (the substrate will be "sticky") and the isotope effects thereby suppressed. With the λPPase enzyme pNPP exhibits a K_M value of 14 mM, a value 30-fold higher than the K_M of a phosphoprotein substrate.[16] This fact gives us a reasonable expectation that the ratio k_2/k_{-1} will be small with pNPP. The ratio k_3/k_{-2} reflects the partitioning of the enzyme-substrate complex following the hypothetical conformational change or other nonchemical step. If such an additional step

is not rapidly reversible, then the enzyme-substrate complex will partition completely forward from this step, and the large k_3/k_{-2} ratio will suppress the isotope effects on the chemical step.

In cases where a commitment factor is sufficiently large to suppress but not entirely abolish isotope effects, the magnitudes of the observed isotope effects will often increase at non-optimal pH values due to the slower rate of the chemical step and the resultant lowering of the commitment factor, just as was found with calcineurin.[26] As a test for the degree to which chemistry is rate-limiting, the isotope effects for the λPPase reaction with pNPP were measured at the pH optimum of 7.8 and also at pH 6.0 and 9.0, where catalysis is significantly slower. The magnitudes of the isotope effects are significantly nonzero and, within experimental error, constant over the pH range examined. This strongly suggests that the chemical step is rate-limiting for V/K across the pH range 6.0 to 9.0, and that the isotope effects measured are the intrinsic ones for the enzymatic phosphoryl-transfer step with the native enzyme using pNPP as substrate. Since the chemical step is considerably slower in the H76N mutant and with the native enzyme when Ca^{2+} replaces Mn^{2+}, chemistry should be rate-limiting in those reactions as well.

Compared with the data from the native enzyme, the values of ^{15}(V/K) and of ^{18}(V/K)$_{bridge}$ increase in the reaction of the H76N mutant enzyme. This could indicate a change in the nature of the transition state arising from this mutation; however, an alternative explanation of the data is that the isotope effects are suppressed in the native enzyme but become fully expressed in the slower H76N mutant. This can be ruled out because a commitment factor in the native enzymatic reaction would suppress all of the isotope effects proportionally. Compared to the values for the native reaction, ^{15}(V/K) for the H76N mutant is increased about 2.5-fold while ^{18}(V/K)$_{bridge}$ only increases about 1.3-fold. This means that the changes in the isotope effects caused by the mutation are

the result of a change in the transition state for the phosphoryl transfer reaction. In addition, substitution of Ca^{2+} results in a significant reduction in catalytic rate but no change in the isotope effects as would be expected if the isotope effects were being partially suppressed by commitment factors.

Interpretation of Kinetic Isotope Effects on Phosphoryl Transfer Reactions. Kinetic isotope effects can characterize reactions in detail, in particular yielding information about the structure of the transition state. The transition state for hydrolysis of phosphate monoesters in solution can be described as very loose or dissociative in nature, characterized by extensive bond cleavage to the leaving group, minimal bond formation to the nucleophile, and in which the transferring phosphoryl group resembles metaphosphate ion.[39,40] Phosphodiesters and triesters exhibit successively tighter, more associative transition states characterized by less bond cleavage to the leaving group and greater bond formation to the nucleophile, where the transferring phosphoryl group resembles a pentacoordinate phosphorane.[40] Linear free energy relationships indicate that in diesters and triesters with good leaving groups, these reactions are concerted with no phosphorane intermediate, but that the transition states become tighter (more associative) than in the dissociative transition state of the monoester reaction.[41,42] Isotope effects have been measured for the phosphoryl transfer reactions of a number of phosphate esters in solution.[28,32,36,43-45] The cumulative data indicate that isotope effects can distinguish between these types of transition states. Calculations predict inverse nonbridge [18]O isotope effects for dissociative transition states, and normal values for associative transition states.[36] The experimental nonbridge [18]O isotope effects for monoester reactions under different conditions are all small and inverse (-0.06 to -0.03%), and the nonbridge [18]O isotope effects for diesters and triesters which have been measured are (with a single exception, which may be anomalous) normal (0.40 to 2.50%).

The isotope effects in the leaving group also distinguish between the loose transition states of monoesters and the tighter ones of diesters and triesters. The isotope effects $^{15}(V/K)$ and $^{18}(V/K)_{bridge}$ measure charge delocalization in the leaving group and P–O bond cleavage, respectively. The extensive bond cleavage in the monoester dianion reaction shows bridge ^{18}O isotope effects of 2.02 to 3.0% and ^{15}N isotope effects of 0.28 to 0.39%. The tighter transition states of diesters and triesters with this leaving group exhibit values for the bridge ^{18}O isotope effects in the range of 3.9 to 6.0%, and for the ^{15}N isotope effect of 0.07 to 0.16%.

When protonation of the leaving group occurs in the transition state the normal $^{18}(V/K)_{bridge}$ isotope effect arising from P–O bond cleavage is reduced by the inverse isotope effect arising from protonation. This is just what is observed in the reaction of the pNPP monoanion in solution, where proton transfer from the phosphoryl group to the leaving group occurs during the reaction, and in the reactions of protein-tyrosine phosphatases where protonation of the leaving group is accomplished by a conserved Asp general acid. The maximum $^{18}(V/K)_{bridge}$ effect seen in pNPP reactions in which the leaving group is not protonated is around 3%, the value observed in PTPases when general acid catalysis has eliminated by mutation.[23-25] The equilibrium isotope effect for protonation of p-nitrophenol is -1.5%.[46] Thus when P–O bond cleavage and proton transfer are extensive and synchronous, the observed $^{18}(V/K)_{bridge}$ isotope effect should be close to the product of these values, or about +1.5%. This is close to the value measured in reactions of pNPP with PTPases where protonation of the leaving group occurs in the transition state.[23-25]

Mechanism and Transition State Structure for the λPPase Reaction. The bell-shaped pH-rate profile for k_{cat} indicates that maximal activity depends on a species which must be deprotonated and another which must be protonated. The acidic limb most likely represents the nucleophilic metal-bound water molecule. The species

responsible for the basic limb results not just in smaller values for k_{cat} but also large increases in K_M when it is deprotonated (Table 6-5). The K_M values for the H76N mutant at all pH values are more consistent and are similar to those seen in the native enzyme at high pH, suggesting that protonation of this residue assists in substrate binding.

If the substrate for catalysis were the monoanion of pNPP, the rate should increase at low pH as the fraction of the substrate present in solution as the monoanion increases. The pH-rate profile suggests that the catalytically active form of the substrate is the dianion. Due to problems with substrate inhibition below pH 6.0, the profile could not be extended to low enough pH values where the pK_a of the substrate, which is 4.96 in solution,[47] would be expected to reveal itself. The values for the $^{18}(V/K)_{nonbridge}$ isotope effect give additional evidence that the dianion form of pNPP is the substrate. At pH 6.0 about 10% of the pNPP substrate will be present as the monoanion, whereas at pH 7.8 and 9.0 the concentration of the monoanion will be negligible. Since the isotope effect for protonation of a phosphate monoester is -1.5%[34] and if protonation of the substrate occurs before or during catalysis, the observed isotope effect at this position will be the product of the inverse isotope effect for protonation and that for the phosphoryl transfer step. Since the kinetic $^{18}(V/K)_{nonbridge}$ effects for monoester hydrolysis in all past studies have been very nearly zero, if the monoanionic form is involved then the observed $^{18}(V/K)_{nonbridge}$ effect should be in the neighborhood of the isotope effect for protonation. The inverse values of $^{18}(V/K)_{nonbridge}$ with λPPase were all found to be much less inverse than -1.5% (Table 6-1). Therefore, they represent exactly the magnitude expected for a loose transition state of the dianionic substrate, as in the uncatalyzed reaction in solution.

The possibility that coordination to the metal ions at the active site could result in isotope effects at the nonbridging oxygens atoms also must be considered. Metal analysis shows that the purified enzyme is devoid of iron, and no EPR signals for Fe^{3+} are observed. Therefore, the active form of the enzyme in these experiments is the di-Mn^{2+} [48]

and presumably the di-Ca^{2+} enzyme depending upon which metal ion is supplied in the buffer solution. A few measurements of ^{18}O isotope effects on the complexation of metal ions to pNPP have been reported. Co(III) is capable of forming inert coordination complexes with phosphate esters such as the Co(ethylene diamine)$_2$-pNPP complex, which can be isolated and crystallized. Cleavage of the phosphate oxygen-cobalt bond of this complex results in a kinetic isotope effect of 1.35%,[49] which is close to the equilibrium effect for deprotonation of a phosphate ester. Formation of the more labile complex between Co(cyclen)$_2$ and pNPP results in a smaller equilibrium effects on the coordination of 0.81%.[49] Divalent metal ions should exhibit weaker coordination and therefore yield smaller isotope effects. A study of the effects of magnesium complexation with ATP put an upper limit on the ^{18}O isotope effect of 0.1%.[50]

We sought to measure or at least to estimate the magnitude of the ^{18}O isotope effect for complexation of the pNPP substrate to Ca^{2+}. The log of the stability constant (K is M^{-1}) for the Ca^{2+}-pNPP complex has been reported to be 1.26 ± 0.04, as measured by potentiometric-pH titration.[51] The determination by UV-VIS titration made in this study gave a value of 1.8 which is in reasonable agreement given the less sensitive method of measuring λ_{max}, which changes by only 2 nm from zero to saturating metal ion. However, the results of the ^{31}P NMR experiment indicate that higher order complexes form as the calcium ion concentration is increased beyond the levels which give 1:1 complexation.

The results from the isotope-shift ^{31}P NMR experiment (Figure 6-3) show that there is a very small ^{18}O isotope effect for coordination of Ca^{2+}. The data allow only an estimation to be made for this isotope effect from a comparison of the maximum separation of the signals for the isotopically labeled ligands as compared to the separation observed in the analogous protonation experiment.[34] The change in separation reaches a maximum when the ligand is half protonated (or complexed). The maximum change in

the isotopic separation found in the protonation experiment was 0.015 ppm.[34] At a calcium ion concentration which gives half complexation of pNPP by the UV-VIS data (indicating the 1:1 complex), this change is 0.0014, suggesting this isotope effect is only about 10% as large as that for protonation. In the ^{31}P NMR experiments, complete saturation of the pNPP ligand by ^{31}P NMR could not be achieved and so an exact measurement of the isotope effect for the higher order Ca^{2+}-pNPP complex could not be calculated although the isotope effect clearly is greater than for the 1:1 complex. Using the maximum value observed for the change in the isotopic separation gives an estimated value of -0.24%, which presumably represents the isotope effect for formation of a complex between pNPP and two calcium ions.

The value for the observed $^{18}(V/K)_{nonbridge}$ isotope effect in the λPPase reaction will be the product of the isotope effect for binding and that for catalysis. The small value of the equilibrium isotope effect for coordination of pNPP to two Ca^{2+} ions inferred by the data indicates that binding effects are not likely to be sufficiently large to mask the isotope effect for the phosphoryl transfer reaction. Thus the $^{18}(V/K)_{nonbridge}$ effect for phosphoryl transfer is essentially unity or slightly inverse, not a normal value that would be indicative of the tighter transition states seen in diesters and triesters. This value is also very close to that observed in the reactions of native PTPases (Table 6-2), which indicates that the binuclear metal center does not induce a change in the transferring phosphoryl group in the transition state relative to its structure in solution reactions or reactions of PTPases.

The isotope effects in the leaving group for the reaction of the native λPPase with both Ca^{2+} and Mn^{2+} are similar to those observed in reactions of the native PTPases, where P–O bond cleavage is extensive in the transition state but the leaving group is neutralized by protonation. The small $^{15}(V/K)$ value of 0.06% indicates that a small but measurable negative charge develops on the leaving group in the transition state,

indicating that charge neutralization of the leaving group does not quite keep up with P-O bond cleavage. A similar value was previously found for the native low-molecular weight PTPase Stp-1 (Table 6-2).[23]

One of the unanswered questions for the Ser/Thr phosphatases is whether the histidine residue that is conserved in the region of the active site in Ser/Thr phosphatases functions as a general acid. The precise roles of the metal ions are also not known and it is possible that one or both of them assists in stabilization of the leaving group, analogous to the situation in alkaline phosphatase.[52] Spectroscopic studies have shown that mutation of His76 results in a perturbation of the ligand environment of the binuclear metal center, possibly by disruption of a hydrogen bond between the histidine and a metal-coordinated water molecule.[15]

In the present study mutation of His76 in λPPase to asparagine resulted in an increase in $^{15}(V/K)$ from 0.06 to 0.16% and an increase in $^{18}(V/K)_{bridge}$ from 1.33 to 1.83% (Table 6-1). These increases are analogous to those observed in $^{15}(V/K)$ and $^{18}(V/K)_{bridge}$ in reactions of PTPases that arise from mutation of their general acids (Table 6-2), but the increases in the λPPase case are smaller in magnitude. There are two possible explanations for the smaller increase in these isotope effects. One possibility is that the H76N λPPase reaction proceeds with an earlier transition state in which P-O bond cleavage is less advanced. An alternative explanation is that charge neutralization of the leaving group is accomplished by one of the metal ions, and that the increases in the $^{15}(V/K)$ and $^{18}(V/K)_{bridge}$ isotope effects in the H76N mutant are due to perturbation of the ligand environment which interferes with but does not eliminate this interaction in the transition state, rather than the mutation causing the loss of a hypothetical general acid. The $^{15}(V/K)$ isotope effect arises from contributions from a quinonoid resonance structure of the nitrophenolate anion which involves the nitro substituent.[45] If the phenolic oxygen atom is in the region of a cationic metal ion, then less charge will be delocalized into the

aromatic ring and this isotope effect will be diminished. This explanation of the data also requires that coordination to the metal ion reduces the $^{18}(V/K)_{bridge}$ isotope effect in the same manner as protonation suppresses the normal isotope effect arising from P-O bond cleavage. There is no experimental basis to allow an estimation of the magnitude of an ^{18}O isotope effect for coordination of nitrophenolate ion to a divalent metal ion. Fairly strong phenolate-metal complexes are known in a number of enzymes, both with ligands (purple acid phosphatase),[53] with substrate analogues (tyrosine hydroxylase),[54] and with substrates (pyrocatechase,[55] Mn^{2+}-dependent catechol dioxygenase).[56] Thus the possibility of a significant isotope effect for such an interaction cannot be dismissed.

The pH-rate profile of the H76N mutant was also determined in an attempt to ascertain the role of this residue. If His76 functions as a general acid in catalysis, the basic limb of the pH-rate profile for the H76N mutant should be lost. The data for the native enzyme and the H76N mutant are shown in Table 6-5 and Figure 6-4. The basic limb that is present in the pH-rate profile of the native enzyme is smaller in the H76N mutant, but is not eliminated. Kinetic data were difficult to obtain due to substrate inhibition at low pH, which required the use of higher metal ion concentrations, and increasing K_M values for substrate at higher pH. It is noteworthy that in the native enzyme the K_M increases at high pH to values that are very similar to those found across the entire pH range in the H76N mutant. This implies that protonation of His76 electrostatically assists in substrate binding (though actual proton transfer to the substrate to form the monoanion is ruled out by the $^{18}(V/K)_{nonbridge}$ isotope effects as discussed earlier). Similar electrostatic assistance in stabilization of the transition state is a reasonable assumption. These facts, and the perturbation of the metal center which results from the H76N mutation, make it difficult to interpret the pH-rate dependency strictly for or against a role for His76 as a general acid. In sum, neither the isotope effects nor the kinetic data allow a definitive answer to this question.

It is noteworthy that the H76N mutation has no effect on the $^{18}(V/K)_{nonbridge}$ isotope effect. In all of the PTPases it has been found that loss, or even partial interference with the effectiveness of neutralization of the leaving group by the general acid always resulted in normal $^{18}(V/K)_{nonbridge}$ isotope effects. This was attributed to more nucleophilic participation in the transition state, which can be rationalized by the need for more of a push to expel the leaving group when charge neutralization is lost.[23-25] In the H76N mutant of λPPase the leaving group also departs bearing more of a negative charge, but there is no change in the $^{18}(V/K)_{nonbridge}$ isotope effect, giving no evidence that this results in additional nucleophilic participation. This may be a result of the different nucleophile in the λPPase reaction (an oxyanion versus a thiolate in the PTPases) or may be due to other electrostatic influences in the catalytic site.

In summary the isotope effect data are most consistent with a transition state for the λPPase reaction which is very similar to those of the PTPase reactions. In the reactions of the native PTPases the observed $^{15}(V/K)$ and $^{18}(V/K)_{bridge}$ isotope effects resulting from bond cleavage and charge development are reduced by protonation of the leaving group. It is conceivable that in the λPPase reaction no such neutralization occurs and that the observed $^{15}(V/K)$ and $^{18}(V/K)_{bridge}$ isotope effects only serendipitously resemble these isotope effects in the PTPase reactions, and instead reflect an earlier transition state with bond cleavage much less advanced in a tighter transition state, more similar to reactions typical of diesters or triesters. If no neutralization of the leaving group occurs in the λPPase reaction, it is difficult to explain why the $^{15}(V/K)$ and $^{18}(V/K)_{bridge}$ isotope effects increase in the H76N mutant. In addition, phosphoryl transfer transition states with tighter transition states are characterized by normal $^{18}(V/K)_{nonbridge}$ isotope effects, while the small inverse values for $^{18}(V/K)_{nonbridge}$ seen in this study are characteristic of the loose transition states of monoester reactions. It may also be conceivable that the $^{18}(V/K)_{nonbridge}$ isotope effects for λPPase are altered by binding to the

binuclear metal center in such a way that they also merely serendipitously resemble the isotope effects seen with monoesters. However, two of the experimental observations made above provide a strong counter to this proposal. First, the solution results with Ca^{2+} are nearly identical with those where Mn^{2+} is present. Additionally, it was noted that the H76N mutation, which is known to perturb the metal center, alters the isotope effects in the leaving group but *does not change* the $^{18}(V/K)_{nonbridge}$ isotope effect. Both of these facts suggest strongly that this isotope effect is not significantly altered by substrate binding. Thus the simplest explanation of the data is that the transition state for the λPPase reaction is similar to those of the reactions of PTPases despite the very different catalytic machinery used by these enzymes.

Conclusions

It has been suggested that the presence of positive charge in phosphatases around the transferring phosphoryl group implies a transition state with associative character and considerable nucleophilic participation[57,58] in contrast to the reaction in solution, which is dissociative or loose in nature. The data obtained in this study do not lend support to the notion that the binuclear center in the λPPase induces such a mechanistic change. The isotope effects are most consistent with a reaction similar to the reaction in solution and in the reactions of native PTPases, which is noteworthy in light of the vastly different catalytic machinery utilized by the two classes of phosphatases. The substitution of Ca^{2+} for Mn^{2+} in the binuclear metal center does not result in a change in the transition state for phosphoryl transfer. The H76N mutation results in small changes in the isotope effects, indicative of greater negative charge borne on the leaving group in the transition state. Neither the isotope effect data nor the pH-rate data clearly answer the question of whether His76 functions as a general acid in the enzymatic reaction, and it is still uncertain whether this residue or the metal ions participate in charge neutralization of the leaving

group. The kinetic data indicate that substrate binding is assisted when His76 is
protonated.

References

(1)   Zhang, Z. Y.; Wang, Y.; Dixon, J. E. *Pro. Natl. Acad. Sci. U.S.A.* **1994**, *91*, 1624-1627.

(2)   Lohse, D. L.; Denu, J. M.; Santoro, N.; Dixon, J. E. *Biochem.* **1997**, *36*, 4568-4575.

(3)   Guan, K. L.; Dixon, J. E. *J. Biol. Chem.* **1991**, *266*, 17026-17030.

(4)   Cho, H.; Krishnaraj, R.; Bannwarth, W.; Walsh, C. T.; Anderson, K. S. *J. Am. Chem. Soc.* **1992**, *114*, 7296-7298.

(5)   Rusnak, F.; Yu, L.; Mertz, P. *J. Biol. Inorg. Chem.* **1996**, *1*, 388-396.

(6)   Lohse, D. L.; Denu, J. M.; Dixon, J. E. *Structure* **1995**, *3*, 987-990.

(7)   Barford, D.; Das, A. K.; Egloff, M. P. *Annu. Rev. Biophys. Biomol. Struct.* **1998**, *27*, 133-164.

(8)   Goldberg, J.; Huang, H. B.; Kwon, Y. G.; Greengard, P.; Nairn, A. C.; Kuriyan, J. *Nature* **1995**, *376*, 745-753.

(9)   Egloff, M. P.; Cohen, P. T.; Reinemer, P.; Barford, D. *J. Mol. Biol.* **1995**, *254*, 942-959.

(10) Griffith, J. P.; Kim, J. L.; Kim, E. E.; Sintchak, M. D.; Thomson, J. A.; Fitzgibbon, M. J.; Fleming, M. A.; Caron, P. R.; Hsiao, K.; Navia, M. A. *Cell* **1995**, *82*, 507-522.

(11) Kissinger, C. R.; Parge, H. E.; Knighton, D. R.; Lewis, C. T.; Pelletier, L. A.; Tempczyk, A.; Kalish, V. J.; Tucker, K. D.; Showalter, R. E.; Moomaw, E. W.; Gastinel, L. N.; Habuka, N.; Chen, X.; Maldonado, F.; Barker, J. E.; Bacquet, R.; Villafranca, J. E. *Nature* **1995**, *378*, 641-644.

(12) Das, A. K.; Helps, N. R.; Cohen, P. T.; Barford, D. *EMBO J.* **1996**, *15*, 6798-6809.

(13) Strater, N.; Klabunde, T.; Tucker, P.; Witzel, H.; Krebs, B. *Science* **1995**, *268*, 1489-1492.

(14) Klabunde, T.; Strater, N.; Frolich, R.; Witzel, H.; Krebs, B. *J. Mol. Biol.* **1996**, *259*, 737-748.

(15) Mertz, P.; Yu, L.; Sikkink, R.; Rusnak, F. *J. Biol. Chem.* **1997**, *272*, 21296-21302.

(16) Zhuo, S.; Clemens, J. C.; Hakes, D. J.; Barford, D.; Dixon, J. E. *J. Biol. Chem.* **1993**, *268*, 17754-17761.

(17) Zhuo, S.; Clemens, J. C.; Stone, R. L.; Dixon, J. E. *J. Biol. Chem.* **1994**, *269*, 26234-26238.

(18) Mueller, E. G.; Crowder, M. W.; Averill, B. A.; Knowles, J. R. *J. Am. Chem. Soc.* **1993**, *115*, 2974-2975.

(19) Aquino, M. A.; Lim, J. S.; Sykes, A. G. *J. Chem. Soc. Dalton Trans.* **1994**, 429-436.

(20) Dietrich, M.; Munstermann, D.; Sauerbaum, H.; Witzel, H. *Eur. J. Biochem.* **1991**, *199*, 105-113.

(21) Martin, B. L.; Graves, D. J. *J. Biol. Chem.* **1986**, *261*, 14545-14550.

(22) Martin, B. L.; Graves, D. J. *Biochim. Biophys. Acta* **1994**, *1206*, 136-142.

(23) Hengge, A. C.; Zhao, Y.; Wu, L.; Zhang, Z.-Y. *Biochem.* **1997**, *36*, 7928-7936.

(24) Hengge, A. C.; Denu, J. M.; Dixon, J. E. *Biochem.* **1996**, *35*, 7084-7092.

(25) Hengge, A. C.; Sowa, G. A.; Wu, L.; Zhang, Z.-Y. *Biochem.* **1995**, *34*, 13982-13987.

(26) Hengge, A. C.; Martin, B. L. *Biochem.* **1997**, *36*, 10185-10191.

(27) Simopoulos, T. T.; Jencks, W. P. *Biochem.* **1994**, *33*, 10375-10380.

(28) Hengge, A. C.; Edens, W. A.; Elsing, H. *J. Am. Chem. Soc.* **1994**, *116*, 5045-5049.

(29) Herschlag, D.; Jencks, W. P. *J. Am. Chem. Soc.* **1987**, *109*, 4665-4674.

(30) Cleland, W. W. *Biochem.* **1964**, *3*, 480-482.

(31) O'Leary, M. H.; Marlier, J. F. *J. Am. Chem. Soc.* **1979**, *101*, 3300-3306.

(32) Caldwell, S. R.; Raushel, F. M.; Weiss, P. M.; Cleland, W. W. *Biochem.* **1991**, *30*, 7444-7450.

(33) Ellison, L. R.; Robinson, M. J. *J. Chem Soc., Chem. Commun.* **1983**, 745.

(34) Knight, W. B.; Weiss, P. M.; Cleland, W. W. *J. Am. Chem. Soc.* **1986**, *108*, 2759-2761.

(35) Lanzetta, P. A.; Alvarez, L. J.; Reinach, P. S.; Candia, O. A. *Anal. Biochem.* **1979**, *100*, 95-97.

(36) Weiss, P. M.; Knight, W. B.; Cleland, W. W. *J. Am. Chem. Soc.* **1986**, *108*, 2761-2762.

(37) Cleland, W. W. *Bioorg. Chem.* **1987**, *15*, 283-302.

(38) Northrop, D. B. In *Isotope Effects on Enzyme-Catalyzed Reactions*; Cleland, W. W., O'Leary, M. H., Northrop, D. B., Eds.; University Park Press: Baltimore, MD, 1977, p 303.

(39) Hengge, A. C. In *Comprehensive Biological Catalysis*; Sinnott, M., Ed.; Academic Press: San Diego, CA, 1998; Vol. 1, pp 517-542.

(40) Thatcher, G. R. J.; Kluger, R. *Adv. Phys. Org. Chem.* **1989**, *25*, 99-265.

(41) Davis, A. M.; Hall, A. D.; Williams, A. *J. Am. Chem. Soc.* **1988**, *110*, 5105-5108.

(42) Ba-Saif, S. A.; Waring, M. A.; Williams, A. *J. Am. Chem. Soc.* **1990**, *112*, 8115-8120.

(43) Hengge, A. C.; Tobin, A. E.; Cleland, W. W. *J. Am. Chem. Soc.* **1995**, *117*, 5919-5926.

(44) Hengge, A. C.; Cleland, W. W. *J. Am. Chem. Soc.* **1991**, *113*, 5835-5841.

(45) Hengge, A. C.; Cleland, W. W. *J. Am. Chem. Soc.* **1990**, *112*, 7421-7422.

(46) Hengge, A. C.; A., H. R. *J. Am. Chem. Soc.* **1994**, *116*, 11256-11263.

(47) Bourne, N.; Williams, A. *J. Org. Chem.* **1984**, *49*, 1200-1204.

(48) Rusnak, F.; Yu, L.; Todorovic, S.; Mertz, P. *submitted* **1999**.

(49) Rawlings, J.; Hengge, A. C.; Cleland, W. W. *J. Am. Chem. Soc.* **1997**, *119*, 542-549.

(50) Jones, J. P.; Weiss, P. M.; Cleland, W. W. *Biochem.* **1991**, *30*, 3634-3639.

(51) Massoud, S. S.; Sigel, H. *Inorg. Chem.* **1988**, *27*, 1447-1453.

(52) Kim, E. E.; Wyckoff, H. W. *J. Mol. Biol.* **1991**, *218*, 449-464.

(53) Vincent, J. B.; Olivier-Lilley, G. L.; Averill, B. A. *Chem. Rev.* **1990**, *90*, 1447-1467.

(54) Michaud-Soret, I.; Andersson, K. K.; Que Jr., L.; Haavik, J. *Biochem.* **1995**, *34*, 5504-5510.

(55) Que, J. L.; Heistand 2d, R. H.; Mayer, R.; Roe, A. L. *Biochem.* **1980**, *19*, 2588-2593.

(56) Whiting, A. K.; Boldt, Y. R.; Hendrich, M. P.; Wackett, L. P.; Que Jr., L. *Biochem.* **1996**, *35*, 160-170.

(57) Schlichting, I.; Reinstein, J. *Biochem.* **1997**, *36*, 9290-9296.

(58) Mildvan, A. S. *Proteins* **1997**, *24*, 401-416.

CHAPTER 7

A MECHANISTIC STUDY OF SULFATE ESTER HYDROLYSIS AND THE EXTENT TO WHICH IT RESEMBLES PHOSPHATE MONOESTER HYDROLYSIS

Abstract: Based on the results of kinetic studies and the use of several mechanistic probes, the resemblance between sulfate monoester hydrolysis and phosphate monoester hydrolysis has often been inferred. A further exploration of the relationship between these very similar reactants was undertaken that incorporated the use of kinetic isotope effects and a study of the kinetics of the reaction in *tert*-amyl alcohol, using *p*-nitrophenyl sulfate as the substrate. In contrast to the *p*-nitrophenyl phosphate dianion, which reacts nearly 9,000-fold faster in *tert*-amyl alcohol, the rate of solvolysis for *p*-nitrophenyl sulfate is actually 40-fold slower. An evaluation of the activation parameters in *tert*-amyl alcohol showed that this rate reduction is primarily entropic in nature. The most logical explanation for this is a difference in the solvation of ground and transition states for the two reactants. Kinetic isotope effects were evaluated for the reaction of *p*-nitrophenyl sulfate in neutral solution, where the monoanion is the primary form of the substrate observed, and in acidic solution where it is believed that the protonated species is the reactant. For the monoanion at 85 °C, isotope effects were $^{15}k = 0.26\pm.01\%$, $^{18}k_{bridge} = 2.1\pm.1\%$, and $^{18}k_{nonbridge} = -0.49\pm.03\%$; under acidic conditions at 65 °C, they were $^{15}k = 0.02\pm.01\%$, $^{18}k_{bridge} = 0.69\pm.02\%$, and $^{18}k_{nonbridge} = 0.67\pm.01\%$. These results indicate that the mechanism proceeds by a concerted, highly dissociative transition state, regardless of pH. Although the isotope effects infer a sulfur center with bonding character that closely resembles sulfur trioxide, no evidence was found of a free sulfur trioxide intermediate. The overall conclusion, in spite of the anomalous activation entropy in aqueous solution, is that the sulfate monoester mechanism is indeed very similar to that of the phosphate monoester.

Introduction

In a classic experiment more than a century ago, Baumann[1] administered phenol to a patient and showed that it was excreted as phenyl sulfate. This was the first demonstration of biological sulfation as an important detoxification mechanism. In subsequent experiments it was shown that the metabolism of drugs often culminates in the excretion of sulfated forms of the drugs, and this process is the subject of a large body of medical literature.[2] Detoxification is merely one of the roles of sulfation reactions, and sulfate monoesters are found among all classes of natural products, including examples such as nucleotides, peptides and proteins, polysaccharides, steroids, and lipids. Sulfate monoesters of steroids are key intermediates in the biosynthesis of steroids, where the sulfate moiety enables intermediates to be kept in circulation as hormone precursors.[3] Deficiency in steroid sulfatases can lead to excessive excretion of steroid sulfates and problems in pregnancy and childbirth.[4] As a result of these many key roles in biochemical systems, there has been significant recent interest in the mechanism of hydrolysis of sulfate esters and biological sulfuryl transfer.

As widely distributed in nature as sulfate monoesters are, equally ubiquitous are the varieties of sulfatase enzymes which catalyze the hydrolysis of the ester linkage as shown in Figure 7-1A and 7-1B.[5] Transfer of the SO_3^- group from a reactant to an acceptor molecule is generically termed sulfuryl transfer; when the acceptor is water, the reaction is termed hydrolysis. Several hypotheses have been proposed in the literature concerning mechanistic similarities between the chemistry of sulfate and phosphate esters.[6-10] Even more significantly, the case has been made for an evolutionary relationship between phosphatase and sulfatase enzymes.[11] In spite of its biological importance, sulfate ester chemistry has been the subject of fewer studies than other hydrolytic mechanisms (e.g., amide, carboxyl ester hydrolysis, phosphate ester hydrolysis). The published studies have shed some light on the mechanism of

uncatalyzed sulfate ester hydrolysis, although some apparently contradictory data have not been satisfactorily explained. The development of new synthetic methods has allowed the application of heavy atom isotope effects to the solution chemistry of sulfate esters. From these data, some of the recent assertions concerning mechanisms of biochemical sulfate ester hydrolysis and sulfuryl transfer can be reexamined.

It has been stated that the solution hydrolysis of sulfate esters resembles that of phosphate esters. In the solution chemistry of phosphate monoesters, the monoester may exist in one of three protonation states: the neutral species, the monoanion, or the dianion. The neutral species is present only in minute quantities in aqueous solution, but the monoanion and dianion (Figure 7-1C and 7-1D) are both observable at biological pHs, and the monoanion is 60 times more reactive than the dianion. This rate difference is the result of the entropic advantage of the intramolecular transfer of the proton to the leaving group. This transfer allows the leaving group to depart as an uncharged molecule, and
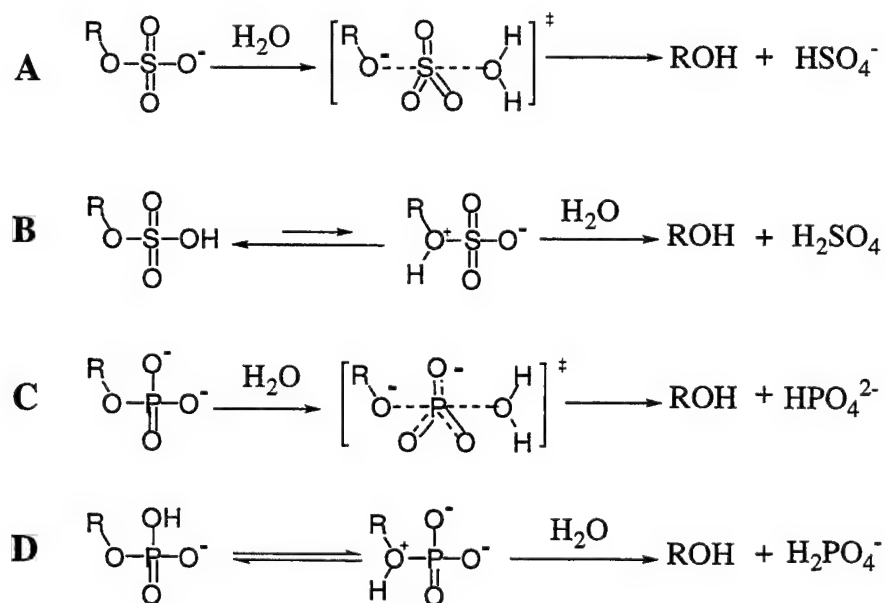
Figure 7-1. Proposed mechanisms for hydrolysis of sulfate and phosphate monoesters. A and B show the sulfate monoanion and neutral species, respectively. C and D show the phosphate dianion and monoanion.

therefore does not require extensive solvent rearrangement to accomodate a charged leaving group. This infers a further entropic advantage for the monoanion reaction over the dianion.

Sulfate monoesters may exist in either of two protonation states, namely the anion (Figure 7-1A) or the neutral species (Figure 7-1B). There is evidence that different mechanisms are followed by these species. At readily attainable pHs, the predominant form of the sulfate monoester is the monoanion (see Figure 1-14). This structure more closely resembles the phosphate dianion, as both lack the intramolecular availability of the proton to facilitate leaving group departure. Therefore, the standard of comparison between phosphate and sulfate monoester chemistry is the comparison of phosphate dianion to sulfate monoanion (Figure 7-1A and 7-1C). There is general agreement that the phosphate monoester is hydrolyzed through a dissociative transition state with little nucleophilic involvement.[12] In contrast, the uncertainty surrounding the mechanism of sulfate monoester hydrolysis is demonstrated by the description of this mechanism in a recent review as "predominantly dissociative in nature with some associative character."[13]

Earlier studies established kinetic parameters that allow the parallel to be drawn between sulfate monoester monoanions and phosphate monoester dianions. Both species demonstrate similar pH/rate profiles with a plateau at neutral values and acid and base catalyzed rate enhancements at pH extremes.[7,14] Studies of phosphate hydrolysis determined a β_{LG} of -1.23[15] and a β_{NUC} of 0.13,[14] while similar studies of sulfate hydrolysis found a β_{LG} of -1.2 [8] and a β_{NUC} of 0.20.[7] These values suggest a reaction where the departure of the leaving group is advanced and there is little nucleophilic participation, and the remarkable similarity of the parameters appears to indicate that the reactions proceed along nearly identical paths. Since the solution hydrolysis of the phosphate monoester dianion proceeds through a highly dissociative, metaphosphate-like transition state, it has been inferred that in the transition state of the sulfate monoanion

reaction the sulfuryl group resembles sulfur trioxide.[10,16] However, the validity of interpreting Brønsted parameters in terms of transition state bonding is not universally accepted.[17] The possibility of a fully dissociative mechanism proceeding by way of a free SO_3 intermediate has been ruled out by stereochemical studies; incubation of phenyl [(R)-^{16}O, ^{17}O, ^{18}O] sulfate with an acceptor alcohol in carbon tetrachloride solution was found to form product of exclusively inverted configuration.[18]

One important difference was found in the kinetic studies of these two related species. An analysis of the aqueous activation parameters for the *p*-nitrophenyl phosphate (pNPP) dianion yielded $\Delta H^{\ddagger}$ of 30.6 kcal/mol and $\Delta S^{\ddagger}$ of +3.5 eu at 39 °C,[14] while a similar study of the *p*-nitrophenyl sulfate (pNPS) monoanion obtained $\Delta H^{\ddagger}$ of 24.6 kcal/mol and $\Delta S^{\ddagger}$ of -18.5 eu at 35 °C.[7] This suggests a difference in the molecularity of the transition states of the two species. The small positive entropy of activation of the pNPP dianion is certainly consistent with a mechanism that proceeds by a unimolecular dissociation that leads to the transition state. The negative value for the hydrolysis of the corresponding sulfate indicates a decrease in entropy as the reaction coordinate moves from ground state to transition state. Large negative values for activation entropy are usually interpreted as indicative of associative transition states. Such transition states are most often associated with activation entropies on the order of -20 to -30 eu.[19] The relatively modest value for the neutral hydrolysis of pNPS may indicate the increased involvement of solvent in the stabilization of the transition state as opposed to a transition state which is more bimolecular than that of the related phosphate. In neither case is there any strong evidence of a free metaphosphate or sulfur trioxide intermediate.

One of the general observations in phosphate solvolysis is the increase in rate as the percent of organic solvent in the aqueous solution is changed from zero to nearly pure organic solvent.[20] A detailed study of the nature of this rate enhancement and the thermodynamic consequences of the transfer from aqueous solvent to nonaqueous solvent

has been reported previously.[21] In other investigations of the effect of organic solvent, specifically in the case of the phosphate dianion, isotopic labeling was used to synthesize a chiral phosphate. Solvolysis in of the chiral species in *tert*-butyl alcohol led to a racemic product.[22] This prompted the conclusion that a free metaphosphate intermediate was indeed formed in a solvent less nucleophilic than water. Kinetic studies of sulfate esters in solvents other than water showed some cases of rate enhancement[7-9] but this was not always the outcome. This parallel with phosphate monoester chemistry gives support to the potential for existence of the sulfur trioxide intermediate in the solvolysis of sulfate monoesters in nonaqueous solvents.

The pH-rate profile for pNPS hydrolysis shows an increase in rate as the proton activity of the solution increases. This cannot be attributed to a substrate that is entirely in a different protonation state, for the pK_a of pNPS is such that a fully protonated species is not attainable in aqueous solution. The pK_a of unsubstituted sulfuric acid is on the order of -3.[23,24] With phosphoric acid, the substitution of the *p*-nitrophenyl group causes a negative shift in pK_a by about two units.[25] Assuming a similar effect on the sulfate, the pK_a of pNPS would be on the order of -5. Given these assumptions, for experiments performed in 10 N HCl the sulfate is only about 1/10,000 in the protonated state. However, the rate of reaction of this species is so much higher than the monoanion, the assertion can be made that observation of chemical trends in strong acid actually do reflect the chemistry of the protonated species.

In the acidic hydrolysis of sulfate esters, reduced values for β_{LG} ($\beta_{LG} = -0.22$ in acid versus $\beta_{LG} = -1.2$ in basic solution)[8] relative to the reaction of the sulfate monoanion and solvent isotope effects of 2.43[9] have been observed. This has led to the proposal that the hydrolysis of the neutral species proceeds via a two-step pathway involving equilibrium proton transfer to the incipient leaving group oxygen, followed by O–S bond cleavage, as shown in Figure 7-1B. The intermediacy of free SO_3 is often assumed but

has never been explicitly proven. Stereochemical studies, such as those described for the reaction of the anionic species, have not been performed for the acid hydrolysis reaction.

In order to further the knowledge of the details of the sulfate hydrolysis reaction, studies to parallel those conducted on phosphate esters were conducted with pNPS. Here we report kinetic data and activation parameters in aqueous solution and in *tert*-amyl alcohol. Synthetic techniques were employed to prepare labeled substrates that allowed determination of kinetic isotope effects for aqueous hydrolysis under conditions that reflect monoanion chemistry, and in both 1.0 N and 10 N HCl, which provide some insight into the chemistry of the neutral species. The substrate, with the positions at which isotope effects have been measured indicated, is shown in Figure 7-2.

The data reported here are significant in that this is the first time heavy-atom secondary kinetic isotope effects have been measured for sulfate monoesters. Comparison of these results with similar studies of phosphate esters will allow inferences to be made concerning the mechanism of sulfate ester solvolysis.

$a = {}^{18}k_{nonbridge}$, secondary isotope effect, reflects changing bond order to nonbridge oxygens

$b = {}^{18}k_{bridge}$, primary isotope effect, it is the bond to this atom that is cleaved as the leaving group departs

$c = {}^{15}k$, secondary isotope effect, reflects extent of negative charge development on the leaving group
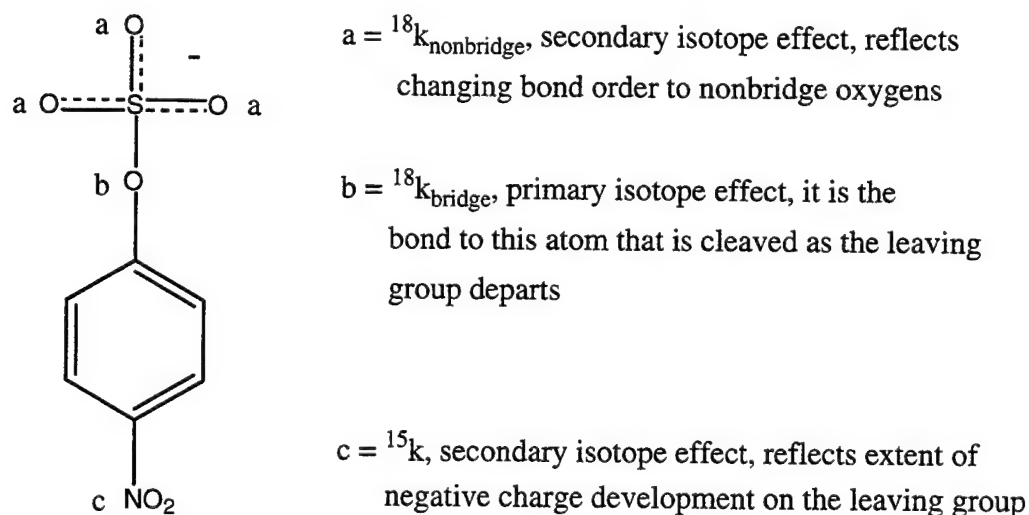
Figure 7-2. The substrate used for kinetic isotope effects experiments, *p*-nitrophenyl sulfate, with the positions at which isotope effects were measured indicated.

Experimental

Synthesis of Reagents.

(a) Unlabeled pNPS synthesis. The substrate used for the study of sulfate ester hydrolysis was pNPS. The potassium salt of pNPS was obtained from a commercial source, but was found to contain excessive free nitrophenol. This commercial potassium salt was used for some work, but most kinetic work was done using locally synthesized salts. Two different methods were used to synthesize pNPS in an effort to optimize the process for the later synthesis of labeled compounds.

The first method employed used a sulfur trioxide-pyridine complex in a modification of the method of Benkovic and Dunikoski.[26] Commercially obtained sulfur trioxide-pyridine complex was purified by suspending 4 g of complex in 50 mL of cool CCl_4, which was then washed with ice water. Impurities were observed in the water layer. The organic layer was filtered through $MgSO_4$, then dried by first by rotary evaporation, then under vacuum. The dried sulfur trioxide-pyridine complex which was not used immediately was stored in a dessicator. A 6.1-mmol quantity (0.97 g) of the sulfur trioxide-pyridine complex was added to 7 mL of dry pyridine at 65 °C with stirring. The complex would not dissolve readily by itself but immediately went into solution on addition of 3.5 mmol (490 mg) of p-nitrophenol, which was added all at once, and the solution was stirred for 10 min. The p-nitrophenol was a commercial product, recrystallized from toluene and stored under vacuum. After stirring, 8 mL of benzene was added and the resulting solution was stirred at 90 °C for 4 h. At the end of this time the solution appeared bi-phasic; an additional 10 mL of benzene was added and the solution was allowed to cool. The product and pyridinium salt byproducts precipitated in the cool benzene which formed a solid gel-like mass. The solids were removed by filtration. All of the dried product was then dissolved in 0.5 N KOH which resulted in a very intensely colored, red/purple solution. Under the assumption that this was free

phenol, the pH of the solution was reduced and an ether extraction performed to remove free phenol, but little was found. The pH was raised back to 13–14, the volume was reduced by rotovap, and the solution was chilled to precipitate the potassium salt of pNPS. Some of the intense color of the solution was found to carry over into the crystalline product, but based on NMR analysis of the crystalline material, did not represent a significant impurity. Subsequent recrystallizations from aqueous KOH produced white crystalline product in 59% yield.

The method of Burkhardt and Lapworth was also employed to produce pNPS.[27] To a solution of N,N-dimethylanaline (1.58 mL, 12.5 mmol) in 12.5 mL CS_2 at -16 to -21 °C, chlorosulfonic acid (2.32 mL, 35 mmol) was added dropwise with stirring. The chlorosulfonic acid was added in roughly a 40% stoichiometric excess to allow for any quenching effect of adventitious water. The mixture was warmed to 35–40 °C, then dry p-nitrophenol (3.5 g, 25 mmol) was added. The solution was stirred for 1 to 1.5 h at this temperature, then allowed to come to room temperature and stirred overnight. The following day, the mixture was cooled to 0 °C and was rapidly mixed with chilled 4 N KOH. The mixture was filtered immediately, and the solid washed with chilled 95% ethanol. The crude product was recrystallized from 90% ethanol to yield a white crystalline product.

Both of the above methods were repeated many times in efforts to optimize yield prior to the synthesis of labeled compounds. The resulting unlabeled crude products were combined and the potassium salt of pNPS was purified by recrystallization. This provided an abundant source of pNPS for kinetic and spectrophotometric studies. For kinetic studies and other experiments done in tert-amyl alcohol, the low solubility of the potassium salt of pNPS proved problematic. In these cases, the tetrabutylammonium salt of pNPS was prepared. Two synthetic routes were used to convert the potassium salt;

both produced the tetrabutylammonium salt cleanly, but the product was difficult to obtain in a crystalline form.

The first method employed was an ion exchange using DOWEX 50X8-100 cation exchange resin, which was converted from the proton form to the tetrabutylammonium form with 0.1 N tetrabutylammonium hydroxide. The tetrabutylammonium hydroxide solution was a dilution of a commercial aqueous preparation. The resin was used in a 300 times excess of the stoichiometric amount required based on the exchange capacity of the resin. The resin was repeatedly soaked in freshly replaced solutions of 0.1 N tetrabutylammonium hydroxide until the pH of the mixture remained basic. The resin was then washed with distilled deionized water until the conductivity fell to background level. The potassium salt was introduced in a solution of about 10 mM strength, and collected in fractions. Fractions which tested positively by UV absorbance for the sulfate were combined and rotovapped to reduce volume. Final concentration was done by lyophilization.

An alternative method was found which involves a metathesis reaction.[28] Two solutions are prepared in distilled deionized water: 150 mg (0.6 mmol) of the potassium salt of pNPS is dissolved in 6 mL, and 200 mg (0.6 mmol) of tetrabutylammonium hydrogen sulfate is dissolved in 1 mL. The two solutions are combined. The cloudy aqueous mixture is extracted four times with a like volume of dichloromethane. The organic layers are dried over anhydrous magnesium sulfate, the solvent removed under reduced pressure, and then dried under vacuum. The resulting suspension of the tetrabutylammonium salt of pNPS was evaluated for purity by NMR and then dissolved directly in *tert*-amyl alcohol for solution experiments. Alternatively, the product can be resuspended in water and lyophilized to produce a dry product.

(b) Preparation of labeled pNPS substrates. The kinetic isotope effect studies required the preparation of four different isotopomers. Based on the isotopomer

required, one or more of the methods described above was employed. Preparation of substrates for isotope effects experiments requires a synthetic route which labels a specific atom or atoms in the compound. The measurement of the effect of ^{15}N labeling in the nitro functional group on the nitrophenyl leaving group can be done with pNPS that has ^{15}N at natural abundance in the nitro group. This is because the isotope ratio mass spectrometer that is used to quantify the enrichment or depletion of ^{15}N provides the most accurate results when the ^{15}N /^{14}N ratio is close to natural abundance. Therefore, no special synthesis is required for this compound.

The tracking of the kinetic effect of ^{18}O substitution in both the bridging position between the phenyl ring and sulfur, and in the nonbridge oxygens on the sulfur is done by the remote label method.[29] Evaluation of ^{18}O isotope effects at either position requires the preparation of two isotopomers, one with ^{14}N in the nitro group and all oxygens at natural abundance, and the other with ^{15}N in the nitro group and the oxygen atom or atoms of interest replaced with ^{18}O. The ^{14}N isotopomer is then mixed with the ^{15}N /^{18}O isotopomer in approximately a 270:1 ratio to bring the ^{14}N /^{15}N ratio into agreement with natural abundance, as shown in Figure 7-3.

To prepare the ^{18}O bridge labeled substrate, the starting point for this process is
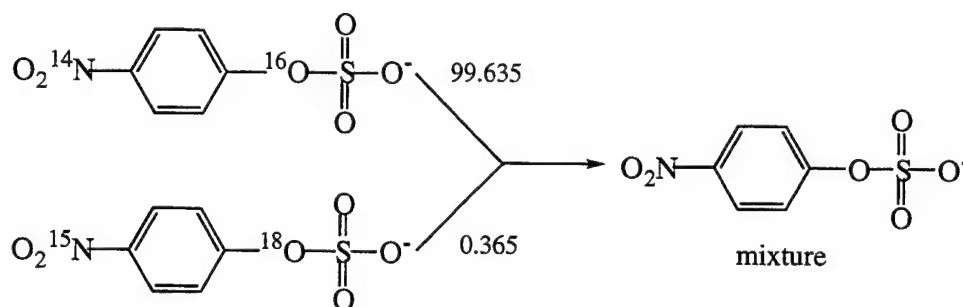
Figure 7-3. Remote labeled mixture preparation. Two preparations of pNPS, one with pure ^{14}N in the remote reporter position and natural abundance oxygen in the position of interest, and the other with ^{15}N in the reporter position and ^{18}O in the position of interest, are combined in a ratio such that the mixture has ^{15}N at or near natural abundance.

the preparation of ^{14}N labeled *p*-nitrophenol, the synthesis of which has been described earlier.[30] Then the [15]N /^{18}O labeled phenol is prepared as described by Hengge et al.[31] These two isotopomers are mixed as described in the paragraph above. The isotopically mixed phenol can now be used in the synthesis of pNPS by the sulfur trioxide-pyridine complex method to produce bridge labeled substrate.

The preparation of the [18]O nonbridge labeled substrate also begins with the [14]N *p*-nitrophenol; however, in this case the phenol is used to produce ^{14}N-pure pNPS, also using the sulfur trioxide-pyridine complex method. The next step is the most difficult part of the process of producing the nonbridge labeled mixture: the synthesis of the ^{15}N labeled pNPS with all of the nonbridge oxygens replaced with [18]O. This synthesis proceeds through the chlorosulfonic acid method, but requires that the chlorosulfonic acid be synthesized locally, in order to incorporate the [18]O. Two different methods were tested for the evolution of chlorosulfonic acid: the method of Thorpe,[32] which produces chlorosulfonic acid from sulfuric acid and phosphorus oxychloride, and the method of Williamson,[33] which reacts sulfuric acid with phosphorus pentachloride. Highest efficiency, relative to the amount of sulfuric acid used, was found with the latter method.

Due to the high cost of the [18]O labeled sulfuric acid and the relatively small amount of labeled compound used to prepare the substrate mixture, the reaction was performed on a very small scale. The acid used in this synthesis was 95% H_2SO_4 in H_2O, with the acid being 95% overall atom percent [18]O. The acid was purchased in a 0.5-g vial from Isotec and used as received. Of this 0.5 g of material, there is 4.5 mmol of H_2SO_4, before allowing for losses on transfer of the material from the shipping vial to the reaction vessel. To this acid, which was placed in a cooled, dried, small-scale condenser/reactor under nitrogen, was added 0.50 g (2.4 mmol) of phosphorus pentachloride, a commercial product that was used as received. The mixture was slowly heated to 75 °C and held at this temperature for 2 h. The mixture was transferred to a miniature reactor/still where it

was heated under anhydrous nitrogen to 110 °C, at which point the byproduct phosphorus

oxychloride (bp = 105 °C) (0.3 g) was distilled out of the mixture. After maintaining the

mixture at this temperature for about one hour, the receiver was switched and the

temperature raised to 165 °C. The labeled chlorosulfonic acid (bp=156 °C) was collected

in the tared receiver. This chlorosulfonic acid was weighed (0.136 g, yield 24% relative

to sulfuric acid), with the measured amount providing the stoichiometric basis for the

addition of ^{15}N labeled *p*-nitrophenol and other reagents as described above in the method

of Burkhardt and Lapworth.[27] Due to the small amount of chlorosulfonic acid produced,

it was not used in excess. Phenol was added in 1:1 stoichiometric ratio and

dimethylanaline was added in 0.5:1 ratio. Following the precipitation of the potassium

salt of pNPS with KOH, 50 mg of crude product was obtained. A schematic of this

synthesis process is shown in Figure 7-4. The crude product contained both the desired

product and another *para*-substituted aromatic compound which had not been seen in

synthesis practice runs. Three successive recrystallizations were required to obtain 18 mg

of product that showed no detectable impurity by NMR. This represents 1.5% yield

relative to the labeled sulfuric acid starting material. The level of purity of product

required in order to obtain a suitable isotopically labeled substrate justifies the selectivity
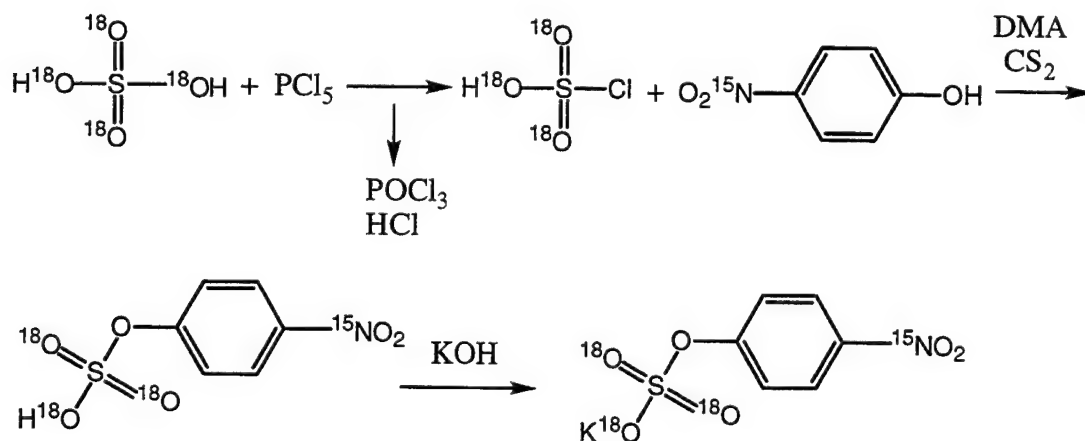
Figure 7-4. Synthetic scheme for preparation of $^{15}N/^{18}O_{3(nonbridge)}$ pNPS.

that leads to yields this low. The ^{15}N /^{18}O pNPS obtained was then mixed with the ^{14}N pure compound to simulate the natural abundance of ^{15}N as shown in Figure 7-3. From the 18 mg of product isolated, more than 4.5 g of labeled mixture was prepared.

In order to accurately calculate the intrinsic kinetic isotope effect in any reaction from the observed isotope effect, the level of isotopic incorporation in the labeled compounds must be accurately known. The ^{15}N /^{18}O pNPS was prepared from labeled sulfuric acid that included 5% water and was net 95% (atom %) in ^{18}O. By tracking the mole percent of ^{18}O in the starting sulfuric acid through to the chlorosulfonic acid intermediate product, the maximum possible percentage of pNPS product with ^{18}O on all three nonbridge oxygens is 80%. Any contact with atmospheric moisture or adventitious water in other reagents will further reduce this maximum. This percentage is therefore the upper bound on the extent to which the product pNPS will be ^{18}O labeled in all three nonbridging oxygen positions. The actual percent incorporation was measured by matrix assisted laser desorption/ionization time-of-flight mass spectometry, using a nitrogen laser at 337 nm and a 2.1 m linear TOF mass spectrometer, as shown in Figure 7-5. A complete description of the instrumentation is available elsewhere.[34] By integration of the results of this mass spectrum, it was possible to estimate that 64.6% of the product was triple labeled in the nonbridge position, with the remainder double labeled. This percentage was used in the mathematic correction of the observed isotope effect as described previously in this work.

Kinetic Experiments. The monohydrate of the potassium salt of pNPS was used as the substrate in all aqueous kinetic experiments. Typical concentrations of pNPS substrate used for kinetic runs were 5-10 mM. In cases where the reaction half lives were very long, concentrations as high as 80 mM were used in order to obtain measurable changes in the composition of the reaction mixture using the initial rates method. Thermostatically controlled water baths or dry blocks were used to maintain reaction
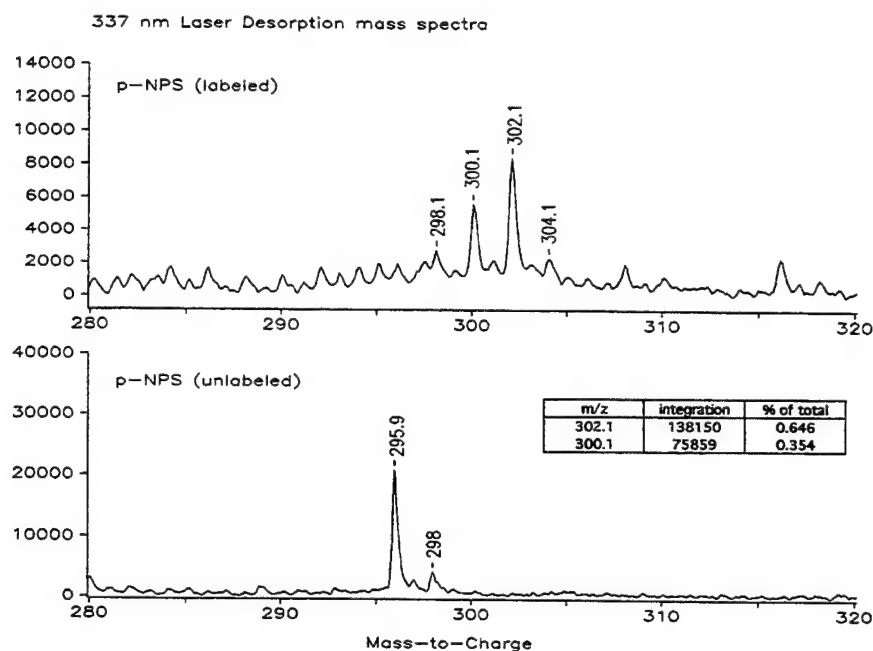
Figure 7-5. MALDI/TOF mass spectrum for double labeled pNPS substrate compared to spectrum for unlabeled material. Integration provided figures for extent of isotopic incorporation in the substrate.

temperatures over the course of the experiments.

Reaction progress was monitored spectrophotometrically by tracking the evolution of the p-nitrophenol hydrolysis product. The pK_a of this phenol is 7.14 and the phenolate ion has an intense absorbance peak at 400 nm (ε=18,320 M^{-1}cm^{-1}).[15] Aqueous reactions under basic conditions were performed in 100 mM TRIS buffer at pH 9.0. At this pH, the phenol was present primarily as the phenolate ion and reaction progress could be tracked directly. Reactions at moderate temperatures were performed in a sealed 3-mL cuvette in a thermostat controlled block in a spectrophotometer. For reactions at higher temperatures and reactions in acidic solution, reactions were performed in sealed tubes. Over time aliquots were removed and added to measured portions of 0.1 N NaOH. This solution was then analyzed spectrophotometrically to determine the concentration of free phenol. The plot of absorbance versus time over the first 1–5% of reaction was analyzed by assuming first-order kinetics using the initial rates method. To determine the initial

substrate concentration, an aliquot of the reaction mixture was subjected to complete hydrolysis in a measured amount of 1.0 N HCl, which was heated at 80 °C for 4 h then analyzed by the same method as the reaction mixture.

Reactions in *tert*-amyl alcohol were performed in much the same manner as the aqueous reactions. To enhance the solubility of the pNPS in the alcohol, the tetrabutylammonium salt was used for these experiments. Dry pNPS substrate was dissolved directly in the alcohol. Evolution of free phenol was quantified by mixing aliquots of the reaction solution in measured portions of 50% aqueous ethanol, which was 0.1 N in NaOH. The ethanol/water mixture was used to facilitate the solubility of *tert*-amyl alcohol in the basic assay solution. The solutions were then analyzed spectrophotometrically for phenolate ion at 405 nm (the λ_{max} is slightly shifted in the ethanolic solution).

Reactions performed in 10 N HCl provided some challenges in terms of kinetic control. At this concentration of acid, the hydrolysis rate was very high, hence time spent in mixing the reactant into the solution was critical. To get the reactants combined and the acid concentration to 10 N, the pNPS was dissolved in a small measured volume of water. The volume of water was calculated to bring a measured volume of concentrated HCl to 10 N when the two were combined. The mixing of these two solutions generated a substantial amount of heat. The heat of reaction and the heat capacity of the solution were calculated, and the solution was cooled to a temperature below the desired reaction temperature such that when the reactants were combined the heat evolved would not raise the temperature of the mixture above the desired temperature. In order to stop these reactions, the 10 N acid was rapidly combined with 10 times its volume of 1.0 N NaOH. A small (<5%) excess of base was used to insure the resulting solution would be basic, as the reaction is much slower in aqueous base than in acid. To mitigate the heat evolved when the acid and base were combined, the 1.0 N base solution was cooled to its freezing

point before they were mixed. To measure the reaction extent, an aliquot of the 10 N acid mixture was removed and rapidly combined with a measured portion of 1.0 N NaOH just prior to the neutralization of the bulk of the solution. To measure initial concentration of substrate, an aliquot of the 10 N acid mixture was placed in a measured portion of 1.0 N HCl and allowed to react to completion, as described above.

Kinetic Isotope Effect Determinations. Isotope effect experiments were run in 100 mM CHES buffer at pH 9.0 at 85 °C, in 1.0 N HCl at 65 °C and 21 °C, and in 10 N HCl at 15 °C. Experiments were performed in triplicate with individual experiments stopped at extents of substrate turnover ranging from 30% to 60%. Extents of reaction were measured as described above in the kinetic methods. Reactions were stopped either by chilling the basic solutions or by neutralization of the acidic reactions. Reaction solutions were titrated to pH 5 and extracted three times with an equivalent volume of ethyl ether to quantitatively remove the p-nitrophenol which was the product of the hydrolysis of the pNPS. The aqueous layer was evaporated briefly under vacuum to remove dissolved ether, then sufficient 10 N HCl was added to bring the solution to at least 1.0 N in HCl. The solutions were heated overnight to completely hydrolyze the remaining pNPS. They were then titrated back to pH 5 and extracted with ether, the p-nitrophenol in this ether fraction representing the residual substrate from the initial reaction. The ether fractions were dried over magnesium sulfate, filtered, and the solvent removed by rotary evaporation. The p-nitrophenol was sublimed under vacuum at 90 °C, and 1.0–1.5-mg samples were prepared for isotopic analysis using an ANCA-NT combustion system in tandem with a Europa 20-20 isotope ratio mass spectrometer.

Isotope effects were calculated from the isotopic ratio at partial reaction in the para-nitrophenol product (R_p), in the residual substrate (R_s), and in the starting material (R_o) as described earlier in this work. The ^{18}O isotope effects were measured by the remote label method[29] as has been described previously for solution reactions of

p-nitrophenyl phosphate.[31] These experiments yield an observed isotope effect which is the product of the effect due to both the ^{15}N and the [18]O substitution. The observed isotope effects from these experiments were corrected for the ^{15}N effect and for incomplete levels of isotopic incorporation in the starting material.[35]

Results

Kinetic Reactions of pNPS in *tert*-Amyl Alcohol and Aqueous Solution. Values of the first-order rate constants for the reactions of pNPS anion in aqueous solution at pH 9.0 and in neat *tert*-amyl alcohol were determined by following the liberation of *p*-nitrophenolate anion spectrophotometrically. Under assumption of first-order kinetics and initial rates conditions, linear plots yielded rate constants. The variation of rate constants with temperature for these reactions gave linear Eyring plots (Figure 7-6) which were used to calculate the enthalpies and entropies of activation. The enthalpy of activation was calculated from the slope of the plot, while the free energy of activation was calculated at a specific temperature by equation 1, where R is the gas constant, T is in Kelvin, k_T is the rate constant at that temperature (sec^{-1}), h is the Planck constant, and k is the Boltzmann constant.[7] Entropy of activation was then calculated from equation 2.

$$\Delta G^{\ddagger} = -RT \ln (k_T h/kT) \tag{1}$$

$$\Delta S^{\ddagger} = (\Delta H^{\ddagger} - \Delta G^{\ddagger}) / T \tag{2}$$

The monoanion of pNPS was found to undergo sulfuryl transfer to solvent approximately 40 times slower in *tert*-amyl alcohol than in water. This is in drastic contrast to the solvolysis of *p*-nitrophenyl phosphate, which was approximately 9000-fold faster in *tert*-amyl alcohol. Tables 7-1A and 7-1B show the rate and activation parameter data together with literature values for the corresponding reaction of the
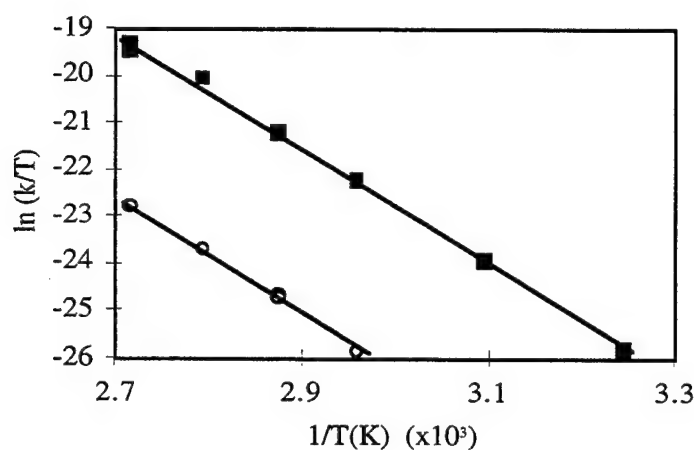
Figure 7-6. Eyring plot for pNPS in aqueous solution and in *tert*-amyl alcohol. Filled squares represent individual determinations of k (sec^{-1}) in aqueous solution, hollow circles represent data points for *tert*-amyl alcohol.

Table 7-1. Rates and Activation Parameters for Reactions of *p*-Nitrophenyl Sulfate Monoanion and *p*-Nitrophenyl Phosphate Dianion

	aqueous		
	literature values	this work	*tert*-amyl alcohol
A. *p*-nitrophenyl phosphate dianion			
k at 39 C, s^{-1}	1.6×10^{-8}		1.4×10^{-4}
$k_{solv}/k_{aqueous}$	1		8750
$\Delta H^{\ddagger}$, kcal/mol	30.6		30.9 ± 0.3
$\Delta S^{\ddagger}$, eu	+ 3.5		+ 23.0 ± 0.3
$\Delta G^{\ddagger}$, kcal/mol	29.5		23.7 ± 0.3
source	Kirby and Jencks[14]		Hoff and Hengge[21]
B. *p*-nitrophenyl sulfate monoanion			
k at 35 C, s^{-1}	1.48×10^{-7}	1.12×10^{-7}	
k at 65 C, s^{-1}			1.19×10^{-7}
$k_{solv}/k_{aqueous}$ at 65 C		1	0.027
$\Delta H^{\ddagger}$, kcal/mol	24.6	24.4 ± 0.2	25.0 ± 0.7
$\Delta S^{\ddagger}$, eu	- 18.5	-19.5 ± 0.2	- 24.5 ± 0.5
$\Delta G^{\ddagger}$, kcal/mol	30.2	30.4 ± 0.2	33.3 ± 0.7
source	Benkovic and Benkovic[7]	this work	this work

p-nitrophenyl phosphate dianion. Table 7-2 shows the variance in the activation parameters with temperature. The kinetic data from which the Eyring plots were derived are in Table 7-3.

Kinetic Isotope Effects. The isotope effects for the solution reactions of pNPS and the standard errors for these isotope effects are given in Table 7-4. The isotope effects obtained from isotopic ratios of product and those obtained from isotopic ratios of residual substrate agreed within experimental error in all cases and were averaged together to give the results shown in the table. Six or more determinations of each isotope effect were made. Isotope effects were measured for the pNPS monoanion at pH 9.0, and also under conditions where the substrate was partially protonated in 1.0 N HCl, and under conditions where protonation was slightly more enhanced in 10 N HCl. The values for the ^{18}O isotope effects have been corrected for the ^{15}N effect and for levels of isotopic incorporation. Due to the variation in isotope effects with temperature, it is desirable to perform experiments at the same temperatures where different solutions conditions are to be compared. However, due to the wide variation in the reactivity of pNPS in acidic and basic solutions, higher temperatures were used in some experiments to enhance reaction rates. These temperature differences were minimized to insure that the temperature-induced differences in isotope effects between sets of experiments were less than the experimental error. In order to provide results in 1.0 N HCl to compare to both the very slow monoanion reaction, and the very fast reaction in 10 N HCl, the isotope effects in 1.0 N HCl were evaluated at two different temperatures. This provides a useful illustration of the magnitude and direction of temperature effects on isotope effects. Table 7-4 also provides isotope effects with *p*-nitrophenyl phosphate taken from previous studies for the purpose of comparison. Raw data and calculations are in Appendix B, Tables B-27 through B-30.

Table 7-2. Activation Parameters as a Function of Temperature[a]

A. Reactions in aqueous solution

T (°C)	35[b]	35	50	65	75	95
k (1/sec)	1.48×10^{-7}	1.12×10^{-7}	7.80×10^{-7}	4.47×10^{-6}	1.28×10^{-5}	8.5×10^{-5}
$\Delta G^{\ddagger}$ (kcal/mol)		30.35	30.61	30.89	31.10	31.54
$\Delta H^{\ddagger}$ (kcal/mol)	24.6	24.35	24.35	24.35	24.35	24.35
$\Delta S^{\ddagger}$ (eu)	-18.5	-19.49	-19.39	-19.36	-19.40	-19.55
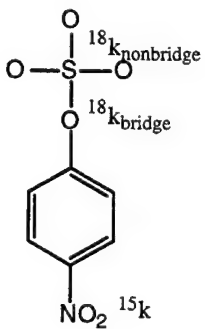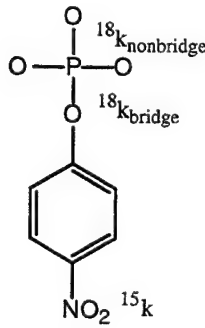
B. Reactions in *tert*-amyl alcohol

T (°C)	65	75	85	95
k (1/sec)	1.19×10^{-7}	3.96×10^{-7}	1.10×10^{-6}	2.76×10^{-6}
$\Delta G^{\ddagger}$ (kcal/mol)	33.33	33.50	33.76	34.05
$\Delta H^{\ddagger}$ (kcal/mol)	25.04	25.04	25.04	25.04
$\Delta S^{\ddagger}$ (eu)	-24.53	-24.32	-24.36	-24.49

[a]Calculated by the method of Benkovic and Benkovic[7] using average of measured rate constants. [b]Data from Benkovic and Benkovic.[7]

Table 7-3. Kinetic Data Used for Eyring Plots and Calculation of Activation Parameters

A. aqueous data		B. *tert*-amyl alcohol data	
Temp (°C)	k (s⁻¹)	Temp (°C)	k (s⁻¹)
95	1.29×10^{-6}	95	4.60×10^{-8}
95	1.52×10^{-6}	85	1.83×10^{-8}
95	1.46×10^{-6}	75	6.75×10^{-9}
85	7.03×10^{-7}	75	6.53×10^{-9}
75	2.17×10^{-7}	65	1.98×10^{-9}
75	2.07×10^{-7}		
75	2.18×10^{-7}		
65	7.25×10^{-8}		
65	7.42×10^{-8}		
65	7.70×10^{-8}		
65	7.57×10^{-8}		
65	7.30×10^{-8}		
65	7.22×10^{-8}		
50	1.31×10^{-8}		
50	1.29×10^{-8}		
35	1.83×10^{-9}		
35	1.90×10^{-9}		

Table 7-4. Kinetic Isotope Effects for the Solvolysis of pNPS and pNPP[a]

A. sulfate isotope effects	aqueous, monoanion pH 9.0, 85 °C	aqueous, anion/neutral, 1.0 N HCl, 65 °C	aqueous, anion/neutral, 1.0 N HCl, 21 °C	aqueous, anion/neutral, 10 N HCl, 15 °C
$^{18}k_{nonbridge}$	-0.49 (3)	0.67 (1)	0.83 (2)	0.98 (3)
$^{18}k_{bridge}$	2.1 (1)	0.69 (2)	0.97 (2)	1.01 (2)
^{15}k	0.26 (1)	0.02 (1)	0.02 (1)	0.04 (1)

B. phosphate isotope effects[b]	aqueous, monoanion pH 3.5, 95 °C	aqueous, dianion pH 10, 95 °C	t-butanol, dianion 30 °C
$^{18}k_{nonbridge}$	2.24 (5)	-0.07 (5)	-0.03 (16)
$^{18}k_{bridge}$	1.06 (3)	2.3 (5)	2.0 (1)
^{15}k	0.05 (2)	0.34 (2)	0.39 (3)

[a]Results for the sulfate monoester are from this work, phosphate results are as reported elsewhere. Isotope effects are all shown as percents, with negative numbers representing an inverse effect. Standard errors in the last digit are shown in parentheses. [b]From Hengge et al.[31]

Discussion

Kinetic Data. The rate constant for hydrolysis and the activation parameters calculated here agree well with those reported earlier.[7,8] The negative entropy of activation for the aqueous hydrolysis of the monoanion has always produced some concern when all of the evidence is combined into a coherent model of the mechanism of this reaction. In our hands the entropy of activation is a slightly more negative number, -19.5 versus -18.5 eu. The individual activation parameters reported in Table 7-1 are calculated at a single temperature: 35 °C for the aqueous reactions and 65 °C for the reaction in *tert*-amyl alcohol. However, the calculated values were very consistent across the entire temperature range evaluated, as shown in Table 7-2.

The change of reaction solvent and sulfuryl acceptor to *tert*-amyl alcohol represents a change in the ability of the solvent to solvate both the ground state and the transition state. In a detailed study of similar solvent effects on the pNPP dianion, it was found that the transfer from aqueous solution to *tert*-amyl alcohol was accompanied by both a destabilization of the ground state, and a stabilization of the transition state, resulting in an 8750-fold increase in reaction rate.[21] The quandary at this point is that the same exchange of solvent causes a 40-fold decrease in reaction rate with the sulfate monoanion, a species that physically resembles the phosphate dianion and demonstrates striking similar chemical trends. It is possible that this can be explained in terms of the relative entropic cost of the rearrangement of the different solvents to accomodate charged species, and the extent to which charge is dispersed in ground state and transition state.

When the phosphate dianion ground state is transferred from water to *tert*-amyl alcohol, it is partially desolvated and some of the charge stabilization afforded by the water is lost. Per data cited in Chapter 4, a free energy change of about +6 kcal/mol results from this change of solvent. Although a similar solvent effect study has not been conducted with the sulfate, the kinetic data show that the reaction is slowed on transfer to

tert-amyl alcohol. This could be due to a stabilization of the ground state as a result of the transfer, or due to a destabilization of the transition state, or to a combination of changes that serves to increase the activation energy. A potential major difference in the two very similar species is the amount and dispersion of negative charge over the molecule. With the net charge of minus one for the sulfate, the charge could be more dispersed than that of the phosphate, which has a net charge of minus two.

In order to compare the dispersion of charge in the ground state of the phosphate and sulfate, semiempirical calculations were done at the PM3 level[36] on the two anions using the MOPAC® software package.[37] The phosphate must be modeled in the presence of solvent due to its instability in the gas phase; therefore, both sulfate and phosphate were modeled using a continuum solvent simulation (COSMO),[38] with the dielectric constant for water and that for *tert*-butanol used in separate simulations. Mulliken charges were calculated for atoms, and dipole moments and heats of formation were calculated for the molecules. In both solvents, the finding was that the charge per atom was lower in the sulfate. In particular, when the nascent metaphosphate group was compared to the corresponding SO_3 group, there were 0.8 more units of negative charge on the phosphorus moiety. Experimental results have shown that the ground state of the pNPP dianion is better stabilized in water than in *tert*-amyl alcohol. These computational results imply that this may be due to locations of high charge density in the ground state, which are better solvated in the solvent of high dielectric constant. The corresponding locations in the sulfate have much lower charge densities. When this computational result is combined with the experimental kinetic data, the inference can be drawn that ground state stabilization for the pNPS monoanion is not very different in the two solvents.

The computational results also produced an interesting difference in the heats of formation in the two solvents. When the pNPP dianion was transferred from water to tert-butanol, there was an increase in 30 kcal/mol in the heat of formation. With pNPS,

the transfer produced an increase of only 13 kcal/mol. Though both indicate a destabilization, this is a relatively low level of theory, and solvent was modeled as a continuum, which does not account well for solvation energies. The important aspect of this result is that it supports, albeit indirectly, the experimentally observed reduction in rate constant for pNPS in *tert*-amyl alcohol.

In a continuation of this logic with the transition states, the other possible explanation for lower sulfate reaction rates in *tert*-amyl alcohol is that the transition state is destabilized, relative to water. Isotope effects with the phosphate dianion show that the transition state is highly dissociative, with one of the negative charges dispersed through the phenyl ring and the other dispersed over the metaphosphate-like center of the transition state. This probably represents more dispersed charge than in the ground state. These dispersed charges are solvated by the *tert*-amyl alcohol at a very low entropic cost, which lowers the entropy of activation and consequently the free energy of activation in *tert*-amyl alcohol when compared to water. With the analogous sulfate monoanion, the charge in the ground state begins dispersed with about 50% on the nonbridge oxygens and 50% on the bridge oxygen. The ^{15}N isotope effects show that virtually the entire negative charge is concentrated on the leaving group in the transition state. Kinetic results support the notion that as the sulfate moves to transition state, and the sulfate center begins to resemble the uncharged sulfur trioxide, all negative charge would have to be accommodated in the leaving group. The sulfate monoanion lacks the push of the negatively charged phosphoryl center, which forced delocalization of the leaving group negative charge into the nitro group. The lower ^{15}k with pNPS may indicate that more charge is localized on the leaving group oxygen in the transition state. This therefore supports the inference that the pNPS transition state could be stabilized more in water, while the pNPP transition state is stabilized more in *tert*-amyl alcohol.

A picture of a transition state begins to emerge that largely resembles that of the

phosphate dianion, however it contains subtle differences capable of having significant effects on the energetics of solvation. Solvation can be the most important aspect of a mechanism, in terms of the change from ground state to transition state. Support for this assertion is provided by earlier computational studies, which have demonstrated that differential solvation of transition states is primarily responsible for rate differences between cyclic and acyclic phosphate esters.[39] Another possible interpretation is that when comparing the evidence for pNPS to that for the pNPP, there are indications that the transition state may not be as dissociative. The β_{NUC} is slightly larger, the activation enthalpy is not as large. What is lacking at this point is sufficient experimental evidence to definitively attribute the cause of the change in reaction rate of pNPS on transfer from water to *tert*-amyl alcohol to solvent effects with the transition state.

Isotope Effects and the Sulfate Monoester Hydrolysis Transition State. In alkaline solution, the ^{15}N kinetic isotope effects (KIE) are normal and significant; 0.26% is about three-quarters of the effect observed with the phosphate dianion (0.39%).[31] The ^{15}N equilibrium isotope effect (EIE) for the deprotonation of *p*-nitrophenol was reported earlier as 0.23%.[40] Note that with the phosphate dianion in aqueous solution and in *tert*-amyl alcohol, the ^{15}N KIE is larger than the ^{15}N EIE. This is hypothesized to be due to the proximity of the leaving group to the negatively charged phosphate center, which electrostatically favors the quinonoid resonance form, which is responsible for the expression of an ^{15}N kinetic isotope effect. The sulfate transition state lacks this negatively charged reaction center; therefore, the ^{15}K for deprotonation should represent an upper bound on the magnitude of the ^{15}k for the sulfate. The fact that the ^{15}N KIE for the hydrolysis is approximately equal to the ^{15}N equilibrium isotope effect for deprotonation suggests that the transition state involves a leaving group that has little or no bond order remaining to the sulfur center.

The primary isotope effect $^{18}k_{bridge}$ should be a normal isotope effect as the S–O

bond is broken as the leaving group departs. The 2.1% isotope effect observed indicates that the S–O bond is almost completely broken in the transition state. The magnitude of the isotope effect is consistent with the $^{18}k_{bridge}$ of 2.3% observed with the phosphate dianion. Note that for the phosphate monoanion, the pre-equilibrium protonation of the leaving group produces an inverse isotope effect which reduces the observed $^{18}k_{bridge}$ to 1.1%. This mitigating effect is not present for the sulfate monoanion. Given the indication from ^{15}k that the S–O bond is virtually completely broken, as discussed above, the 2.1% $^{18}k_{bridge}$ is likely an upper bound on this isotope effect. The slightly higher isotope effect with the phosphate, compared to the sulfate, suggests a slightly stronger bond in the phosphate. Under the assumption that bond length correlates with bond strength, crystallographic data were compiled to test this hypothesis. Bond lengths were very close when comparing analogous sulfates and phosphates, and there was no systematic correlation. The phosphate had the shorter bond in ethyl esters, while the sulfate had the shorter bond with the p-nitrophenyl esters (ethyl phosphate dianion 1.56 ± 0.02 Å[41] and ethyl sulfate monoanion 1.60 ± 0.01 Å;[42] p-nitrophenyl phosphate dianion 1.66 ± 0.01 Å[43] and p-nitrophenyl sulfate monoanion 1.62 ± 0.01 Å [unpublished data from this lab]). This conflicting data may mean that this isotope effect difference is only on the order of experimental error.

The $^{18}k_{nonbridge}$ isotope effect is inverse and is much larger than the corresponding isotope effect with the phosphate dianion (-0.49% versus -0.07%). This is clearly suggestive of a change from a structure with five bonds to the nonbridge oxygens, to one with six bonds, as shown in Figure 7-1A. The fact that this isotope effect is so clearly inverse is a strong refutation of any hypothesized mechanistic explanation that involves an associative transition state. Associative transition states in the hydrolysis of phosphate esters typically have normal isotope effects of over 1%.[35] Thus the transition state most likely does resemble free sulfur trioxide, but this species is not an observable

intermediate. The transition state is an unstable point on the reaction path, and there is the weak but observable dependence of reaction kinetics on nucleophile character which must be considered. Therefore, this isotope effect result by itself cannot be said to provide evidence of free sulfur trioxide, but it is powerful evidence in favor of a very dissociative transition state.

Isotope effects were measured for the solution reaction of pNPS in acid conditions for comparison with the reaction under alkaline conditions. The reaction is 10^5-fold faster at 35 °C in 1.0 N HCl compared to the rate in aqueous buffer at pH 9.0,[8] and thus it was anticipated that significant differences in the transition state structure might be observed. Kinetic isotope effects are sensitive to the reaction temperature, but due to extreme differences in reactivity these two systems could not be investigated at the same temperature. A compromise was reached, with the alkaline reaction done at 85 °C and the 1.0 N HCl reaction at 65 °C. Thus any differences in isotope effect caused by temperature differences should be little more than the experimental error. With the acidic reaction, one of the most telling changes is the reduction in ^{15}k. This shows that the extent of negative charge delocalization into the nitrophenyl group is greatly reduced. The KIE is significantly different from zero, but it is very low. Compared to the same KIE with the pNPP monoanion, where protonation of the leaving group is believed to be a preequilibrium process that narrowly precedes leaving group departure, the sulfate isotope effects are less than half as large. This suggests that the leaving group in the transition state is a nearly completely protonated species.

There are two potential sources for the proton on the leaving group in this reaction: the solvent or the proton on the nonbridge oxygen. A previously observed solvent isotope effect ($k_D/k_H = 2.43$)[9] supports the solvent as the source for the proton, with the proton transfer followed by a extremely fast decomposition of the bridge oxygen protonated form of the substrate. A close examination of the monoanion isotope effects

results compared with the acidic results reveals an alternative source of the proton. The isotope effect on protonation/deprotonation has an absolute value of about 1.5%, normal for deprotonation and inverse for protonation. This figure is approximately the same for both the phenolic (bridge) protonation and the phosphate (nonbridge) protonation reactions.[44,45] For hydrolysis of the monoanion, the 2.1% $^{18}k_{bridge}$ was interpreted as representing a nearly completely broken S–O bond. If this oxygen is protonated in the transition state, and is bond is still nearly completely cleaved, this 2.1% isotope effect should be reduced by the effect of the -1.5% for protonation, resulting in an isotope effect of about +0.6%. This is a very good match with the observed $^{18}k_{bridge}$ for the reaction in 1.0 N HCl. If the same mathematic treatment is applied to $^{18}k_{nonbridge}$, the 1.5% for deprotonation is multiplied by the -0.49% obtained with the monoanion to arrive at a predicted isotope effect of about +1% for $^{18}k_{nonbridge}$ in acidic solution. This is close to the value observed.

Nucleophilic participation can influence nonbridge isotope effects by perturbing the degree of freedom of the nonbridge oxygen bonds. It is logical to infer that the alkaline hydrolysis of pNPS requires more nucleophilic participation than the acidic hydrolysis, because in the acidic hydrolysis the protonated leaving group should be more activated and require less nucleophilic push to reach the transition state. Evidence from phosphate esters, which relates the trend toward more associative transition states as the extent of alkylation increases with increasingly normal isotope effects, shows that nucleophilic participation causes the nonbridge isotope effects to become more normal. It is possible that a slight increase in the extent of nucleophilic involvement as the reaction goes from acidic to alkaline solution causes a slight normal effect to be expressed in the monoanion $^{18}k_{nonbridge}$. If the full inverse value of the change in bond order with the monoanion was able to be observed, it might account for the small difference between the observed $^{18}k_{nonbridge}$ of 0.67% and the predicted value of 1%. There is no other evidence

in these results to suggest that this small normal isotope effect in the acidic hydrolysis of the sulfate represents a more associative transition state.

The change in isotope effects discussed above clearly supports the assertion that there are two different mechanisms involved in sulfate ester hydrolysis. However, it is not reasonable for us to claim that we have been investigating the chemistry of the protonated species without including some qualifications. Based on pK_a, in 1.0 N HCl the substrate is only present in the protonated form at a ratio of less than 1 in 10,000. There is a large difference in reaction rate for the protonated and unprotonated species, but exactly how large this difference is cannot be measured. If the rate of reaction of the protonated species is five or more orders of magnitude higher than that of the anionic species, then it is possible that at low pH the mechanistic probes used are providing information on the chemistry of the protonated species. In an effort to probe further the change in going from alkaline to acid conditions, the same experiments were performed in 10 N HCl. Though the percentage of substrate present in the protonated form increases by an order of magnitude with this change, the percentage is still very small in absolute terms.

In 10 N HCl, the reaction is quite rapid with a half life of under 2 min at 15 °C. In order to provide isotope effects for comparison without applying artificial corrections for temperature, the 1.0 N HCl work was repeated at 21 °C. The small temperature difference in these two reactions reduces the correction due to temperature to much less than the experimental error. A comparison of the measured isotope effects in 1.0 N HCl at 65 °C and 21 °C shows no change in the ^{15}k. This is consistent with the role of the ^{15}N isotope effect as a reporter for delocalization of charge into the nitrophenyl group. This delocalization should be fairly independent of the temperature of the reaction. There is a change of about 40% in the value of $^{18}k_{bridge}$, which is a primary isotope effect and should be sensitive to temperature. The proportion of the change in $^{18}k_{nonbridge}$ is

somewhat smaller (24%), consistent with its role as a secondary isotope effect.

When the results from the 10 N HCl solution are compared to those from the 1.0 N HCl, all isotope effects are seen to increase, but the increases in $^{18}k_{bridge}$ and in ^{15}k are so small that they cannot be distinguished from experimental error. This suggests that under these conditions the extent to which the scissile S-O bond is broken and the extent of charge development in the leaving group is the same as it was in 1.0 N HCl. The modest increase in $^{18}k_{nonbridge}$ may be due to a slight shift in the character of the transition state, but any change from the mechanism in 1.0 N HCl is minimal.

Summary and Conclusions

The question that this work sought to answer was a resolution of the extent to which the mechanism of sulfate monoester hydrolysis resembles phosphate monoester hydrolysis. Based on a comparison using the relatively good leaving group *p*-nitrophenol, the mechanisms can be said to be strikingly similar. For the reaction of the sulfate monoanion, the transition state is like that of the phosphate dianion; a late, dissociative concerted transition state as shown in Figure 7-1A. When the stabilization of ground and transition states by solvent is perturbed by changing from water to a nonaqueous solvent, phosphate has been shown to proceed through a free metaphosphate intermediate. No evidence was found to support an analogous free intermediate in the nonaqueous reaction of *p*-nitrophenyl sulfate. Although isotope effects indicate that the bonding of the nonbridge oxygens does shift to suggest the formation of a sulfur trioxide-like transition state, there still appears to be nucleophilic involvement in the activated complex. Earlier kinetic studies had inferred the existence of a change in mechanism as the hydrolysis reaction was performed under more acidic conditions. The change in mechanism was confirmed by isotope effects experiments, which showed evidence of proton transfer from nonbridge oxygen to bridge oxygen in the transition state. Under

acid conditions the transition state retains the predominantly dissociative nature of the reaction in neutral solution, and appears to proceed through a concerted mechanism. The apparently incongruous finding of a large negative entropy of activation for the neutral hydrolysis can be explained by a consideration of the effects of solvation of the ground state and transition state for the reaction. Considering all of the evidence gathered in this study, it is concluded that the mechanism of sulfate monoester hydrolysis is virtually identical to that of phosphate monoester hydrolysis.

References

(1) Baumann, E. *Ber. Dtsch. Chem. Ges.* **1876**, *9*, 54-58.

(2) Mulder, G. J. *Sulfation of Drugs and Related Compounds*; CRC Press: Boca Raton, FL, 1981.

(3) Bernstein, S.; Solomon, S. *The Chemistry and Biochemistry of Steroid Conjugates*; Springer-Verlag: Berlin, 1970.

(4) Shapiro, L. J.; Cousins, L.; Fluharty, A. L.; Stevens, R. L.; Kihara, H. *Pediatr. Res.* **1977**, *11*, 894-897.

(5) Gregory, J. D.; Robbins, P. W. *Ann. Rev. Biochem.* **1960**, *29*, 347.

(6) Kaiser, E. T.; Panar, M.; Westheimer, F. H. *J. Am. Chem. Soc.* **1963**, *85*, 602.

(7) Benkovic, S. J.; Benkovic, P. A. *J. Am. Chem. Soc.* **1966**, *88*, 5504-5511.

(8) Fendler, E. J.; Fendler, J. H. *J. Org. Chem.* **1968**, *33*, 3852-3859.

(9) Kice, J. L.; Anderson, J. M. *J. Am. Chem. Soc.* **1966**, *88*, 5242-5245.

(10) Bourne, N.; Hopkins, A.; Williams, A. *J. Am. Chem. Soc.* **1985**, *107*, 4327-4331.

(11) O'Brien, P. J.; Herschlag, D. *J. Am. Chem. Soc.* **1998**, *120*, 12369-12370.

(12) Hengge, A. C. In *Comprehensive Biological Catalysis*; Sinnott, M., Ed.; Academic Press: San Diego, CA, 1998; Vol. 1, pp 517-542.

(13) Leyh, T. S. *Crit. Rev. Biochem. Molec. Biol.* **1993**, *28*, 515-542.

(14) Kirby, A. J.; Jencks, W. P. *J. Am. Chem. Soc.* **1965**, *87*, 3209-3216.

(15) Kirby, A. J.; Varvoglis, A. G. *J. Am. Chem. Soc.* **1967**, *89*, 415-423.

(16) D'Rozario, P.; Smyth, R. L.; Williams, A. *J. Am. Chem. Soc.* **1984**, *106*, 5027-5028.

(17) Pross, S.; Shaik, S. S. *New J. Chem.* **1971**, *13*, 427.

(18) Chai, C. L. L.; Hepburn, T. W.; Lowe, G. *J. Chem. Soc. Chem. Commun.* **1991**, 1403-1405.

(19) Benkovic, S. J.; Hevey, R. C. *J. Am. Chem. Soc.* **1970**, *92*, 4971-4977.

(20) Abell, K. W. Y.; Kirby, A. J. *Tet. Lett.* **1986**, *27*, 1085-1088.

(21) Hoff, R. H.; Hengge, A. C. *J. Org. Chem.* **1998**, *63*, 6680-6688.

(22) Friedman, J. M.; Freeman, S.; Knowles, J. R. *J. Am. Chem. Soc.* **1988**, *110*, 1268-1275.

(23) Luder, W. F.; Zuffanti, S. *The Electronic Theory of Acids and Bases*; 2nd ed.; Dover Publications: New York, 1961.

(24) Shriver, D. F.; Atkins, P.; Langford, C. H. *Inorganic Chemistry*; 2nd ed.; W.H. Freeman and Company: New York, 1994.

(25) Bourne, N.; Williams, A. *J. Org. Chem.* **1984**, *49*, 1200-1204.

(26) Benkovic, S. J.; Dunikoski, L. K. J. *Biochemistry* **1970**, *9*, 1390-1397.

(27) Burkhardt, G. N.; Lapworth, A. *J. Chem. Soc.* **1926**, 684-687.

(28) Wang, Z. Y.; Just, G. *Synth. Comm.* **1988**, *18*, 469-473.

(29) O'Leary, M. H.; Marlier, J. F. *J. Am. Chem. Soc.* **1979**, *101*, 3300-3306.

(30) Hengge, A. C.; Cleland, W. W. *J. Am. Chem. Soc.* **1991**, *113*, 5835-5841.

(31) Hengge, A. C.; Edens, W. A.; Elsing, H. *J. Am. Chem. Soc.* **1994**, *116*, 5045-5049.

(32) Thorpe, T. E. *J. Chem. Soc.* **1880**, *37*, 327-394.

(33) Williamson, A. *Proc. Roy. Soc.* **1854/55**, *7*, 11-15.

(34) Brown, R. S.; Lennon, J. J. *Anal. Chem.* **1995**, *67*, 1998-2003.

(35) Caldwell, S. R.; Raushel, F. M.; Weiss, P. M.; Cleland, W. W. *Biochemistry* **1991**, *30*, 7444-7450.

(36) Stewart, J. J. P. *J. Comp. Chem.* **1989**, *10*, 209.

(37) Stewart, J. P. P. *MOPAC 93.00*; Fujitsu Limited: Tokyo, 1993.

(38) Klamt, A.; Schurmann, G. *Journal of the Chemical Society, Perkin Transactions 2* **1993**, 799-805.

(39) Dejaegere, A.; Karplus, M. *J. Am. Chem. Soc.* **1993**, *115*, 5316-5317.

(40) Hengge, A. C.; Cleland, W. W. *J. Am. Chem. Soc.* **1990**, *112*, 7421-7422.

(41) McDonald, W. S.; Cruickshank, D. W. J. *Acta Crystallogr.* **1971**, *B27*, 1315-1319.

(42) Truter, M. R. *Acta Crystallogr.* **1958**, *11*, 680.

(43) Jones, P. G.; Sheldrick, G. M.; Kirby, A. J.; Abell, K. W. Y. *Acta Crystallogr.* **1984**, *C40*, 550-552.

(44) Knight, W. B.; Weiss, P. M.; Cleland, W. W. *J. Am. Chem. Soc.* **1986**, *108*, 2759-2761.

(45) Hengge, A. C.; Hess, R. A. *J. Am. Chem. Soc.* **1994**, *116*, 11256-11263.

CHAPTER 8

CONCLUSION

Much of the research discussed in the previous chapters has involved purely nonenzymatic chemistry. However, the underlying motivation behind the pure chemistry research into phosphoryl transfer has been the desire to improve the understanding of the nature of the catalytic advantage afforded by similar enzymatic reactions. One of the most fundamental questions was the extent to which this catalytic advantage stems from changes in mechanism as the reaction is switched from uncatalyzed routes to enzymatic. Based on the evidence gathered in this study, it appears a change in mechanism is not involved.

The initial approach to the investigation of catalytic rate enhancement focused on an explanation of previously observed rate enhancements involving phosphoryl transfer in mixed organic/aqueous or pure organic solvents. The first phase of this study focused on how the mechanism changed as the reaction was transferred from water to a much more weakly hydrogen bonding solvent, *tert*-amyl alcohol. This solvent was chosen due to its immiscibility with water, a property that was exploited in partitioning studies, as well as due to the large difference in its ability to solvate charged species. The initial findings in this solvent showed a large rate acceleration. The immediate conclusion was that transfer to this solvent mimicked the transfer from bulk water to the desolvating environment of an enzymatic active site, and that this desolvation was responsible for part of the catalytic advantage observed with enzymatic systems. Comparison of activation parameters in water with those in nonaqueous solvent showed virtually identical enthalpy of activation, with the difference in free energy of activation due almost entirely to differences in the entropy of activation. Earlier isotope effects experiments had shown that the transition state in a similar nonaqueous solvent, *tert*-butanol, was almost identical to that in the aqueous reaction. The evaluation of the reaction rates for a series of substituted aryl

phosphate found a linear free energy relationship in *tert*-amyl alcohol, with the same dependency on the leaving group as was observed in aqueous solution, a further affirmation of the similarity in mechanism in the two solvents. Therefore, the difference in the activation entropy had to be related to the differential solvation of the ground states and transition states in the two solvents.

A study of the partitioning of bis-tetrabutylammonium phenyl phosphate between water and *tert*-amyl alcohol, which provided data on the equilibrium concentrations in the two solvents, allowed an approximate evaluation of the difference in the ground state free energies in each solvent. From this the free energy of transfer for the compound was calculated. In order to obtain the more meaningful free energy of transfer for the dianion, the extrathermodynamic assumption was employed. This allowed the theoretical isolation of the dianion from the counterions, with the finding that the phosphate dianion ground state was significantly destabilized on transfer into *tert*-amyl alcohol. It was finally determined that the transfer from water into *tert*-amyl alcohol caused both a destabilization of the ground state, and an even larger stabilization of the transition state. These two entropic solvent-based interactions were responsible for the rate enhancement seen in *tert*-amyl alcohol.

The source of entropic advantage in *tert*-amyl alcohol is postulated to be the lack of requirement for solvent reorganization. As the dianion shifts from ground state to transition state, it goes from a molecule with a net negative charge of two, localized on the phosphate oxygens, to two separate charged species. For a highly organized solvent like water, there is a high entropic cost for this rearrangement. In a less organized solvent like *tert*-amyl alcohol, the cost is much lower. The implications for enzymatic phosphoryl transfer are that a similar entropic advantage is derived from the transfer from bulk solvent into the active site. Thus a significant portion of the rate enhancement observed with enzymatic phosphoryl transfer is hypothesized to be due purely to entropy.

The phosphate monoanion has much less relevance in terms of application as a model of enzymatic pathways; however, the impact of the change in solvent was investigated for this species also. It was found that transfer to *tert*-amyl alcohol actually had the opposite effect on reaction rates with the monoanion. While there was a similar entropic advantage from the solvent transfer, it was more than compensated for by an unfavorable change in the enthalpy of activation. The explanation for this change centers on the potential for solvent involvement in the transfer of a proton from a nonbridge oxygen to the oxygen of the scissile P–O bond. Without the facile proton transfer medium afforded by water, there is a much higher enthalpic cost of making this proton transfer. Since the leaving group departs as an uncharged species, the solvation effects seen with the dianion reaction are not present. Hence the enthalpic contributions to the energy of activation dominate the thermodynamics of the reaction. Again, what is seen is a change in the ability of solvent to play its role in solvation of reactants and transition state, but no fundamental change in the nature of the mechanism.

Sulfuryl transfer has long been postulated to be similar in chemistry and mechanism to phosphoryl transfer. Kinetic parameters and mechanistic probes have provided many examples of these similarities. However, the fact that the entropies of activation for sulfuryl transfer are so different from those for phosphoryl transfer has caused some concern on the part of many researchers. Activation parameters for the hydrolysis of the sulfate monoanion in aqueous solution were reevaluated for comparison with historical results, with a good match obtained.

The sulfate reactions were also performed in *tert*-amyl alcohol, providing a parallel for the work done with phosphoryl transfer. As in the solvent change with phosphates, there was only a minor change in enthalpy of activation, while most of the difference was in entropy of activation; however, the entropy change was unfavorable. This is consistent with the reaction in *tert*-amyl alcohol occurring at a rate about 1/40 of the rate in water.

One of the controversies surrounding the comparison of the sulfuryl transfer mechanism with phosphoryl transfer has been the fact that the entropy of activation in aqueous solution was so large and negative. Large negative entropies of activation are usually indications that a reaction is bimolecular. The phosphate mechanism, which is nearly a unimolecular dissociation, has an activation entropy that is small and positive. The large difference between the two systems certainly suggests that they might have different molecularities. Isotope effects experiments were performed with *p*-nitrophenyl sulfate in aqueous solutions that ranged from a buffered pH of 9.0 to 10 N HCl. Under conditions wherein the monoanion chemistry dominated, the isotope effects were found to clearly resemble those for *p*-nitrophenyl phosphate. The picture painted of the transition state was one with advanced cleavage of the scissile S–O bond, negative charge fully developed on the leaving group, and indication that there was little nucleophilic involvement. When the isotope effects were considered for the reaction conditions where the neutral mechanism was expressed, the transition state was largely unchanged, except for the superposition of the effects of proton transfer from the nonbridge oxygen to the bridge oxygen. In summary of all of these results with the sulfate, it appears that it is reasonable to state that the sulfate and phosphate monoester mechanisms are essentially the same. The differences in entropy of activation that were observed are an expression of the tremendous impact of solvation on the entropy and overall free energy changes of reactive systems.

Lessons learned from the solution chemistry analysis of these two systems were then applied to the study of enzymatic systems. With the *Yersinia* PTPase, an isotope effect titration demonstrated the gradual extinction of the effect of the general acid in the catalytic transition state. Site-directed mutation allowed the study of the impact of individual residues on the structure of the transition state. Other studies with isotope effects had demonstrated the ability of these probes to differentiate between associative

and dissociative mechanisms. With the wild type enzyme, the isotope effects showed a dissociative transition state, but with little charge development on the leaving group. Experiments with enzyme having mutations to the general acid itself; to Arg409, which has substrate binding and general acid positioning roles; and to Trp354, which interacts with Arg409 and acts as a hinge for general acid movement, show that all had impacts on the functioning of the general acid. Regardless of the extent to which the general acid was disabled, there was no significant shift toward an associative reaction. Double mutants were employed to isolate the impacts of the Arg409 interaction with the substrate to see if the positive charge in the active site would interact differently when the general acid was not there. Again, no major increase in the associative character of the transition state was seen. Based on all of this evidence, the conclusion is that the interaction of the substrate with the positive charge of the active site serves to stabilize the dissociative transition state, but does not alter it. Specifically, the positive charge at the active site does not cause a shift toward an associative mechanism.

The exploration of enzymatic catalysis of phosphoryl transfer was continued with the investigation of the lambda Ser/Thr protein phosphatase. The positive charge in the active site of this enzyme is provided by two metal ions bearing multiple positive charges, rather than by an amino acid side chain, as in the *Yersinia* PTPase. This system is also different in that it is believed that the phosphoryl group is transferred directly to the nucleophilic water, rather than to a protein nucleophile. The investigation with this system again centered on the role of the positive charge in the catalytic rate enhancements observed. The results of isotope effects experiments indicated that the transition state of the enzymatic reaction resembles that of aqueous phosphoryl transfer, with a late, dissociative transition state. The role of the metal ions is unclear, but may include altering the pK_a of a bound water to enhance its nucleophilicity. It was found that the metal ions in the active site could be changed, and that the isotope effects remained constant. A key

residue was mutated from histidine to asparagine, and though the extent of negative charge on the leaving group increased, the isotope effects were unchanged for the nonbridge oxygens. Thus the dissociative character of the transition state was not decreased.

From these results with the *p*-nitrophenyl phosphate dianion in aqueous solution, from the activation parameters and isotope effects, and from the enzymatic isotope effects experiments, the mechanism by which phosphoryl transfer is accomplished is seemingly invariant. At least for phosphate monoester chemistry with a relatively activated leaving group, the reaction is dissociative, and there is little need for nucleophilic assistance to achieve the transition state. In the gas phase, the *p*-nitrophenyl phosphate dianion is unstable and dissociates spontaneously. In aqueous solution the dianion is unreactive, stabilized by the solvation of the water molecules. In this environment, the mechanism is concerted, and proceeds through a dissociative, late transition state. Intuitively, it would seem that in an aqueous environment the maximum nucleophilic push would be required to make the reaction move in the forward direction, yet indications are that there is virtually the same extent of nucleophilic involvement as in *tert*-butanol or *tert*-amyl alcohol, where the reaction rate is four orders of magnitude higher. Other workers have noted that the phosphoryl transfer mechanism seems to be invariant regardless of how good the leaving group is.[1,2] Recent computational evidence was published that presented a means by which the dissociative transition state could be stabilized by positive charge interacting with the nonbridge oxygens.[3] It is the finding of this research that, for the *p*-nitrophenyl phosphate monoester, the mechanism is invariant whether or not an enzyme is involved. The experimental evidence presented here provides proof that the imputed ability of positive charge in the enzyme active site to stabilize a dissociative transition state is a reality.

References

(1)   Herschlag, D.; Jencks, W. P. *J. Am. Chem. Soc.* **1989**, *111*, 7587-7596.

(2)   Herschlag, D.; Jencks, W. P. *J. Am. Chem. Soc.* **1987**, *109*, 4665-4674.

(3)   Alhambra, C.; Wu, L.; Zhang, Z. Y.; Gao, J. *J. Am. Chem. Soc.* **1998**, *120*, 3858-3866.

APPENDICES

Appendix A. Copyright Permissions

5 March 1999

Copyright Office, Publications Div.
American Chemical Society
1155 Sixteenth Street
Washington, DC 20036

Richard H. Hoff
Dept. of Chemistry and Biochemistry
Utah State University
Logan, UT 84322-0300
Phone (435) 797-0023
FAX (435) 797-3390

Dear Sirs:

I am in the process of preparing my dissertation in the Department of Chemistry and
Biochemistry Department at Utah State University. I hope to complete my assembly of the
dissertation in April of 1999.

I am The first author of the journal articles referred to on the following pages, all of which
have appeared in ACS publications. These reports are an essential part of my dissertation
research and I would like to use the articles, as written, as chapters in the dissertation.
Please note that Utah State University sends dissertations to University Microfilms
International Dissertation services to be made available for reproduction.

I will include an acknowledgment to each article on the first page of the dissertation chapter
in which it appears. Copyright and permission information will be included in a special
appendix. If you require a different acknowledgment, please so indicate.

I am including a letter of permission for each article. Please indicate your approval by
signing in the space provided and include any other form necessary to confirm permission.
If any fees are required, please let me know.

If any additional information is required I can be reached by e-mail at <slr5h@cc.usu.edu>
or by phone as shown above.

Thank you very much for your assistance.

Sincerely,

Richard H. Hoff

American Chemical Society

MEMORANDUM

TO: Richard H. Hoff, Dept. of Chemistry and Biochemistry
        Utah State University, Logan, UT 84322-0300

FROM: C. Arleen Courtney, Assistant Copyright Administrator   *C. Arleen Courtney*

Thank you for your recent request for permission to include your paper(s) or portions of your paper(s) in your thesis. Permission is now automatically granted; please pay special attention to the implications paragraph below. The Joint Board/Council Committees on Copyrights and Publications recently approved the following:

Copyright permission for published and submitted material from theses and dissertations
ACS extends blanket permission to students to include in their theses and dissertations their own articles, or portions thereof, that have been published in ACS journals or submitted to ACS journals for publication, provided that the ACS copyright credit line is noted on the appropriate page(s).

Publishing implications of electronic publication of theses and dissertation material
Students and their mentors should be aware that posting of theses and dissertation material on the Web prior to submission of material from that thesis or dissertation to an ACS journal may affect publication in that journal. Whether Web posting is considered prior publication may be evaluated on a case-by-case basis by the journal's editor. If an ACS journal editor considers Web posting to be "prior publication", the paper will not be accepted for publication in that journal.

If your paper has not yet been published by ACS, we have no objection to your including part or all of it in your thesis in print and microfilm formats; please note, however, that electronic distribution or Web posting of the unpublished paper as part of your thesis in electronic formats might jeopardize publication of your paper by ACS. Please print the following credit line on the first page of your article: "Reproduced (or 'Reproduced in part') with permission from [JOURNAL NAME], in press (or 'submitted for publication'). Unpublished work copyright [CURRENT YEAR] American Chemical Society." Include appropriate information.

If your paper has already been published by ACS and you want to include part or all of it in your thesis or dissertation, please print the ACS copyright credit line on the first page of your article: "Reproduced (or 'Reproduced in part') with permission from [FULL REFERENCE CITATION.] Copyright [YEAR] American Chemical Society." Include appropriate information.

Note: If you plan to submit your thesis to UMI or to another dissertation distributor, you should not include the unpublished ACS paper in your thesis if the thesis will be disseminated electronically, until ACS has published your paper. After publication of the paper by ACS, you may release the entire thesis for electronic dissemination; ACS's copyright credit line should be printed on the first page of the ACS paper.

Permission is not granted to post any published or unpublished ACS articles on any Web site.

Thank you for writing. Questions? Please call me at 202/872-4368 or send e-mail to copyright@acs.org.   9/1/98

5 March 1999

Pamela Mertz   Richard H. Hoff
Department of Chemistry & Biochemistry   Dept. of Chemistry and Biochemistry
University of Massachusetts   Utah State University
285 Old Westport Road   Logan, UT 84322-0300
North Dartmouth, MA 02747.   Phone (435) 797-0023
                                           FAX (435) 797-3390

Dear Pam:

I am in the process of preparing my dissertation in Chemistry and Biochemistry Department at Utah State University. I hope to complete my assembly of the dissertation in April of 1999.

I am requesting your permission to include the draft of our manuscript "The Transition State of the Phosphoryl Transfer Reaction Catalyzed by the Lambda Ser/Thr Protein Phosphatase," in its entirety as a chapter in my dissertation. I feel that the arguments and conclusions drawn from our isotope effects experiments will be best developed when considered in conjunction with the data that you collected and provided on the enzyme. I will acknowledge your contributions to this part of my dissertation by the inclusion of a footnote on the title page for that chapter. Additionally, a copy of this letter will become an Appendix to the dissertation. I have included a sample of this title page. Please advise me of any changes you require.

Please indicate your approval of this request by signing the endorsement below. If you have any questions, please call me at the number above.

If possible, please provide your reply immediately. Thank you very much for your consideration.

Richard H. Hoff

I hereby give permission to Richard H. Hoff to reprint the manuscript "The Transition State of the Phosphoryl Transfer Reaction Catalyzed by the Lambda Ser/Thr Protein Phosphatase," co-authored by Richard H. Hoff, Pamela Mertz, Frank Rusnak, and Alvan C. Hengge in his dissertation.

Signed _Pamela S. Mertz_   Date _3/9/99_

5 March 1999

Dr. Yen-Fang Keng
Department of Molecular Pharmacology
Albert Einstein College of Medicine
1300 Morris Park Avenue
Bronx, NY 10461

Richard H. Hoff
Dept. of Chemistry and Biochemistry.
Utah State University
Logan, UT 84322-0300
Phone (435) 797-0023
FAX (435) 797-3390

Dear Dr. Keng:

I am in the process of preparing my dissertation in Chemistry and Biochemistry Department at Utah State University. I hope to complete my assembly of the dissertation in April of 1999.

I am requesting your permission to include the draft of our manuscript "The Effects on the Functioning of the General Acid Catalyst from Mutations of the Invariant Tryptophan and Arginine Residues in the Protein-Tyrosine Phosphatase from *Yersinia*," in its entirety as a chapter in my dissertation. I feel that the arguments and conclusions drawn from our isotope effects experiments will be best developed when considered in conjunction with the data that you collected and provided on the enzyme. I will acknowledge your contributions to this part of my dissertation by the inclusion of a footnote on the title page for that chapter. Additionally, a copy of this letter will become an Appendix to the dissertation. I have included a sample of this title page. Please advise me of any changes you require.

Please indicate your approval of this request by signing the endorsement below. If you have any questions, please call me at the number above.

If possible, please provide your reply immediately. Thank you very much for your consideration.

Richard H. Hoff

_____

I hereby give permission to Richard H. Hoff to reprint the manuscript "The Effects on the Functioning of the General Acid Catalyst from Mutations of the Invariant Tryptophan and Arginine Residues in the Protein-Tyrosine Phosphatase from *Yersinia*," co-authored by Richard H. Hoff, Alvan C. Hengge, Yen-Fang Keng, and Zhong-Yin Zhang in his dissertation.

Signed _Yen-fang Keng_   Date _March 9, 1999_

5 March 1999

Dr. Zhong-Yin Zhang
Department of Molecular Pharmacology
Albert Einstein College of Medicine
1300 Morris Park Avenue
Bronx, NY 10461

Richard H. Hoff
Dept. of Chemistry and Biochemistry.
Utah State University
Logan, UT 84322-0300
Phone (435) 797-0023
FAX (435) 797-3390

Dear Dr. Zhang:

I am in the process of preparing my dissertation in Chemistry and Biochemistry Department at Utah State University. I hope to complete my assembly of the dissertation in April of 1999.

I am requesting your permission to include the draft of our manuscript "The Effects on the Functioning of the General Acid Catalyst from Mutations of the Invariant Tryptophan and Arginine Residues in the Protein-Tyrosine Phosphatase from *Yersinia*," in its entirety as a chapter in my dissertation. I feel that the arguments and conclusions drawn from our isotope effects experiments will be best developed when considered in conjunction with the data that you collected and provided on the enzyme. I will acknowledge your contributions to this part of my dissertation by the inclusion of a footnote on the title page for that chapter. Additionally, a copy of this letter will become an Appendix to the dissertation. I have included a sample of this title page. Please advise me of any changes you require.

Please indicate your approval of this request by signing the endorsement below. If you have any questions, please call me at the number above.

If possible, please provide your reply immediately. Thank you very much for your consideration.

Richard H. Hoff

I hereby give permission to Richard H. Hoff to reprint the manuscript "The Effects on the Functioning of the General Acid Catalyst from Mutations of the Invariant Tryptophan and Arginine Residues in the Protein-Tyrosine Phosphatase from *Yersinia*," co-authored by Richard H. Hoff, Alvan C. Hengge, Yen-Fang Keng, and Zhong-Yin Zhang in his dissertation.

Signed _____   Date 3/9/99

5 March 1999

Dr Frank Rusnak
Section of Hematology Research
Dept. of Biochemistry and Molecular
    Biology
Mayo Clinic and Foundation
Rochester, MN 55905

Richard H. Hoff
Dept. of Chemistry and Biochemistry.
Utah State University
Logan, UT 84322-0300
Phone (435) 797-0023
FAX (435) 797-3390

Dear Dr. Rusnak:

I am in the process of preparing my dissertation in the Chemistry and Biochemistry
Department at Utah State University. I hope to complete my assembly of the dissertation
in April of 1999.

I am requesting your permission to include the draft of our manuscript "The Transition
State of the Phosphoryl Transfer Reaction Catalyzed by the Lambda Ser/Thr Protein
Phosphatase," in its entirety as a chapter in my dissertation. I feel that the arguments and
conclusions drawn from our isotope effects experiments will be best developed when
considered in conjunction with the data that you collected and provided on the enzyme. I
will acknowledge your contributions to this part of my dissertation by the inclusion of a
footnote on the title page for that chapter. Additionally, a copy of this letter will become an
Appendix to the dissertation. I have included a sample of this title page. Please advise me
of any changes you require.

Please indicate your approval of this request by signing the endorsement below. If you
have any questions, please call me at the number above.

If possible, please provide your reply immediately. Thank you very much for your
consideration.

Richard H. Hoff

I hereby give permission to Richard H. Hoff to reprint the manuscript "The Transition State
of the Phosphoryl Transfer Reaction Catalyzed by the Lambda Ser/Thr Protein
Phosphatase," co-authored by Richard H. Hoff, Pamela Mertz, Frank Rusnak, and Alvan
C. Hengge in his dissertation.

Signed _____   Date __3/8/99__

Appendix B. Kinetic Isotope Effect Data

Data Sheets. The following pages are data sheets on which the raw data reported by the isotope ratio mass spectrometer were recorded and converted to the isotope effects reported in the text. Each experiment is recorded on a separate sheet, sheets are collected according to subject and each page is labeled as a table. As a heading on each sheet, experimental conditions are noted. In the upper left corner of the sheet, the isotope ratio in the substrate is recorded. In the main body of the sheet, the isotope ratio from each sample is recorded as either a "P delta" (product), or "RS delta" (residual substrate). These deltas are then converted into ratios that compare the $^{15}N/^{14}N$ ratio in the sample to the $^{15}N/^{14}N$ ratio in the substrate, these ratios of ratios are the R_s and R_p. The extent of reaction is recorded andthese data are input into equations for the calculation of isotope effects. The calculated isotope effects are listed in two columns, one derived from product and one derived from residual substrate. For the ^{15}N experiments, the calculation stops here with an average of all of the results for that one experiment.

For ^{18}O experiments, the isotope effects need to be corrected as described in Chapter 5 for incomplete isotopic incorporation in the substrates. Hence the data sheets for these experiments include a section that lists the pertinent correction factors. Additional fields are added on to the main body of the data sheet for calculation of the corrections and calculation of the final, corrected isotope effect. As in the case with the ^{15}N experiments, isotope effects derived from product and residual substrate analysis are all averaged to yield an overall isotope effect. The isotope effects on these data sheets are per atom isotope effects and must be raised to the power of the number of discriminating atoms to give a total effect. Some of these overall effects also require correction for pH, as described in Chapter 5.

In addition to the data and calculations, the data sheets also include any administrative notes that may affect the handling of a particular set of results. In these raw data, all isotope effects are expressed as deviations from unity, not as percents.

Table B-1. *Yersinia*, Wild-Type, ^{15}N Isotope Effects, Variable pH

YOP51* WT, 35C, pH 9.0, 15 N effects, Run #1 — exp:9/4/97, res:12/1/97

Delta TC/Sm		
1.430	0.85	pH estimated at 8.75
1.020	1.13	
1.070	0.91	
1.430	0.87	
1.020	1.23	
0.870		
1.075	1.0011	

sample#	P Delta	RS Delta	Rp	Rs	f	IE(Rs,Ro)	IE(Rp,Ro)
A1	0.89	2.37	1.00089	1.00237	0.53	1.001715	1.000277
A2	0.41	2.34	1.00041	1.00234	0.53	1.001675	
B1	1.29	2.42	1.00129	1.00242	0.58	1.001550	
B2	0.84	1.94	1.00084	1.00194	0.58		1.000374
C1	0.71	2.14	1.00071	1.00214	0.35		1.000456
C2	0.4	1.86	1.0004	1.00186	0.35	1.001822	1.000844
					Mean	1.001690	1.000488
					SD	0.000112	0.000248
					overall	1.00109	
					SD	0.000667	
					SE	0.00024	

YOP51* WT, 35C, pH 9.0, 15 N effects, Run #2 — exp:10/15/97, res:12/1/97

Delta TC/Sm		
1.075	1.0011	pH estimated 8.5

sample#	P Delta	RS Delta	Rp	Rs	f	IE(Rs,Ro)	IE(Rp,Ro)
A1	1.23	1.57	1.001230	1.001570	0.33		0.999810
A2	1.16	1.86	1.001160	1.001860	0.33	1.001960	0.999896
B1	1.3	2.32	1.001300	1.002320	0.48	1.001904	0.999683
B2	0.94	2.41	1.000940	1.002410	0.48	1.002041	1.000191
C1	0.74	1.83	1.000740	1.001830	0.31	1.002035	1.000406
C2	1.02	2.12	1.001020	1.002120	0.31		1.000067
					Mean	1.001985	1.000009
					SD	0.000066	0.000265
					overall	1.00080	
					SD	0.001040	
					SE	0.00033	

YOP51* WT, 35C, pH 10.0, 15 N effects — 1/20/98

Delta TC/Sm		
1.430	0.85	Actual pH estimated at 9.5 due to substrate acidity effects
1.340	1.2	pH not measured after dissolving substrate in buffer
1.320	1.41	
1.150	1.31	
1.020	1.13	
1.070	0.91	
1.430	0.87	
1.020	1.23	
0.870		
1.151	1.0012	

sample#	P Delta	RS Delta	Rp	Rs	f	IE(Rs,Ro)	IE(Rp,Ro)
A1	0.21	1.91	1.00021	1.00191	0.297	1.002156	1.001127
A2	0.09	1.99	1.00009	1.00199	0.297	1.002384	1.001271
B1	0.45	2.31	1.00045	1.00231	0.409	1.002206	1.000921
B2	0.37	2.29	1.00037	1.00229	0.409	1.002167	1.001027
C1	0.36	2.42	1.00036	1.00242	0.527	1.001695	1.001176
C2	0.34	2.42	1.00034	1.00242	0.527	1.001695	1.001206
					Mean	1.002051	1.001121
					SD	0.000287	0.000128
					overall	1.00159	
					SD	0.000529	
					SE	0.00019	

Table B-2. *Yersinia*, Wild-Type, ^{15}N Isotope Effects, Higher pH

YOP51* WT, 35C, pH 10.0, 15 N effects	exp 2/6/98
	res 2/18/98

Delta TC/Sm

1.950	1.68
1.98	2.03
2.15	2.23
2.08	2.11
2.12	2.17
2.04	2.01
2.06	2.09
2.04	2.07
2.051	1.0021

Actual pH is 10.0
pH measured and adjusted after dissolving substrate in buffer

sample#	P Delta	RS Delta	Rp	Rs	f	IE(Rs,Ro)	IE(Rp,Ro)
A1	0.35	2.60	1.00035	1.00260	0.237	1.002033	1.001952
A2	0.48	2.61	1.00048	1.00261	0.237	1.002070	1.001802
B1	0.60	2.86	1.00060	1.00286	0.311	1.002172	1.001757
B2	0.77	2.90	1.00077	1.00290	0.311	1.002280	1.001551
C1	0.61	3.15	1.00061	1.00315	0.431	1.001948	1.001934
C2	0.60	3.09	1.00060	1.00309	0.431	1.001842	1.001947
					Mean	1.002058	1.001824
					SD	0.000156	0.000157
					overall	1.00194	
					SD	0.000193	
					SE	0.00006	

YOP51* WT, 35C, pH 9.0, 15 N effects	exp 2/6/98
	res 2/18/98

Delta TC/Sm

1.950	1.68
1.98	2.03
2.15	2.23
2.08	2.11
2.12	2.02
2.12	2.17
2.01	2.12
2.04	2.01
2.06	2.09
2.04	2.07
2.054	1.0021

Actual pH is 9.0
pH measured and adjusted after dissolving substrate in buffer

sample#	P Delta	RS Delta	Rp	Rs	f	IE(Rs,Ro)	IE(Rp,Ro)
A1	2.64	2.49	1.00264	1.00249	0.367		
A2	1.29	2.50	1.00129	1.00250	0.367	1.000974	1.000967
B1	1.31	2.71	1.00131	1.00271	0.444	1.001116	1.001011
B2	1.34	2.77	1.00134	1.00277	0.444	1.001218	1.000970
C1	1.49	3.33	1.00149	1.00333	0.532		1.000843
C2	1.56	3.20	1.00156	1.00320	0.532		
					Mean	1.001103	1.000948
					SD	0.000123	0.000073
					overall	1.00101	
					SD	0.000120	
					SE	0.00005	

YOP51* WT, 35C, pH 10.5, 15 N effects	exp 4/1/98
	res 4/2/98

Delta TC/Sm

1.96	2.12
2.00	2.01
2.12	2.09
2.04	2.07
2.06	1.94
1.85	2.00
2.022	1.002

Actual pH is 10.5
Enzyme has very low activity at pH 10.5 and quickly
denatures. Excessive quantities of enzyme required
for limited reaction extent. Problems with sublimation
procedure may effect RS numbers - high 15N content.

sample#	P Delta	RS Delta	Rp	Rs	f	IE(Rs,Ro)	IE(Rp,Ro)
A1	1.09	2.88	1.00109	1.00288	0.257	1.002890	1.001084
A2	0.94	2.87	1.00094	1.00287	0.257	1.002856	1.001258
B1	0.10	2.21	1.00010	1.00221	0.119	1.001482	1.002049
B2	-0.06	2.24	0.99994	1.00224	0.119	1.001719	1.002220

Reaction extent

0.091	0.047
0.354	0.390
0.257	0.119

Mean	1.002237	1.001653
SD	0.000741	0.000565
overall	1.00194	
SD	0.000685	
SE	0.00024	

Table B-3. *Yersinia*, Wild-Type, ^{18}O Isotope Effects, pH 9.0

YOP51* WT pH 9.0, bridge

TC	Rinf.		y fraction of 18-O in double labeled cpd	x fraction of 15-N in double labeled cpd	z fraction of 15-N in 14-N labeled cpd	b fraction of 15-N in mixture	15-N isotope effect	number of discrimin. atoms			
6.97	6.93										
7.07	7.02										
7.05	7.58										
7.36											
7.14	1.0071		0.87	0.99	0.0001	0.00369	1.0010	1			

Sample#	P Delta	RS Delta	Rp	Rs	f	IE(Rs,Ro)	IE(Rp,Ro)	corrected ---IE(Rs)	corrected ---IE(Rp)	Q1	A1	a2
Bridge A	-7.42	18.402	0.9926	1.0184	0.448	1.019067	1.020026	1.021369	1.022508	0.02727	1.01854	1.01952
Bridge A	-6.86	18.454	0.9931	1.0185	0.448	1.019156	1.019245	1.021475	1.021580	0.02727	1.01863	1.01872
Bridge B	-5.612	21.328	0.9944	1.0213	0.526	1.019112	1.019040	1.021423	1.021337	0.02727	1.01859	1.01851
Bridge B	-5.888	20.965	0.9941	1.0210	0.526	1.018617	1.019457	1.020835	1.021832	0.02727	1.01808	1.01894
Bridge C	-6.697	18.865	0.9933	1.0189	0.451	1.019661	1.019079	1.022075	1.021384	0.02727	1.01915	1.01855
Bridge C	-7.048	18.664	0.9930	1.0187	0.451	1.019321	1.019569	1.021671	1.021966	0.02727	1.01880	1.01906

	Rxn extent						
A	B	C		Mean	1.019156	1.019403	1.021475	1.021768
0.0755	0.092	0.0765		Sd	0.000341	0.000369	0.000405	0.000438
0.1685	0.175	0.1695		overall	1.019279		1.021621	
0.44807	0.5257	0.4513		Sd	0.000363		0.000430	
				SE	0.000105		0.000124	

YOP51* WT, 35C pH 9.0, non-bridge 18O

TC	Rinf.		y fraction of 18-O in double labeled cpd	x fraction of 15-N in double labeled cpd	z fraction of 15-N in 14-N labeled cpd	b fraction of 15-N in mixture	15-N isotope effect	number of discrimin. atoms			
-2.86	-2.17										
-2.11											
-2.12											
-2.33											
-2.318	0.9977		0.946	0.97	0.0001	0.00365	1.0010	3			

Sample#	P Delta	S Delta	Rp	Rs	f	IE(Rs,Ro)	IE(Rp,Ro)	corrected ---IE(Rs)	corrected ---IE(Rp)	Q1	A1	a2
non-B A	-4.699	-0.719	0.9953	0.9993	0.437	1.002795	1.003232	1.000622	1.000774	0.02814	1.00061	1.00076
non-B A	-4.628	-0.443	0.9954	0.9996	0.437	1.003279	1.003135	1.000791	1.000740	0.02814	1.00078	1.00073
non-B B	-3.915	0.7354	0.9961	1.0007	0.582	1.003516	1.002558	1.000873	1.000540	0.02814	1.00086	1.00053
non-B B	-4.362	0.9071	0.9956	1.0009	0.582	1.003714	1.003277	1.000942	1.000790	0.02814	1.00092	1.00078
non-B C	-4.529	-0.434	0.9955	0.9996	0.470	1.002980	1.003102	1.000687	1.000729	0.02814	1.00067	1.00072
non-B C	-4.35	-0.337	0.9957	0.9997	0.470	1.003135	1.002850	1.000740	1.000641	0.02814	1.00073	1.00063

						Mean	1.003236	1.003026	1.000776	1.000702
						Sd	0.000340	0.000273	0.000118	0.000095
						overall	1.003131		1.000739	
						Sd	0.000314		0.000109	
						SE	0.000091		0.000045	

Table B-4. *Yersinia*, R409K Mutant, All Isotope Effects, pH 6.0

YOP51*/R409K, pH 6.0, 31°C, ^{15}N

Exp: 12/15/98
Res: 12/19/98

Delta TC/Sm	
0.060	0.170
0.150	0.160
0.090	
0.120	
0.125	1.0001

sample#	P Delta	RS Delta	Rp	Rs	f	IE(Rs,Ro)	IE(Rp,Ro)
A1	-1.13	1.71	0.99887	1.00171	0.528	1.002112	1.001872
A2	-1.08	1.59	0.99892	1.00159	0.528	1.001952	1.001798
B1	-1.19	1.54	0.99881	1.00154	0.483	1.002150	1.001864
B2	-1.2	1.54	0.99880	1.00154	0.483	1.002150	1.001878

Rxn extent						
A	B	C		Mean	1.002091	1.001853
				SD	0.000094	0.000037
159.229	133.64					
301.444	276.89			overall	1.001972	
0.528	0.483			SD	0.000144	
				SE	0.000051	

YOP51* /R409K, pH 6.0, 31°C, bridge ^{18}O

exp: 12/15/98
res: 12/19/98

TC	Rinf.
1.73	1.98
1.85	
2.33	
2.03	
1.984	1.002

		y fraction of 18-O in double labeled cpd	x fraction of 15-N in double labeled cpd	z fraction of 15-N in 14-N labeled cpd	b fraction of 15-N in mixture	15-N isotope effect	number of discrimin. atoms
		0.93	0.99	0.0002	0.00365685	1.0020	1

Sample#	P Delta	RS Delta	Rp	Rs	f	IE(Rs,Ro)	IE(Rp,Ro)	corrected ---IE(Rs)	corrected ---IE(Rp)	Q1	A1	a2
Bridge A	-13.86	26.32	0.9861	1.0263	0.611	1.026072	1.026681	1.027375	1.028069	0.05504	1.02541	1.02605
Bridge A	-13.77	26.24	0.9862	1.0262	0.611	1.025985	1.026527	1.027276	1.027894	0.05504	1.02532	1.02589
Bridge B	-15.72	20.73	0.9843	1.0207	0.541	1.024376	1.027193	1.025442	1.028653	0.05504	1.02362	1.02659
Bridge B	-16.04	20.86	0.9840	1.0209	0.541	1.024547	1.027693	1.025638	1.029222	0.05504	1.02380	1.02712
Bridge C	-14.18	24.41	0.9858	1.0244	0.594	1.025156	1.026577	1.026331	1.027950	0.05504	1.02444	1.02594
Bridge C	-14.14	24.26	0.9859	1.0243	0.594	1.024985	1.026510	1.026137	1.027874	0.05504	1.02426	1.02587
Bridge D	-14.05	25.01	0.9860	1.0250	0.601	1.025388	1.026595	1.026595	1.027972	0.05504	1.02469	1.02596
Bridge D	-13.89	24.83	0.9861	1.0248	0.601	1.025187	1.026326	1.026366	1.027665	0.05504	1.02448	1.02568

Rxn extent							
A	B	C	D	Mean	1.025212	1.026763	1.026395
							1.028162
140.868	138.76	154.41	139.664	Sd	0.000605	0.000452	0.000690
							0.000515
230.516	256.43	259.84	232.562	overall	1.025987		1.027279
0.611	0.541	0.594	0.601	Sd	0.000953		0.001086
				SE	0.000275		0.000271

YOP51*/R409K, pH 6.0, 31°C, bridge

exp: 11/27/98
res: 12/8/98

TC	Rinf.
1.73	
1.85	
2.33	
1.97	1.002

		y fraction of 18-O in double labeled cpd	x fraction of 15-N in double labeled cpd	z fraction of 15-N in 14-N labeled cpd	b fraction of 15-N in mixture	15-N isotope effect from 12/98	number of discrimin. atoms
		0.93	0.99	0.0002	0.0036568	1.0020	1

Sample#	P Delta	RS Delta	Rp	Rs	f	IE(Rs,Ro)	IE(Rp,Ro)	corrected ---IE(Rs)	corrected ---IE(Rp)	Q1	A1	a2
Bridge A		21.310		1.0213	0.497	1.028600		1.030256		0.055043	1.028079	0.000000
Bridge A		21.210		1.0212	0.497	1.028449		1.030085		0.055043	1.027920	0.000000
Bridge B	-17.64	14.820	0.9824	1.0148	0.405	1.025135	1.026163	1.026308	1.027479	0.055043	1.024421	1.025507
Bridge B	-17.66	14.790	0.9823	1.0148	0.405	1.025075	1.026191	1.026240	1.027510	0.055043	1.024358	1.025535
Bridge C	-17.32	15.710	0.9827	1.0157	0.400	1.027349	1.025616	1.028831	1.026855	0.055043	1.026759	1.024928
Bridge C	-17.19	15.830	0.9828	1.0158	0.400	1.027593	1.025440	1.029109	1.026655	0.055043	1.027016	1.024743

Rxn extent							
A	B	C		Mean	1.027033	1.025852	1.028471
							1.027125
103.092	87.846	85.184		Sd	0.001569	0.000382	0.001788
							0.000435
207.339	216.73	212.71		overall	1.026561		1.027933
0.497	0.405	0.400		Sd	0.001337		0.001524
				SE	0.000386		0.000482

Table B-5. *Yersinia*, R409K Mutant, All Isotope Effects, Varying pH

| YOP51* R409K, 31°C pH 6.0, non-bridge 18O | | | | | | | exp: 11/27/98 res: 12/8/98 |

TC	Rinf.		y fraction of 18-O in double labeled cpd	x fraction of 15-N in double labeled cpd	z fraction of 15-N in 14-N labeled cpd	b fraction of 15-N in mixture	15-N isotope effect	number of discrimin. atoms
2.01								
1.97								
2.05								
2.05								
2.02	1.002		0.87	0.99	0.0001	0.003657	1.0020	3

Sample#	P Delta	S Delta	Rp	Rs	f	IE(Rs,Ro)	IE(Rp,Ro)	corrected ---IE(Rs)	corrected ---IE(Rp)	Q1	A1	a2
non-B A	-4.22	5.76	0.9958	1.0058	0.398	1.007400	1.008161	1.001936	1.002207	0.027520	1.001852	1.002111
non-B A	-4.03	5.99	0.9960	1.0060	0.398	1.007858	1.007911	1.002099	1.002118	0.027520	1.002008	1.002026
non-B B	-3.97	6.56	0.9960	1.0066	0.429	1.008136	1.008061	1.002198	1.002172	0.027520	1.002103	1.002077
non-B B	-3.93	6.54	0.9961	1.0065	0.429	1.008100	1.008006	1.002186	1.002152	0.027520	1.002091	1.002059
non-B C	-3.93	6.62	0.9961	1.0066	0.448	1.007775	1.008155	1.002070	1.002205	0.027520	1.001980	1.002109
non-B C	-3.87	6.60	0.9961	1.0066	0.448	1.007741	1.008072	1.002058	1.002176	0.027520	1.001968	1.002081
					Mean	1.007835	1.008061	1.002091	1.002172			
					Sd	0.000269	0.000094	0.000096	0.000034			

	Rxn extent	
A	B	C
98.494	106.48	104.54
247.599	248.27	233.51
0.398	0.429	0.448

	overall	1.007948		1.002131
	Sd	0.000226		0.000080
	SE	0.000065		0.000023

| YOP51*/R409K, pH 6.0, 39°C | | 11/21/97 |

Delta TC/Sm	
0.718	0.837
0.974	0.510
0.531	
0.74093	1.0007

This experiment has reliability problems due to low extent of reaction. Repeated this experiment with better results, got different result, but one that looks much more reliable.

sample#	P Delta	RS Delta	Rp	Rs	f	IE(Rs,Ro)	IE(Rp,Ro)
A1	-0.206	0.8229	0.99979	1.00082	0.177	1.000421	1.001046
A2	0.0351	1.2851	1.00004	1.00129	0.177		1.000779
B1	0.0476	0.526	1.00005	1.00053	0.165	0.998810	1.000760
B2	0.1796	0.5276	1.00018	1.00053	0.165	0.998819	1.000615
C1	-0.368	0.5859	0.99963	1.00059	0.181	0.999225	1.001227
C2	-0.326	0.8937	0.99967	1.00089	0.181	1.000765	1.001182
					Mean	0.999608	1.000935
					SD	0.000923	0.000251
					overall	1.000332	
					SD	0.000923	
					SE	0.000278	

| YOP51*/R409K, pH 9.0, 39°C | | 11/21/97 |

Delta TC/Sm	
0.718	0.837
0.974	0.510
0.531	
0.74093	1.0007

sample#	P Delta	RS Delta	Rp	Rs	f	IE(Rs,Ro)	IE(Rp,Ro)
A1	-0.685	0.933	0.99932	1.00093	0.209	1.000821	1.001608
A2	-1.607	0.941	0.99839	1.00094	0.209	1.000852	1.002650
B1	-1.240	1.190	0.99876	1.00119	0.181	1.002253	1.002195
B2	-1.366	0.985	0.99863	1.00098	0.181	1.001222	1.002335
C1	-1.461	0.807	0.99854	1.00081	0.214		1.002494
C2	-1.243	1.264	0.99876	1.00126	0.214	1.002173	1.002245
					Mean	1.001464	1.002254
					SD	0.000702	0.000358
					overall	1.001895	
					SD	0.000657	
					SE	0.000190	

Table B-6. *Yersinia*, D356N Mutant, All Isotope Effects, pH 9.0

YOP51* D356N, 35C, pH 9.0, 15 N effects   exp:4/1/98   res:4/2/98

Delta TC/Sm		
1.96	2.12	pH 9.0 actual
2.00	2.01	
2.12	2.09	
2.04	2.07	
2.06	1.94	
1.85	2.00	
2.022	1.002	

sample#	P Delta	RS Delta	Rp	Rs	f	IE(Rs,Ro)	IE(Rp,Ro)
A1	0.47	3.48	1.00047	1.00348	.427	1.002622	1.002074
A2	0.35	3.51	1.00035	1.00351	.427	1.002676	1.002235
B1	0.39	3.52	1.00039	1.00352	.391	1.003020	1.002112
B2	0.37	3.57	1.00037	1.00357	.391	1.003121	1.002138
C1	0.86	4.30	1.00086	1.0043	.494	1.003342	
C2	0.74	4.20	1.00074	1.0042	.494	1.003195	1.001836

Extent							
0.1495	0.1355	0.1755			Mean	1.002996	1.002079
0.3505	0.3463	0.355			SD	0.000289	0.000148
0.42653	0.3912	0.4944					
					overall	1.00258	
					SD	0.000529	
					SE	0.00016	

YOP51*/D356N pH 9.0, 35C, bridge

TC	Rinf.		y fraction of 18-O in double labeled cpd	x fraction of 15-N in double labeled cpd	z fraction of 15-N in 14-N labeled cpd	b fraction of 15-N in mixture	15-N isotope effect	number of discrimin. atoms
6.97	6.93							
7.07	7.02							
7.05	7.58							
7.36								
7.14	1.0071		0.87	0.99	0.0001	0.00369	1.0026	1

Sample#	P Delta	RS Delta	Rp	Rs	f	IE(Rs,Ro)	IE(Rp,Ro)	corrected ---IE(Rs)	corrected ---IE(Rp)	Q1	A1	a2
Bridge A	-12.8	28.170	0.9872	1.0282	0.517	1.029190	1.029687	1.031491	1.032082	0.027273	1.027286	1.027796
Bridge A	-13.15	27.780	0.9869	1.0278	0.517	1.028638	1.030218	1.030836	1.032714	0.027273	1.02672	1.028341
Bridge B	-11.88	31.330	0.9881	1.0313	0.564	1.029450	1.029938	1.031801	1.032382	0.027273	1.027553	1.028054
Bridge B	-11.72	31.500	0.9883	1.0315	0.564	1.029661	1.029682	1.032052	1.032077	0.027273	1.027769	1.027791
Bridge C	-11.93	32.010	0.9881	1.0320	0.547	1.031804	1.029379	1.034602	1.031717	0.027273	1.029969	1.027481
Bridge C	-11.86	31.750	0.9881	1.0318	0.547	1.031466	1.029270	1.034199	1.031587	0.027273	1.029621	1.027368

Rxn extent									
A	B	C							
0.089	0.095	0.094			Mean	1.030035	1.029696	1.032497	1.032093
0.089	0.095	0.093			Sd	0.001290	0.000350	0.001535	0.000416
0.172	0.169	0.171			overall	1.029865		1.032295	
	0.168				Sd	0.000919		0.001093	
0.51744	0.5638	0.5468			SE	0.000265		0.000315	

YOP51*/D356N, 35C, pH 9.0, non-bridge 18O

TC	Rinf.		y fraction of 18-O in double labeled cpd	x fraction of 15-N in double labeled cpd	z fraction of 15-N in 14-N labeled cpd	b fraction of 15-N in mixture	15-N isotope effect	number of discrimin. atoms
-2.86	-2.17							
-2.11								
-2.12								
-2.33								
-2.318	0.9977		0.946	0.97	0.0001	0.00365	1.0026	3

Sample#	P Delta	S Delta	Rp	Rs	f	IE(Rs,Ro)	IE(Rp,Ro)	corrected ---IE(Rs)	corrected ---IE(Rp)	Q1	A1	a2
non-B A	-6.33	2.12	0.9937	1.0021	.534	1.005845	1.006058	1.001136	1.001210	0.028142	1.001115	1.001188
non-B A	-6.45	2.14	0.9936	1.0021	.534	1.005872	1.006240	1.001145	1.001273	0.028142	1.001124	1.00125
non-B B	-6.18	3.26	0.9938	1.0033	.628	1.005677	1.006626	1.001077		0.028142	1.001058	1.001382
non-B B	-5.68	3.34	0.9943	1.0033	.628	1.005759	1.005766	1.001106	1.001108	0.028142	1.001086	1.001088
non-B C	-5.70	4.65	0.9943	1.0047	.662	1.006462	1.006136		1.001237	0.028142	1.001326	1.001214
non-B C	-5.42	4.72	0.9946	1.0047	.662	1.006527	1.005626		1.001060	0.028142	1.001348	1.001041

Rxn extent									
A	B	C							
.094	.108	.113			Mean	1.00602358	1.00607536	1.00111594	1.00117746
.094	.106	.112			Sd	0.00037177	0.00035553	3.0743E-05	8.9905E-05
.177	.169	.170			overall	1.00604947		1.00115	
.175	.172	.170			Sd	0.00034786		7.3805E-05	
0.53409	0.6276	0.6618			SE	0.00010042		2.4602E-05	

Table B-7. *Yersinia*, Various Mutants, [15]N Isotope Effects, pH 9.0

YOP51* D356N, 35C, pH 9.0, 15 N effects						exp:10/15/97 res:12/1/97	
Delta TC/Sm							
1.430	0.85	pH estimated at 8.5, not measured					
1.020	1.13						
1.070	0.91						
1.430	0.87						
1.020	1.23						
0.870							
1.075	1.0011						

sample#	P Delta	RS Delta	Rp	Rs	f	IE(Rs,Ro)	IE(Rp,Ro)
A1	0.20	4.26	1.00020	1.00426	.610	1.003384	1.001454
A2	0.40	4.38	1.00040	1.00438	.610	1.003512	1.001122
B1	-0.47	3.71	0.99953	1.00371	.525	1.003545	1.002295
B2	-0.35	3.61	0.99965	1.00361	.525	1.003410	1.002116
C1	-0.10	3.10	0.99990	1.00310	.371	1.004378	1.001495
C2	0.12	3.08	1.00012	1.00308	.371	1.004334	1.001215

Extent							
0.146	0.126	0.109			Mean	1.003760	1.001616
0.145	0.128	0.108			SD	0.000465	0.000481
0.237	0.242	0.29					
0.24	0.242	0.295			overall	1.00269	
0.61006	0.5248	0.3709			SD	0.001207	
					SE	0.00035	

YOP51* W354A, 35C, pH 9.0, 15 N effects						exp:9/6/97 res:12/1/97	
Delta TC/Sm							
1.430	0.85	pH estimated at 8.52 due to substrate effect					
1.020	1.13	pH not measured/adjusted aafter substrate addition					
1.070	0.91						
1.430	0.87						
1.020	1.23						
0.870							
1.075	1.0011						

sample#	P Delta	RS Delta	Rp	Rs	f	IE(Rs,Ro)	IE(Rp,Ro)
A1	-0.35	2.48	0.99965	1.00248	.291		1.001702
A2	-0.22	2.52	0.99978	1.00252	.291		1.001546
B1	0.4	3.79	1.0004	1.00379	.579	1.003142	1.001073
B2	0.18	3.46	1.00018	1.00346	.579	1.002760	1.001423
C1	0.19	2.58	1.00019	1.00258	.442	1.002579	1.001202
C2	0.09	2.46	1.00009	1.00246	.442	1.002373	1.001338

					Mean	1.002714	1.001381
					SD	0.000326	0.000228
					overall	1.00191	
					SD	0.000734	
					SE	0.00023	

Table B-8. *Yersinia*, W354A Mutant, ^{15}N and ^{18}O Isotope Effects, pH 6.0

YOP51* W354A, 35C, pH 6.0, 15 N effects   1/20/98

Delta TC/Sm

1.020	1.23
1.020	1.13
1.340	1.2
1.320	1.41
1.150	1.31
1.070	0.91
0.870	
1.152	1.0012

pH estimated at 5.84 due to acidic effects of substrate
pH not measured after addition of substrate to buffer

sample#	P Delta	RS Delta	Rp	Rs	f	IE(Rs,Ro)	IE(Rp,Ro)
A1	-0.3	2.51	0.9997	1.00251	.391	1.002896	1.001781
A2	-0.21	2.46	0.99979	1.00246	.391	1.002795	1.001664
B1	0.2	2.91	1.0002	1.00291	.543	1.002344	1.001328
B2	0.07	3.02	1.00007	1.00302	.543	1.002484	1.001525
C1	0.14	3.59	1.00014	1.00359	.601	1.002738	1.001533
C2	0.1	3.48	1.0001	1.00348	.601	1.002618	1.001599
					Mean	1.002646	1.001572
					SD	0.000206	0.000152
					overall	1.00211	
					SD	0.000587	
					SE	0.00019	

YOP51*-W354A, 35°C, pH 6.0, bridge

substrate: 1/28/98   exp: 2/6/98   res: 2/18/98

TC	Rinf.
2.23	2.21
2.35	1.93
2.51	2.05
2.42	2.08
2.2225	1.0022

y fraction of 18-O in double labeled cpd	x fraction of 15-N in double labeled cpd	z fraction of 15-N in 14-N labeled cpd	b fraction of 15-N in mixture	15-N isotope effect	number of discrimin. atoms
0.93	0.99	0.0002	0.003672	1.0021	1

Sample#	P Delta	RS Delta	Rp	Rs	f	IE(Rs,Ro)	IE(Rp,Ro)	corrected ---IE(Rs)	corrected ---IE(Rp)	Q1	A1	a2
Br A	-18.50	20.10	0.9815	1.0201	0.469	1.028722	1.029436	1.030230	1.031043	0.05481	1.02805	1.02881
Br A	-18.40	19.83	0.9816	1.0198	0.469	1.028280	1.029291	1.029726	1.030878	0.05481	1.02759	1.02865
Br B	-13.83	34.10	0.9862	1.0341	0.653	1.030509	1.028853	1.032266	1.030379	0.05481	1.02994	1.02819
Br B	-13.85	33.98	0.9862	1.0340	0.653	1.030392	1.028889	1.032134	1.030420	0.05481	1.02982	1.02823
Br C	-11.06	43.44	0.9889	1.0434	0.742	1.030640	1.028409	1.032417	1.029873	0.05481	1.03008	1.02772
Br C	-11.02	43.32	0.9890	1.0433	0.742	1.030550	1.028323	1.032314	1.029774	0.05481	1.02998	1.02763

	Rxn extent	
A	B	C
0.114	0.156	0.167
0.243	0.239	0.225
0.4691	0.6527	0.7422

	IE(Rs,Ro)	IE(Rp,Ro)	corrected ---IE(Rs)	corrected ---IE(Rp)
Mean	1.029849	1.028867	1.031514	1.030395
Sd	0.001056	0.000449	0.001204	0.000512
overall	1.029358		1.030954	
Sd	0.000928		0.001059	
SE	0.000268		0.000306	

YOP51*-W354A, 35°C, pH 6.0, non-bridge

substrate: 1/98   exp: 2/6/98   res: 2/18/98

TC	Rinf.
-8.5	-10.11
-8.49	-10.11
-10.11	-10.11
-10.11	-10.11
-9.705	0.9903

y fraction of 18-O in double labeled cpd	x fraction of 15-N in double labeled cpd	z fraction of 15-N in 14-N labeled cpd	b fraction of 15-N in mixture	15-N isotope effect	number of discrimin. atoms
0.87	0.99	0.0001	0.003626	1.0021	3

Sample#	P Delta	RS Delta	Rp	Rs	f	IE(Rs,Ro)	IE(Rp,Ro)	corrected ---IE(Rs)	corrected ---IE(Rp)	Q1	A1	a2
NB A	-12.79	-4.12	0.9872	0.9959	0.550	1.007095	1.004782		1.000954	0.02776	1.00170	1.00091
NB A	-13.03	-4.11	0.9870	0.9959	0.550	1.007108	1.005155		1.001088	0.02776	1.00171	1.00104
NB B	-12.25	-2.03	0.9878	0.9980	0.564	1.009377	1.004017	1.002592	1.000681	0.02776	1.00248	1.00065
NB B	-12.29	-1.98	0.9877	0.9980	0.564	1.009439	1.004080	1.002614	1.000704	0.02776	1.00250	1.00067
NB C	-10.61	2.48	0.9894	1.0025	0.743	1.009073	1.001948	1.002483		0.02776	1.00238	0.99995
NB C	-10.64	2.39	0.9894	1.0024	0.743	1.009006	1.002013	1.002460		0.02776	1.00235	0.99997

	Rxn extent	
A	B	C
0.1295	0.1315	0.168
0.2355	0.233	0.226
0.5499	0.5644	0.7434

	IE(Rs,Ro)	IE(Rp,Ro)	corrected ---IE(Rs)	corrected ---IE(Rp)
Mean	1.008516	1.003666	1.002537	1.000857
Sd	0.001109	0.001374	0.000077	0.000197
overall	1.006091		1.001697	
Sd	0.002799		0.000909	
SE	0.000808		0.000321	

Table B-9. *Yersinia*, W354A Mutant, ^{15}N and ^{18}O Isotope Effects, pH 9.0

YOP51* W354A, 35C, pH 9.0, 15 N effects

exp 3/20/98
res 3/28/98

pH actual is 9.0

Delta TC/Sm	
2.120	1.85
2.010	2.12
2.040	2.01
2.060	2.09
2.040	2.07
2.000	1.94
2.029	1.002

sample#	P Delta	RS Delta	Rp	Rs	f	IE(Rs,Ro)	IE(Rp,Ro)
A1	0.55	3.26	1.00055	1.00326	.406	1.002360	1.001940
A2	0.39	3.26	1.00039	1.00326	.406	1.002360	1.002150
B1	0.64	3.81	1.00064	1.00381	.545	1.002259	1.002112
B2	0.6	3.7	1.0006	1.0037	.545	1.002120	1.002173
C1	0.91	4.3	1.00091	1.0043	.669	1.002050	1.002045
C2	0.91	4.31	1.00091	1.00431	.669	1.002059	1.002045

Rxn extent		
A	B	C
0.104	0.139	0.17
0.256	0.255	0.254
0.406	0.545	0.669

Mean	1.002201	1.002077
SD	0.000144	0.000085
overall	1.00214	
SD	0.000130	
SE	0.00004	

YOP51*-W354A, 35°C, pH 9.0, bridge

substrate: 1/28/98

exp: 3/20/98
res: 3/28/98

TC	Rinf.
1.9	1.87
1.94	1.78
1.77	1.79
1.75	1.85
1.8313	1.0018

y fraction of 18-O in double labeled cpd	x fraction of 15-N in double labeled cpd	z fraction of 15-N in 14-N labeled cpd	b fraction of 15-N in mixture	15-N isotope effect	number of discrimin. atoms
0.93	0.99	0.0002	0.003672	1.0021	1

Sample#	P Delta	RS Delta	Rp	Rs	f	IE(Rs,Ro)	IE(Rp,Ro)	corrected ---IE(Rs)	corrected ---IE(Rp)	Q1	A1	a2
Br A	-20.51	16.62	0.9795	1.0166	0.399	1.029588	1.029734	1.031180	1.031348	0.05481	1.02893	1.02909
Br A	-20.58	16.61	0.9794	1.0166	0.399	1.029567	1.029830	1.031157	1.031456	0.05481	1.02891	1.02919
Br B	-15.36	29.55	0.9846	1.0296	0.582	1.032328	1.027810	1.034306	1.029154	0.05481	1.03183	1.02706
Br B	-15.68	29.48	0.9843	1.0295	0.582	1.032245	1.028336	1.034211	1.029753	0.05481	1.03174	1.02761
Br C	-13.64	35.43	0.9864	1.0354	0.648	1.032615	1.027593	1.034633	1.028907	0.05481	1.03213	1.02683
Br C	-13.71	35.29	0.9863	1.0353	0.648	1.032477	1.027720	1.034475	1.029051	0.05481	1.03198	1.02696

Rxn extent		
A	B	C
0.0735	0.1175	0.128
0.184	0.202	0.1975
0.3995	0.5817	0.6481

Mean	1.031470	1.028504	1.033327	1.029945
Sd	0.001471	0.001022	0.001678	0.001165
overall	1.029987		1.031636	
Sd	0.001964		0.002240	
SE	0.000567		0.000647	

YOP51*-W354A, 35°C, pH 9.0, non-bridge

substrate: 1/98

exp: 3/20/98
res: 3/28/98

TC	Rinf.
-8.5	-8.37
-8.49	-8.20
-9.15	-8.61
-9.24	-8.41
-8.621	0.9914

y fraction of 18-O in double labeled cpd	x fraction of 15-N in double labeled cpd	z fraction of 15-N in 14-N labeled cpd	b fraction of 15-N in mixture	15-N isotope effect	number of discrimin. atoms
0.87	0.99	0.0001	0.003626	1.0021	3

Sample#	P Delta	RS Delta	Rp	Rs	f	IE(Rs,Ro)	IE(Rp,Ro)	corrected ---IE(Rs)	corrected ---IE(Rp)	Q1	A1	a2
NB A	-13.14	-6.09	0.9869	0.9939	0.464	1.004103	1.006356	1.000701	1.001505	0.02776	1.00067	1.00144
NB A	-13.20	-6.17	0.9868	0.9938	0.464	1.003973	1.006441	1.000655	1.001535	0.02776	1.00063	1.00147
NB B	-12.96		0.9870	1.0000	0.536		1.006613		1.001596	0.02776	0.00000	1.00153
NB B	-13.00		0.9870	1.0000	0.536		1.006674		1.001618	0.02776	0.00000	1.00155
NB C	-12.35	-4.13	0.9877	0.9959	0.568	1.005414	1.005912	1.001169	1.001347	0.02776	1.00112	1.00129
NB C	-12.36	-4.21	0.9876	0.9958	0.568	1.005318	1.005928	1.001135	1.001352	0.02776	1.00109	1.00129

Rxn extent		
A	B	C
0.120	0.122	0.142
0.259	0.228	0.250
0.4642	0.5363	0.568

Mean	1.004702	1.006321	1.000915	1.001492
Sd	0.000770	0.000331	0.000275	0.000118
overall	1.005673		1.001261	
Sd	0.000978		0.000349	
SE	0.000282		0.000110	

Table B-10. *Yersinia*, W354F Mutant, ^{15}N and ^{18}O Isotope Effects, pH 6.0

YOP51* W354F, 35C, pH 6.0, 15 N effects 1/20/98

Delta TC/Sm	
1.430	0.85
1.020	1.13
1.340	1.2
1.320	1.41
1.150	1.31
1.070	0.91
1.430	0.87
1.020	1.23
0.870	
1.151	1.0012

pH estimated at 5.84 due to acidic effects of substrate
pH not measured after addition of substrate to buffer

sample#	P Delta	RS Delta	Rp	Rs	f	IE(Rs,Ro)	IE(Rp,Ro)
A1	0.34	2.24	1.00034	1.00224	.465	1.001742	1.001126
A2	0.52	2.28	1.00052	1.00228	.465	1.001806	1.000876
B1	0.53	2.57	1.00053	1.00257	.555	1.001753	1.000955
B2	0.66	2.55	1.00066	1.00255	.555	1.001728	1.000755
C1	0.7	2.85	1.0007	1.00285	.601	1.001849	1.000738
C2	0.79	2.77	1.00079	1.00277	.601	1.001762	1.000591
					Mean	1.001773	1.000840
					SD	0.000046	0.000188
					overall	1.00131	
					SD	0.000504	
					SE	0.00016	

YOP51*-W354F, 35°C, pH 6.0, bridge
substrate: 1/28/98
exp: 2/6/98
res: 2/18/98

TC	Rinf.
2.23	2.21
2.35	1.93
2.51	2.05
2.42	2.08
2.2225	1.0022

y fraction of 18-O in double labeled cpd	x fraction of 15-N in double labeled cpd	z fraction of 15-N in 14-N labeled cpd	b fraction of 15-N in mixture	15-N isotope effect	number of discrimin. atoms
0.93	0.99	0.0002	0.003672	1.0013	1

Sample#	P Delta	RS Delta	Rp	Rs	f	IE(Rs,Ro)	IE(Rp,Ro)	corrected ---IE(Rs)	corrected ---IE(Rp)	Q1	A1	a2
Bridge A	-13.94	26.97	0.9861	1.0270	0.427	1.045843	1.021918		1.023411	0.05481	1.04703	1.02174
Bridge A	-14.03		0.9860	1.0000	0.427		1.022042		1.023552	0.05481	0.00000	1.02187
Bridge B	-8.85	34.09	0.9912	1.0341	0.716	1.025470	1.022331	1.027460	1.023882	0.05481	1.02549	1.02217
Bridge B	-8.84	33.87	0.9912	1.0339	0.716	1.025293	1.022311	1.027257	1.023859	0.05481	1.02530	1.02215
Bridge C	-7.21	14.40	0.9928	1.0144	0.743	1.008977	1.020142		1.021390	0.05481	1.00808	1.01986
Bridge C	-7.35	14.43	0.9927	1.0144	0.743	1.008999	1.020443		1.021732	0.05481	1.00811	1.02018
					Mean	1.022916	1.021531	1.027358	1.022971			
					Sd	0.015214	0.000977	0.000143	0.001112			
					overall	1.022161		1.024068				
					Sd	0.009674		0.002239				
					SE	0.002793		0.000791				

Rxn extent		
A	B	C
0.102	0.168	0.127
0.239	0.2345	0.171
0.4268	0.7164	0.7427

YOP51*-W354F, 35°C, pH 6.0, non-bridge
substrate: 1/98
exp: 2/6/98
res: 2/18/98

TC	Rinf.
-8.5	-10.11
-8.49	-10.11
-10.11	-10.11
-10.11	-10.11
-9.705	0.9903

y fraction of 18-O in double labeled cpd	x fraction of 15-N in double labeled cpd	z fraction of 15-N in 14-N labeled cpd	b fraction of 15-N in mixture	15-N isotope effect	number of discrimin. atoms
0.87	0.99	0.0001	0.003626	1.0013	3

Sample#	P Delta	RS Delta	Rp	Rs	f	IE(Rs,Ro)	IE(Rp,Ro)	corrected ---IE(Rs)	corrected ---IE(Rp)	Q1	A1	a2
Bridge A	-11.50	-3.62	0.9885	0.9964	0.430	1.011002	1.002438		1.000405	0.02776	1.00331	1.00039
Bridge A	-11.43	-3.64	0.9886	0.9964	0.430	1.010966	1.002343		1.000370	0.02776	1.00329	1.00035
Bridge B	-11.50	-2.99	0.9885	0.9970	0.578	1.007891	1.002883	1.002350	1.000564	0.02776	1.00225	1.00054
Bridge B	-11.45	-3.06	0.9886	0.9969	0.578	1.007808	1.002803	1.002321	1.000535	0.02776	1.00222	1.00051
Bridge C	-10.55	-0.73	0.9895	0.9993	0.783	1.005949	1.002014	1.001658	1.000253	0.02776	1.00159	1.00024
Bridge C	-10.45	-0.84	0.9896	0.9992	0.783	1.005876	1.001776	1.001632	1.000168	0.02776	1.00156	1.00016
					Mean	1.008249	1.002376	1.001990	1.000382			
					Sd	0.002289	0.000433	0.000399	0.000155			
					overall	1.005312		1.001025				
					Sd	0.003446		0.000869				
					SE	0.000995		0.000307				

Rxn extent		
A	B	C
0.099	0.1165	0.1835
0.23	0.2015	0.2345
0.4304	0.5782	0.7825

Table B-11. *Yersinia,* W354F Mutant, ^{15}N and ^{18}O Isotope Effects, pH 9.0

YOP51* W354F, 35C, pH 9.0, 15 N effects   exp 3/20/98   res 3/28/98

Delta TC/Sm	
2.120	1.85
2.010	2.12
2.040	2.01
2.060	2.09
2.040	2.07
2.000	1.94
2.029	1.002

pH actual is 9.0

sample#	P Delta	RS Delta	Rp	Rs	f	IE(Rs,Ro)	IE(Rp,Ro)
A1	0.57	3.31	1.00057	1.00331	.366	1.002807	1.001848
A2	0.54	3.3	1.00054	1.0033	.366	1.002785	1.001886
B1	0.77	3.95	1.00077	1.00395	.544	1.002444	1.001911
B2	0.82	3.94	1.00082	1.00394	.544	1.002432	1.001835
C1	1.32	5.55	1.00132	1.00555	.800	1.002209	1.001760
C2	1.24	5.59	1.00124	1.00559	.800	1.002209	1.001958

	Rxn extent			
A	B	C	Mean	1.002477	1.001866
0.072	0.105	0.156	SD	0.000270	0.000069
0.1965	0.193	0.195			
0.366	0.544	0.800	overall	1.00217	
			SD	0.000370	
			SE	0.00012	

YOP51*-W354F, 35°C, pH 9.0, bridge

substrate: 1/28/98   exp: 3/20/98   res: 3/28/98

TC	Rinf.
1.9	1.87
1.94	1.78
1.77	1.79
1.75	1.85
1.8313	1.0018

y fraction of 18-O in double labeled cpd	x fraction of 15-N in double labeled cpd	z fraction of 15-N in 14-N labeled cpd	b fraction of 15-N in mixture	15-N isotope effect	number of discrimin. atoms
0.93	0.99	0.0002	0.003672	1.0022	1

Sample#	P Delta	RS Delta	Rp	Rs	f	IE(Rs,Ro)	IE(Rp,Ro)	corrected ---IE(Rs)	corrected ---IE(Rp)	Q1	A1	a2
Br A	-20.85	16.54	0.9792	1.0165	0.414	1.028003	1.030610	1.029336	1.032308	0.05481	1.02723	1.02998
BrA	-20.89	16.60	0.9791	1.0166	0.414	1.028120	1.030665	1.029469	1.032371	0.05481	1.02735	1.03004
BrB	-15.25	32.04	0.9848	1.0320	0.563	1.037276	1.026938	1.039917	1.028122	0.05481	1.03702	1.02610
BrB	-15.13	32.04	0.9849	1.0320	0.563	1.037276	1.026745	1.039917	1.027903	0.05481	1.03702	1.02590
BrC	-11.39	44.34	0.9886	1.0443	0.761	1.029892	1.029618	1.031489	1.031178	0.05481	1.02922	1.02893
BrC	-11.46		0.9885		0.761		1.029777		1.031358	0.05481	0.00000	1.02910

	Rxn extent			
A	B	C	Mean	1.032113	1.029059	1.034026	1.030540
0.075	0.104	0.137	Sd	0.004772	0.001770	0.005445	0.002018
0.181	0.184	0.180					
0.4144	0.5625	0.7611	overall	1.030447		1.032124	
			Sd	0.003636		0.004148	
			SE	0.001050		0.001251	

YOP51*-W354F, 35°C, pH 9.0, non-bridge

substrate: 1/98   exp: 3/20/98   res: 3/28/98

TC	Rinf.
-8.5	-8.37
-8.49	-8.20
-9.15	-8.61
-9.24	-8.41
-8.621	0.9914

y fraction of 18-O in double labeled cpd	x fraction of 15-N in double labeled cpd	z fraction of 15-N in 14-N labeled cpd	b fraction of 15-N in mixture	15-N isotope effect	number of discrimin. atoms
0.87	0.99	0.0001	0.003626	1.0022	3

Sample#	P Delta	RS Delta	Rp	Rs	f	IE(Rs,Ro)	IE(Rp,Ro)	corrected ---IE(Rs)	corrected ---IE(Rp)	Q1	A1	a2
NB A	-12.26	-2.49	0.9877	0.9975	0.693	1.005246	1.007039	1.001097	1.001737	0.02776	1.00105	1.00166
NB A	-12.29	-2.58	0.9877	0.9974	0.693	1.005169	1.007097	1.001070	1.001757	0.02776	1.00102	1.00168
NB B	-12.66	-3.73	0.9873	0.9963	0.634	1.004921	1.007045	1.000982	1.001739	0.02776	1.00094	1.00166
NB B	-12.60	-3.72	0.9874	0.9963	0.634	1.004931	1.006940	1.000985	1.001702	0.02776	1.00094	1.00163
NB C	-13.34	-5.83	0.9867	0.9942	0.472	1.004420	1.006694	1.000803	1.001614	0.02776	1.00077	1.00154
NB C	-13.42	-5.78	0.9866	0.9942	0.472	1.004499	1.006808	1.000831	1.001654	0.02776	1.00080	1.00158

	Rxn extent			
A	B	C	Mean	1.004864	1.006937	1.000961	1.001700
0.122	0.097	0.081	Sd	0.000340	0.000157	0.000121	0.000056
0.176	0.153	0.171					
0.6932	0.634	0.4721	overall	1.005901		1.001331	
			Sd	0.001112		0.000396	
			SE	0.000321		0.000125	

Table B-12. *Yersinia*, R409A Mutant, ^{15}N and ^{18}O Isotope Effects, pH 6.0

YOP51*/R409A, 35C, pH 6.0

exp: 4/15/98
res: 5/7/98

Delta TC/Sm	
2.060	1.85
1.800	2.12
2.01	1.94
2.09	
2.07	
1.993	1.002

sample#	P Delta	RS Delta	Rp	Rs	f	IE(Rs,Ro)	IE(Rp,Ro)
A1	0.93	2.20	1.00093	1.00220	0.118	1.001656	1.001131
A2	0.99	2.24	1.00099	1.00224	0.118	1.001976	1.001067
B1	1.01	2.49	1.00101	1.00249	0.198	1.002249	1.001099
B2	1.09	2.24	1.00109	1.00224	0.198	1.001118	1.001009

Rxn extent				Mean	1.001750	1.001076
A	B			SD	0.000486	0.000052
0.045	0.127					
0.3823	0.64			overall	1.001413	
0.118	0.198			SD	0.000482	
				SE	0.000170	

YOP51*-R409A, 35°C, pH 6.0, bridge

substrate: 1/28/98

exp: 4/20/98
res: 5/7/98

TC	Rinf.		y fraction of 18-O in double labeled cpd	x fraction of 15-N in double labeled cpd	z fraction of 15-N in 14-N labeled cpd	b fraction of 15-N in mixture	15-N isotope effect	number of discrimin. atoms
1.63	1.87							
1.62	1.78							
1.77	1.79							
1.75	1.85							
1.7575	1.0018		0.93	0.99	0.0002	0.003656	1.0014	1

Sample#	P Delta	RS Delta	Rp	Rs	f	IE(Rs,Ro)	IE(Rp,Ro)	corrected ---IE(Rs)	corrected ---IE(Rp)	Q1	A1	a2
Bridge A	-15.33	7.56	0.9847	1.0076	0.269	1.018819	1.020370	1.019764	1.021530	0.0551	1.0184	1.0200
Bridge A	-15.50	7.63	0.9845	1.0076	0.269	1.019049	1.020576	1.020027	1.021765	0.0551	1.0186	1.0202
Bridge B	-15.31	5.79	0.9847	1.0058	0.212	1.017162	1.019569	1.017879	1.020618	0.0551	1.0166	1.0191
Bridge B	-15.24	5.82	0.9848	1.0058	0.212	1.017291	1.019487	1.018026	1.020525	0.0551	1.0167	1.0191

Rxn extent			Mean	1.018080	1.020000	1.018924	1.021110
A	B		Sd	0.000992	0.000553	0.001129	0.000630
0.087	0.107						
0.324	0.505		overall	1.019040		1.020017	
0.2685	0.2119		Sd	0.001267		0.001442	
			SE	0.000366		0.000510	

YOP51*-R409A, 35°C, pH 6.0, non-bridge

substrate: 1/98

exp: 4/20/98
res: 5/7/98

TC	Rinf.		y fraction of 18-O in double labeled cpd	x fraction of 15-N in double labeled cpd	z fraction of 15-N in 14-N labeled cpd	b fraction of 15-N in mixture	15-N isotope effect	number of discrimin. atoms
-10.11	-9.93							
-8.49	-9.74							
-9.15	-8.61							
-9.24	-10.11							
-9.423	0.9906		0.87	0.99	0.0001	0.003626	1.0014	3

Sample#	P Delta	RS Delta	Rp	Rs	f	IE(Rs,Ro)	IE(Rp,Ro)	corrected ---IE(Rs)	corrected ---IE(Rp)	Q1	A1	a2
Bridge A	-13.59	-8.43	0.9864	0.9916	0.270	1.003186	1.004967	1.000634	1.001269	0.0278	1.0006	1.0012
Bridge A	-13.65	-8.42	0.9864	0.9916	0.270	1.003218	1.005039	1.000645	1.001295	0.0278	1.0006	1.0012
Bridge B	-13.35	-9.93	0.9867	0.9901	0.229	0.998036	1.004547	0.998791	1.001120	0.0278	0.9988	1.0011
Bridge B	-13.29	-9.94	0.9867	0.9901	0.229	0.997997	1.004477	0.998777	1.001095	0.0278	0.9988	1.0010

Rxn extent			Mean	1.000609	1.004757	0.999712	1.001195
A	B		Sd	0.002994	0.000286	0.001071	0.000102
0.081	0.100						
0.300	0.434		overall	1.002683		1.000453	
0.2705	0.2293		Sd	0.002965		0.001060	
			SE	0.000856		0.000375	

Use only product data due to low reaction extent and wide variance of product and residual substrate numbers

Table B-13. *Yersinia*, R409A Mutant, ^{15}N Isotope Effects, pH 6.0

	YOP51* R409A, 35°C, pH 6.0, ^{15}N effects						1/26/98
Delta TC/Sm							
1.98	2.03	(Actual pH estimated is 5.84)					
2.15	2.23						
2.08	2.11						
2.12	2.02						
2.12	2.17						
2.01	2.12						
2.04	2.01						
2.06	2.09						
2.04	2.07						
2.081	1.0021						

sample#	P Delta	RS Delta	Rp	Rs	f	IE(Rs,Ro)	IE(Rp,Ro)
A1	2.11	2.88	1.002110	1.002880	.167		0.999968
A2	1.60	2.79	1.001600	1.002790	.167		1.000526
B1	1.85	2.61	1.001850	1.002610	.187	1.002558	1.000256
B2	1.51	2.64	1.001510	1.002640	.187	1.002703	1.000633
C1	1.49	2.54	1.001490	1.002540	.179	1.002330	1.000652
C2	1.19	2.49	1.001190	1.002490	.179	1.002076	1.000983
					Mean	1.002417	1.000503
					SD	0.000275	0.000352
					overall	1.00127	
					SD	0.001035	
					SE	0.00033	

Table B-14. *Yersinia*, R409A/D356A Mutant, ^{15}N and ^{18}O Isotope Effects, pH 6.0

YOP51*/R409A-D356A, 31°C, pH 6.0, ^{15}N

exp: 11/27/98
res: 12/8/98

Delta TC/Sm
0.060
-0.080
0.090

0.0233 1.0000

sample#	P Delta	RS Delta	Rp	Rs	f	IE(Rs,Ro)	IE(Rp,Ro)
A1	-1.7	2.03	0.9983	1.00203	0.445	1.003420	1.002350
A2	-1.78	2.04	0.99822	1.00204	0.445	1.003437	1.002459
B1	-2.02	0.97	0.99798	1.00097	0.340	1.002282	1.002538
B2	-1.99	0.85	0.99801	1.00085	0.340	1.001992	1.002501
C1	-1.83	1.04	0.99817	1.00104	0.406	1.001958	1.002435
C2	-1.88	1.09	0.99812	1.00109	0.406	1.002054	1.002501

Rxn extent

A	B	C
9.765	8.401	9.548
21.96	24.705	23.546
0.445	0.340	0.406

Mean	1.002524	1.002464
SD	0.000710	0.000067
overall	**1.002494**	
SD	0.000482	
SE	**0.000139**	

YOP51* R409A-D356A, pH 6.0, 31°C, bridge ^{18}O

exp: 11/27/98
res: 12/8/98

TC Rinf.
1.73
1.85
2.33
1.97 1.002

y fraction of 18-O in double labeled cpd	x fraction of 15-N in double labeled cpd	z fraction of 15-N in 14-N labeled cpd	b fraction of 15-N in mixture	15-N isotope effect	number of discrimin. atoms
0.93	0.99	0.0002	0.0036568	1.0025	1

Sample#	P Delta	RS Delta	Rp	Rs	f	IE(Rs,Ro)	IE(Rp,Ro)	corrected ---IE(Rs)	corrected ---IE(Rp)	Q1	A1	a2
Bridge A	-19.08	24.48	0.9809	1.0245	0.554	1.028301	1.032953	1.029305	1.034610	0.0550	1.0272	1.0321
Bridge A	-19.00	24.50	0.9810	1.0245	0.554	1.028326	1.032825	1.029335	1.034464	0.0550	1.0272	1.0320
Bridge B	-22.32	14.58	0.9777	1.0146	0.405	1.024715	1.032537	1.025221	1.034136	0.0550	1.0234	1.0317
Bridge B	-22.35	14.36	0.9777	1.0144	0.405	1.024276	1.032578	1.024721	1.034183	0.0550	1.0230	1.0317
Bridge C	-21.50	17.44	0.9785	1.0174	0.414	1.029553	1.031673	1.030732	1.033150	0.0550	1.0285	1.0308
Bridge C	-21.62	17.51	0.9784	1.0175	0.414	1.029689	1.031839	1.030888	1.033339	0.0550	1.0287	1.0309

Rxn extent

A	B	C
9.765	7.75	7.998
17.629	19.154	19.337
0.554	0.405	0.414

Mean	1.027477	1.032401	1.028367	1.033980
Sd	0.002387	0.000526	0.002719	0.000600
overall	1.02993878		**1.031174**	
Sd	0.00305417		0.00348072	
SE	0.00088166		0.0010048	

YOP51* R409A-D356A, 31°C pH 6.0, non-bridge ^{18}O

exp: 11/27/98
res: 12/8/98

TC Rinf.
2.01
1.97
2.05
2.05
2.02 1.002

y fraction of 18-O in double labeled cpd	x fraction of 15-N in double labeled cpd	z fraction of 15-N in 14-N labeled cpd	b fraction of 15-N in mixture	15-N isotope effect	number of discrimin. atoms
0.87	0.99	0.0001	0.003657	1.0025	3

Sample#	P Delta	S Delta	Rp	Rs	f	IE(Rs,Ro)	IE(Rp,Ro)	corrected ---IE(Rs)	corrected ---IE(Rp)	Q1	A1	a2
non-B A	-2.49	7.80	0.9975	1.0078	0.564	1.007046	1.007093	1.001597	1.001623	0.0275	1.0015	1.0016
non-B A	-2.52	7.61	0.9975	1.0076	0.564	1.006740	1.007093	1.001515	1.001640	0.0275	1.0014	1.0016
non-B B	-3.15	6.12	0.9969	1.0061	0.482	1.006246	1.007335	1.001338	1.001726	0.0275	1.0013	1.0017
non-B B	-3.06	6.22	0.9969	1.0062	0.482	1.006399	1.007207	1.001393	1.001681	0.0275	1.0013	1.0016
non-B C	-1.59	7.97	0.9984	1.0080	0.576	1.006949	1.005722	1.001589	1.001152	0.0275	1.0015	1.0011
non-B C	-1.63	7.92	0.9984	1.0079	0.576	1.006890	1.005786	1.001568	1.001175	0.0275	1.0015	1.0011

Rxn extent

A	B	C
12.462	10.85	11.067
22.082	22.509	19.215
0.564	0.482	0.576

Mean	1.006699	1.006698	1.001500	1.001500
Sd	0.000306	0.000738	0.000109	0.000263
overall	1.006699		**1.001500**	
Sd	0.000539		0.000192	
SE	0.000156		0.000055	

Table B-15. *Yersinia*, R409A/D356N Mutant, ^{15}N and [18]O Isotope Effects, pH 6.0

YOP51*/R409A-D356N, 31°C, pH 6.0, [15]N

exp: 12/5/98
res: 12/14/98

Delta TC/Sm
0.060
-0.080
0.090
-0.050
0.120
0.028 1.0000

sample#	P Delta	RS Delta	Rp	Rs	f	IE(Rs,Ro)	IE(Rp,Ro)
A1	-1.79	1.53	0.99821	1.00153	0.452	1.002500	1.002498
A2	-1.66	1.4	0.99834	1.0014	0.452	1.002283	1.002319
B1	-1.71	1.67	0.99829	1.00167	0.468	1.002609	1.002426
B2	-1.72	1.53	0.99828	1.00153	0.468	1.002386	1.002440

	Rxn extent	
A	B	C
13.02	13.95	
28.792	29.829	
0.452	0.468	

Mean	1.002445	1.002421
SD	0.000141	0.000075
overall	1.002433	
SD	0.000105	
SE	0.000037	

YOP51* R409A-D356N, pH 6.0, 31°C, bridge [18]O

exp: 12/5/98
res: 12/14/98

TC	Rinf.		y fraction of 18-O in double labeled cpd	x fraction of 15-N in double labeled cpd	z fraction of 15-N in 14-N labeled cpd	b fraction of 15-N in mixture	15-N isotope effect	number of discrimin. atoms
1.73	1.98							
1.85								
2.33								
2.03								
1.984	1.002		0.93	0.99	0.0002	0.00365685	1.0024	1

Sample#	P Delta	RS Delta	Rp	Rs	f	IE(Rs,Ro)	IE(Rp,Ro)	corrected ---IE(Rs)	corrected ---IE(Rp)	Q1	A1	a2
Bridge A	-15.98	34.23	0.9840	1.0342	0.610	1.034800	1.030264	1.036790	1.031615	0.055042	1.034127	1.029337
Bridge A	-15.60	34.08	0.9844	1.0341	0.610	1.034635	1.029614	1.036602	1.030874	0.055042	1.033953	1.028651
Bridge B	-18.25	26.81	0.9818	1.0268	0.514	1.035103	1.030174	1.037136	1.031512	0.055042	1.034447	1.029242
Bridge B	-18.35	26.91	0.9817	1.0269	0.514	1.035247	1.030326	1.037301	1.031686	0.055042	1.034599	1.029403

	Rxn extent	
A	B	C
14.105	13.547	
23.119	26.352	
0.610	0.514	

Mean	1.034946	1.030095	1.036957	1.031422
Sd	0.000279	0.000326	0.000318	0.000372
overall	1.03252055		1.03419	
Sd	0.00260857		0.00297609	
SE	0.00075303		0.00105221	

YOP51* R409A-D356N, 31°C pH 6.0, non-bridge [18]O

exp: 12/15/98
res: 12/19/98

TC	Rinf.		y fraction of 18-O in double labeled cpd	x fraction of 15-N in double labeled cpd	z fraction of 15-N in 14-N labeled cpd	b fraction of 15-N in mixture	15-N isotope effect	number of discrimin. atoms
2.01								
2.14								
2.05								
2.05								
2.0625	1.0021		0.87	0.99	0.0001	0.003657	1.0024	3

Sample#	P Delta	S Delta	Rp	Rs	f	IE(Rs,Ro)	IE(Rp,Ro)	corrected ---IE(Rs)	corrected ---IE(Rp)	Q1	A1	a2
non-B A	-2.10	7.29	0.9979	1.0073	0.526	1.007014	1.006200	1.001634	1.001344	0.02752	1.001563	1.001286
non-B A	-2.06	7.25	0.9979	1.0073	0.526	1.006960	1.006141	1.001615	1.001323	0.02752	1.001545	1.001265
non-B B	-1.53	8.70	0.9985	1.0087	0.617	1.006925	1.006038	1.001602	1.001286	0.02752	1.001533	1.00123
non-B B	-1.41	8.58	0.9986	1.0086	0.617	1.006799	1.005835	1.001558	1.001214	0.02752	1.00149	1.001161

	Rxn extent	
A	B	C
118.29	163.14	
224.79	264.37	
0.526	0.617	

Mean	1.006924	1.006053	1.001602	1.001292
Sd	0.000091	0.000160	0.000032	0.000057
overall	1.006489		1.001447	
Sd	0.000481		0.000171	
SE	0.000139		0.000061	

Table B-16. *Yersinia*, R409K/D356A Mutant, ^{15}N and ^{18}O Isotope Effects, pH 6.0

YOP51*/R409K-D356A, 31°C, pH 6.0, ^{15}N

exp: 12/5/98
res: 12/14/98

Delta TC/Sm	
0.060	
-0.080	
0.090	
-0.050	
0.120	
0.028	1.0000

sample#	P Delta	RS Delta	Rp	Rs	f	IE(Rs,Ro)	IE(Rp,Ro)
A1	-1.76	1.32	0.99824	1.00132	0.425	1.002341	1.002391
A2	-1.76	1.32	0.99824	1.00132	0.425	1.002341	1.002391
B1	-1.47	1.14	0.99853	1.00114	0.390	1.002255	1.001940
B2	-1.52	1.21	0.99848	1.00121	0.390	1.002397	1.002005

Rxn extent		
A	B	C
11.811	10.416	
27.816	26.718	
0.425	0.390	

Mean	1.002334	1.002182
SD	0.000059	0.000243
overall	1.002258	
SD	0.000183	
SE	0.000065	

YOP51* R409K-D356A, pH 6.0, 31°C, bridge ^{18}O

exp: 12/5/98
res: 12/14/98

TC	Rinf.
1.73	1.98
1.85	
2.33	
2.03	
1.984	1.002

y fraction of 18-O in double labeled cpd	x fraction of 15-N in double labeled cpd	z fraction of 15-N in 14-N labeled cpd	b fraction of 15-N in mixture	15-N isotope effect	number of discrimin. atoms
0.93	0.99	0.0002	0.00365685	1.0023	1

Sample#	P Delta	RS Delta	Rp	Rs	f	IE(Rs,Ro)	IE(Rp,Ro)	corrected ---IE(Rs)	corrected ---IE(Rp)	Q1	A1	a2
Bridge A	-14.86	34.11	0.9851	1.0341	0.622	1.033541	1.028850	1.035558	1.030208	0.0550	1.0330	1.0280
Bridge A	-14.79		0.9852		0.622		1.028729		1.030069	0.0550	0.0000	1.0279
Bridge B	-16.49	28.96	0.9835	1.0290	0.576	1.031948	1.029690	1.033741	1.031165	0.0550	1.0313	1.0289
Bridge B	-16.40	28.77	0.9836	1.0288	0.576	1.031719	1.029543	1.033479	1.030997	0.0550	1.0311	1.0288

Rxn extent		
A	B	C
14.756	13.423	
23.729	23.302	
0.622	0.576	

Mean	1.032402	1.029203	1.034259	1.030610
Sd	0.000992	0.000484	0.001133	0.000551
overall	1.03057414		1.032174	
Sd	0.00183575		0.002094	
SE	0.00052994		0.00079146	

YOP51* R409K-D356A, 31°C pH 6.0, non-bridge ^{18}O

exp: 12/15/98
res: 12/19/98

TC	Rinf.
2.01	1.98
1.97	2.14
2.05	
2.05	
2.0333	1.002

y fraction of 18-O in double labeled cpd	x fraction of 15-N in double labeled cpd	z fraction of 15-N in 14-N labeled cpd	b fraction of 15-N in mixture	15-N isotope effect	number of discrimin. atoms
0.87	0.99	0.0001	0.003657	1.0023	3

Sample#	P Delta	S Delta	Rp	Rs	f	IE(Rs,Ro)	IE(Rp,Ro)	corrected ---IE(Rs)	corrected ---IE(Rp)	Q1	A1	a2
non-B A	-3.89	6.36	0.9961	1.0064	0.421	1.007939	1.007913	1.002026	1.002017	0.0275	1.0019	1.0019
non-B A	-3.93	6.41	0.9961	1.0064	0.421	1.008031	1.007967	1.002059	1.002036	0.0275	1.0020	1.0019
non-B B	-2.86	8.95	0.9971	1.0090	0.592	1.007735	1.007937	1.001953	1.002025	0.0275	1.0019	1.0019
non-B B	-2.87	8.81	0.9971	1.0088	0.592	1.007578	1.007953	1.001897	1.002031	0.0275	1.0018	1.0019

Rxn extent		
A	B	C
102.34	142.98	
242.9	241.56	
0.421	0.592	

Mean	1.007821	1.007943	1.001984	1.002027
Sd	0.000204	0.000023	0.000073	0.000008
overall	1.007882		1.002006	
Sd	0.000149		0.000053	
SE	0.000043		0.000019	

Table B-17. _Yersinia, R409K/D356N Mutant, ^{15}N and ^{18}O Isotope Effects, pH 6.0_

YOP51*/R409K-D356N, 31°C, pH 6.0, ^{15}N

exp: 12/15/98
res: 12/19/98

Delta TC/Sm	
0.060	0.17
0.150	0.16
0.090	0.12
-0.050	
0.100	1.0001

sample#	P Delta	RS Delta	Rp	Rs	f	IE(Rs,Ro)	IE(Rp,Ro)
A1	-1.51	1.17	0.99849	1.00117	0.360	1.002398	1.002033
A2	-1.47	1.17	0.99853	1.00117	0.360	1.002398	1.001982
B1	-1.58	1.17	0.99842	1.00117	0.371	1.002313	1.002140
B2	-1.46	1.28	0.99854	1.00128	0.371	1.002551	1.001987

Rxn extent		
A	B	C
120.7	98.126	
334.83	264.62	
0.360	0.371	

Mean	1.002415	1.002036
SD	0.000099	0.000073
overall	1.002225	
SD	0.000218	
SE	0.000077	

YOP51* R409K-D356N, pH 6.0, 31°C, bridge ^{18}O

exp: 12/15/98
res: 12/19/98

TC	Rinf.		y fraction of 18-O in double labeled cpd	x fraction of 15-N in double labeled cpd	z fraction of 15-N in 14-N labeled cpd	b fraction of 15-N in mixture	15-N isotope effect	number of discrimin. atoms
1.73	1.98							
1.85								
2.33								
2.03								
1.984	1.002		0.93	0.99	0.0002	0.00365685	1.0022	1

Sample#	P Delta	RS Delta	Rp	Rs	f	IE(Rs,Ro)	IE(Rp,Ro)	corrected ---IE(Rs)	corrected ---IE(Rp)	Q1	A1	a2
Bridge A	-19.90	18.52	0.9801	1.0185	0.424	1.030575	1.029774	1.032213	1.031299	0.0550	1.0299	1.0290
Bridge A	-20.05	18.55	0.9800	1.0186	0.424	1.030632	1.029983	1.032278	1.031537	0.0550	1.0300	1.0293
Bridge B	-19.08	20.48	0.9809	1.0205	0.467	1.029899	1.029886	1.031442	1.031426	0.0550	1.0292	1.0292
Bridge B	-19.09	20.63	0.9809	1.0206	0.467	1.030147	1.029900	1.031724	1.031443	0.0550	1.0294	1.0292

Rxn extent		
A	B	C
117.99	111.97	
278.26	239.55	
0.424	0.467	

Mean	1.030313	1.029886
Sd	0.000351	0.000086
overall	1.03009956	
Sd	0.00032893	
SE	9.4955E-05	

corrected	corrected
1.031914	1.031426
0.000400	0.000098
1.03167	
0.00037514	
0.00014179	

YOP51* R409K-D356N, 31°C pH 6.0, non-bridge ^{18}O

exp: 12/15/98
res: 12/19/98

TC	Rinf.		y fraction of 18-O in double labeled cpd	x fraction of 15-N in double labeled cpd	z fraction of 15-N in 14-N labeled cpd	b fraction of 15-N in mixture	15-N isotope effect	number of discrimin. atoms
2.01	1.98							
1.97	2.14							
2.05								
2.05								
2.0333	1.002		0.87	0.99	0.0001	0.003657	1.0022	3

Sample#	P Delta	S Delta	Rp	Rs	f	IE(Rs,Ro)	IE(Rp,Ro)	corrected ---IE(Rs)	corrected ---IE(Rp)	Q1	A1	a2
non-B A	-3.33	7.29	0.9967	1.0073	0.457	1.008638	1.007416	1.002286	1.001851	0.0275	1.0022	1.0018
non-B A	-3.41	7.19	0.9966	1.0072	0.457	1.008473	1.007527	1.002228	1.001891	0.0275	1.0021	1.0018
non-B B	-3.75	6.50	0.9963	1.0065	0.453	1.007416	1.007971	1.001851	1.002049	0.0275	1.0018	1.0020
non-B B	-3.66	6.57	0.9963	1.0066	0.453	1.007533	1.007846	1.001893	1.002004	0.0275	1.0018	1.0019

Rxn extent		
A	B	C
112.27	111.67	
245.59	246.26	
0.457	0.453	

Mean	1.008015	1.007690
Sd	0.000630	0.000261
overall	1.007853	
Sd	0.000479	
SE	0.000138	

corrected	corrected
1.002065	1.001949
0.000224	0.000093
1.002007	
0.000170	
0.000060	

Table B-18. VHR Enzyme, ^{15}N Isotope Effects, pH 6.0 and 9.0

VHR, 35C, pH 9.0, 15 N effects — exp:4/1/98 res:4/2/98

Delta TC/Sm

1.96	2.12
2.00	2.01
2.12	2.09
2.04	2.07
2.06	1.94
1.85	2.00
2.022	1.002

sample#	P Delta	RS Delta	Rp	Rs	f	IE(Rs,Ro)	IE(Rp,Ro)
A1	1.74	2.13	1.00174	1.00213	.083		1.000294
A2	1.45	2.25	1.00145	1.00225	.083		1.000596
B1	1.70	2.25	1.0017	1.00225	.327	1.000575	1.000394
B2	1.75	2.20	1.00175	1.0022	.327	1.000449	1.000333
C1	1.77	2.14	1.00177	1.00214	.232	1.000447	1.000288
C2	1.64	2.26	1.00164	1.00226	.232		1.000436

						IE(Rs,Ro)	IE(Rp,Ro)
					Mean	1.000491	1.000390
					SD	0.000074	0.000116

Extent

0.025	0.192	0.116
0.302	0.587	0.497
0.083	0.327	0.232

overall	1.00042
SD	0.000111
SE	0.00004

VHR, 35C, pH 6.0, 15 N effects — exp:4/1/98 res:4/2/98

Delta TC/Sm

1.96	2.12
2.00	2.01
2.12	2.09
2.04	2.07
2.06	1.94
1.85	2.00
2.022	1.002

sample#	P Delta	RS Delta	Rp	Rs	f	IE(Rs,Ro)	IE(Rp,Ro)
A1	1.82	2.41	1.00182	1.00241	.748	1.000281	1.000434
A2	1.87	2.58	1.00187	1.00258	.748	1.000404	1.000326

						IE(Rs,Ro)	IE(Rp,Ro)
					Mean	1.000342	1.000380
					SD	0.000087	0.000076

Extent

0.494		
0.660		
0.748		

overall	1.00036
SD	0.000070
SE	0.00002

Table B-19. STP Enzyme, [15]N Isotope Effects, pH 6.0 and 9.0

STP, 35C, pH 9.0, 15 N effects exp:4/1/98 res:4/2/98

Delta TC/Sm

1.96	2.12
2.00	2.01
2.12	2.09
2.04	2.07
2.06	1.94
1.85	2.00
2.022	1.002

sample#	P Delta	RS Delta	Rp	Rs	f	IE(Rs,Ro)	IE(Rp,Ro)
A1	1.54	2.62	1.00154	1.00262	.486	1.000899	1.000683
A2	1.45	2.56	1.00145	1.00256	.486	1.000809	1.000811
B1	1.62	2.56	1.00162	1.00256	.471	1.000845	1.000560
B2	1.46	2.65	1.00146	1.00265	.471	1.000987	1.000784
C1	1.64	2.65	1.00164	1.00265	.593	1.000698	1.000617
C2	1.64	2.83	1.00164	1.00283	.593	1.000898	1.000617

	IE(Rs,Ro)	IE(Rp,Ro)
Mean	1.000856	1.000679
SD	0.000098	0.000100

Extent

0.158	0.168	0.214
0.326	0.357	0.361
0.486	0.471	0.593

overall	1.00077
SD	0.000132
SE	0.00004

STP, 35C, pH 6.0, 15 N effects exp:4/1/98 res:4/2/98

Delta TC/Sm

1.96	2.12
2.00	2.01
2.12	2.09
2.04	2.07
2.06	1.94
1.85	2.00
2.022	1.002

sample#	P Delta	RS Delta	Rp	Rs	f	IE(Rs,Ro)	IE(Rp,Ro)
A1	1.82	2.41	1.00182	1.00241	.486	1.000583	1.000286
A2	1.87	2.58	1.00187	1.00258	.486	1.000839	1.000215

	IE(Rs,Ro)	IE(Rp,Ro)
Mean	1.000711	1.000250
SD	0.000181	0.000050

Extent

0.158
0.326
0.486

overall	1.00048
SD	0.000287
SE	0.00008

Table B-20. PP2C Enzyme, ^{15}N Isotope Effects, Under Varying Conditions

PP2C, pH 7.5, 35C, Mn
15N isotope effects

Delta TC/Sm	
1.020	
0.870	
0.850	
1.230	
1.130	
0.910	
0.870	
0.983	1.001

sample#	P Delta	RS Delta	Rp	Rs	f	IE(Rs,Ro)	IE(Rp,Ro)
A1	1.20	0.95	1.00120	1.00095	.320		0.999735
A2	1.54	1.24	1.00154	1.00124	.320	1.000666	0.999321
B1	1.54	1.41	1.00154	1.00141	.361	1.000954	0.999298
B2	2.06	1.52	1.00206	1.00152	.361	1.001199	
C1	1.42	1.47	1.00142	1.00147	.388	1.000992	0.999436
C2	1.47	1.36	1.00147	1.00136	.388	1.000768	0.999372
					Mean	1.000916	0.999433
					SD	0.000207	0.000177
					overall	**1.000174**	
					SD	0.000803	
					SE	**0.000254**	

PP2C, Acetate buffer, pH 6.0, T=35 C
Rxn mixture includes DTT, MnCl$_2$

exper: 1/29/99
results: 2/17/99

Delta TC/Sm	
-0.200	
-0.290	
-0.210	
-0.320	
-0.255	0.9997

sample#	P Delta	RS Delta	Rp	Rs	f	IE(Rs,Ro)	IE(Rp,Ro)
A1	-0.160	0.520	0.99984	1.00052	0.541	1.000996	0.999856
A2	-0.270	0.400	0.99973	1.0004	0.541	1.000842	1.000023
B1	-0.090	0.480	0.99991	1.00048	0.5669	1.000879	0.999742
B2	0.010	0.430	1.00001	1.00043	0.5669	1.000819	0.999585
C1	-0.230	0.570	0.99977	1.00057	0.6123	1.000871	0.999958
C2	-0.210	0.490	0.99979	1.00049	0.6123	1.000787	0.999925

Rxn Extent		
A	B	C
0.507	0.534	0.558
0.399	0.401	0.388
0.541	0.5669	0.6123

Mean	1.000866	0.999848
SD	0.000072	0.000161
overall	**1.000357**	
SD	0.000544	
SE	**0.000157**	

Table B-21. Lambda Enzyme, All Isotope Effects, pH 7.8

Lamda WT, 30C, pH 7.8, 15 N effects

Delta	TC/Sm
1.98	2.03
2.15	2.23
2.12	2.02
2.12	2.17
2.01	2.12
2.04	2.01
2.04	2.07
2.07929	1.00208

sample#	P Delta	RS Delta	Rp	Rs	f	IE(Rs,Ro)	IE(Rp,Ro)
A1	2.45	2.97	1.00245	1.00297	0.420	1.001634	0.999508
A2	2.46	3.03	1.00246	1.00303	0.420	1.001744	0.999495
B1	1.97	3.05	1.00197	1.00305	0.550	1.001214	1.000167
B2	1.82	2.92	1.00182	1.00292	0.550	1.001051	
C1	2.17	3.04	1.00217	1.00304	0.557	1.001178	0.999860
C2	2.17	2.92	1.00217	1.00292	0.557	1.001031	0.999860

		IE(Rs,Ro)	IE(Rp,Ro)
Mean		1.001309	0.999778
SD		0.000305	0.000282
overall		1.00061	
SD		0.000847	
SE		0.00026	

Lambda WT, pH 7.8, bridge
substrate 1/28/98

TC	Rinf.
2.23	2.21
2.35	1.93
2.51	
2.42	
2.275	1.00228

y fraction of 18-O in double labeled cpd	x fraction of 15-N in double labeled cpd	z fraction of 15-N in 14-N labeled cpd	b fraction of 15-N in mixture	15-N isotope effect	number of discrimin. atoms
0.93	0.99	0.0002	0.003672	1.0006	1

Sample#	P Delta	RS Delta	Rp	Rs	f	IE(Rs,Ro)	IE(Rp,Ro)	corrected ---IE(Rs)	corrected ---IE(Rp)	Q1	A1	a2
Bridge A	-7.52	9.44	0.9925	1.0094	0.477	1.011112	1.013880	1.011917	1.015066	0.054814	1.011074	1.013996
Bridge A	-7.62	9.26	0.9924	1.0093	0.477	1.010831	1.014023	1.011598	1.015228	0.054814	1.010777	1.014147
Bridge B	-5.68	13.21	0.9943	1.0132	0.642	1.010676	1.013950	1.011422	1.015145	0.054814	1.010614	1.01407
Bridge B	-5.84	13.07	0.9942	1.0131	0.642	1.010539	1.014233	1.011266	1.015467	0.054814	1.010469	1.014368
Bridge C	-3.03	20.57	0.9970	1.0206	0.785	1.011908	1.012610	1.012823		0.054814	1.011914	1.012655
Bridge C	-2.97	20.60	0.9970	1.0206	0.785	1.011928	1.012467	1.012845		0.054814	1.011935	1.012504

		IE(Rs,Ro)	IE(Rp,Ro)	corrected ---IE(Rs)	corrected ---IE(Rp)
Mean		1.011166	1.013527	1.011979	1.015226
Sd		0.000613	0.000777	0.000697	0.000173
overall		1.012346		1.013278	
Sd		0.001402		0.001759	
SE		0.000405		0.000556	

Rxn extent		
A	B	C
#DIV/0!	#DIV/0!	#DIV/0!

Lambda WT, 30C, pH 7.8, non-bridge 18O
substrate 1/98

exp:1/31/98
res: 2/6/98

TC	Rinf.
-10.11	-10.18
-10.09	-10.1
-10.06	
-10.11	
-10.108	0.98989

y fraction of 18-O in double labeled cpd	x fraction of 15-N in double labeled cpd	z fraction of 15-N in 14-N labeled cpd	b fraction of 15-N in mixture	15-N isotope effect	number of discrimin. atoms
0.87	0.99	0.0001	0.003626	1.0006	3

Sample#	P Delta	S Delta	Rp	Rs	f	IE(Rs,Ro)	IE(Rp,Ro)	corrected ---IE(Rs)	corrected ---IE(Rp)	Q1	A1	a2
non-B A	-9.04	-10.94	0.9910	0.9891	0.438	0.998544	0.998542	0.999259	0.999258	0.027756	0.999291	0.99929
non-B A	-9.03	-10.98	0.9910	0.9890	0.438	0.998474	0.998528	0.999234	0.999253	0.027756	0.999267	0.999286
non-B B	-9.04	-11.45	0.9910	0.9886	0.690	0.998843	0.997951	0.999366	0.999046	0.027756	0.999394	0.999088
non-B B	-9.03	-11.45	0.9910	0.9886	0.690	0.998843	0.997931	0.999366	0.999040	0.027756	0.999394	0.999081
non-B C	-8.96	-11.92	0.9910	0.9881	0.652	0.998268	0.997943	0.999160	0.999044	0.027756	0.999196	0.999085
non-B C	-9.01	-12.02	0.9910	0.9880	0.652	0.998172	0.998032	0.999126	0.999076	0.027756	0.999164	0.999116

		IE(Rs,Ro)	IE(Rp,Ro)	corrected ---IE(Rs)	corrected ---IE(Rp)
Mean		0.998524	0.998155	0.999252	0.999120
Sd		0.000282	0.000297	0.000101	0.000106
overall		0.998339		0.999186	
Sd		0.000337		0.000121	
SE		0.000097		0.000035	

Table B-22. Lambda Enzyme, All Isotope Effects, pH 6.0

Lamda WT, 30C, pH 6.0, 15 N effects

Delta	TC/Sm
1.98	2.03
2.15	2.23
2.12	2.02
2.12	2.17
2.01	2.12
2.04	2.01
2.08333	1.00208

sample#	P Delta	RS Delta	Rp	Rs	f	IE(Rs,Ro)	IE(Rp,Ro)
A1	2.61	2.99	1.00261	1.00299	0.335		0.999351
A2	2.21	2.74	1.00221	1.00274	0.335	1.001608	0.999844
B1	1.84	2.83	1.00184	1.00283	0.407	1.001427	1.000319
B2	1.78	2.75	1.00178	1.00275	0.407	1.001274	1.000398
C1	2.29	2.84	1.00229	1.00284	0.496	1.001103	0.999704
C2	2.14	2.86	1.00214	1.00286	0.496	1.001132	0.999919
					Mean	1.001309	0.999922
					SD	0.000211	0.000391
					overall	1.00055	
					SD	0.000786	
					SE	0.00024	

Lambda WT, pH 6.0, bridge
substrate 1/28/98

TC	Rinf.
2.23	2.21
2.35	1.93
2.51	
2.42	
2.275	1.00228

y fraction of 18-O in double labeled cpd	x fraction of 15-N in double labeled cpd	z fraction of 15-N in 14-N labeled cpd	b fraction of 15-N in mixture	15-N isotope effect	number of discrimin. atoms
0.93	0.99	0.0002	0.003672	1.0006	1

Sample#	P Delta	RS Delta	Rp	Rs	f	IE(Rs,Ro)	IE(Rp,Ro)	corrected ---IE(Rs)	corrected ---IE(Rp)	Q1	A1	a2
Bridge A	-7.93	9.60	0.9921	1.0096	0.488	1.010997	1.014638	1.011856		0.054814	1.011017	1.014861
Bridge A	-7.93	9.70	0.9921	1.0097	0.488	1.011148	1.014638	1.012028		0.054814	1.011177	1.014861
Bridge B	-5.25	14.89	0.9948	1.0149	0.653	1.011959	1.013433	1.012949	1.014627	0.054814	1.012032	1.013589
Bridge B	-5.15	15.00	0.9949	1.0150	0.653	1.012064	1.013254	1.013069	1.014422	0.054814	1.012143	1.013399
Bridge C	-5.70	12.98	0.9943	1.0130	0.611	1.011380	1.013330	1.012292	1.014509	0.054814	1.011422	1.013480
Bridge C	-5.69	12.92	0.9943	1.0129	0.611	1.011316	1.013313	1.012219	1.014490	0.054814	1.011354	1.013462
					Mean	1.011477	1.013768	1.012402	1.014512			
					Sd	0.000436	0.000677	0.000495	0.000085			
					overall	1.012623		1.013246				
					Sd	0.001313		0.001151				
					SE	0.000379		0.000364				

Lambda WT, 30C pH 6.0, non-bridge 18O
substrate 1/98   exp:1/31/98   res: 2/6/98

TC	Rinf.
-10.11	-10.18
-10.09	-10.10
-10.06	
-10.11	
-10.108	0.98989

y fraction of 18-O in double labeled cpd	x fraction of 15-N in double labeled cpd	z fraction of 15-N in 14-N labeled cpd	b fraction of 15-N in mixture	15-N isotope effect	number of discrimin. atoms
0.87	0.99	0.0001	0.003626	1.0006	3

Sample#	P Delta	S Delta	Rp	Rs	f	IE(Rs,Ro)	IE(Rp,Ro)	corrected ---IE(Rs)	corrected ---IE(Rp)	Q1	A1	a2
non-B A	-10.45	-10.22	0.9896	0.9898	0.385	0.999768	1.000445	0.999719	0.999961	0.027756	0.999731	0.999963
non-B A	-10.38	-10.24	0.9896	0.9898	0.385	0.999726	1.000354		0.999929	0.027756	0.999717	0.999932
non-B B	-10.24	-9.99	0.9898	0.9900	0.418	1.000221	1.000177	0.999881	0.999865	0.027756	0.999886	0.999871
non-B B	-10.16	-10.03	0.9898	0.9900	0.418	1.000146	1.000069	0.999855	0.999827	0.027756	0.999861	0.999834
non-B C	-10.20	-9.99	0.9898	0.9900	0.512	1.000167	1.000135	0.999862	0.999851	0.027756	0.999868	0.999857
non-B C	-10.26	-9.89	0.9897	0.9901	0.512	1.000307	1.000224		0.999882	0.027756	0.999916	0.999887
					Mean	1.000056	1.000234	0.999829	0.999886			
					Sd	0.000246	0.000141	0.000074	0.000050			
					overall	1.000145		0.999863				
					Sd	0.000212		0.000064				
					SE	0.000061		0.000020				

Table B-23. Lambda Enzyme, All Isotope Effects, pH 9.0

Lamda WT, pH 9.0, ^{15}N effects

exp:2/26/98
res:3/16/98

Delta	TC/Sm
1.98	2.03
1.86	2.01
2.08	2.11
2.12	2.02
2.12	1.85
2.01	2.12
2.06	2.09
2.03286	1.00203

sample#	P Delta	RS Delta	Rp	Rs	f	IE(Rs,Ro)	IE(Rp,Ro)
A1	1.69	2.53	1.00169	1.00253	0.353		1.000429
A2	1.63	2.44	1.00163	1.00244	0.353	1.000933	1.000504
B1	1.68	2.59	1.00168	1.00259	0.448	1.000937	1.000481
B2	1.89	2.57	1.00189	1.00257	0.448	1.000904	
C1	1.67	2.65	1.00167	1.00265	0.591	1.000689	1.000586
C2	1.57	2.50	1.00157	1.00250	0.591	1.000521	1.000747

	Rxn extent				
A	B	C	Mean	1.000797	1.000549
0.1385	0.1795	0.2105	SD	0.000185	0.000124
0.392	0.401	0.356	overall	1.00067	
0.353	0.448	0.591	SD	0.000198	
			SE	0.00006	

Lambda WT, pH 9.0, bridge

substrate 1/28/98

exp:2/26/98
res:3/16/98

TC	Rinf.
2.23	2.21
2.35	1.93
2.51	1.77
2.42	1.75
1.49	1.87
1.47	1.78
1.85	1.79
1.95857	1.00196

y fraction of 18-O in double labeled cpd	x fraction of 15-N in double labeled cpd	z fraction of 15-N in 14-N labeled cpd	b fraction of 15-N in mixture	15-N isotope effect	number of discrimin. atoms
0.93	0.99	0.0002	0.003672	1.0007	1

Sample#	P Delta	RS Delta	Rp	Rs	f	IE(Rs,Ro)	IE(Rp,Ro)	corrected ---IE(Rs)	corrected ---IE(Rp)	Q1	A1	a2
Bridge A	-7.82	8.85	0.9922	1.0089	0.362	1.015488	1.012440	1.016825	1.013359	0.054814	1.015629	1.012412
Bridge A	-7.74	8.87	0.9923	1.0089	0.362	1.015533	1.012338	1.016877	1.013242	0.054814	1.015677	1.012304
Bridge B	-6.39	12.18	0.9936	1.0122	0.569	1.012207	1.013170	1.013093	1.014188	0.054814	1.012165	1.013182
Bridge B	-6.50	11.88	0.9935	1.0119	0.569	1.011846	1.013344	1.012683	1.014387	0.054814	1.011785	1.013366

					Mean	1.013768	1.012823	1.014870	1.013794
					Sd	0.002017	0.000508	0.002294	0.000578
					overall	1.013296		1.014332	
					Sd	0.001453		0.001652	
					SE	0.000514		0.000584	

Lambda WT, pH 9.0, non-bridge ^{18}O

substrate 1/98

exp:2/26/98
res:3/16/98

TC	Rinf.	TC values from 3/16/98 data only, previous average was -10.5
-8.37		
-8.20		
-8.61		
-8.41		
#####	0.99160	

y fraction of 18-O in double labeled cpd	x fraction of 15-N in double labeled cpd	z fraction of 15-N in 14-N labeled cpd	b fraction of 15-N in mixture	15-N isotope effect	number of discrimin. atoms
0.87	0.99	0.0001	0.003626	1.0007	3

Sample#	P Delta	S Delta	Rp	Rs	f	IE(Rs,Ro)	IE(Rp,Ro)	corrected ---IE(Rs)	corrected ---IE(Rp)	Q1	A1	a2
non-B A	-7.7	-9.9	0.9923	0.9901	0.579	0.998250	0.998883	0.999132	0.999359	0.027756	0.999170	0.999387
non-B A	-7.7	-9.94	0.9923	0.9901	0.579	0.998203	0.998883	0.999115	0.999359	0.027756	0.999154	0.999387
non-B B	-7.69	-10.35	0.9923	0.9897	0.610	0.997909	0.998816	0.999010	0.999335	0.027756	0.999053	0.999364
non-B B	-7.79	-10.42	0.9922	0.9896	0.610	0.997834	0.998984	0.998983	0.999395	0.027756	0.999027	0.999421
non-B C	-7.86	-10.76	0.9921	0.9892	0.669	0.997846	0.999010	0.998987	0.999405	0.027756	0.999031	0.999430
non-B C	-7.82	-10.67	0.9922	0.9893	0.669	0.997928	0.998936	0.999017	0.999378	0.027756	0.999059	0.999405

	Rxn extent				Mean	0.997995	0.998919	0.999041	0.999372
A	B	C			Sd	0.000184	0.000072	0.000066	0.000026
0.1835	0.2045	0.217							
0.317	0.3355	0.3245			overall	0.998457		0.999206	
0.579	0.610	0.669			Sd	0.000501		0.000179	
					SE	0.000144		0.000052	

Table B-24. Lambda Enzyme, ^{15}N and $^{18}O_{bridge}$, pH 7.8, Ca^{2+} Replaces Mn^{2+}

Lamda WT, pH 7.8, Ca replaces Mn, 15 N effects

exp:2/26/98
res:3/16/98

Delta	TC/Sm
1.86	2.01
2.08	2.11
2.12	2.02
2.12	1.85
2.01	2.12
2.04	2.07
2.03417	1.00203

sample#	P Delta	RS Delta	Rp	Rs	f	IE(Rs,Ro)	IE(Rp,Ro)
A1	1.51	2.33	1.00151	1.00233	0.284	1.000886	1.000621
A2	1.57	2.27	1.00157	1.00227	0.284	1.000706	1.000550
B1	1.61	2.57	1.00161	1.00257	0.406	1.001026	1.000556
B2	1.68	2.70	1.00168	1.00270	0.406		1.000464
C1	1.81	2.61	1.00181	1.00261	0.427	1.001033	1.000299
C2	1.80	2.58	1.00180	1.00258	0.427	1.000979	1.000313

	Rxn extent					
A	B	C		Mean	1.000926	1.000467
0.059	0.0825	0.0875		SD	0.000136	0.000135
0.208	0.203	0.205		overall	1.00068	
0.284	0.406	0.427		SD	0.000272	
				SE	0.00008	

Lambda WT, Ca metal, pH 7.8, bridge
substrate 1/28/98

TC	Rinf.
2.23	2.21
2.35	1.93
2.51	
2.42	
2.275	1.00228

	y fraction of 18-O in double labeled cpd	x fraction of 15-N in double labeled cpd	z fraction of 15-N in 14-N labeled cpd	b fraction of 15-N in mixture	15-N isotope effect	number of discrimin. atoms
	0.93	0.99	0.0002	0.003672	1.0007	1

Sample#	P Delta	RS Delta	Rp	Rs	f	IE(Rs,Ro)	IE(Rp,Ro)	corrected ---IE(Rs)	corrected ---IE(Rp)	Q1	A1	a2
Bridge A	-7.20	5.15	0.9928	1.0052	0.265	1.009391	1.011175	1.009889	1.011917	0.0548	1.0092	1.0111
Bridge A	-7.13	5.18	0.9929	1.0052	0.265	1.009490	1.011092	1.010002	1.011822	0.0548	1.0093	1.0110
Bridge B	-6.55	5.14	0.9935	1.0051	0.281	1.008728	1.010523	1.009137	1.011176	0.0548	1.0085	1.0104
Bridge B	-6.77	4.85	0.9932	1.0049	0.281	1.007839	1.010787	1.008127	1.011477	0.0548	1.0076	1.0107

			Mean	1.008862	1.010894	1.009289	1.011598
			Sd	0.000761	0.000298	0.000865	0.000339
			overall	1.009878		1.010443	
			Sd	0.001211		0.001376	
			SE	0.000428		0.000486	

Lambda WT, Ca metal, pH 7.8, bridge
substrate 1/28/98

exp:2/26/98
res:3/16/98

TC	Rinf.
1.75	1.47
1.87	1.85
1.78	
	1.79
1.77	1.49
1.72000	1.00172

	y fraction of 18-O in double labeled cpd	x fraction of 15-N in double labeled cpd	z fraction of 15-N in 14-N labeled cpd	b fraction of 15-N in mixture	15-N isotope effect	number of discrimin. atoms
	0.93	0.99	0.0002	0.003672	1.0007	1

Sample#	P Delta	RS Delta	Rp	Rs	f	IE(Rs,Ro)	IE(Rp,Ro)	corrected ---IE(Rs)	corrected ---IE(Rp)	Q1	A1	a2
Bridge A	-7.51	7.88	0.9925	1.0079	0.440	1.010695	1.012595	1.011371	1.013531	0.0548	1.0106	1.0126
Bridge A	-7.91	7.98	0.9921	1.0080	0.440	1.010870	1.013146	1.011570	1.014157	0.0548	1.0108	1.0132
Bridge B	-8.40	7.76	0.9916	1.0078	0.404	1.011765	1.013360	1.012588	1.014401	0.0548	1.0117	1.0134
Bridge B	-8.14	7.88	0.9919	1.0079	0.404	1.012001	1.013013	1.012856	1.014007	0.0548	1.0119	1.0130
Bridge C	-7.92	8.28	0.9921	1.0083	0.435	1.011558	1.013101	1.012353	1.014107	0.0548	1.0115	1.0131
Bridge C	-7.29	8.30	0.9927	1.0083	0.435	1.011594	1.012238	1.012393	1.013125	0.0548	1.0115	1.0122

	Rxn extent			Mean	1.011414	1.012909	1.012189	1.013888
A	B	C		Sd	0.000517	0.000414	0.000587	0.000471
0.0675	0.066	0.0705		overall	1.012161		1.013038	
0.1535	0.1635	0.162		Sd	0.000899		0.001022	
0.440	0.404	0.435		SE	0.000318		0.000295	

Table B-25. Lambda Enzyme, $^{18}O_{nonbridge}$, pH 7.8, Ca^{2+} Replaces Mn^{2+}

Lambda WT, Ca metal, pH 7.8, non-bridge ^{18}O
substrate 1/98

exp:2/26/98

res:3/16/98

TC	Rinf.	TC values from 3/16/98 data only, previous average was -10.5	y fraction of 18-O in double labeled cpd	x fraction of 15-N in double labeled cpd	z fraction of 15-N in 14-N labeled cpd	b fraction of 15-N in mixture	15-N isotope effect	number of discrimin. atoms
-8.37								
-8.20								
-8.61								
-8.41								
#####	0.99160		0.87	0.99	0.0001	0.003626	1.0007	3

Sample#	P Delta	S Delta	Rp	Rs	f	IE(Rs,Ro)	IE(Rp,Ro)	corrected ---IE(Rs)	corrected ---IE(Rp)	Q1	A1	a2
non-B A	-6.24	-11.16	0.9938	0.9888	0.501	0.995999	0.996865	0.998324	0.998635	0.0278	0.9984	0.9987
non-B A	-6.33	-11.15	0.9937	0.9889	0.501	0.996014	0.996996	0.998329	0.998682	0.0278	0.9984	0.9987
non-B B	-6.33	-11.38	0.9937	0.9886	0.515	0.995850	0.996948	0.998270	0.998664	0.0278	0.9983	0.9987
non-B B	-6.33	-11.31	0.9937	0.9887	0.515	0.995947	0.996948	0.998305	0.998664	0.0278	0.9984	0.9987
non-B C	-3.89	-9.92	0.9961	0.9901	0.341	0.996329	0.994385	0.998442	0.997744	0.0278	0.9985	0.9978
non-B C	-3.89	-9.83	0.9961	0.9902	0.341	0.996545	0.994385	0.998520	0.997744	0.0278	0.9986	0.9978
Non-Br D	-5.81	-10.36	0.9942	0.9896	0.275	0.993873	0.996930	0.997561	0.998658	0.0278	0.9977	0.9987
Non-Br D	-6.04	-10.41	0.9940	0.9896	0.275	0.993718	0.997203	0.997505	0.998756	0.0278	0.9976	0.9988

					Mean	0.996114	0.996088	0.998365	0.998356
					Sd	0.000266	0.001320	0.000095	0.000474

Rxn extent			
A	B	C	D
0.25	0.176	0.052	0.1625
0.4993	0.342	0.1525	0.59125
0.501	0.515	0.341	0.275

overall	0.996101	0.998360
Sd	0.000908	0.000326
SE	0.000262	0.000081

Table B-26. Lambda H76N Mutant, ^{15}N and ^{18}O Isotope Effects, pH 7.8

Lamda H76N, 30C, pH 7.8, 15 N effects

Delta	TC/Sm
1.98	2.03
2.15	2.23
2.12	2.02
2.12	2.17
2.01	2.12
2.04	2.01
2.08333	1.00208

sample#	P Delta	RS Delta	Rp	Rs	f	IE(Rs,Ro)	IE(Rp,Ro)
A1	1.91	3.56	1.00191	1.00356	0.496	1.002154	
A2	1.91	3.55	1.00191	1.00355	0.496	1.002139	
B1	1.36	3.78	1.00136	1.00378	0.489	1.002526	1.001030
B2	1.29	3.57	1.00129	1.00357	0.489	1.002213	1.001129
C1	1.65	3.44	1.00165	1.00344	0.615		1.000724
C2	1.57	3.40	1.00157	1.00340	0.615		1.000858

Mean	1.002258	1.000935
SD	0.000182	0.000180
overall	**1.00160**	
SD	0.000727	
SE	**0.00026**	

Lambda H76N, pH 7.8, bridge
substrate 1/28/98

TC	Rinf.
2.23	2.21
2.35	1.93
2.51	
2.42	
2.275	1.00228

y fraction of 18-O in double labeled cpd	x fraction of 15-N in double labeled cpd	z fraction of 15-N in 14-N labeled cpd	b fraction of 15-N in mixture	15-N isotope effect	number of discrimin. atoms
0.93	0.99	0.0002	0.003672	1.0016	1

Sample#	P Delta	RS Delta	Rp	Rs	f	IE(Rs,Ro)	IE(Rp,Ro)	corrected ---IE(Rs)	corrected ---IE(Rp)	Q1	A1	a2
Bridge A	-11.04	12.54	0.9890	1.0125	0.498	1.015008	1.019366	1.015214	1.020171	0.054814	1.014134	1.018732
Bridge A	-11.10	12.69	0.9889	1.0127	0.498	1.015229	1.019455	1.015466	1.020271	0.054814	1.014368	1.018825
Bridge B	-8.13	18.41	0.9919	1.0184	0.667	1.014737	1.019073	1.014907	1.019837	0.054814	1.013849	1.018423
Bridge B	-8.07	18.41	0.9919	1.0184	0.667	1.014737	1.018962	1.014907	1.019711	0.054814	1.013849	1.018306
Bridge C	-6.66	18.82	0.9933	1.0188	0.771	1.011232	1.020473		1.021430	0.054814	1.010153	1.019900
Bridge C	-6.50	18.85	0.9935	1.0189	0.771	1.011253	1.020104		1.021011	0.054814	1.010174	1.019511

Mean	1.013699	1.019572	1.015123	1.020405
Sd	0.001912	0.000595	0.000270	0.000677
overall	**1.016636**		**1.018292**	
Sd	0.003351		0.002778	
SE	0.000967		0.000879	

Lambda H76N, 30°C, pH 7.8, non-bridge 18O
exp:1/31/98
res:2/6/98

TC	Rinf.
-10.11	-10.18
-10.09	-10.10
-10.06	
-10.11	
-10.108	0.98989

y fraction of 18-O in double labeled cpd	x fraction of 15-N in double labeled cpd	z fraction of 15-N in 14-N labeled cpd	b fraction of 15-N in mixture	15-N isotope effect	number of discrimin. atoms
0.87	0.99	0.0001	0.003626	1.0016	3

Sample#	P Delta	S Delta	Rp	Rs	f	IE(Rs,Ro)	IE(Rp,Ro)	corrected ---IE(Rs)	corrected ---IE(Rp)	Q1	A1	a2
non-B A	-8.38	-10.62	0.9916	0.9894	0.498	0.999250	0.997491	0.999161	0.998530	0.027756	0.999197	0.998594
non-B A		-10.57	1.0000	0.9894	0.498	0.999324	0.985441	0.999187		0.027756	0.999222	0.994446
non-B B	-8.47	-11.02	0.9915	0.9890	0.667	0.999163	0.996989	0.999129	0.998350	0.027756	0.999167	0.998422
non-B B	-8.5	-11.07	0.9915	0.9889	0.667	0.999117	0.997044	0.999113	0.998370	0.027756	0.999151	0.998441
non-B C	-8.56	-10.85	0.9914	0.9892	0.771	0.999492	0.996431	0.999247	0.998150	0.027756	0.999280	0.998230
non-B C	-8.71	-10.94	0.9913	0.9891	0.771	0.999430	0.996776	0.999225	0.998274	0.027756	0.999258	0.998349

Mean	0.999296	0.995029	0.999177	0.998335
Sd	0.000148	0.004710	0.000053	0.000139
overall	0.997162		0.998794	
Sd	0.003881		0.000450	
SE	0.001120		0.000136	

Table B-27. pNPS, Base Hydrolysis, All Isotope Effects, 85 °C, pH 9.0

p-nitrophenyl sulfate - base hydrolysis
^{15}N KIE, 100mM CHES buffer pH9.0, 85°C

Delta TC/Sm	
-3.87	
-3.6	-3.63
-3.6	
-3.57	
-3.654	0.99635

For data set 1, the RXN extents were very small. For small RXN extent, the product numbers are more reliable than the residual substrate. RS numbers were very low. The second run showed numbers consistent with first run product-only results. Some samples were lost during MS analysis with second run. Reported value is average of results of both runs.

sample	P Delta	RS Delta	Rp	Rs	f	IE(Rs,Ro)	IE(Rp,Ro)
A1	-6.17	-3.79	0.9938	0.9962	0.092		1.002658
A2	-6.28	-3.61	0.9937	0.9964	0.092		1.002775
B1	-6.28	-3.6	0.9937	0.9964	0.127		1.002831
B2	-6.25	-3.51	0.9938	0.9965	0.127		1.002798
C1	-6.3	-3.5	0.9937	0.9965	0.146		1.002885
C2	-6.2	-3.42	0.9938	0.9966	0.146		1.002776
2A1		-2.17		0.9978	0.440	1.002574	
2A2		-2.16		0.9978	0.440	1.002591	
2B1	-5.64	-2.28	0.9944	0.9977	0.474	1.002147	1.002803
2B2		-2.28		0.9977	0.474	1.002147	
2C1		-1.57		0.9984	0.555	1.002589	
2C2	-5.44	-1.49	0.9946	0.9985	0.555	1.002689	1.002765

Reaction extent	A	B	C
stop	0.034	0.036	0.043
final	0.369	0.283	0.294
%	0.092	0.127	0.146

	IE(Rs,Ro)	IE(Rp,Ro)
Mean	1.002456	1.002786
SD	0.000243	0.000065
overall	1.002645	
SD	0.000232	
SE	0.000062	

p-nitrophenyl sulfate - base hydrolysis
^{18}O bridge KIE, 100mM CHES buffer pH9.0, 85°C

TC	Rinf.
1.9	2.13
2.13	2.34
2.08	2.29
2.01	2.28
2.145	1.00215

y fraction of 18-O in double labeled cpd	x fraction of 15-N in double labeled cpd	z fraction of 15-N in 14-N labeled cpd	b fraction of 15-N in mixture	15-N isotope effect	number of discrimin. atoms
0.87	0.99	0.0001	0.003658	1.0026	1

Sample#	P Delta	RS Delta	Rp	Rs	f	IE(Rs,Ro)	IE(Rp,Ro)	corrected ---IE(Rs)	corrected ---IE(Rp)	Q1	A1	a2
Bridge A	-5.57	14.880	0.9944	1.0149	0.550	1.016068	1.011868	1.015850		0.02751	1.01376	1.00945
Bridge A	-5.66	14.940	0.9943	1.0149	0.550	1.016145	1.012007	1.015941		0.02751	1.01384	1.00960
Bridge B	-13.28	15.310	0.9867	1.0153	0.462	1.021641	1.021641	1.022296	1.022453	0.02751	1.01934	1.01948
Bridge B	-13.27	15.090	0.9867	1.0151	0.462	1.021144	1.021626	1.021863	1.022436	0.02751	1.01897	1.01946
Bridge C	-11.58	20.060	0.9884	1.0201	0.621	1.018593	1.023416	1.018840	1.024559	0.02751	1.01635	1.02130
Bridge C	-11.45	20.210	0.9886	1.0202	0.621	1.018750	1.023191	1.019027	1.024292	0.02751	1.01651	1.02107

	IE(Rs,Ro)	IE(Rp,Ro)	---IE(Rs)	---IE(Rp)
Mean	1.018701	1.018958	1.018970	1.023435
Sd	0.002338	0.005490	0.002770	0.001149
overall	1.018830		1.020756	
Sd	0.004025		0.003165	
SE	0.001162		0.001001	

Rxn extent	A	B	C
	0.1215	0.1215	0.305
	0.221	0.263	0.491
	0.54977	0.46198	0.62118

p-nitrophenyl sulfate - base hydrolysis
^{18}O non-bridge KIE, 100mM CHES buffer pH9.0, 65°C

TC	Rinf.
-4.02	-4.13
-3.96	
-4.27	
-4.3	
-4.136	0.99586

y fraction of 18-O in double labeled cpd	x fraction of 15-N in double labeled cpd	z fraction of 15-N in 14-N labeled cpd	b fraction of 15-N in mixture	15-N isotope effect	number of discrimin. atoms
0.646	0.99	0.0001	0.003626	1.0026	3

Sample#	P Delta	RS Delta	Rp	Rs	f	IE(Rs,Ro)	IE(Rp,Ro)	corrected ---IE(Rs)	corrected ---IE(Rp)	Q1	A1	a2
Bridge A	-2.23	-8.050	0.9978	0.9920	0.449	0.99343	0.99739	0.99642	0.99796	0.02776	0.99684	0.99820
Bridge A	-2.15	-7.960	0.9979	0.9920	0.449	0.99358	0.99728	0.99648	0.99792	0.02776	0.99689	0.99816
Bridge B	-3.6	-4.150	0.9964	0.9959	0.526	0.99998	0.99920	0.99897	0.99866	0.02776	0.99909	0.99882
Bridge B	-3.62	-4.020	0.9964	0.9960	0.526	1.00016	0.99923	0.99904	0.99868	0.02776	0.99915	0.99883
Bridge C	-4.08	-3.850	0.9959	0.9962	0.522	1.00039	0.99992	0.99913	0.99894	0.02776	0.99923	0.99907
Bridge C	-4.18	-3.950	0.9958	0.9961	0.522	1.00025	1.00007	0.99907	0.99900	0.02776	0.99918	0.99912

	IE(Rs,Ro)	IE(Rp,Ro)	---IE(Rs)	---IE(Rp)
Mean	0.997966	0.998847	0.998184	0.998527
Sd	0.003456	0.001224	0.001343	0.000475
overall	0.998406		0.998356	
Sd	0.002514		0.000977	
SE	0.000726		0.000282	

Rxn extent	A	B	C
	0.459	0.439	0.533
	0.206	0.231	0.278
	0.449	0.526	0.522

Table B-28. pNPS, Acid Hydrolysis, All Isotope Effects, 65 °C, 1.0 N HCl

p-nitrophenyl sulfate - acid hydrolysis
^{15}N KIE, 1N HCl, 65°C

Delta TC/Sm		
-3.87		-3.84
-3.6	-3.63	-3.9
-3.6		-4.11
-3.57		-3.95
-3.654	0.99635	

sample	P Delta	RS Delta	Rp	Rs	f	IE(Rs,Ro)	IE(Rp,Ro)
A1	-3.71	-3.69	0.9963	0.9963	0.242	0.999870	
A2	-3.9	-3.61	0.9961	0.9964	0.242	1.000160	1.000285
B1	-4.08	-3.55	0.9959	0.9965	0.309		1.000518
B2	-4.01	-3.68	0.9960	0.9963	0.309	0.999929	1.000432
C1	-4.19	-3.68	0.9958	0.9963	0.373	0.999944	1.000686
C2	-4.11	-3.65	0.9959	0.9964	0.373	1.000009	1.000584

Reaction extent			
	A	B	C
stop	0.074	0.098	0.119
final	0.306	0.317	0.318
%	0.242	0.309	0.373

	IE(Rs,Ro)	IE(Rp,Ro)
Mean	0.999982	1.000501
SD	0.000111	0.000152
overall	1.000242	
SD	0.000301	
SE	0.000095	

p-nitrophenyl sulfate - acid hydrolysis
^{18}O bridge KIE, 1N HCl, 65°C

TC	Rinf.
1.9	2.13
2.13	2.34
2.08	2.29
2.01	2.28
2.145	1.00215

y fraction of 18-O in double labeled cpd	x fraction of 15-N in double labeled cpd	z fraction of 15-N in 14-N labeled cpd	b fraction of 15-N in mixture	15-N isotope effect	number of discrimin. atoms
0.87	0.99	0.0001	0.003658	1.0002	1

Sample#	P Delta	RS Delta	Rp	Rs	f	IE(Rs,Ro)	IE(Rp,Ro)	corrected ---IE(Rs)	corrected ---IE(Rp)	Q1	A1	a2
Bridge A	-2.78	4.690	0.9972	1.0047	0.367	1.005577	1.006261	1.006306	1.007115	0.027512	1.005482	1.006185
Bridge A	-2.58	4.670	0.9974	1.0047	0.367	1.005533	1.006006	1.006254	1.006813	0.027512	1.005437	1.005922
Bridge B	-2.31	6.060	0.9977	1.0061	0.506	1.005567	1.006480	1.006294	1.007375	0.027512	1.005472	1.006410
Bridge B	-2.34	6.010	0.9977	1.0060	0.506	1.005496	1.006524	1.006210	1.007427	0.027512	1.005398	1.006455
Bridge C	-2.4	6.600	0.9976	1.0066	0.528	1.005937	1.006789	1.006732	1.007740	0.027512	1.005851	1.006727
Bridge C	-2.19	6.500	0.9976	1.0065	0.528	1.005803	1.006474	1.006573	1.007368	0.027512	1.005714	1.006404

Rxn extent		
A	B	C
0.282	0.181	0.256
0.104	0.092	0.135
0.367	0.506	0.528

	IE(Rs,Ro)	IE(Rp,Ro)	corrected ---IE(Rs)	corrected ---IE(Rp)
Mean	1.005652	1.006422	1.006395	1.007306
Sd	0.000176	0.000265	0.000209	0.000313
overall	1.006037		1.006851	
Sd	0.000456		0.000539	
SE	0.000132		0.000156	

p-nitrophenyl sulfate - acid hydrolysis
^{18}O non-bridge KIE, 1N HCl, 65°C

TC	Rinf.
-6.58	-6.58
-6.5	-6.49
-6.34	
-6.52	
-6.5017	0.9935

y fraction of 18-O in double labeled cpd	x fraction of 15-N in double labeled cpd	z fraction of 15-N in 14-N labeled cpd	b fraction of 15-N in mixture	15-N isotope effect	number of discrimin. atoms
0.646	0.99	0.0001	0.003626	1.0002	3

Sample#	P Delta	RS Delta	Rp	Rs	f	IE(Rs,Ro)	IE(Rp,Ro)	corrected ---IE(Rs)	corrected ---IE(Rp)	Q1	A1	a2
NB A	-10.97	-3.840	0.9890	0.9962	0.406	1.005164	1.005927	1.001909	1.002205	0.027756	1.001683	1.001944
NB A	-10.89	-3.870	0.9891	0.9961	0.406	1.005106	1.005821	1.001886	1.002163	0.027756	1.001663	1.001908
NB B	-10.76	-2.770	0.9892	0.9972	0.411	1.007140	1.005672	1.002674	1.002106	0.027756	1.002358	1.001857
NB B	-10.85	-2.860	0.9892	0.9971	0.411	1.006967	1.005793	1.002607	1.002152	0.027756	1.002299	1.001898
NB C	-10.49	-1.960	0.9895	0.9980	0.519	1.006267	1.005942	1.002336	1.002210	0.027756	1.002060	1.001949
NB C	-10.45	-1.970	0.9896	0.9980	0.519	1.006253	1.005882	1.002331	1.002187	0.027756	1.002055	1.001929

Rxn extent		
A	B	C
0.202	0.224	0.208
0.082	0.092	0.108
0.406	0.411	0.519

	IE(Rs,Ro)	IE(Rp,Ro)	corrected ---IE(Rs)	corrected ---IE(Rp)
Mean	1.006149	1.005840	1.002290	1.002171
Sd	0.000864	0.000101	0.000335	0.000039
overall	1.005994		1.002231	
Sd	0.000608		0.000236	
SE	0.000176		0.000068	

Table B-29. pNPS, Acid Hydrolysis, All Isotope Effects, 21 °C, 1.0 N HCl

p-nitrophenyl sulfate - acid hydrolysis
^{15}N KIE, 1 N HCl, 21°C

Delta TC/Sm	
-3.59	-3.35
-3.58	-3.47
-3.65	
-3.46	
-3.5167	0.99648

sample	P Delta	RS Delta	Rp	Rs	f	IE(Rs,Ro)	IE(Rp,Ro)
A1	-3.84	-3.39	0.9962	0.9966	0.423	1.000231	1.000433
A2	-3.63	-3.59	0.9964	0.9964	0.423	0.999866	1.000152
B1	-3.61	-3.41	0.9964	0.9966	0.470	1.000169	1.000131
B2	-3.78	-3.37	0.9962	0.9966	0.470	1.000232	1.000369
C1	-3.73	-3.24	0.9963	0.9968	0.503	1.000397	1.000310
C2	-3.72	-3.33	0.9963	0.9967	0.503	1.000268	1.000295

Reaction extent	A	B	C
stop	0.119	0.149	0.168
final	0.281	0.317	0.334
%	0.423	0.470	0.503

	Mean	1.000194	1.000282
	SD	0.000177	0.000119
	overall	1.000238	
	SD	0.000151	
	SE	0.000048	

p-nitrophenyl sulfate - acid hydrolysis
^{18}O bridge KIE, 1N HCl, 21°C

TC	Rinf.		y fraction of 18-O in double labeled cpd	x fraction of 15-N in double labeled cpd	z fraction of 15-N in 14-N labeled cpd	b fraction of 15-N in mixture	15-N isotope effect	number of discrimin. atoms
1.48	2.01							
1.35	2.19							
1.76								
1.93								
1.78667	1.00179		0.87	0.99	0.0001	0.003658	1.0002	1

Sample#	P Delta	RS Delta	Rp	Rs	f	IE(Rs,Ro)	IE(Rp,Ro)	corrected ---IE(Rs)	corrected ---IE(Rp)	Q1	A1	a2
Bridge A	-4.34	6.700	0.9957	1.0067	0.460	1.007999	1.008506	1.009178	1.009778	0.027512	1.007975	1.008496
Bridge A	-4.5	6.820	0.9955	1.0068	0.460	1.008196	1.008730	1.009410	1.010042	0.027512	1.008177	1.008725
Bridge B	-4.2	7.420	0.9958	1.0074	0.494	1.008303	1.008612	1.009537	1.009903	0.027512	1.008287	1.008604
Bridge B	-4.06	7.110	0.9959	1.0071	0.494	1.007844	1.008409	1.008994	1.009663	0.027512	1.007815	1.008396
Bridge C	-4.01	7.860	0.9960	1.0079	0.484	1.009293	1.008244	1.010637	1.009468	0.027512	1.009241	1.008227
Bridge C	-3.69	7.900	0.9963	1.0079	0.484	1.009293	1.007787	1.010709	1.008926	0.027512	1.009304	1.007757

Rxn extent	A	B	C
	0.104	0.161	0.147
	0.226	0.326	0.304
	0.460	0.494	0.484

	Mean	1.008478	1.008381	1.009744	1.009630
	Sd	0.000628	0.000336	0.000744	0.000397
	overall	1.008430		1.009687	
	Sd	0.000483		0.000572	
	SE	0.000139		0.000165	

p-nitrophenyl sulfate - acid hydrolysis
^{18}O non-bridge KIE, 1N HCl, 21°C

TC	Rinf.		y fraction of 18-O in double labeled cpd	x fraction of 15-N in double labeled cpd	z fraction of 15-N in 14-N labeled cpd	b fraction of 15-N in mixture	15-N isotope effect	number of discrimin. atoms
-5.13	-5.14							
-5.2	-5.12							
-4.7								
-4.6								
-4.9817	0.99502		0.646	0.99	0.0001	0.003626	1.0002	3

Sample#	P Delta	RS Delta	Rp	Rs	f	IE(Rs,Ro)	IE(Rp,Ro)	corrected ---IE(Rs)	corrected ---IE(Rp)	Q1	A1	a2
NB A	-11.31	-2.000	0.9887	0.9980	0.443	1.005135	1.008699	1.001899	1.003278	0.027756	1.001675	1.002890
NB A	-10.97	-1.810	0.9890	0.9982	0.443	1.005464	1.008229	1.002027	1.003097	0.027756	1.001787	1.002730
NB B	-10.94	-1.380	0.9891	0.9986	0.468	1.005759	1.008394	1.002141	1.003160	0.027756	1.001888	1.002786
NB B	-11.21	-1.400	0.9888	0.9986	0.468	1.005727	1.008777	1.002129	1.003308	0.027756	1.001877	1.002917
NB C	-11.23	-0.130	0.9888	0.9999	0.478	1.007537	1.008899	1.002829	1.003356	0.027756	1.002494	1.002959
NB C	-11.04	-0.270	0.9890	0.9997	0.478	1.007318	1.008627	1.002744	1.003251	0.027756	1.002420	1.002866

Rxn extent	A	B	C
	0.125	0.124	0.120
	0.282	0.265	0.251
	0.443	0.468	0.478

	Mean	1.006157	1.008604	1.002295	1.003242
	Sd	0.001012	0.000249	0.000392	0.000096
	overall	1.007381		1.002768	
	Sd	0.001459		0.000564	
	SE	0.000421		0.000163	

Table B-30. pNPS, Acid Hydrolysis, All Isotope Effects, 15 °C, 10 N HCl

p-nitrophenyl sulfate - acid hydrolysis
^{15}N KIE, 10 N HCl, 15°C

Delta TC/Sm	
-3.59	-3.35
-3.58	-3.47
-3.65	
-3.46	
-3.5167	0.99648

sample	P Delta	RS Delta	Rp	Rs	f	IE(Rs,Ro)	IE(Rp,Ro)
A1	-3.75	-3.17	0.9963	0.9968	0.700	1.000289	1.000454
A2	-3.72	-2.96	0.9963	0.9970	0.700	1.000464	1.000396
B1	-3.69	-3.4	0.9963	0.9966	0.630	1.000118	1.000298
B2	-3.92	-3.29	0.9961	0.9967	0.630	1.000229	1.000694
C1	-3.89	-2.72	0.9961	0.9973	0.460		1.000518
C2	-3.91	-3.1	0.9961	0.9969	0.460	1.000680	1.000546
D1	-3.71	-3.38	0.9963	0.9966	0.443	1.000235	1.000264
D2	-3.74	-3.45	0.9963	0.9966	0.443	1.000114	1.000305

Reaction extent						
	A	B	C	D	Mean	1.000356	1.000484
stop	0.263	0.203	0.108	0.12	SD	0.000220	0.000136
final	0.376	0.322	0.235	0.271	overall	1.000426	
%	0.700	0.630	0.460	0.443	SD	0.000182	
					SE	0.000050	

p-nitrophenyl sulfate - acid hydrolysis
^{18}O bridge KIE, 10 N HCl, 15°C

TC	Rinf.		y fraction of 18-O in double labeled cpd	x fraction of 15-N in double labeled cpd	z fraction of 15-N in 14-N labeled cpd	b fraction of 15-N in mixture	15-N isotope effect	number of discrimin. atoms
1.48	2.01							
1.35	2.19							
1.76								
1.93								
1.78667	1.00179		0.87	0.99	0.0001	0.003658	1.0004	1

Sample#	P Delta	RS Delta	Rp	Rs	f	IE(Rs,Ro)	IE(Rp,Ro)	corrected ---IE(Rs)	corrected ---IE(Rp)	Q1	A1	a2
Bridge A	-5.18	6.900	0.9948	1.0069	0.437	1.008955	1.009455	1.010085	1.010677	0.0275	1.0088	1.0093
Bridge A	-5.17	6.920	0.9948	1.0069	0.437	1.008991	1.009441	1.010127	1.010661	0.0275	1.0088	1.0093
Bridge B	-4.05	9.230	0.9960	1.0092	0.546	1.009468	1.008919	1.010692	1.010043	0.0275	1.0093	1.0087
Bridge B	-3.97	9.390	0.9960	1.0094	0.546	1.009672	1.008797	1.010934	1.009897	0.0275	1.0095	1.0086
Bridge C	-3.96	7.950	0.9960	1.0080	0.537	1.008028	1.008687	1.008988	1.009767	0.0275	1.0078	1.0085
Bridge C	-4.32	8.080	0.9957	1.0081	0.537	1.008199	1.009234	1.009189	1.010415	0.0275	1.0080	1.0090

Rxn extent				Mean	1.008885	1.009089	1.010002	1.010243
A	B	C		Sd	0.000660	0.000333	0.000782	0.000395
0.110	0.131	0.145		overall	1.008987		1.010123	
0.252	0.240	0.270		Sd	0.000510		0.000604	
0.437	0.546	0.537		SE	0.000147		0.000174	

p-nitrophenyl sulfate - acid hydrolysis
^{18}O non-bridge KIE, 10 N HCl, 15°C

TC	Rinf.		y fraction of 18-O in double labeled cpd	x fraction of 15-N in double labeled cpd	z fraction of 15-N in 14-N labeled cpd	b fraction of 15-N in mixture	15-N isotope effect	number of discrimin. atoms
-5.13	-5.14							
-5.2	-5.12							
-6.34								
-6.2								
-5.5217	0.99448		0.646	0.99	0.0001	0.003626	1.0004	3

Sample#	P Delta	RS Delta	Rp	Rs	f	IE(Rs,Ro)	IE(Rp,Ro)	corrected ---IE(Rs)	corrected ---IE(Rp)	Q1	A1	a2
NB A	-12.6	-0.880	0.9874	0.9991	0.461	1.007592	1.009917	1.002777	1.003676	0.0278	1.0024	1.0032
NB A	-12.22	-0.770	0.9878	0.9992	0.461	1.007773	1.009381	1.002847	1.003469	0.0278	1.0025	1.0031
NB B	-12.76	-1.000	0.9872	0.9990	0.492	1.006734	1.010486	1.002445	1.003895	0.0278	1.0022	1.0034
NB B	-12.85	1.830	0.9872	1.0018	0.492	1.010979	1.010617		1.003946	0.0278	1.0036	1.0035
NB C	-12.68	-0.440	0.9873	0.9996	0.538	1.006646	1.010927	1.002411	1.004066	0.0278	1.0021	1.0036
NB C	-12.62	-0.640	0.9874	0.9994	0.538	1.006384	1.010835	1.002309	1.004030	0.0278	1.0020	1.0036

Rxn extent				Mean	1.007684	1.010361	1.002558	1.003847
A	B	C		Sd	0.001706	0.000597	0.000238	0.000231
0.130	0.131	0.149		overall	1.009023		1.003261	
0.282	0.266	0.277		Sd	0.001854		0.000709	
0.461	0.492	0.538		SE	0.000535		0.000205	

CURRICULUM VITAE

Richard H. Hoff
(May 1999)

<u>Educational Background:</u>
B.S., United States Military Academy, 1979, Mechanical Engineering.
M.S., Utah State University, 1988, Environmental Engineering.
    Research in the soil-phase photodegradation of a simulated hazardous waste.
Ph.D., Utah State University, 1999, Chemistry.
    Research titled, "Investigation Into The Cleavage of The Ester Bond in Phosphate Monoesters: Enzymatic and Solution Studies of Phosphoryl Transfer Reactions and Comparison with Analogous Sulfuryl Transfer Reactions."

<u>Professional Experience:</u>
Nine years of increasingly challenging management positions in military combat engineering organizations in worldwide locations, culminating in a position as the Chief Executive for a 500 man organization with responsibility for training and evaluating Reserve soldiers and units throughout five western states.

As a member of the teaching faculty at the United States Military Academy, managed increasing teaching responsibilities for three academic years. In the final year, as an Associate Professor, developed, planned and taught a new senior level, semester-long course in Environmental Chemistry.

Served for two years in the military engineer district in Seoul, Korea, with dual responsibilities as the Army Corps of Engineers Environmental Engineer for all US forces in Korea, and as Deputy Project Manager for over $40 million in civil construction.

<u>Publications:</u>
Dupont, R.R., McLean, J.E., Hoff, R.H., Moore, W.M. (1990) "Evaluation of the Use of Solar Irradiation for the Decontamination of Soils Containing Wood Treating Wastes." <u>J. Air Waste Manage. Assoc.</u> **40**(9): 1257-1265.

Hoff, R.H. "Guidance for the Use of Bioremediation for POL Contaminated Soils." U.S. Army Corps of Engineers report to U.S. Forces Korea: Seoul, Korea, 31 January 1994.

Hoff, R.H., Hengge, A.C. (1998) "A Facile High-Yield Synthesis and Purification of Tetrabutylammonium Tetrabutylborate." <u>J. Org. Chem.</u> **63**(1): 195.

Hoff, R.H., Hengge, A.C. (1998) "Entropy and Enthalpy Contributions to Solvent Effects on Phosphate Monoester Solvolysis. The Importance of Entropy Effects in the Dissociative Transition State." <u>J. Org. Chem.</u> **63**(19): 6680-6688.

Hoff, R.H., Mertz, P., Rusnak, F., Hengge, A.C. "The Transition State of the Phosphoryl Transfer Reaction Catalyzed by the Lambda Ser/Thr Protein Phosphatase." Accepted for publication in <u>J. Amer. Chem. Soc.</u>

Hoff, R.H., Hengge, A.C., Keng, Y.F., Zhang, Y.Z., "The Effects on General Acid Catalysis From Mutations of the Invariant Tryptophan and Arginine Residues in the Protein-Tyrosine Phosphatase from *Yersinia.*" Submitted for publication.

Hoff, R.H., Hengge, A.C., Keng, Y.F., Zhang, Y.Z., "The Effect of the Conserved Arginine on the Transition State for Enzymatic Phosphoryl Transfer in the Protein-Tyrosine Phosphatase from *Yersinia*." Submitted for publication.

Hoff, R.H., Hengge, A.C. "The Solvolysis of a Sulfate Monoester. Does the Transition State for Solvolysis Resemble the Transition State of Phosphate Monoesters?" Submitted for publication.

Presentations:
"Thermodynamics and Solvation Effects on Phosphoryl and Sulfuryl Transfer Reactions." Presented at the American Chemical Society National Conference, Las Vegas, Nevada, 7-11 September, 1997.

"Kinetic Isotope Effects in Phosphoryl Transfer Reactions." Presented at the 1998 Gordon Research Conference on Isotopes in Biology and Chemistry, Ventura, California, 12 January 1998.

"The Chemistry Behind the Toxicity of Chemical Weapons, and the Mechanism and Politics of their Destruction." Presented to the Chemistry and Biochemistry Department of USU, April 1998.

"Entropy Effects in the Catalytic Efficiency of Phosphatases." Presented at the 27th Reaction Mechanisms Conference, Asilomar, California, 29 June 1998.

"The Effects on the Functioning of the General Acid Catalyst From Mutations of the Invariant Tryptophan and Arginine Residues in the Protein-Tyrosine Phosphatase from *Yersinia*.." Presented at the 16th Enzyme Mechanisms Conference, Napa, California, 7 January 1999.

Professional Honors:
1998 - Chemistry and Biochemistry Alumni Award
1996 - DeFleury Medal from US Army Engineer Regiment for distinguished service.
1993 - Environmental Professional of the Year, US Forces Korea.
1993 - Golden Apple Award, Department of Defense Schools, Korea.
1992 - Army Achievement Medal for proposing and executing $150K in cost savings on an environmental remediation project.